Nickel N-heterocyclic carbene complexes in homogeneous catalysis

Berding, J.

Nickel N-heterocyclic carbene complexes in homogeneous catalysis

PROEFSCHRIFT

ter verkrijging van

de graad van Doctor aan de Universiteit Leiden,

op gezag van Rector Magnificus prof.mr. P.F. van der Heijden,

volgens besluit van het College voor Promoties

te verdedigen op donderdag 8 oktober 2009

klokke 16.15 uur

door

Joris Berding

geboren te ‘s-Gravenhage in 1980

Samenstelling promotiecommissie

Promotor	Prof.dr. J. Reedijk
Co-promotor	Dr. E. Bouwman
Overige leden	Prof.dr. F.E. Hahn
	(Westfälische Wilhelms-Universität Münster, Duitsland)
	Prof.dr. C.J. Elsevier (Universiteit van Amsterdam, Nederland)
	Prof.dr. G.A. van der Marel
	Prof.dr. J. Brouwer

This work has been supported financially by the National Graduate School Combination NRSC-Catalysis, a joint activity of the graduate schools NIOK, HRSMC, and PTN.

Printed by: Wöhrmann Print Service, Zutphen

Every great advance in science has issued from a new audacity of imagination.
John Dewey, The Quest for Certainty, 1929

voor mijn ouders

Table of contents

List of abbreviations

Acac	Acetylacetonate
Bim	Benzimidazole
Bn	Benzyl
Bu	Butyl
COD	1,4-Cyclooctadiene
COSY	Correlation spectroscopy
COSMO	Conductor-like screening model
Cp	Cyclopentadienyl
Cy	Cyclohexyl
d	Doublet (in NMR) or days
DCM	Dichloromethane
DFT	Density functional theory
DMF	N,N-Dimethylformamide
DMSO	Dimethylsulfoxide
Et	Ethyl
ESI	Electrospray ionization
FT	Fourier transform
GC	Gas chromatography
GPC	Gel permeation chromatography
Im	Imidazole
IMes	1,3-Bis(2,4,6-trimethylphenyl)imidazol-2-ylidene
IPr	1,3-Bis(2,6-diisopropylphenyl)imidazol-2-ylidene
IR	Infra red
MAO	Methylaluminoxane
Me	Methyl
MS	Mass spectroscopy
n.d.	Not determined
NHC	N-heterocyclic carbene
NMR	Nuclear magnetic resonance
OMs	Methylsulfonate (mesylate)
OTf	Trifluoromethylsulfonate (triflate)
OTos	p-Toluenesulfonate (tosylate)
Ph	Phenyl
Pr	Propyl
Py	Pyridine
q	Quartet
RT	Room temperature
s	Singlet
SIMes	1,3-Bis(2,4,6-trimethylphenyl)imidazolin-2-ylidene
t	Triplet
THF	Tetrahydrofuran
TMS	Tetramethylsilane
Xy	Xylyl

Chapter 1

Introduction

Abstract. *The chemistry of N-heterocyclic carbenes (NHCs) is reviewed and discussed. First an overview is given of the electronic structure of free carbenes, followed by a discussion on the structure of transition-metal NHC complexes, with an emphasis on nickel complexes. Then synthetic routes leading to such complexes are evaluated. In addition, an overview of reactions catalyzed by transition-metal NHC complexes is presented, followed by a description of the contents of this thesis.*

1.1 Introduction

An old definition of the word 'carbene' is 'a bitumen soluble in carbon disulfide but insoluble in carbon tetrachloride'.[1] Nowadays, the term carbene is used for a divalent carbon compound in which the carbene carbon atom is linked to two adjacent groups by covalent bonds and has two non-bonding electrons (Figure 1.1), which are either in a singlet or in a triplet state.

A special class of carbenes is the group of N-heterocyclic carbenes (NHCs),[2-9] which is the subject of this thesis. Since the first isolation of a free NHC in 1991,[10] the study and application of these compounds is a fast growing field, as can be seen in Figure 1.2. In this figure the number of hits in a literature search using the SciFinder Scholar program for the phrase 'N-heterocyclic carbene', ordered by year of publication, is depicted.[11] It reveals a linear increase in the number of papers published on this subject between 2002 and 2008.

The great interest for NHCs may mostly be attributed to the fact that they are highly versatile ligands for transition-metal complexes, especially of complexes used in homogeneous catalysis. A famous example of the successful use of NHCs in catalysis is the Grubbs catalyst. The first generation Grubbs catalyst, a ruthenium complex with two phosphane ligands was found to be highly active in the metathesis of olefins. The second generation catalyst, in which one of the phosphane ligands

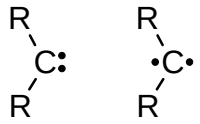

Figure 1.1. Singlet and triplet carbenes.

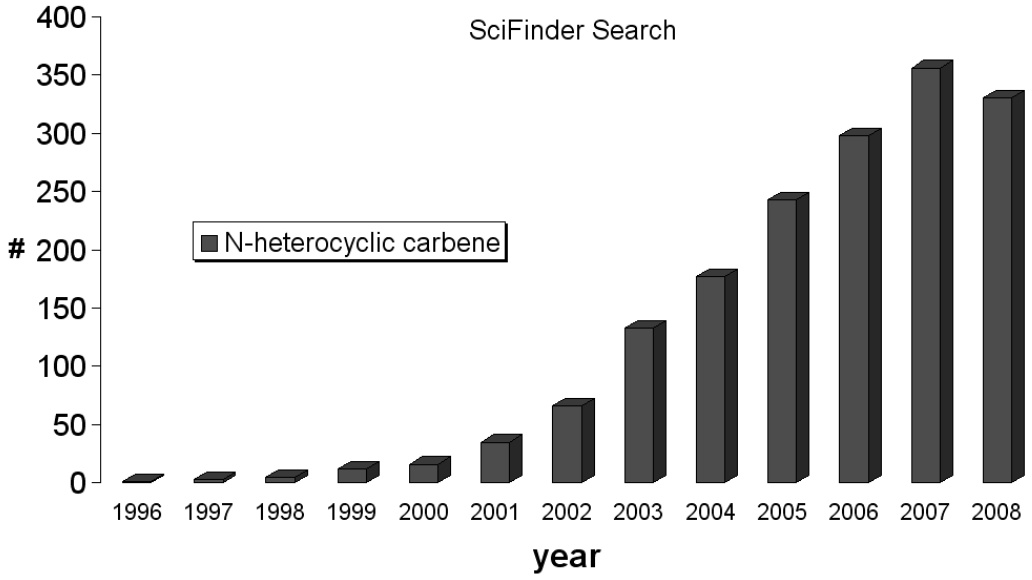

Figure 1.2. Number of papers on the subject of N-heterocyclic carbenes, ordered by publication year, found using the SciFinder Scholar program.

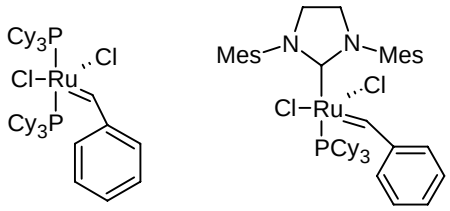

Figure 1.3. First and second generation Grubbs catalysts.

was replaced by a NHC ligand, proved to be even more active and more stable (Figure 1.3).[12] In 2005 Robert Grubbs was awarded the Nobel Prize in chemistry for his work on the metathesis reaction.

In this chapter a short overview is given of the properties of carbenes and of N-heterocyclic carbenes in particular. Then their properties as ligands in transition-metal complexes are discussed, followed by a short overview of catalytic reactions in which NHC complexes have been investigated. The discussion will be focused on the synthesis and use of nickel NHC complexes.

Nomenclature

Some inconsistencies appear to be present in the literature in the nomenclature of imidazole derivatives and carbenes thereof. In this thesis the nomenclature shown in Figure 1.4 will be followed. Furthermore, it should be noted that metal N-heterocyclic carbene complexes derived from imidazole have been depicted differently in literature (Figure 1.4, **A** - **D**). Representation **A** is used throughout this thesis.

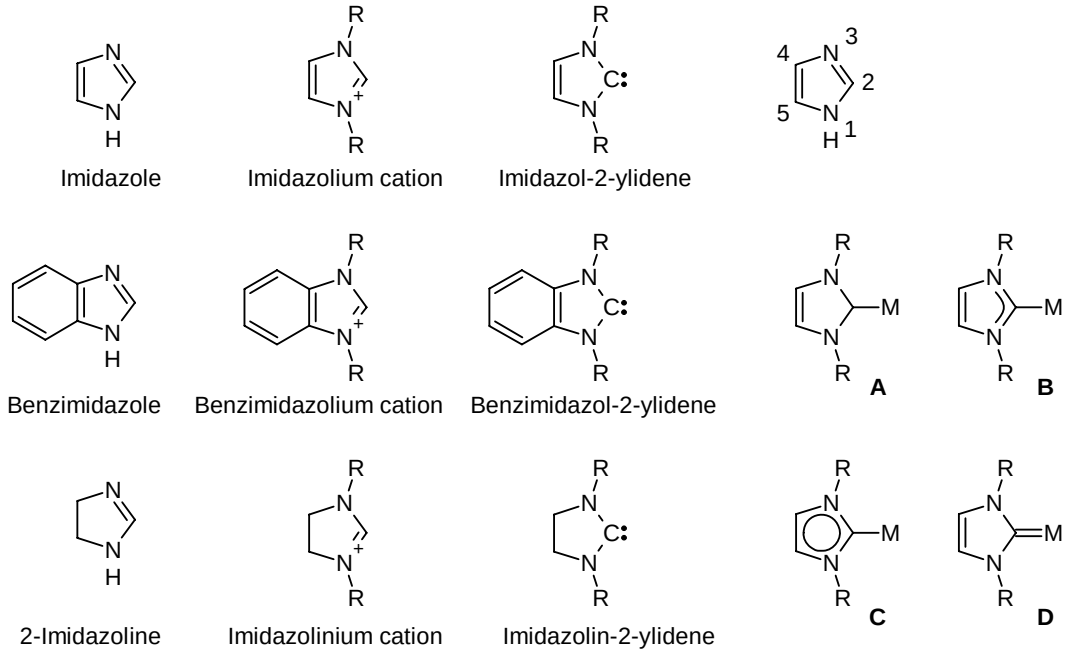

Figure 1.4. Nomenclature of imidazole-derived structures, atom numbering, and a variety of common representations of metal NHC complexes (**A** – **D**).

1.2 Carbenes

Reactants in organic synthesis

Free carbenes are known in organic synthesis as useful reactants. A common reaction involving a carbene is given in Scheme 1.1.[13] In this case, the dichlorocarbene may be generated by reaction of chloroform with a strong base. Subsequent reaction with an olefin leads to the formation of a cyclopropane.

Singlet vs triplet state – theoretical discussion

Having only two substituents, the geometry around the divalent carbene carbon atom can be either bent or linear. The latter geometry is based on an sp-hybridized carbon atom. Most carbenes, however, have an sp^2-hybridized carbon atom and the geometry is not linear. The energy of one p orbital, p_π, does not change by going from the sp to the sp^2-hybridization state. Due to its partial s character the sp^2 orbital, which is described as a σ orbital, is energetically stabilized relative to the original p orbital (Figure 1.5).[7]

The two nonbonding electrons available on the sp^2-hybridized carbene carbon atom can have antiparallel spins, with the two electrons occupying the σ-orbital

Scheme 1.1. Dichlorocarbene in organic synthesis.

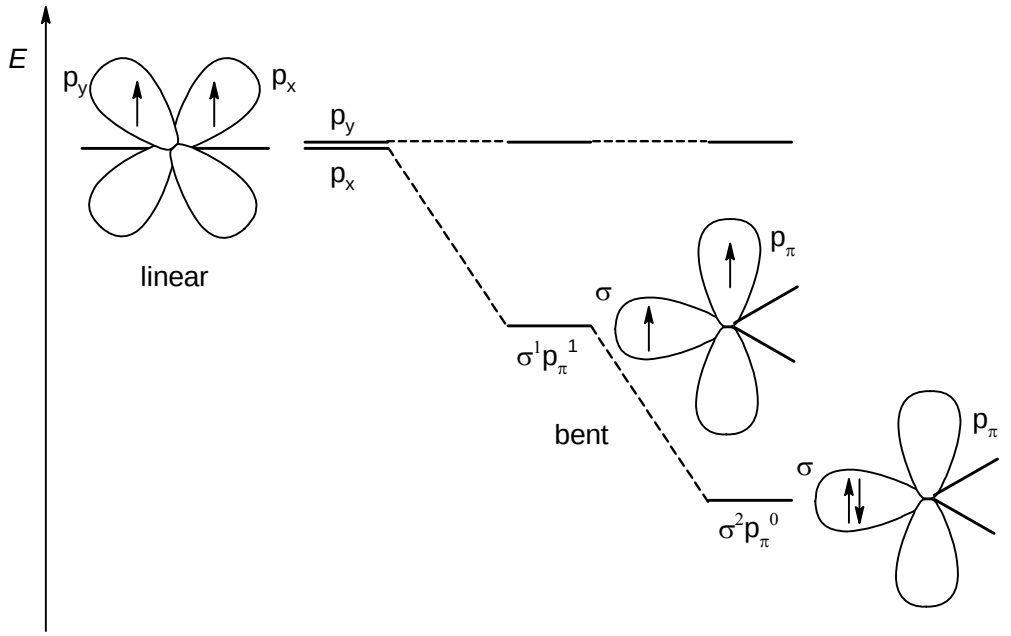

Figure 1.5. Energy diagram with possible electron configurations for the frontier orbitals of carbene carbon atoms.[7]

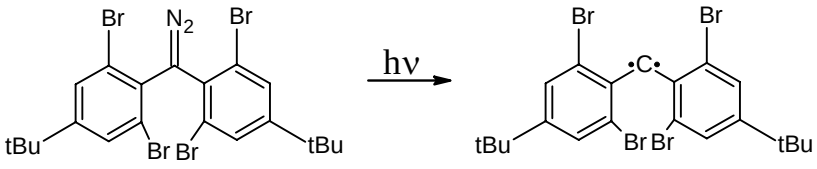

Scheme 1.2. Generation of a triplet carbene.

($\sigma^2p_\pi^0$, singlet state) or parallel spins, with the electrons divided over the two orbitals ($\sigma^1p_\pi^1$, triplet state). A less-stable singlet state with both electrons in the p_π-orbital and an excited singlet state with antiparallel occupation of the two orbitals are theoretically feasible, but are not considered to be of importance.[7]

Whether a carbene is in the singlet or the triplet ground state is determined by the relative energies of the σ and the p_π orbitals. If the gap between the two states is greater than about 40 kcal/mol, a singlet ground state is favored.[14] The relative energies of the two orbitals are determined by the substituents. For instance, large, electron-withdrawing groups give rise to singlet carbenes, while electron-donating groups favor the more reactive triplet state.[3] Three types of substituents may be distinguished: (1) substituents that are part of a conjugated system, (2) substituents that withdraw π electrons from the carbene center and (3) substituents that donate π electrons. To the first type belong triplet carbenes in which the carbene carbon atom has two alkene, alkyne or aryl groups. An example of such a reactive triplet carbene is shown in Scheme 1.2. Even with the steric bulk provided by the substituents, this species has a half-life of 16 seconds in a benzene solution.[15]

Examples of the second type of substituent are π-accepting substituents such as Li, BH_2 or BeH. Often these carbenes have a linear or nearly linear geometry.

Substituents belonging to the third type enhance the nucleophilicity of the carbon atom and the thermodynamic stability. To this type belong N, O, S and P substituents, as well as halides. The interaction of the π electrons of the substituents with the p_π orbital of the carbene center leads to a four-electron-three-center π system, with multiple bond character for the carbene-substituent bond (Figure 1.6).

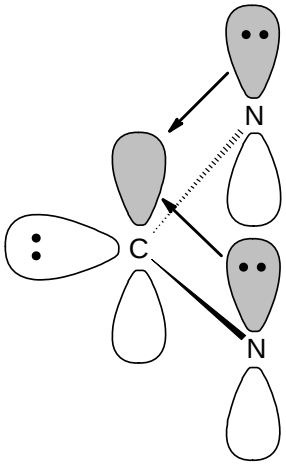

Figure 1.6. Stabilization of NHCs by π interaction.

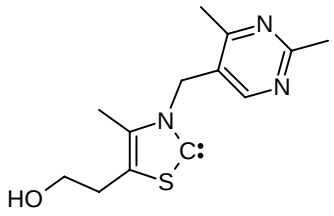

Figure 1.7. N,S-heterocyclic carbene involved in enzymatic benzoin condensation.

Several combinations of heteroatoms (N, O, S, P) are conceivable, and a number of different carbenes with these substituents has been isolated in the solid state.[3] An N,S-substituted heterocyclic carbene was proposed, and later found, to be involved in the enzymatic benzoin condensation in 1958 (Figure 1.7).[16] N-heterocyclic carbenes, in which two N-substituents are incorporated into a 5-membered ring, are the major topic of this work.

Fischer and Schrock carbene complexes

Although many early attempts to prepare or isolate free carbenes failed, complexes of carbenes have been known for decades. The first example of a carbene in coordination chemistry was given by Fischer in 1964 with the synthesis of $W(CO)_5(C(CH_3)OCH_3)$ (Figure 1.8, **A**).[17] The metal-carbon bond of this type of carbene complex is a donor-acceptor bond with σ-donation from the carbene to the metal and π-back donation from the metal to the carbene.[3] Fischer carbenes are generally found with low oxidation state metals with π-accepting ligands and π-donor substituents on the carbene carbon. The Fischer carbene is in a singlet spin state. In contrast, Schrock carbenes are found with high oxidation state metals with non-π-accepting ligands and without π-donor substituents on the carbene carbon. Schrock carbenes are in the triplet spin state. The first example was reported by Schrock in 1974 (Figure 1.8, **B**).[18] Both the Fischer and the Schrock carbenes are commonly depicted with a metal-carbon double bond.

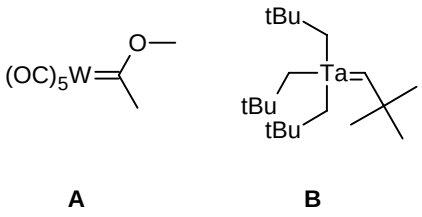

Figure 1.8. Examples of a Fischer (**A**) and a Schrock (**B**) carbene.

1.3 N-Heterocyclic carbenes (free)

Imidazole derivatives

The type of carbene that has received the most attention is the N-heterocyclic carbene (NHC), in which the carbene carbon atom has two nitrogen substituents and is part of a 5-membered ring. In the 1960's attempts to obtain this type of carbenes starting from N,N′-disubstituted imidazolines were made by Wanzlick *et al*.[19] Thermal α-elimination of chloroform from the corresponding imidazole adduct, however, gave the dimerized electron-rich olefin, which was shown not to be in equilibrium with the monomer (Scheme 1.3). In addition, attempts to isolate the free carbene derived from unsaturated N,N′-disubstituted imidazoles were unsuccessful, although the existence of the NHC was proven by trapping the free species as a transition-metal complex.[20]

The first stable carbene was reported by Arduengo *et al*. in 1991 (Figure 1.9).[10] This first example of a stable N-heterocyclic carbene was obtained by deprotonation of the corresponding imidazolium chloride with sodium hydride in the presence of a catalytic amount of DMSO. Some characteristics of the imidazolium salt and the carbene are collected in Table 1.1. The colorless crystals of **B** are thermally stable and

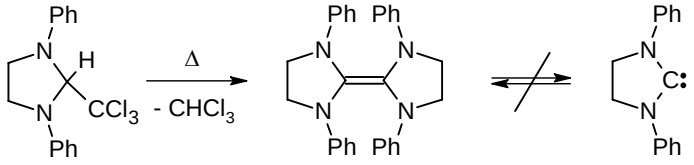

Scheme 1.3. Dimerization of imidazoline-based carbenes.

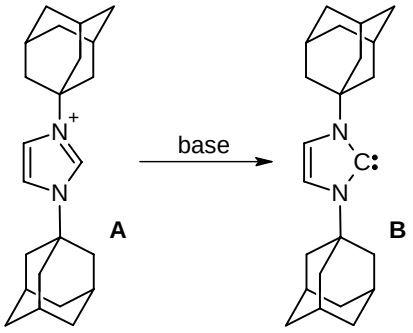

Figure 1.9. 1,3-Diadamanylimidazolium cation **A** and the first isolated N-heterocyclic carbene **B**.

Table 1.1. Some characteristic bond distances (Å), angles (°) and ^{13}C NMR shift (ppm) of structures **A** and **B** (Figure 1.9).

	A BPh_4^-	**B**
C-2 - N-1	1.326	1.367
C-2 - N-3	1.332	1.373
C-4 - C-5	1.334	1.338
N-C-N	109.7	102.2
δ(C) C-2	136	211

melt at 240 °C without decomposition.

The basicity of 1,3-diisopropyl-4,5-dimethylimidazol-2-ylidene in DMSO was reported as pK_a = 24, which makes it more basic than strong nitrogen bases such as 1,8-Diazabicyclo[5.4.0]undec-7-ene (DBU).[21] Other experimental and theoretical investigations revealed similar values for related compounds.[22, 23]

Electronic structure/Stability of imidazol(in)-2-ylidenes

Initially it was thought that the stability of the first isolated free carbene could be explained by the steric properties of the adamantyl groups, however, in 1992 Arduengo showed that 1,3,4,5,-tetramethylimidazol-2-ylidene is a stable solid as well.[24, 25] It has been calculated that the gap between the triplet and the singlet ground state in N-heterocyclic carbenes is about 65-85 kcal/mol, which clearly indicates that the singlet ground state is preferred.[26] The stability of the singlet state is explained by the inductive effect of the σ-electron withdrawing substituents, which stabilizes the σ orbital on the carbene carbon atom, by increasing the singlet-triplet gap. In addition, the singlet state is stabilized by p_π donation from the nitrogen atoms into the empty p_π orbital of the carbene C atom.[27] It was calculated that the highest occupied molecular orbital corresponds to the σ lone pair of the carbene carbon atom.[28]

The tendency of saturated NHCs to dimerize is correlated to their smaller singlet-triplet gap of about 70 kcal/mol, compared to the gap of about 80 kcal/mol for unsaturated NHCs.[26] To obtain the free saturated carbene species, bulky substituents such as 2,4,6-trimethylphenyl are needed.[29, 30]

While unsaturated NHCs do not show a tendency to dimerize and unsaturated NHCs dimerize readily, in the case of benzimidazol-2-ylidenes the equilibrium depends highly on steric parameters.[31] The first free benzimidazol-2-ylidenes were reported by Hahn *et al*.[32] As shown in Scheme 1.4, *o*-phenylenediamines **A** were reacted with thiophosgene to yield the corresponding benzimidazol-2-thiones (**B**), which were treated with potassium to generate either the free carbene (**C**), or the

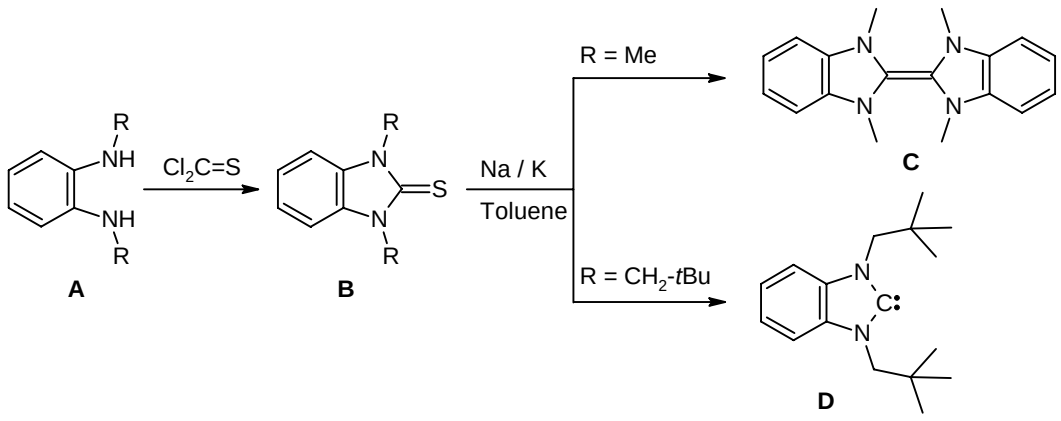

Scheme 1.4. Synthesis of benzimidazol-2-thione **B**, dibenzotetraazafulvalene **C** and benzimidazol-2-ylidene **D**.

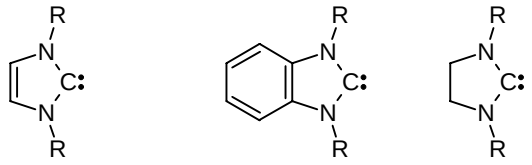

d(C_2) [ppm]	211.4-220.8	231.5 (THF-d_8)	238.2-244.5
N-C-N [°]	101.2(2)-102.2(2)	103.5(1), 104.3(1)	104.7(3)-106.4(1)

Figure 1.10. Comparison of ^{13}C NMR spectroscopic and structural parameters for imidazol-, benzimidazol- and imidazolin-2-ylidene.

dibenzotetraazafulvalene (**D**). The solid-state structures of free benzimidazol-2-ylidenes suggest that, compared to the unsaturated imidazol-2-ylidenes the benzimidazole based carbenes have less aromatic character at the carbene carbon.[33] Furthermore, not only the tendency to dimerize, but also structural and ^{13}C NMR spectroscopic parameters are intermediate between the saturated and unsaturated imidazole-based carbenes (Figure 1.10).

Other N-heterocycles and topologies

An overview of other N-heterocyclic carbene topologies is shown in Figure 1.11. Some have been characterized in the free state, while others have been under investigation as a ligand. The use of these alternative topologies allows for the fine-tuning of the electronic properties of the ligand and the corresponding complex. For instance, the six- and seven-membered ring NHCs (**A**, **B**) have been shown to be more basic than their five-membered analogues and due to the larger NCN angle, the substituents of the larger rings are closer to the metal center.[34] Structure **C** was obtained by reaction of bipyridine with a suitable CH_2-precursor ($[Ph_3AsCH_2OTf]^+$), followed by deprotonation, and may formally be described as a bipyridine complex of singlet carbon.[35] Carbene **D** is another example of a way to bring steric bulk in the vicinity of the metal center. With this oxazoline topology, several chiral ligands have

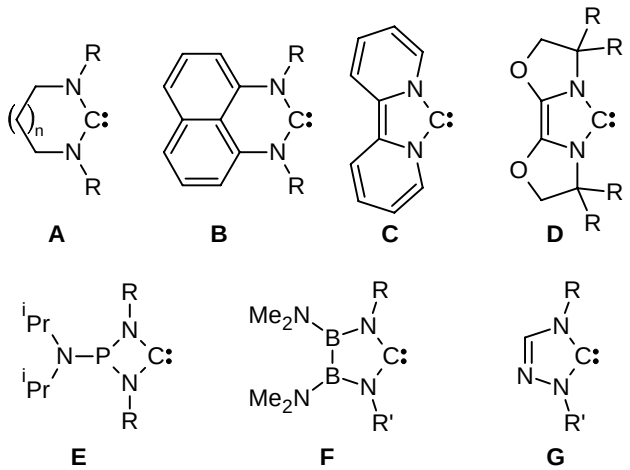

Figure 1.11. Alternative common N-heterocyclic carbene topologies.

been prepared as well.[36]

The backbone of the N-heterocycle is not limited to carbon atoms. Some variations, including phosphorus (**E**)[37] and boron (**F**)[38] containing NHCs have been synthesized as well. The phenyl substituted triazole-based NHC (**G**) was the first commercially available free carbene.[39]

1.4 N-Heterocyclic carbene complexes

1.4.1 General

Even though several N-heterocyclic carbene complexes had been isolated and characterized from the 1960s onward,[20, 40, 41] study of these compounds became widespread only after the isolation of the first free NHC in 1991. Early attempts to trap the free NHC by Öfele and Wanzlick resulted in metal-NHC complexes shown in Figure 1.12, **A** and **B**.[20, 40] Lappert *et al.* used the NHC dimers earlier described by Wanzlick to obtain several transition-metal complexes (**C**).[41]

In NHC complexes the π-back-bonding is less pronounced, in contrast to the Fischer-type carbenes. For this reason, in literature the M-C bond in this type of complex is often depicted as a single bond. A more detailed discussion of the bonding of N-heterocyclic carbenes to transition metals is given in the next section.

1.4.2 Electronic and sterics properties of NHCs

Comparison with phosphanes

NHCs have often been compared to phosphanes, PR_3, the first major class of spectator ligands in homogeneous catalysis. Because of the availability of the Tolman's parameters (electronic parameter Δν, steric parameter Θ) they have predictable and tunable steric and electronic effects.[42] Based on spectroscopic measurements it was concluded early on that NHCs have comparable electronic structures (good σ-donors, poor π-acceptors). Later, it was shown that NHCs are stronger donors than the most basic phosphanes,[43] and that NHCs may also act as a π-acceptor in a number of complexes.[44, 45]

When compared to other σ-donating ligands, NHCs show relatively high

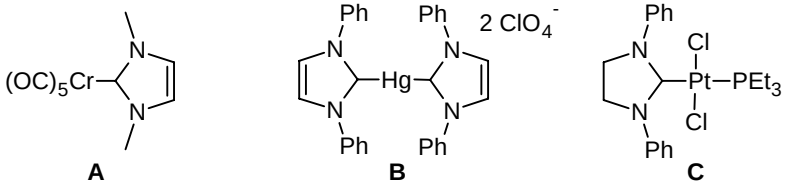

Figure 1.12. Early examples of NHC complexes.

dissociation energies. For example, calculations showed that the loss of PMe_3 from *trans*-[$PdCl_2(PMe_3)$(NHC)] requires 38.4 kcal/mol, while the loss of the NHC (unsubstituted imidazol-2-ylidene) requires 54.4 kcal/mol.[46]

Another important difference between phosphanes and NHCs is the orientation of the steric bulk. In phosphane ligands the three substituents point away from the metal center, while in NHCs the two substituents may flank the metal center. Furthermore, in contrast to phosphanes, the substituents of the NHC are not directly linked to the coordinating atom. This allows, in principle, for the electronic and steric factors to be tuned independently.

Steric parameter

Defining steric parameters for NHCs is subject of ongoing research; however, this is hampered by the fan shape of the NHC ligands compared to the cone shape of the phosphane ligands.[47-50] The cone angle, the parameter used by Tolman to quantify the steric properties of tertiary phosphane ligands, is not a suitable measure of bulk in NHCs. In general, the steric congestion around the metal center is due to the bulkiness of the N-substituents and the metal-carbon distance. Therefore, instead of only one cone angle, two angles may be defined; one angle describing the occupancy of the ligand in the plane of the imidazolium ring, and one angle perpendicular to the plane.[47] Alternatively, the percentage of the volume occupied by ligand atoms in a 3 Å sphere around the metal center may be calculated (Figure 1.13).[51, 52] A plot of the (calculated) bond dissociation energy against the (calculated) volume percentage showed a linear correlation between the two parameters, thereby showing the usefulness of these models.[52]

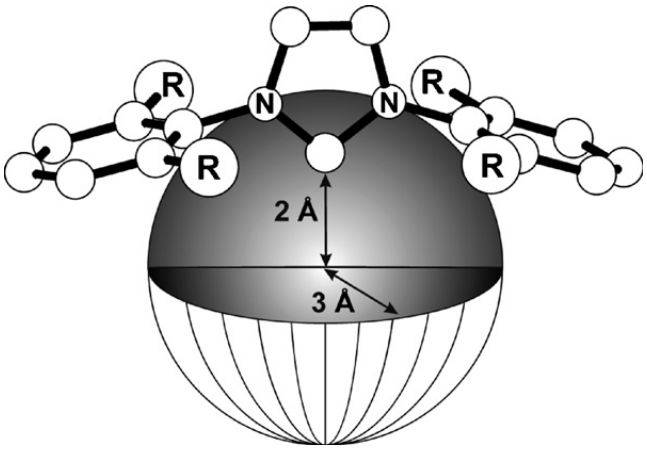

Figure 1.13. Representation of the sphere dimensions for steric parameter determination of NHC ligands (Figure was reproduced from ref. 51).

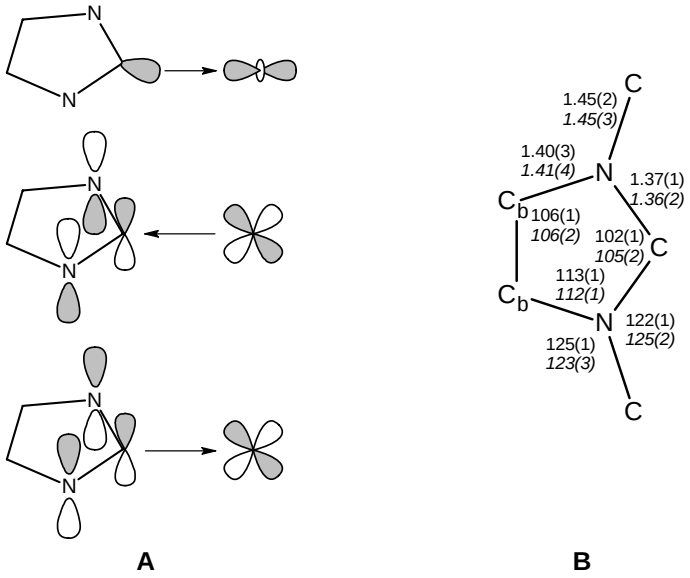

Figure 1.14. The three bonding contributions to the NHCs to metal centers (**A**), and comparison of average bond distances (Å) and angles (°) of 13 examples of free NHCs and 156 NHC complexes (in italics) (**B**).

Electronic structure

Initially, NHC ligands were considered to be almost pure σ-donors, through donation of the σ electrons of the carbene carbon atom into an empty d orbital of the metal. More recently it has been suggested that NHCs are electronically more flexible, since filled and empty π and π* orbitals on the NHC ring may contribute to the NHC-metal bond (Figure 1.14, **A**).[53] Electron rich metals may be stabilized through additional back donation of d electrons of the metal to a π* orbital of the NHC, while electron-deficient metals can be stabilized through donation of π electrons of the NHC into an empty d orbital of the metal.[52] The structure of the five-membered ring changes only slightly on going from the free carbene species to the metal complex, as can be seen from a comparison of the solid state structures of free NHCs and metal NHC compounds. Selected bond distances and angles averaged over a number of NHCs and complexes are given in Figure 1.14, **B**.[54]

Several studies have been performed in order to determine the bond dissociation energy of metal-NHC bonds and to quantify the contribution of π electrons to the metal-NHC bond in various systems. For example, in several studies the carbonyl stretching frequencies of metal (Ni, Ir) NHC carbonyl complexes have been determined experimentally[50] and by quantum chemical calculation[55]. Comparison of different NHCs and phosphanes showed that the difference between various NHCs is not very large and that NHCs are better σ-donors than phosphanes. In addition, attempts were undertaken to measure calorimetrically the bond dissociation energy (BDE) of a number of $NiL(CO)_n$ complexes.[56] Depending on the complex and the bulk of the ligand the BDE of the Ni-NHC bond was measured to be about 30-40 kcal/mol.

Density functional calculations on d^{10} metal NHC complexes such as $Ni(NHC)(CO)_2$ revealed as much as 25% π contribution to the total bonding interaction in the case of nickel(0), most of which is due to back donation.[45] Other studies revealed that the π contribution decreases in the order Ni > Pd > Pt.[57]

The investigations regarding the nature of various metal-NHC bonds were reviewed in 2008.[27]

1.4.3 Other topologies

Abnormal binding

The C-4 and C-5 CH groups of imidazolium salts are quite acidic. This is clear for example, from the fact that the backbone of IMes (1,3-bis(2,4,6-trimethylphenyl)imidazol-2-ylidene) is readily chlorinated by CCl_4.[58] In 2002 Gründemann *et al*. reported a pyridine functionalized imidazolium ligand that, on reacting with $IrH_5(PPh_3)_2$, gave a mixture of two carbene complexes: one with regular binding at C-2 and one with binding at C-4, as shown in Scheme 1.5.[59, 60] This binding motive was coined abnormal binding.

Once the normal or abnormal compounds have formed they do not easily interconvert, even not after prolonged heating in DMSO. IR-spectroscopy data suggest that abnormal C-4 bound NHCs would be substantially stronger electron donors than normal C-2 bound carbenes,[61] which may be beneficial for some catalytic applications. For instance, it was shown that palladium complexes bearing two NHCs (IMes), one in the normal, one in the abnormal binding mode, could be used as active catalysts in C-C coupling reactions.[62] When the two ligands are both in the normal binding mode the catalyst is inactive. Whether the normal or the abnormal complex is obtained depends on the reaction conditions: when cesium carbonate is used as a base, abnormal binding occurs more frequently.

More recently, abnormal NHCs have been observed with other metals, such as rhodium,[63] osmium,[64] and platinum.[65] The abnormal binding of NHC ligands was reviewed in 2007.[66]

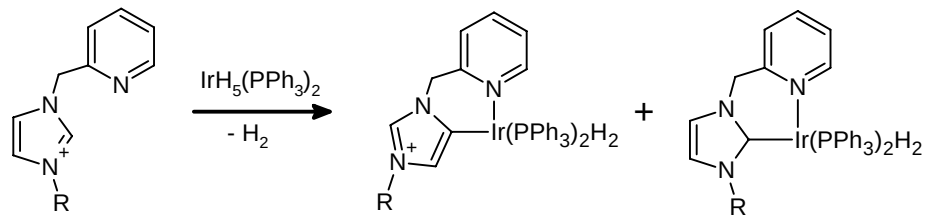

Scheme 1.5. Abnormal binding mode in NHC coordination. BF_4 anions are not shown.

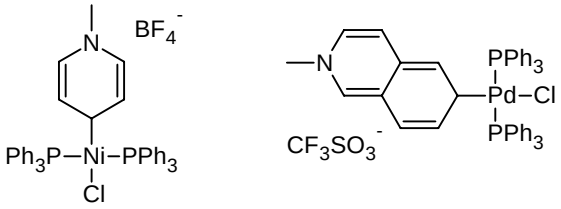

Figure 1.15. Examples of transition metal rNHC complexes.

Remote N-heterocyclic carbenes

A new class of metal NHC complexes was discovered recently, in which the heteroatom is not directly bound to the carbene carbon atom. Even though to date free remote N-heterocyclic carbenes (rNHCs) have not been isolated, a number of rNHC metal complexes have been prepared via oxidative addition of d^{10} metal centers into a suitable carbon-halide bond.[67, 68] Two examples of rNHC metal complexes are depicted in Figure 1.15. A number of rNHC metal complexes have been used in catalytic reactions.[68]

1.4.4 Decomposition pathways

Although NHCs are usually considered to be spectator ligands and some NHC complexes are stable in boiling solvents in air, they are not always inert. Potential decomposition or deactivation pathways are depicted in Scheme 1.6 and include reductive elimination of the carbene with a *cis*-coordinated ligand (**A**),[69] decomplexation or displacement by a competing ligand (**B**),[70] C-H or C-C activation of a substituent (**C**).[71] Another pathway leads to abnormal binding of the carbene ligand (see for example section 1.4.3). The rate of reductive elimination is considered

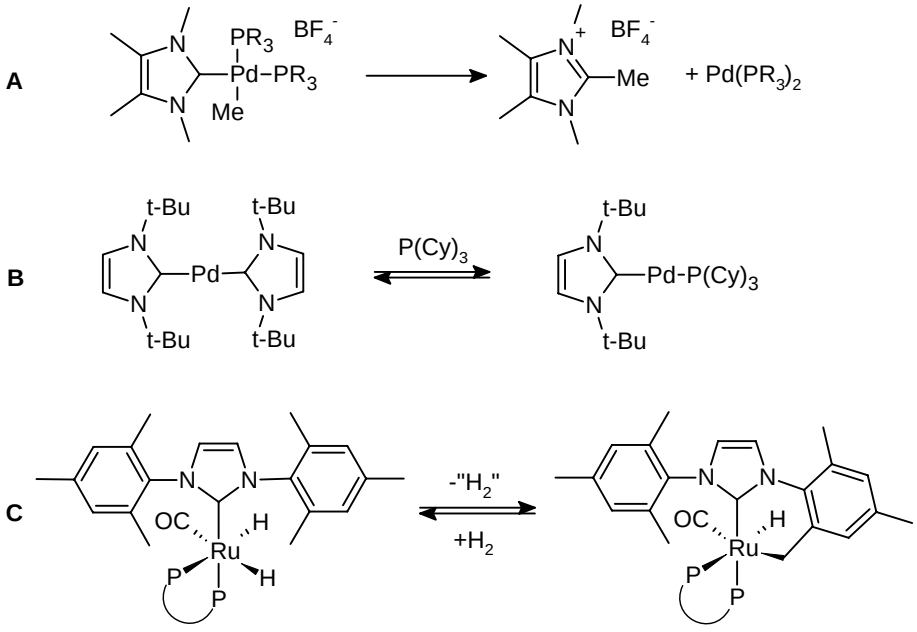

Scheme 1.6. Examples of possible decomposition pathways of NHC complexes.

to be lowered by the use of bidentate ligands, because of restriction of the bite angle.[72]

The imidazol-2-ylidene C=C (back-bone) double bond is relatively inert, possibly because of the aromatic character of the ring. For example, IMes is unchanged when $RhCl(H)_2(IMes)_2$ is used as a catalyst in a hydrogenation reaction. Because catalysts are rarely recovered, it is difficult to say whether imidazol-2-ylidenes remain unsaturated in all cases.

The reactivity of stable NHCs towards O_2, CO, NO and water was reported in 2001.[73] It was shown that 1,3-di-*tert*-butylimidazol-2-ylidene and its saturated analogue were stable towards O_2 and CO. Reactions with NO yielded the C-2 ketone and reactions with water gave the hydrolysis products (*e.g.* R-N=CHCH$_2$-N(CHO)-R). The air sensitivity is therefore due to the attack of water, which in the case of the imidazolin-2-ylidene is very fast. The hydrolysis of the imidazol-2-ylidene requires months to complete. Furthermore, it was reported that in the presence of platinum the imidazol-2-ylidene could be hydrogenated to the corresponding imidazolidine.

The stability and reactivity of NHC complexes was reviewed in 2004.[74]

1.4.5 Chelating N-heterocyclic carbene ligands

Given the successful use of chelating phosphane ligands in transition-metal catalyzed homogeneous catalysis, several studies into the properties of chelating N-heterocyclic carbenes have been undertaken. A 2004 review on chelating NHCs concludes: "In view of the increasing success of monodentate NHCs in catalysis, we can expect a rise in the use of chelating NHCs".[43] Indeed, since then many complexes bearing chelating NHCs have been reported as homogeneous catalysts.[72, 75]

A first advantage of chelating NHCs is the entropically enhanced stability. For example, pincer-type complex **A** (Figure 1.16) can be refluxed for 24 hours in dimethylacetamide (bp 165 °C) in air without decomposition, while bisNHC complex **B** deposits Pd black after 8 hours of reflux in the same solvent.[76] Furthermore, the bridging moiety provides another means of fine-tuning the properties of the complex, by modulation of the bite angle and a more rigid conformation, as shown in Figure 1.17.[75]

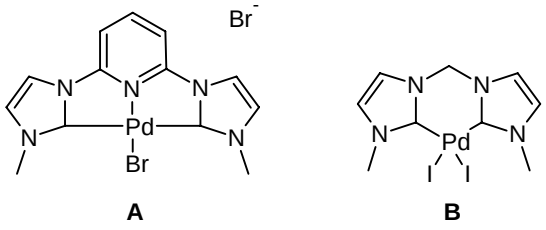

A **B**

Figure 1.16. Palladium complexes of chelating NHC ligands.

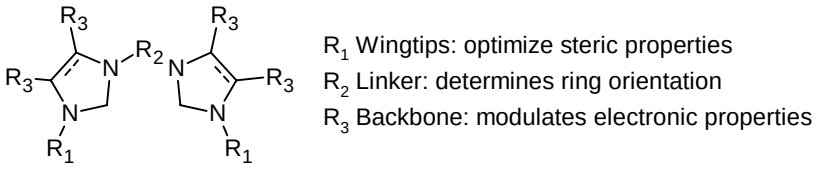

Figure 1.17. Influence of various substituents of chelating N-heterocyclic carbenes on the properties of the corresponding complex. Reproduced from ref. 75.

It has been noted that the effect of the linker on the bite angle of bisNHCs is small, in comparison with bisphosphanes. This is due to rotation of the imidazole rings out of the preferred orientation perpendicular to the coordination plane.

A disadvantage of chelating NHCs may be the irreversible coordination of the NHC to transition metals. Therefore, in some cases care must be taken because of the possibility that a chelating ligand binds monodentately,[77] or that it will bind two metal centers.[78, 79]

The properties of functionalized NHCs were reviewed in 2007,[80] and 2008.[72]

1.4.6 Nickel complexes

Monodentate nickel NHC complexes

The main focus of the research described in this thesis lies on the synthesis and use of nickel complexes of N-heterocyclic carbenes. In this section an overview is given of the most common nickel NHC complexes reported to date.

The first isolated Ni NHC complex was serendipitously synthesized by reaction between DMF and a Ni(SNNS) complex to yield a dinuclear nickel(II) complex bearing two (SCS) pincer-type ligands of a saturated NHC with thiophenolate substituents (Figure 1.18).[81] This complex is highly stable and does not decompose in concentrated H_2SO_4, although strong nucleophiles (Nu), such as PMe_3 are able to react to give mononuclear Ni(SCS)Nu complexes. Two years later the first isolated nickel(0) NHC complex was reported by Arduengo *et al*.[25] Coordination of the free carbene IMes to $Ni(COD)_2$ gave a $Ni(NHC)_2$ species, which was shown to exhibit a nearly linear geometry. The nickel complexes of monodentate NHC ligands isolated since, may be divided into five categories, depicted in Figure 1.19.

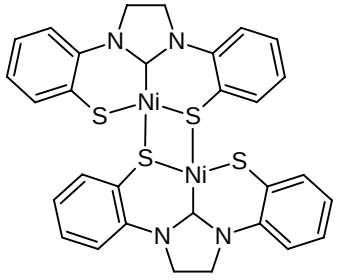

Figure 1.18. The first isolated nickel NHC complex reported in literature.

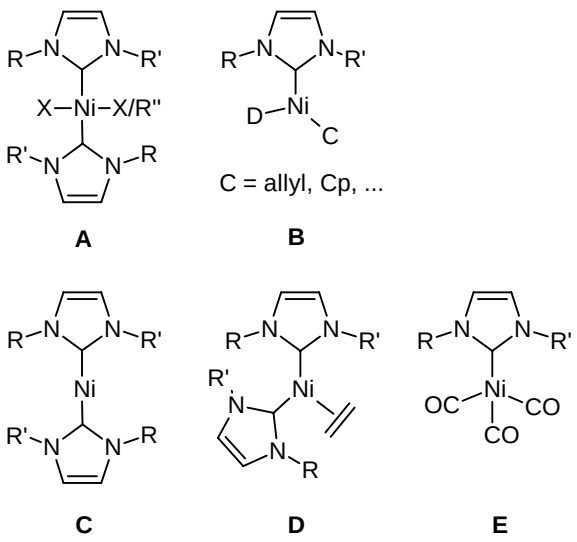

Figure 1.19. Overview of types of nickel complexes with monodentate NHC ligands isolated to date. For clarity, only unsaturated NHCs are shown.

The largest category (**A**) is that of nickel(II) complexes with two monodentate NHCs and two additional anionic groups. In most cases two halides are present, [82-84] but two pseudohalides, such as cyanide, have been used as well.[85] In addition, structures with one halide and one alkyl or aryl substituent on the nickel ion have been isolated.[86] These complexes are the result of oxidative addition of alkyl or aryl halides to the corresponding Ni(0) species. A second type of nickel NHC complex has one monodentate NHC, one anionic carbon-donor moiety, such as cyclopentadienyl,[87] or allyl,[88] and one additional anionic ligand, such as a halide,[87]or a thiophenolate (**B**).[89] The other types comprise Ni(0) NHC species (**C**), the first of which includes Arduengo's $Ni(IMes)_2$ and a $Ni(NHC)_3$ species.[90] Furthermore, some $Ni(0)(NHC)_2$ complexes bearing an additional olefin or alkyne coordinated to the nickel center have been characterized (**D**).[90] The last category of common Ni(0) NHC complexes consists of complexes with the general formula $Ni(NHC)_n(CO)_m$ (**E**). Several combinations of *n* and *m* have been found, depending mainly on the size of the NHC. These complexes were prepared mainly to study the electronic properties of N-heterocyclic carbenes.[50]

Chelating NHC ligands

Nickel complexes bearing polydentate ligands may be divided into two groups: (1) those where all the donor groups are NHCs and (2) those where, next to one NHC other donor groups (P, N, O, S, olefin) are present. Only a few members of the first group were successfully prepared, and are shown in Figure 1.21. Examples are a nickel dihalide complex bearing a cyclophane-based bisNHC,[91] and a nickel dihalide complex of a *trans* chelating bisNHC ligand with a BINOL-derived bridge have been obtained to date.[92] Other nickel complexes bearing one bisNHC include a dimethyl complex Ni(C^C)Me_2,[78] and a cationic complex bearing one bisNHC, one phosphane

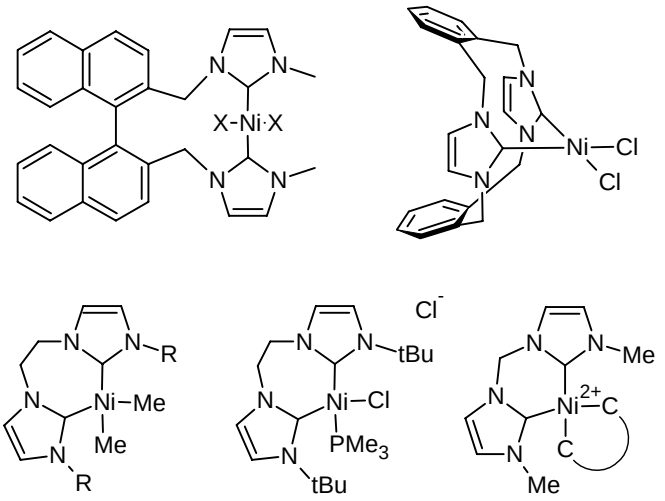

Figure 1.21. Known nickel complexes with chelating bisNHC ligands (C = NHC).

ligand and one halide.[93] Attempts to prepare complexes of the type $Ni(C\hat{}C)_2X_2$, where C^C is a chelating bisNHC in which the two NHCs are linked with one alkyl chain bridge and X is a halide, lead to homoleptic $Ni(C\hat{}C)_2$ complexes,[77, 93, 94] or intractable mixtures.[78] In comparison, palladium dihalide complexes bearing chelating bisNHC ligands are ubiquitous.[95, 96]

The group of nickel complexes with donor-functionalized polydentate ligands mainly consists of compounds with bidentate ligands. Three examples are shown in Figure 1.20. The most common neutral donor moieties are phosphanes,[97] and pyridines,[98, 99] while anionic donor moieties include amido,[100] and phenolato groups.[101-103] Most complexes are obtained as the homoleptic complex with two ligands (**A** or **C**) or the dihalide complex with one chelating ligand (**B**). Recently, some penta- and hexacoordinated nickel complexes with various N-donor functionalized NHC ligands have been reported, as well.[104]

Tridentate NHC ligands are mainly of the pincer type. In addition to the (SCS) pincer-type complexes mentioned before, several others have been reported, for example with a (CNC) donor configuration.[105] Few other tridentate ligands have been investigated, such as a (CNO^-) ligand.[106] As nickel prefers a square planar geometry, an additional donor ligand is required for this type of ligands. To fill all four

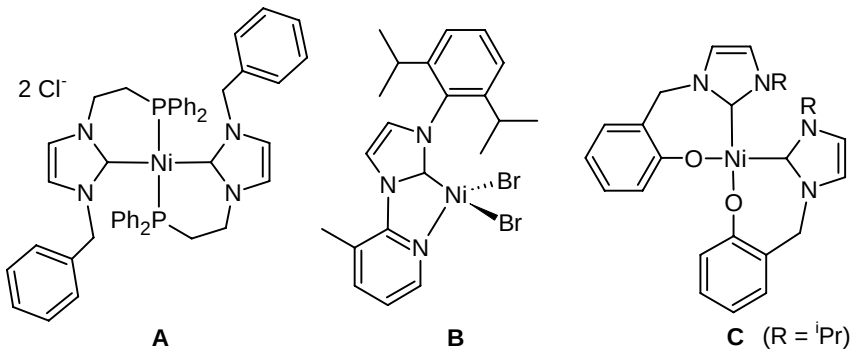

Figure 1.20. Nickel(II) NHC complexes with coordinating pendant arms.

coordination sites a number of tetradentate NHC ligands have been prepared, including a macrocyclic ligand of two NHCs and two pyridines,[107] and ligands consisting of two coupled pyridine functionalized NHCs.[108]

1.5 Synthetic methods

1.5.1 Free carbene

In order to obtain a transition-metal complex of an N-heterocyclic carbene, it is often required to synthesize the NHC in the free state. Three common routes to generate the free carbene are depicted in Scheme 1.7. In this scheme, only unsaturated imidazole rings are shown, although in principle these methods may be used to generate saturated and benzimidazole-based NHCs. Generally, carbenes derived from imidazoles are obtained by deprotonation of the 1,3-disubstituted imidazolium salts. A number of different bases and solvents have been reported in the literature for this reaction. An early example is the use of NaH in THF, sometimes in combination with a catalytic amount of KO^{t}Bu. If the imidazole has base-sensitive substituents more selective bases may be used, such as *sec*-BuLi or KN(SiMe$_3$)$_2$.[2, 93] Alternatively, the carbene may be generated by addition of a base (NaH or KNH$_2$) to a suspension of the imidazolium salt in liquid ammonia. This technique, introduced by Herrmann *et al*.[109] yields the carbene within minutes and was shown to be especially useful for deprotonation of diimidazolium salts. Other methods leading to the free NHC include the desulfurization of imidazol-2-thiones with potassium,[30, 32] and the thermolysis of 2-alkoxy substituted NHC-precursors (Scheme 1.7).[12]

In the case of imidazolin-2-ylidenes and benzimidazol-2-ylidenes, the free NHC may be in equilibrium with its dimeric species, as discussed in section 1.3. Still, the free species may be present long enough to be able to coordinate to a metal center.

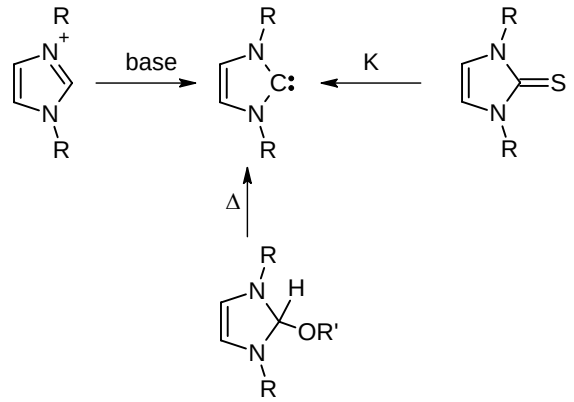

Scheme 1.7. Methods for the generation of a free NHC.

1.5.2 Carbene complexes

Carbene complexes prepared from the free carbene

A number of strategies may be distinguished in the synthesis of coordination complexes with carbenes. The majority of NHC complexes have been obtained by substitution of another ligand on the metal center. The first strategy is to mix a suitable metal ion with a free carbene, as shown in Scheme 1.8, **A**. The free carbene may be obtained by methods discussed in the previous section.

For example, treatment of bis(1,5-cyclooctadienyl)nickel(0) with two equivalents of IMes (1,3-bis(2,4,6-trimethylphenyl)imidazol-2-ylidene) in THF yielding $Ni(IMes)_2$ was reported in 1994.[25] Another example, in which phosphane ligands are replaced by NHCs, has been reported by Herrmann *et al*. in 1997:[110] $NiX_2(PPh_3)_2$ (X = Cl, Br) is reacted with 1,3-dicyclohexylimidazol-2-ylidene (ICy) yielding $NiX_2(ICy)_2$. An example of the synthesis of a coordination complex with a chelating NHC was published by Douthwaite *et al*.:[78] when $Ni(bipy)Me_2$ is reacted with 1,2-ethylene-3,3'-di-*tert*-butyl-diimidazol-2,2'-diylidene at –78 °C the chelating bisNHC ligand replaces the bipy and the complex $[Ni(bisNHC)Me_2]$ is formed.

Alternatively, the carbene may be generated *in situ*, by reaction of the precursor imidazolium salt with an additional external base. For example, a nickel complex with two aryloxo-functionalized NHCs could be prepared by treatment of the ligand precursor salt with $NaN(SiMe_3)_2$ and $Ni(PPh_3)_2Br_2$ in a one-pot procedure.[101]

In the second strategy, an imidazolium salt is deprotonated by reaction with a basic ligand of a suitable metal precursor generating the carbene *in situ* (Scheme 1.8, **B**). An early example of this route is the reaction of $Hg(OAc)_2$ with an imidazolium salt to yield the mercury NHC complex as reported by Wanzlick in 1968.[20]

Nickel NHC complexes may be obtained by reacting $Ni(OAc)_2$ with the imidazolium halide with the loss of acetic acid. This is an example of a reaction in which the carbene is generated *in situ* by a basic metal precursor. In the case that the imidazolium salt has a low melting point, this reaction may even be performed

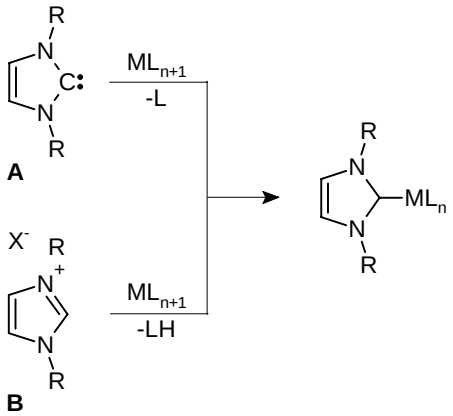

Scheme 1.8. Reactions leading to transition metal carbene complexes.

without solvent.[82] Alternatively, an additional low-melting, non-reactive salt (ionic liquid) may be added, such as tetrabutylammonium halide, to act as the solvent.[83] When the reaction is finished the salt may be removed by washing with water. Alternatively, $Ni(Cp)_2$ (nickelocene) may be used as a metal precursor with a basic ligand, although in this case only one ligand is replaced.[111]

Nickel(0) complexes may be obtained by reaction of the free carbene with a suitable nickel(0) species, such as $Ni(COD)_2$. Alternatively, the nickel(0) NHC species may be obtained by reductive elimination of ethane from the $Ni(NHC)_2Me_2$ complex.[112]

Alternative, less common strategies leading to NHC complexes are discussed below.

Transmetalation: the Ag_2O route

In recent publications, a number of carbene complexes has been obtained *via* a transmetalation procedure.[98, 113-116] First, the silver complex is obtained by a reaction of an imidazolium salt with Ag_2O. Then, the NHC is transferred from the silver atom to another transition metal, as shown in Scheme 1.9.

In a typical example 1,3-dialkylimidazolium halide is reacted with Ag_2O in dichloromethane at room temperature yielding the complex [Ag(imidazol-2-ylidene)$_2$][AgX_2]. This complex is subsequently reacted with $[M(COD)Cl_2]$ or $[MCl_2(MeCN)_2]$ to yield the transition-metal complex. This procedure has already been applied with monodentate imidazole carbene ligands, chelating imidazole-based dicarbene ligands and benzimidazole-based carbenes with transmetalation to transition metals, including Pd, Au, Rh, Ir, and Ni. The molecular structures of silver(I) NHC complexes and their use in transmetalation reactions have been reviewed in 2005 and 2007.[53, 117]

In addition to silver NHC complexes, other agents have been developed for transmetalation reactions. For instance, imidazolium salts were reacted with $LiBEt_3H$ to yield the imidazol-2-ylidene-BEt_3 adduct.[118] In subsequent reactions this BEt_3 could be replaced by BH_3, BF_3, and $Mo(CO)_5$. In addition, complexes of the type $[M(NHC)(CO)_5]$ (M = Cr, Mo, W) may be used as NHC-transfer agents.[119]

The generation of silver(I) NHC complexes and the transmetalation reaction of NHCs from silver(I) complexes to other metals will be discussed in more detail in Chapter 2.

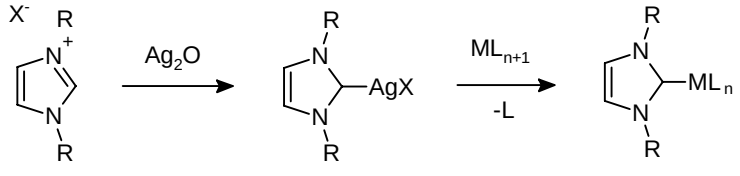

Scheme 1.9. The transmetalation route leading to transition metal NHC complexes.

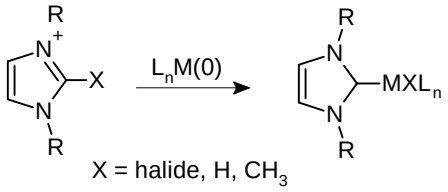

Scheme 1.10. The oxidative insertion of a zerovalent transition-metal complex into a C-X bond.

Oxidative insertion

In the early 1970s the synthesis of several N,S- and N,O-heterocyclic carbene complexes by oxidative addition of a C–Cl bond to suitable Ir, Pd, Pt, and Ni complexes were reported (Scheme 1.10).[120] Later, similar reactions were performed to obtain N-heterocyclic carbene complexes, by oxidative addition of other C–X bonds,[121, 122] In addition, oxidative addition of the C–Cl bond of acyclic carbene precursors to Ni(0) and Pd(0) complexes has been performed.[123]

An example of the oxidative addition of a 2-H imidazolium salt was reported by Clement *et al*. in 2004.[124] It involves the addition of 2-H-1,3-dialkylimidazolium salt (with non-coordinating anions) to coordinatively unsaturated $M(NHC)_2$ complexes (M = Ni, Pd) furnishing a stable $[M(NHC)_3H]^+$ complex.

Insertion into electron rich C=C bonds

Insertion of a coordinatively unsaturated electrophilic metal complex into the C=C bond of bis(imidazolin-2-ylidene)-based electron-rich olefins is one of the early methods for the synthesis of metal NHC complexes and is known as the Lappert method (Scheme 1.11).[41] This method has been applied mainly for unsaturated NHCs and benzimidazole-based carbenes and for a number of metals, including Pt, Ni, Rh, Pd, W, Cr, Co and Fe.[9] In addition the method may be used to obtain metal complexes of chelating bisNHCs by insertion into N,N′-bridged tetraazafulvalenes.[125]

Synthesis by ring closure on the metal

A conceptually different approach towards benzimidazol-2-ylidene complexes was introduced by Hahn *et al*. in 2003. Instead of using a preformed benzimidazole-scaffold, the imidazole ring was closed while the carbene carbon atom precursor was already attached to the metal by starting from the isocyanide complex (Scheme 1.12).[126] This type of template synthesis yields one of the few examples where the N-substituents are protons, which may subsequently be replaced in a substitution

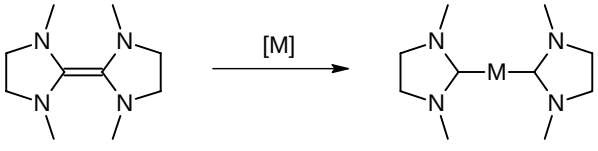

Scheme 1.11. Insertion of a metal fragment into the C=C bond of a tetraazafulvalene.

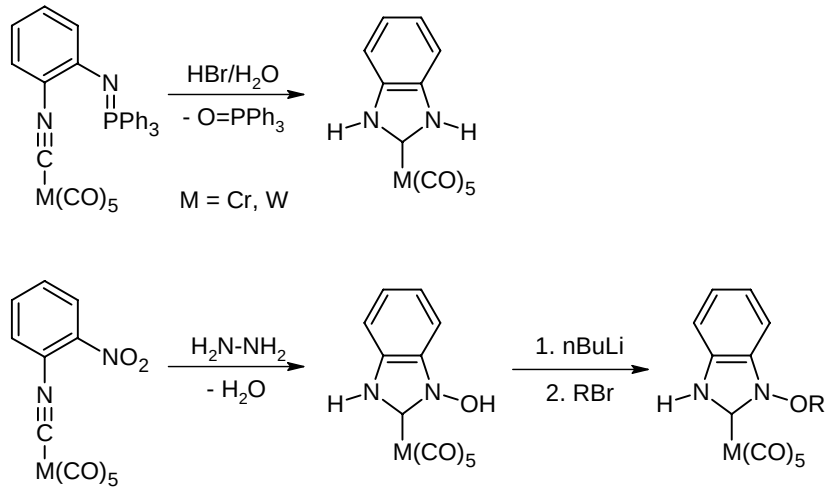

Scheme 1.12. Ring-closing routes towards benzimidazole-based carbene complexes.

reaction. Following a similar scheme, starting from the *o*-NO_2 phenyl isocyanide, an O-R substituted benzimidazol-2-ylidene could be obtained.[127]

1.6 Catalysis

1.6.1 General

In the past few years N-heterocyclic carbenes have been applied in a large variety of research areas. Apart from an interest from a fundamental point of view, NHC complexes have for example been studied as antibiotics (with silver),[128] anticancer drugs (with gold and palladium),[129, 130] and examples of NHCs in building blocks for supramolecular chemistry,[131] and NHC complex polymers are starting to attract attention.[103, 132] It has been shown that a number of reactions may be catalyzed by free NHCs.[133] For example, 1,3-diadamantylimidazol-2-ylidene (IAd) has been shown to catalyze the transesterification of methyl acetate with benzyl alcohol at room temperature,[134] while several other NHCs have been used as ring-opening polymerization catalysts.[135]

The most studied application of NHCs, however, is as a spectator ligand in homogeneous transition-metal catalyzed reactions. Soon after the first isolation of a free NHC, Herrmann *et al*.[136] recognized the potential of this class of compounds, and with the similarity of the electronic properties of phosphane ligands in mind, attempts were made to modify known transition metal catalysts with NHCs. Early successful examples include $Pd(NHC)_2X_2$ complexes in the Heck reaction,[136] Rh(NHC)(COD)Cl complexes in the hydrosilylation of alkenes,[137] $[Pd(C\hat{}C)(MeCN)_2]^{2+}$ complexes in CO/ethylene copolymerization,[138] and $Ru(NHC)_2Cl_2(=CHPh)$ in olefin metathesis.[139] Inspired by these early successes the field of NHC transition-metal catalysis developed rapidly and was already reviewed in 2002.[140]

A number of examples in which a known phosphane-based catalyst is modified by replacing one or more of the phosphane ligands with NHCs have been reported. For example, modifications of Crabtree's catalyst $[Ir(cod)(py)(PCy_3)]PF_6$,[141] Wilkinson's catalyst $[RhCl(PPh_3)_3]$,[142] and Grubbs catalyst $[RuCl_2(PPh_3)_2(=CHPh)]$[139] have been reported. More recently, catalytic reactions which are catalyzed uniquely by transition metal NHC complexes are being disclosed. For instance, the use of nickel NHC complexes for catalytic dehydrogenation of ammonia-borane (H_3N-BH_3) for chemical hydrogen storage was recently published.[143]

Due to the stability of the metal-carbene bond, it is assumed that during the catalytic cycle the carbene ligand remains coordinated to the metal. Therefore, in contrast to metal phosphane catalysts, no excess ligand is needed to bring the catalytic reaction to completion. Often the metal NHC catalyst is introduced into the reaction mixture as a preformed complex, although the use of an *in situ* mixture of free carbene or carbene precursor and a suitable metal complex has been reported, as well. The use of preformed NHC complexes avoids handling of free carbenes, while an *in situ* mixture allows for the ligand to metal ratio to be optimized more easily.

In the following sections the most common NHC-complex catalyzed reactions will be discussed, with an emphasis on nickel and other group 10 transition metals. Two types of reactions that are encountered frequently in literature will be reviewed separately, followed by an overview of less common reactions. The reactions that are regularly reported are C-C coupling reactions with aryl halides and olefin metathesis.

Cross-coupling reactions with aryl halides

The vast majority of studies on NHC transition-metal catalyzed reactions has focused on C-C coupling reactions, with an emphasis on coupling reactions with aryl halides. In most cases palladium is the preferred metal, although in some cases also nickel is used. The most common C-C coupling reactions are shown in Scheme 1.13.[144-146] The successful use of NHCs is mostly due to the thermal stability of the metal-NHC bond, as these coupling reactions often require elevated temperatures and previously studied phosphane complexes suffered from degradation. The use of palladium NHC complexes as catalysts in cross coupling reactions was reviewed in 2008.[4]

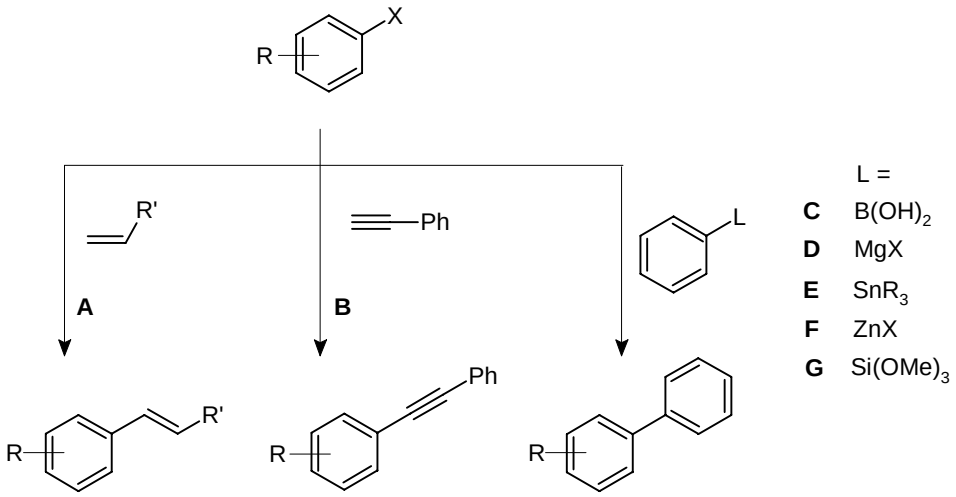

Scheme 1.13. C-C couplings reactions with aryl halides (X = I, Br, Cl): A = Heck reaction, B = Alkyne coupling, C = Suzuki reaction, D = Kumada cross-coupling, E = Stille reaction, F = Negishi coupling, G = siloxane cross-coupling.

Olefin metathesis

A general reaction scheme of olefin metathesis is shown in Scheme 1.14.[147] Homogeneous catalysts for this reaction were devised by Grubbs ($RuCl_2(PCy_3)_2(=CHPh)$)[148] and Schrock ($Mo(OR)_2(=N\text{-}Ar)(=C\text{-}Ar)$).[149] In general, in order to catalyze olefin metathesis a catalyst is needed that has an alkylidene ligand ($=CR_2$) in its active species. A number of metals (Mo, W, Ru, Ta) is known to be able to coordinate alkylidene ligands and to perform these reactions.[147] So far, from these transition metals ruthenium is the only one used in combination with NHC ligands.

Based on the Grubbs-type metathesis catalysts, a number of ruthenium NHC alkylidene complexes were used to perform ring-opening metathesis polymerization (ROMP) and ring-closing metathesis (RCM) reactions.[139] The activity of the known catalyst $RuCl_2(PCy_3)_2(=CHPh)$ was comparable to the activity of the complexes with two IPr ligands instead of phosphanes, leading to high yields in both reactions, although the new complex was found to be more stable. It was reported that a similar complex (second generation Grubbs catalyst) bearing one phosphane ligand (PCy_3) and one SIMes (1,3-bis(2,4,6-trimethylphenyl)imidazolin-2-ylidene) is even more active as metathesis catalyst.[12, 150, 151]

More recently, the O-donor functionalized NHCs were investigated in the ruthenium-catalyzed asymmetric olefin metathesis reactions.[152]

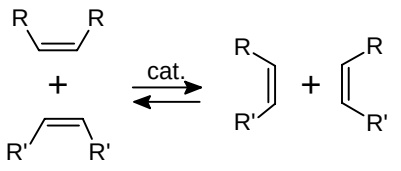

Scheme 1.14. General olefin metathesis reaction.

Other catalytic reactions

Apart from the reactions mentioned in the previous sections, in the literature a large number of reactions has been reported to be catalyzed by transition-metal NHC complexes. As these reactions have not had received a lot of attention, they are not discussed here in detail. Some examples are given in Table 1.2.

Table 1.2. Miscellaneous reactions involving NHC complexes as catalysts.

Reaction	metal center	ref.
Hydrosilylation of alkynes	Rh, Pt	79, 153
Hydrosilylation of ketones	Rh	154
Hydrogenation	Ru, Ir, Pd	155, 141, 156
Furan synthesis	Ru	157
Aryl halide amination	Pd	158
Ethene polymerization	Ti, V, Cr	159, 160
Ethene/CO copolymerization	Pd	138
Hydroformylation	Co, Rh	161, 162
Alkyne coupling	Ru	163
Allylic acetate rearrangement	Au	164
Atom-transfer radical polymerization	Fe	165
Pauson-Khand reaction	Co	166
Hydroamination of olefins	Cu	167

In general, it may be concluded that N-heterocyclic carbenes are versatile ligands capable of stabilizing a variety of metal centers. If an NHC is used as a ligand instead of a phosphane-based ligand a more stable, and often more active catalyst is obtained in a large number of cases.[2]

1.6.2 Nickel NHC complexes in catalysis

Even though palladium is often the transition metal of choice for catalytic applications in C–C cross coupling reactions, the use of nickel-based catalysts still has a number of advantages: nickel often has a higher reactivity towards aryl chlorides, is cheaper than palladium, and is often easier to remove from the final products.[168] Nickel NHC complexes have been used in a variety of catalytic organic transformations. A short overview of common reaction types is given in this section.

Reactions with aryl halides

In section 1.6.1, a number of C–C cross–coupling reactions starting from aryl halides was listed. In addition to the numerous examples of these reactions catalyzed by palladium compounds, several nickel NHC catalysts have been studied, for instance in the Heck,[105] and Negishi[169] cross-couplings. Several efforts were made to catalyze the Suzuki coupling of aryl halides with aryl boronic acids with nickel NHC

complexes. In some cases the addition of phosphanes to the reaction mixture was necessary to reach full conversion,[100, 170] although a recent example avoids this addition by using phosphane-functionalized NHCs.[97] The Kumada cross-coupling has been studied a number of times and will be discussed in Chapter 4-6. In addition to the cross-coupling reactions mentioned before, the cross-coupling of aryltitanium alkoxides (Ar-Ti(OEt)$_3$) with aryl halides, catalyzed by an *in situ* mixture of Ni(acac)$_2$ and IPr·HCl was investigated.[171] It was found that this reaction runs under mild conditions, leading to a broad scope with high functional-group tolerance.

Other reactions starting with aryl halides include the following. Complexes of the type Ni(Cp)(NHC)Cl, which were obtained by reaction of nickelocene (Ni(Cp)$_2$) and bulky imidazol(in)ium halides, were successfully used for the dehalogenation of 4-bromotoluene in the presence of NaO^{i}Pr as a base (Scheme 1.15, **A**).[172] In addition, it was shown that the same complexes could be used for the catalytic aryl amination of aryl halides with morpholine in good yields with KO^{t}Bu as a base and at elevated temperatures (**B**). Benzimidazole-based carbene ligands were used in the nickel catalyzed Ullmann reaction with bromobenzene and 4-bromoanisole in molten tetrabutylammonium bromide to yield symmetric biaryls (**C**).[173] The coupling of aryl chlorides was unsuccessful in this reaction. Nickel(0) complexes bearing two monodentate NHCs could be used for the catalytic aromatic C-S coupling of aryl bromides with thiophenols (**D**),[174] and catalytic C-N coupling of aryl chlorides and with anilines and aryl diamines (**E**).[175]

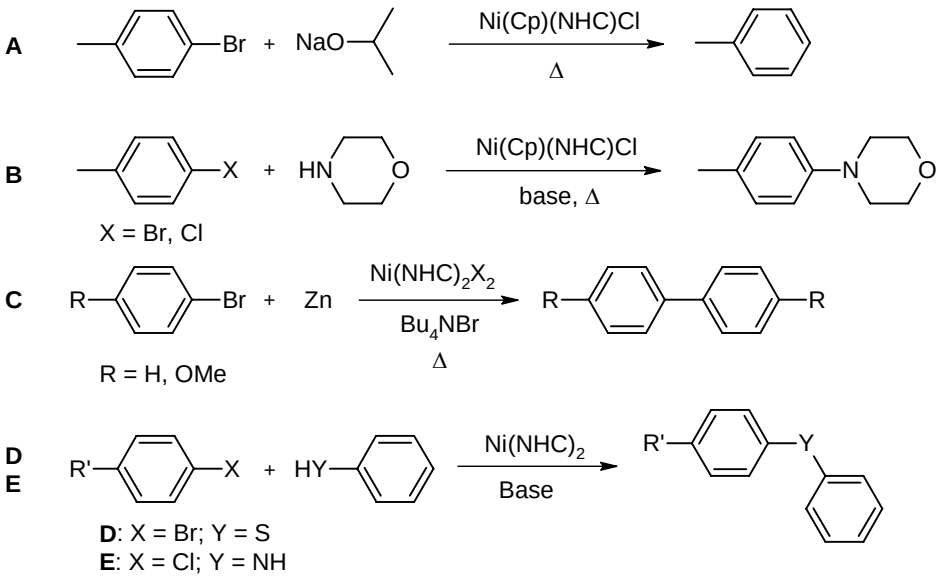

Scheme 1.15. Aryl halide dehalogenation, amination, homocoupling, aryl amination and aryl thioether formation.

Reactions involving double bonds

A number of variations on catalytic reactions involving C–C double and triple bonds have been disclosed. For instance, the nickel-catalyzed coupling of 1,3-dienes and aldehydes with $HSiEt_3$ is shown in Scheme 1.16, **A**.[176] The nickel NHC complex is generated *in situ* by addition of BuLi to a mixture of $NiCl_2$ and imidazolium salt. The (*Z*)-alkene is obtained in moderate to high yield. Interestingly, when a phosphane ligand is used instead of the NHC, the reaction yields the (*E*)-alkene. Jamison *et al.* used an *in situ* mixture of $Ni(COD)_2$ and IPr (1,3-(2,6-diisopropylphenyl)imidazol-2-ylidene) to catalyze the coupling of olefins with aldehydes (**B**)[177] and terminal olefins with isocyanates to yield acrylamides (**C**).[178] Similar conditions were used to couple two isocyanates with alkynes to give pyrimidine diones (**D**).[179] A reaction of diynes with nitriles catalyzed by an *in situ* prepared nickel NHC complex under basic conditions was reported to give a variety of substituted pyridines (**E**, X = $C(CO_2Me)_2$, H_2CCH_2, O, NTs).[180] Vinyl cyclopropanes could successfully be isomerized to the corresponding cyclopentenes by addition of a mixture of a Ni(0) precursor and a

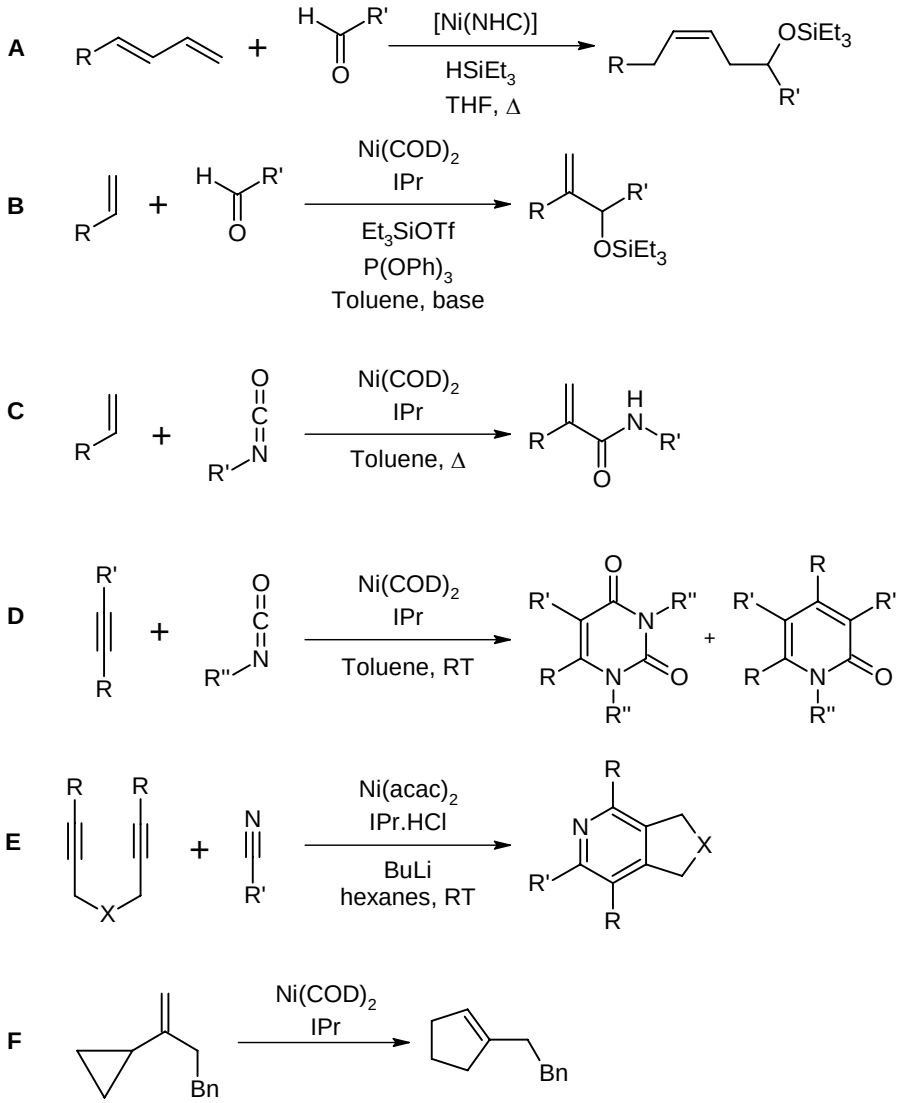

Scheme 1.16. Organic transformations of C-C multiple bonds catalyzed by nickel NHC complexes.

bulky NHC (**F**).[181]

Other reactions with C–C double bonds in which nickel NHC complexes have been studied are for example the polymerization of styrene,[106, 182] and dimerization of ethene.[183, 184] Often in these reaction the Ni(II) is activated by methylaluminoxane ((-O-Al(Me)$_2$-)$_n$).

Two other nickel NHC complex catalyzed reactions involve hydrogen transfer. It was shown that treatment of various imines with NaO^{i}Pr in the presence of catalytic amounts of Ni(0) and IMes yielded the corresponding amines by transfer hydrogenation.[185] A reaction of catalytic amounts of Ni(0) and a triazol-5-ylidene with H_3NBH_3 leads to the rapid production of dihydrogen gas by dehydrogenation,[143] which, interestingly, was shown to proceed through hydrogen transfer of ammonia-borane to the carbene carbon, followed by C-H activation by the nickel species.[186]

The types of homogeneous catalysis under investigation in this thesis will be presented and discussed in the respective chapters.

1.7 Aim and outline of this thesis

The aim of the research described in this thesis has been to synthesize new nickel complexes with chelating N-heterocyclic carbene based ligands and to use these complexes in homogeneous catalysis.

In the current chapter an overview has been given of the chemistry of N-heterocyclic carbenes and their properties, complexes, and applications in homogeneous catalysis. In Chapter 2 the synthesis and solid-state structure of a monodentate NHC silver(I) complex is described and compared to literature. In addition, the silver complex is used to obtain the corresponding nickel NHC complex. The use of nickel(II) complexes of monodentate NHC ligands in the catalytic hydrosilylation of alkynes is discussed in Chapter 3. In the next three chapters investigations into the Kumada cross-coupling of aryl halides and aryl Grignard reagents are presented. The synthesis of nickel complexes bearing chelating benzimidazole-based bisNHC ligands is described in Chapter 4, together with the use of these novel complexes in this catalytic reaction. Nickel complexes bearing chelating NHC ligands with pendant anionic moieties were synthesized and used in the same catalytic reaction, which is described in Chapter 5. An attempt to rationalize the results described in Chapter 4 by using density functional theoretical calculations is discussed in Chapter 6 and includes the calculation of the full catalytic cycle and a possible route leading to the experimentally observed sideproducts. A number of the complexes were also used in the catalytic vinyl polymerization of norbornene, of which the results are presented in Chapter 7. Chapter 8 contains an evaluation and concluding remarks, as well as future prospects. In addition, the microwave-assisted synthesis of diimidazolium salts, which are potential precursors for chelating

biscarbene complexes, and a comparison to conventional syntheses, are briefly discussed in Appendix A.

Parts of this thesis have been published.[187-189]

1.8 References

(1) Doering, W. V. E.; Knox, L. H. *J. Am. Chem. Soc.* **1956**, *78*, 4947.
(2) Herrmann, W. A.; Kocher, C. *Angew. Chem. Int. Ed.* **1997**, *36*, 2163.
(3) Bourissou, D.; Guerret, O.; Gabbai, F. P.; Bertrand, G. *Chem. Rev.* **2000**, *100*, 39.
(4) Kantchev, E. A. B.; O'Brien, C. J.; Organ, M. G. *Angew. Chem. Int. Ed.* **2007**, *46*, 2768.
(5) de Fremont, P.; Marion, N.; Nolan, S. P. *Coord. Chem. Rev.* **2009**, *253*, 862.
(6) Boeda, F.; Nolan, S. P. *Annu. Rep. Prog. Chem., Sect. B* **2008**, *104*, 184.
(7) Hahn, F. E.; Jahnke, M. C. *Angew. Chem. Int. Ed.* **2008**, *47*, 3122.
(8) Weskamp, T.; Bohm, V. P. W.; Herrmann, W. A. *J. Organomet. Chem.* **2000**, *600*, 12.
(9) Lappert, M. F. *J. Organomet. Chem.* **2005**, *690*, 5467.
(10) Arduengo, A. J.; Harlow, R. L.; Kline, M. *J. Am. Chem. Soc.* **1991**, *113*, 361.
(11) SciFinder is a registered trademark of the American Chemical Society.
(12) Scholl, M.; Ding, S.; Lee, C. W.; Grubbs, R. H. *Org. Lett.* **1999**, *1*, 953.
(13) Doering, W. V.; Hoffmann, A. K. *J. Am. Chem. Soc.* **1954**, *76*, 6162.
(14) Hoffmann, R.; Zeiss, G. D.; Vandine, G. W. *J. Am. Chem. Soc.* **1968**, *90*, 1485.
(15) Tomioka, H.; Hattori, M.; Hirai, K.; Murata, S. *J. Am. Chem. Soc.* **1996**, *118*, 8723.
(16) Breslow, R. *J. Am. Chem. Soc.* **1958**, *80*, 3719.
(17) Fischer, E. O.; Maasbol, A. *Angew. Chem. Int. Ed.* **1964**, *3*, 580.
(18) Schrock, R. R. *J. Am. Chem. Soc.* **1974**, *96*, 6796.
(19) Wanzlick, H. W. *Angew. Chem. Int. Ed.* **1962**, *74*, 129.
(20) Wanzlick, H. W.; Schonher.Hj *Angew. Chem. Int. Ed.* **1968**, *7*, 141.
(21) Alder, R. W.; Allen, P. R.; Williams, S. J. *J. Chem. Soc.-Chem. Commun.* **1995**, 1267.
(22) Amyes, T. L.; Diver, S. T.; Richard, J. P.; Rivas, F. M.; Toth, K. *J. Am. Chem. Soc.* **2004**, *126*, 4366.
(23) Magill, A. M.; Cavell, K. J.; Yates, B. F. *J. Am. Chem. Soc.* **2004**, *126*, 8717.
(24) Arduengo, A. J.; Dias, H. V. R.; Harlow, R. L.; Kline, M. *J. Am. Chem. Soc.* **1992**, *114*, 5530.
(25) Arduengo, A. J.; Gamper, S. F.; Calabrese, J. C.; Davidson, F. *J. Am. Chem. Soc.* **1994**, *116*, 4391.
(26) Heinemann, C.; Thiel, W. *Chem. Phys. Lett.* **1994**, *217*, 11.
(27) Jacobsen, H.; Correa, A.; Poater, A.; Costabile, C.; Cavallo, L. *Coord. Chem. Rev.* **2009**, *253*, 687.
(28) Arduengo, A. J.; Bock, H.; Chen, H.; Denk, M.; Dixon, D. A.; Green, J. C.; Herrmann, W. A.; Jones, N. L.; Wagner, M.; West, R. *J. Am. Chem. Soc.* **1994**, *116*, 6641.
(29) Arduengo, A. J.; Goerlich, J. R.; Marshall, W. J. *J. Am. Chem. Soc.* **1995**, *117*, 11027.
(30) Denk, M. K.; Thadani, A.; Hatano, K.; Lough, A. J. *Angew. Chem. Int. Ed.* **1997**, *36*, 2607.
(31) Liu, Y. F.; Lindner, P. E.; Lemal, D. M. *J. Am. Chem. Soc.* **1999**, *121*, 10626.
(32) Hahn, F. E.; Wittenbecher, L.; Boese, R.; Blaser, D. *Chem.-Eur. J.* **1999**, *5*, 1931.
(33) Korotkikh, N. I.; Raenko, G. F.; Pekhtereva, T. M.; Shvaika, O. P.; Cowley, A. H.; Jones, J. N. *Russ. J. Org. Chem.* **2006**, *42*, 1822.
(34) Iglesias, M.; Beetstra, D. J.; Knight, J. C.; Ooi, L. L.; Stasch, A.; Coles, S.; Male, L.; Hursthouse, M. B.; Cavell, K. J.; Dervisi, A.; Fallis, I. A. *Organometallics* **2008**, *27*, 3279.
(35) Weiss, R.; Reichel, S.; Handke, M.; Hampel, F. *Angew. Chem. Int. Ed.* **1998**, *37*, 344.
(36) Glorius, F.; Altenhoff, G.; Goddard, R.; Lehmann, C. *Chem. Commun.* **2002**, 2704.
(37) Despagnet-Ayoub, E.; Grubbs, R. H. *J. Am. Chem. Soc.* **2004**, *126*, 10198.
(38) Krahulic, K. E.; Enright, G. D.; Parvez, M.; Roesler, R. *J. Am. Chem. Soc.* **2005**, *127*, 4142.
(39) Enders, D.; Breuer, K.; Runsink, J.; Teles, J. H. *Liebigs Ann.* **1996**, 2019.
(40) Ofele, K. *J. Organomet. Chem.* **1968**, *12*, 42.

(41) Cardin, D. J.; Cetinkay.B; Lappert, M. F.; Manojlov, L.; Muir, K. W. *Chem. Commun.* **1971**, 400.
(42) Tolman, C. A. *Chem. Rev.* **1977**, *77*, 313.
(43) Peris, E.; Crabtree, R. H. *Coord. Chem. Rev.* **2004**, *248*, 2239.
(44) Radius, U.; Bickelhaupt, F. M. *Organometallics* **2008**, *27*, 3410.
(45) Jacobsen, H.; Correa, A.; Costabile, C.; Cavallo, L. *J. Organomet. Chem.* **2006**, *691*, 4350.
(46) Schwarz, J.; Bohm, V. P. W.; Gardiner, M. G.; Grosche, M.; Herrmann, W. A.; Hieringer, W.; Raudaschl-Sieber, G. *Chem.-Eur. J.* **2000**, *6*, 1773.
(47) Huang, J. K.; Schanz, H. J.; Stevens, E. D.; Nolan, S. P. *Organometallics* **1999**, *18*, 2370.
(48) Hillier, A. C.; Sommer, W. J.; Yong, B. S.; Petersen, J. L.; Cavallo, L.; Nolan, S. P. *Organometallics* **2003**, *22*, 4322.
(49) Dorta, R.; Stevens, E. D.; Hoff, C. D.; Nolan, S. P. *J. Am. Chem. Soc.* **2003**, *125*, 10490.
(50) Dorta, R.; Stevens, E. D.; Scott, N. M.; Costabile, C.; Cavallo, L.; Hoff, C. D.; Nolan, S. P. *J. Am. Chem. Soc.* **2005**, *127*, 2485.
(51) Diez-Gonzalez, S.; Nolan, S. P. *Coord. Chem. Rev.* **2007**, *251*, 874.
(52) Cavallo, L.; Correa, A.; Costabile, C.; Jacobsen, H. *J. Organomet. Chem.* **2005**, *690*, 5407.
(53) Garrison, J. C.; Youngs, W. J. *Chem. Rev.* **2005**, *105*, 3978.
(54) Baba, E.; Cundari, T. R.; Firkin, I. *Inorg. Chim. Acta* **2005**, *358*, 2867.
(55) Gusev, D. G. *Organometallics* **2009**, *28*, 763.
(56) Scott, N. M.; Clavier, H.; Mahjoor, P.; Stevens, E. D.; Nolan, S. P. *Organometallics* **2008**, *27*, 3181.
(57) Penka, E. F.; Schlapfer, C. W.; Atanasov, M.; Albrecht, M.; Daul, C. *J. Organomet. Chem.* **2007**, *692*, 5709.
(58) Arduengo, A. J.; Davidson, F.; Dias, H. V. R.; Goerlich, J. R.; Khasnis, D.; Marshall, W. J.; Prakasha, T. K. *J. Am. Chem. Soc.* **1997**, *119*, 12742.
(59) Crabtree, R. H. *Pure Appl. Chem.* **2003**, *75*, 435.
(60) Grundemann, S.; Kovacevic, A.; Albrecht, M.; Faller, J. W.; Crabtree, R. H. *J. Am. Chem. Soc.* **2002**, *124*, 10473.
(61) Chianese, A. R.; Kovacevic, A.; Zeglis, B. M.; Faller, J. W.; Crabtree, R. H. *Organometallics* **2004**, *23*, 2461.
(62) Lebel, H.; Janes, M. K.; Charette, A. B.; Nolan, S. P. *J. Am. Chem. Soc.* **2004**, *126*, 5046.
(63) Yang, L.; Kruger, A.; Neels, A.; Albrecht, M. *Organometallics* **2008**, *27*, 3161.
(64) Eguillor, B.; Esteruelas, M. A.; Olivan, M.; Puerta, M. *Organometallics* **2008**, *27*, 445.
(65) Bacciu, D.; Cavell, K. J.; Fallis, I. A.; Ooi, L. L. *Angew. Chem. Int. Ed.* **2005**, *44*, 5282.
(66) Arnold, P. L.; Pearson, S. *Coord. Chem. Rev.* **2007**, *251*, 596.
(67) Schuster, O.; Raubenheimer, H. G. *Inorg. Chem.* **2006**, *45*, 7997.
(68) Schneider, S. K.; Rentzsch, C. F.; Krueger, A.; Raubenheimer, H. G.; Herrmann, W. A. *J. Mol. Catal. A-Chem.* **2007**, *265*, 50.
(69) McGuinness, D. S.; Saendig, N.; Yates, B. F.; Cavell, K. J. *J. Am. Chem. Soc.* **2001**, *123*, 4029.
(70) Titcomb, L. R.; Caddick, S.; Cloke, F. G. N.; Wilson, D. J.; McKerrecher, D. *Chem. Commun.* **2001**, 1388.
(71) Chilvers, M. J.; Jazzar, R. F. R.; Mahon, M. F.; Whittlesey, M. K. *Adv. Synth. Catal.* **2003**, *345*, 1111.
(72) Normand, A. T.; Cavell, K. J. *Eur. J. Inorg. Chem.* **2008**, 2781.
(73) Denk, M. K.; Rodezno, J. M.; Gupta, S.; Lough, A. J. *J. Organomet. Chem.* **2001**, *617*, 242.
(74) Crudden, C. M.; Allen, D. P. *Coord. Chem. Rev.* **2004**, *248*, 2247.
(75) Mata, J. A.; Poyatos, M.; Peris, E. *Coord. Chem. Rev.* **2007**, *251*, 841.
(76) Peris, E.; Loch, J. A.; Mata, J.; Crabtree, R. H. *Chem. Commun.* **2001**, 201.
(77) Herrmann, W. A.; Schwarz, J.; Gardiner, M. G. *Organometallics* **1999**, *18*, 4082.
(78) Douthwaite, R. E.; Green, M. L. H.; Silcock, P. J.; Gomes, P. T. *Organometallics* **2001**, *20*, 2611.
(79) Poyatos, M.; Mas-Marza, E.; Mata, J. A.; Sanau, M.; Peris, E. *Eur. J. Inorg. Chem.* **2003**, 1215.
(80) Lee, H. M.; Lee, C. C.; Cheng, P. Y. *Curr. Org. Chem.* **2007**, *11*, 1491.
(81) Sellmann, D.; Prechtel, W.; Knoch, F.; Moll, M. *Organometallics* **1992**, *11*, 2346.

(82) McGuinness, D. S.; Mueller, W.; Wasserscheid, P.; Cavell, K. J.; Skelton, B. W.; White, A. H.; Englert, U. *Organometallics* **2002**, *21*, 175.
(83) Huynh, H. V.; Holtgrewe, C.; Pape, T.; Koh, L. L.; Hahn, E. *Organometallics* **2006**, *25*, 245.
(84) Koziol, A.; Pasynkiewicz, S.; Pietrzykowski, A.; Jerzykiewicz, L. B. *Collect. Czech. Chem. Commun.* **2007**, *72*, 609.
(85) Liu, Q. X.; Xu, F. B.; Li, Q. S.; Song, H. B.; Zhang, Z. Z. *Organometallics* **2004**, *23*, 610.
(86) Schaub, T.; Fischer, P.; Steffen, A.; Braun, T.; Radius, U.; Mix, A. *J. Am. Chem. Soc.* **2008**, *130*, 9304.
(87) Ritleng, V.; Barth, C.; Brenner, E.; Milosevic, S.; Chetcuti, M. J. *Organometallics* **2008**, *27*, 4223.
(88) Dible, B. R.; Sigman, M. S. *Inorg. Chem.* **2006**, *45*, 8430.
(89) Malyshev, D. A.; Scott, N. M.; Marion, N.; Stevens, E. D.; Ananikov, V. P.; Beletskaya, I. P.; Nolan, S. P. *Organometallics* **2006**, *25*, 4462.
(90) Schaub, T.; Backes, M.; Radius, U. *Organometallics* **2006**, *25*, 4196.
(91) Baker, M. V.; Skelton, B. W.; White, A. H.; Williams, C. C. *J. Chem. Soc.-Dalton Trans.* **2001**, 111.
(92) Clyne, D. S.; Jin, J.; Genest, E.; Gallucci, J. C.; RajanBabu, T. V. *Org. Lett.* **2000**, *2*, 1125.
(93) Douthwaite, R. E.; Haussinger, D.; Green, M. L. H.; Silcock, P. J.; Gomes, P. T.; Martins, A. M.; Danopoulos, A. A. *Organometallics* **1999**, *18*, 4584.
(94) Herrmann, W. A.; Schwarz, J.; Gardiner, M. G.; Spiegler, M. *J. Organomet. Chem.* **1999**, *575*, 80.
(95) Ahrens, S.; Zeller, A.; Taige, M.; Strassner, T. *Organometallics* **2006**, *25*, 5409.
(96) Lee, H. M.; Lu, C. Y.; Chen, C. Y.; Chen, W. L.; Lin, H. C.; Chiu, P. L.; Cheng, P. Y. *Tetrahedron* **2004**, *60*, 5807.
(97) Lee, C. C.; Ke, W. C.; Chan, K. T.; Lai, C. L.; Hu, C. H.; Lee, H. M. *Chem.-Eur. J.* **2007**, *13*, 582.
(98) Wang, X.; Liu, S.; Jin, G. X. *Organometallics* **2004**, *23*, 6002.
(99) Winston, S.; Stylianides, N.; Tulloch, A. A. D.; Wright, J. A.; Danopoulos, A. A. *Polyhedron* **2004**, *23*, 2813.
(100) Liao, C. Y.; Chan, K. T.; Chang, Y. C.; Chen, C. Y.; Tu, C. Y.; Hu, C. H.; Lee, H. M. *Organometallics* **2007**, *26*, 5826.
(101) Li, W. F.; Sun, H. M.; Wang, Z. G.; Chen, M. Z.; Shen, Q.; Zhang, Y. *J. Organomet. Chem.* **2005**, *690*, 6227.
(102) Waltman, A. W.; Ritter, T.; Grubbs, R. H. *Organometallics* **2006**, *25*, 4238.
(103) Boydston, A. J.; Rice, J. D.; Sanderson, M. D.; Dykhno, O. L.; Bielawski, C. W. *Organometallics* **2006**, *25*, 6087.
(104) Zhang, X. M.; Lilu, B.; Liu, A. L.; Xie, W. L.; Chen, W. Z. *Organometallics* **2009**, *28*, 1336.
(105) Inamoto, K.; Kuroda, J.; Hiroya, K.; Noda, Y.; Watanabe, M.; Sakamoto, T. *Organometallics* **2006**, *25*, 3095.
(106) Li, W. F.; Sun, H. M.; Chen, M. Z.; Wang, Z. G.; Hu, D. M.; Shen, Q.; Zhang, Y. *Organometallics* **2005**, *24*, 5925.
(107) Baker, M. V.; Skelton, B. W.; White, A. H.; Williams, C. C. *Organometallics* **2002**, *21*, 2674.
(108) Chiu, P. L.; Lai, C. L.; Chang, C. F.; Hu, C. H.; Lee, H. M. *Organometallics* **2005**, *24*, 6169.
(109) Herrmann, W. A.; Kocher, C.; Goossen, L. J.; Artus, G. R. J. *Chem.-Eur. J.* **1996**, *2*, 1627.
(110) Herrmann, W. A.; Gerstberger, G.; Spiegler, M. *Organometallics* **1997**, *16*, 2209.
(111) Abernethy, C. D.; Cowley, A. H.; Jones, R. A. *J. Organomet. Chem.* **2000**, *596*, 3.
(112) Danopoulos, A. A.; Pugh, D. *Dalton Trans.* **2008**, 30.
(113) Wang, H. M. J.; Lin, I. J. B. *Organometallics* **1998**, *17*, 972.
(114) McGuinness, D. S.; Cavell, K. J. *Organometallics* **2000**, *19*, 741.
(115) Chianese, A. R.; Li, X. W.; Janzen, M. C.; Faller, J. W.; Crabtree, R. H. *Organometallics* **2003**, *22*, 1663.
(116) Bonnet, L. G.; Douthwaite, R. E.; Hodgson, R. *Organometallics* **2003**, *22*, 4384.
(117) Lin, I. J. B.; Vasam, C. S. *Coord. Chem. Rev.* **2007**, *251*, 642.
(118) Yamaguchi, Y.; Kashiwabara, T.; Ogata, K.; Miura, Y.; Nakamura, Y.; Kobayashi, K.; Ito, T. *Chem. Commun.* **2004**, 2160.

(119) Liu, S. T.; Reddy, K. R. *Chem. Soc. Rev.* **1999**, *28*, 315.
(120) Fraser, P. J.; Roper, W. R.; Stone, F. G. A. *J. Chem. Soc.-Dalton Trans.* **1974**, 102.
(121) Furstner, A.; Seidel, G.; Kremzow, D.; Lehmann, C. W. *Organometallics* **2003**, *22*, 907.
(122) McGuinness, D. S.; Cavell, K. J.; Yates, B. F.; Skelton, B. W.; White, A. H. *J. Am. Chem. Soc.* **2001**, *123*, 8317.
(123) Kremzow, D.; Seidel, G.; Lehmann, C. W.; Furstner, A. *Chem. Eur. J.* **2005**, *11*, 1833.
(124) Clement, N. D.; Cavell, K. J.; Jones, C.; Elsevier, C. J. *Angew. Chem. Int. Ed.* **2004**, *43*, 1277.
(125) Hahn, F. E.; von Fehren, T.; Wittenbecher, L.; Frohlich, R. *Z. Naturforsch.(B)* **2004**, *59*, 541.
(126) Hahn, F. E.; Langenhahn, V.; Meier, N.; Lugger, T.; Fehlhammer, W. P. *Chem.-Eur. J.* **2003**, *9*, 704.
(127) Hahn, F. E.; Plumed, C. G.; Munder, M.; Lugger, T. *Chem.-Eur. J.* **2004**, *10*, 6285.
(128) Kascatan-Nebioglu, A.; Panzner, M. J.; Tessier, C. A.; Cannon, C. L.; Youngs, W. J. *Coord. Chem. Rev.* **2007**, *251*, 884.
(129) Horvath, U. E. I.; Bentivoglio, G.; Hummel, M.; Schottenberger, H.; Wurst, K.; Nell, M. J.; van Rensburg, C. E. J.; Cronje, S.; Raubenheimer, H. G. *New J. Chem.* **2008**, *32*, 533.
(130) Ray, S.; Mohan, R.; Singh, J. K.; Samantaray, M. K.; Shaikh, M. M.; Panda, D.; Ghosh, P. *J. Am. Chem. Soc.* **2007**, *129*, 15042.
(131) Han, Y.; Huynh, H. V.; Tan, G. K. *Organometallics* **2007**, *26*, 6447.
(132) Boydston, A. J.; Williams, K. A.; Bielawski, C. W. *J. Am. Chem. Soc.* **2005**, *127*, 12496.
(133) Enders, D.; Niemeier, O.; Henseler, A. *Chem. Rev.* **2007**, *107*, 5606.
(134) Grasa, G. A.; Kissling, R. M.; Nolan, S. P. *Org. Lett.* **2002**, *4*, 3583.
(135) Kamber, N. E.; Jeong, W.; Waymouth, R. M.; Pratt, R. C.; Lohmeijer, B. G. G.; Hedrick, J. L. *Chem. Rev.* **2007**, *107*, 5813.
(136) Herrmann, W. A.; Elison, M.; Fischer, J.; Kocher, C.; Artus, G. R. J. *Angew. Chem. Int. Ed.* **1995**, *34*, 2371.
(137) Hill, J. E.; Nile, T. A. *J. Organomet. Chem.* **1977**, *137*, 293.
(138) Gardiner, M. G.; Herrmann, W. A.; Reisinger, C. P.; Schwarz, J.; Spiegler, M. *J. Organomet. Chem.* **1999**, *572*, 239.
(139) Weskamp, T.; Schattenmann, W. C.; Spiegler, M.; Herrmann, W. A. *Angew. Chem. Int. Ed.* **1998**, *37*, 2490.
(140) Herrmann, W. A. *Angew. Chem. Int. Ed.* **2002**, *41*, 1291.
(141) Lee, H. M.; Jiang, T.; Stevens, E. D.; Nolan, S. P. *Organometallics* **2001**, *20*, 1255.
(142) Grasa, G. A.; Moore, Z.; Martin, K. L.; Stevens, E. D.; Nolan, S. P.; Paquet, V.; Lebel, H. *J. Organomet. Chem.* **2002**, *658*, 126.
(143) Keaton, R. J.; Blacquiere, J. M.; Baker, R. T. *J. Am. Chem. Soc.* **2007**, *129*, 1844.
(144) Herrmann, W. A.; Reisinger, C. P.; Spiegler, M. *J. Organomet. Chem.* **1998**, *557*, 93.
(145) Bohm, V. P. W.; Weskamp, T.; Gstottmayr, C. W. K.; Herrmann, W. A. *Angew. Chem. Int. Ed.* **2000**, *39*, 1602.
(146) Herrmann, W. A.; Bohm, V. P. W.; Gstottmayr, C. W. K.; Grosche, M.; Reisinger, C. P.; Weskamp, T. *J. Organomet. Chem.* **2001**, *617*, 616.
(147) Furstner, A. *Angew. Chem. Int. Ed.* **2000**, *39*, 3013.
(148) Nguyen, S. T.; Grubbs, R. H.; Ziller, J. W. *J. Am. Chem. Soc.* **1993**, *115*, 9858.
(149) Schrock, R. R.; Murdzek, J. S.; Bazan, G. C.; Robbins, J.; Dimare, M.; Oregan, M. *J. Am. Chem. Soc.* **1990**, *112*, 3875.
(150) Huang, J. K.; Stevens, E. D.; Nolan, S. P.; Petersen, J. L. *J. Am. Chem. Soc.* **1999**, *121*, 2674.
(151) Furstner, A.; Thiel, O. R.; Ackermann, L.; Schanz, H. J.; Nolan, S. P. *J. Org. Chem.* **2000**, *65*, 2204.
(152) Van Veldhuizen, J. J.; Gillingham, D. G.; Garber, S. B.; Kataoka, O.; Hoveyda, A. H. *J. Am. Chem. Soc.* **2003**, *125*, 12502.
(153) Poyatos, M.; Maisse-Francois, A.; Bellemin-Laponnaz, S.; Gade, L. H. *Organometallics* **2006**, *25*, 2634.

(154) Duan, W. L.; Shi, M.; Rong, G. B. *Chem. Commun.* **2003**, 2916.
(155) Lee, H. M.; Smith, D. C.; He, Z. J.; Stevens, E. D.; Yi, C. S.; Nolan, S. P. *Organometallics* **2001**, *20*, 794.
(156) Sprengers, J. W.; Wassenaar, J.; Clement, N. D.; Cavell, K. J.; Elsevier, C. J. *Angew. Chem. Int. Ed.* **2005**, *44*, 2026.
(157) Kucukbay, H.; Cetinkaya, B.; Guesmi, S.; Dixneuf, P. H. *Organometallics* **1996**, *15*, 2434.
(158) Grasa, G. A.; Viciu, M. S.; Huang, J. K.; Nolan, S. P. *J. Org. Chem.* **2001**, *66*, 7729.
(159) Aihara, H.; Matsuo, T.; Kawaguchi, H. *Chem. Commun.* **2003**, 2204.
(160) McGuinness, D. S.; Gibson, V. C.; Steed, J. W. *Organometallics* **2004**, *23*, 6288.
(161) van Rensburg, H.; Tooze, R. P.; Foster, D. F.; Slawin, A. M. Z. *Inorg. Chem.* **2004**, *43*, 2468.
(162) Chen, A. C.; Ren, L.; Decken, A.; Crudden, C. M. *Organometallics* **2000**, *19*, 3459.
(163) Baratta, W.; Herrmann, W. A.; Rigo, P.; Schwarz, J. *J. Organomet. Chem.* **2000**, *594*, 489.
(164) de Fremont, P.; Marion, N.; Nolan, S. P. *J. Organomet. Chem.* **2009**, *694*, 551.
(165) Louie, J.; Grubbs, R. H. *Chem. Commun.* **2000**, 1479.
(166) Gibson, S. E.; Johnstone, C.; Loch, J. A.; Steed, J. W.; Stevenazzi, A. *Organometallics* **2003**, *22*, 5374.
(167) Munro-Leighton, C.; Delp, S. A.; Blue, E. D.; Gunnoe, T. B. *Organometallics* **2007**, *26*, 1483.
(168) Tucker, C. E.; de Vries, J. G. *Top. Catal.* **2002**, *19*, 111.
(169) Xi, Z. X.; Zhou, Y. B.; Chen, W. Z. *J. Org. Chem.* **2008**, *73*, 8497.
(170) Xi, Z. X.; Zhang, X. M.; Chen, W. Z.; Fu, S. Z.; Wang, D. Q. *Organometallics* **2007**, *26*, 6636.
(171) Manolikakes, G.; Dastbaravardeh, N.; Knochel, P. *Synlett* **2007**, 2077.
(172) Kelly, R. A.; Scott, N. M.; Diez-Gonzalez, S.; Stevens, E. D.; Nolan, S. P. *Organometallics* **2005**, *24*, 3442.
(173) Huynh, H. V.; Wong, L. R.; Ng, P. S. *Organometallics* **2008**, *27*, 2231.
(174) Zhang, Y. G.; Ngeow, K. C.; Ying, J. Y. *Org. Lett.* **2007**, *9*, 3495.
(175) Kuhl, S.; Fort, Y.; Schneider, R. *J. Organomet. Chem.* **2005**, *690*, 6169.
(176) Sato, Y.; Sawaki, R.; Mori, M. *Organometallics* **2001**, *20*, 5510.
(177) Ho, C. Y.; Jamison, T. F. *Angew. Chem. Int. Ed.* **2007**, *46*, 782.
(178) Schleicher, K. D.; Jamison, T. F. *Org. Lett.* **2007**, *9*, 875.
(179) Duong, H. A.; Louie, J. *Tetrahedron* **2006**, *62*, 7552.
(180) Tekavec, T. N.; Louie, J. *J. Org. Chem.* **2008**, *73*, 2641.
(181) Zuo, G.; Louie, J. *Angew. Chem. Int. Ed.* **2004**, *43*, 2277.
(182) Campora, J.; de la Tabla, L. O.; Palma, P.; Alvarez, E.; Lahoz, F.; Mereiter, K. *Organometallics* **2006**, *25*, 3314.
(183) Li, W. F.; Sun, H. M.; Chen, M. Z.; Shen, Q.; Zhang, Y. *J. Organomet. Chem.* **2008**, *693*, 2047.
(184) MacKinnon, A. L.; Baird, M. C. *J. Organomet. Chem.* **2003**, *683*, 114.
(185) Kuhl, S.; Schneider, R.; Fort, Y. *Organometallics* **2003**, *22*, 4184.
(186) Yang, X. Z.; Hall, M. B. *J. Am. Chem. Soc.* **2008**, *130*, 1798.
(187) Berding, J.; Kooijman, H.; Spek, A. L.; Bouwman, E. *J. Organomet. Chem* **2009**, *694*, 2217.
(188) Berding, J.; Lutz, M.; Spek, A. L.; Bouwman, E. *Organometallics* **2009**, *28*, 1845.
(189) Berding, J.; van Dijkman, T. F.; Lutz, M.; Spek, A. L.; Bouwman, E. *Dalton Trans.* **2009**, 6948.

Chapter 2

Another silver complex of 1,3-dibenzylimidazol-2-ylidene: structure and reactivity[†]

Abstract. *The reaction of 1,3-dibenzylimidazolium bromide ($Bn_2Im{\cdot}HBr$) with silver(I) oxide yields the dinuclear compound $\{(Bn_2Im)AgBr\}_2$, as determined with X-ray crystallography. The structure turned out to differ significantly from the mononuclear complex $(Bn_2Im)_2AgBr$ that was reported during the current study. It appears that the kind of structure is the result of different crystallization conditions. A new classification of solid-state structures of these and other silver(I) complexes containing monodentate N-heterocyclic carbenes is presented. The silver complex was used to synthesize the novel compound trans-$[(Bn_2Im)_2NiBr_2]$.*

[†] Based on: J. Berding, H. Kooijman, A. L. Spek, E. Bouwman, *J. Organomet. Chem.*, **2009**, *694*, 2217.

2.1 Introduction

In recent years the study and application of N-heterocyclic carbenes (NHCs) has increased rapidly, most notably as spectator ligands in various homogeneous catalysts.[1] As these ligands are strong σ-donors, they form stable transition-metal NHC complexes with strong metal-carbon bonds. Many synthetic methods leading to these useful carbene complexes have been investigated. One of these methods is the generation of a silver(I) NHC complex, followed by transfer of the carbene to another transition metal.[2] Such a reaction has successfully been applied to a variety of metals, including rhodium, iridium, gold, palladium, and nickel,[2] and may lead to NHC complexes that cannot be obtained via other synthetic routes, such as the addition of the free carbene to a metal salt. Furthermore, Ag NHC complexes have been used as catalysts,[3, 4] and as antimicrobial agent.[5]

Three common approaches toward the synthesis of Ag NHC complexes are: (1) the reaction of a free NHC with silver salts, (2) the reaction of azolium salts with silver salts under basic phase-transfer conditions and (3) the reaction of azolium salts with silver bases. The latter method, in which Ag_2O is used as a base (Equation 1) is now by far the most commonly employed.[2] Soon after the first report in 1998,[6] the Ag_2O route was recognized for its attractive features, such as its stability towards air and the tolerance towards other reactive hydrogen atoms.

$$2\ NHC{\cdot}HX + Ag_2O \rightarrow 2\ (NHC)AgX + H_2O \qquad (1)$$

During the research described in this thesis attempts have been made to prepare nickel(II)-NHC complexes with the aid of silver(I) NHC intermediates. During these studies the unusual structure of $[(NHC)_2AgBr]$, in which NHC is 1,3-dibenzylimidazol-2-ylidene, was reported,[7] whereas with the same NHC and the same synthetic procedure the current study resulted in the isolation of the compound $\{(NHC)AgBr\}_2$. In this chapter, the synthesis and crystal structure of this compound is reported, including an attempt to rationalize the formation of the different complexes. Moreover, the subsequent transmetalation of the carbene from silver(I) to nickel(II) is described.

2.2 Results and Discussion

2.2.1 Synthesis of the silver complex

The ligand precursor 1,3-dibenzylimidazolium bromide ($Bn_2Im{\cdot}HBr$, **1**) was obtained by the alkylation of *N*-benzylimidazole with benzyl bromide in hot 1,4-dioxane. In accordance with the general reaction for the generation of silver-NHC complexes (Equation 1) and the literature procedure,[7] **1** was reacted with 0.5 equivalents of silver(I) oxide in dichloromethane. This reaction yielded an off-white solid product, which was assumed to be compound **2** (Scheme 2.1).[7] The ^1H NMR

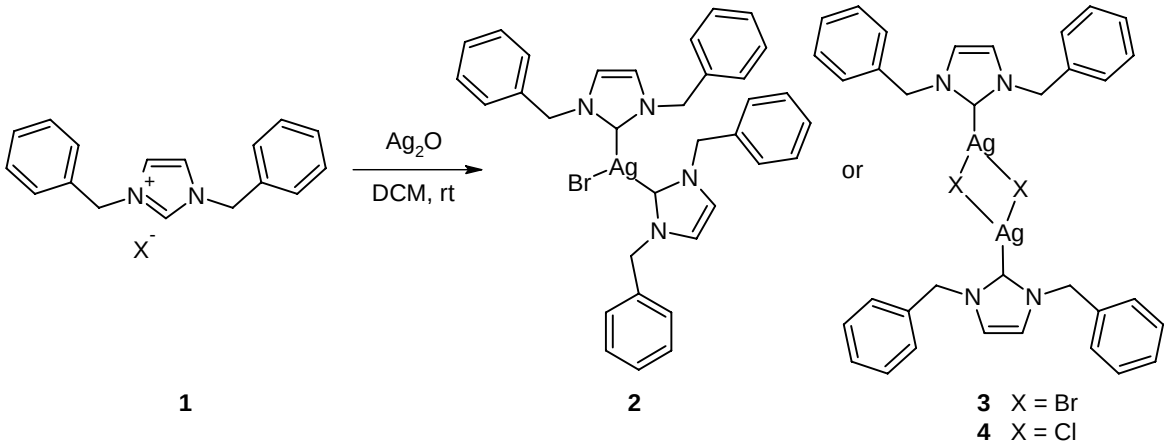

Scheme 2.1. Reaction of imidazolium halide with Ag_2O, yielding **2** or **3**(**4**).

spectrum of this solid product in CD_2Cl_2 lacked the downfield NCHN signal, indicating successful carbene formation, while the ^{13}C NMR spectrum showed the Ag-C resonance at 182 ppm. No ^{13}C–$^{107/109}Ag$ coupling was observed, consistent with the fluxional behavior known for other Ag(I) NHC complexes.[6] The elemental analysis, however, revealed a clear 1:1:1 ligand to silver to bromide ratio, in disagreement with the reported structure **2**. To elucidate the identity of this new compound **3**, its solid-state structure was determined.

2.2.2 X-ray crystal structure determination of the silver complex 3

Single crystals suitable for X-ray diffraction were obtained by slow diffusion of diethyl ether into a chloroform solution of the silver compound at room temperature. The complex has a dinuclear solid-state structure (**3**), as depicted in Figure 2.1. In the structure of **3**, two (Bn_2Im)AgBr moieties are present around an inversion center to give a dinuclear species with, in addition to the end-on Ag–Br bond, side-on Ag…Br interaction. The Ag_2Br_2 4-membered ring is planar with an Ag–Ag distance of 4.0296(6) Å. The two bridging bromide ions are asymmetrically bound with Ag–Br distances of 2.4913(5) and 3.0415(5) Å. The Ag1–C2 distance is comparable to those in other silver-carbene complexes.[8] The silver center is shifted slightly out of the trigonal [CBr_2] coordination plane, while the plane through the imidazole ring is rotated with respect to the Ag_2Br_2-plane by 36.82(12)°. A weak stacking interaction of the aromatic phenyl side groups is observed in the crystal structure with a center-to-center distance of 3.90 Å, with the center of one ring directly above the quaternary carbon of the other ring (Figure 2.2). Several similar {(NHC)AgX}$_2$ structures have been reported in literature (see below).

Apart from the mononuclear compound **2,** in which two NHC ligands are bound to one silver ion (Scheme 2.1), Newman *et al.*[7] obtained the dinuclear {(Bn_2Im)AgCl}$_2$ (**4**) with a structure similar to **3**, with only minor differences in bond

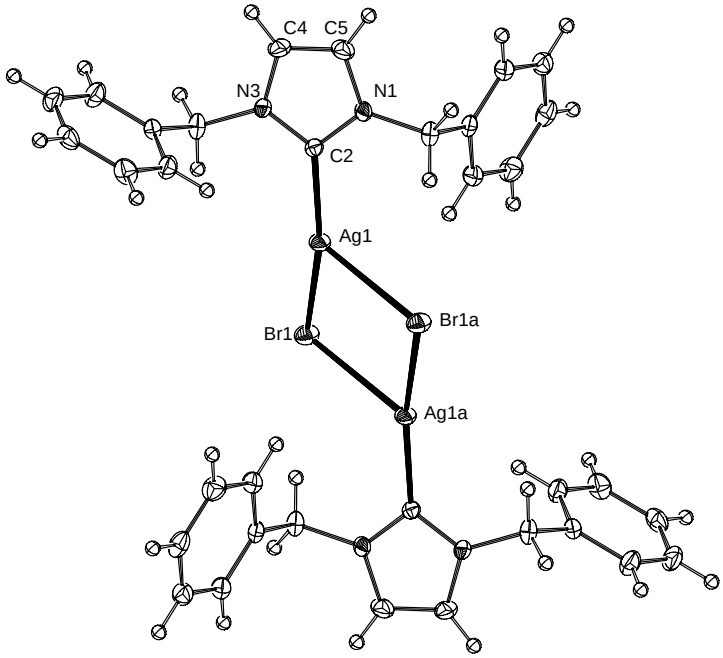

Figure 2.1. ORTEP projection of **3** with displacement ellipsoids drawn at the 50% probability level. The molecule is located at a crystallographic inversion centre. Symmetry transformation used to generate equivalent atoms: –x, 1–y, 1–z. Selected bond distances (Å) and angles (°): Ag1–C2 2.102(2); Ag1–Br1 2.4913(5); Ag1–Br1a 3.0415(5); N1–C2 1.355(3); N3–C2 1.471(4); C4–C5 1.349(4); Ag1–Ag1a 4.0296(6); Br1–Ag1–C2 159.30(6); Br1a–Ag1–C2 112.77(6); Br1–Ag1–Br1a 87.05(2); Ag1–Br1–Ag1a 92.95(2); N1–C2–N3 104.21(18).

lengths and angles; e.g., the carbene–silver distances are 2.090(2) and 2.102(2) Å, respectively. Only the distance between the silver center and the closest halide is significantly different due to the different van der Waals radii of Br^- and Cl^-. The two silver-carbene bond lengths in **2** of 2.116(4) and 2.117(4) Å are slightly longer than those in **3**. The silver-bromide distance of 2.89 Å in **2** is intermediate between the two

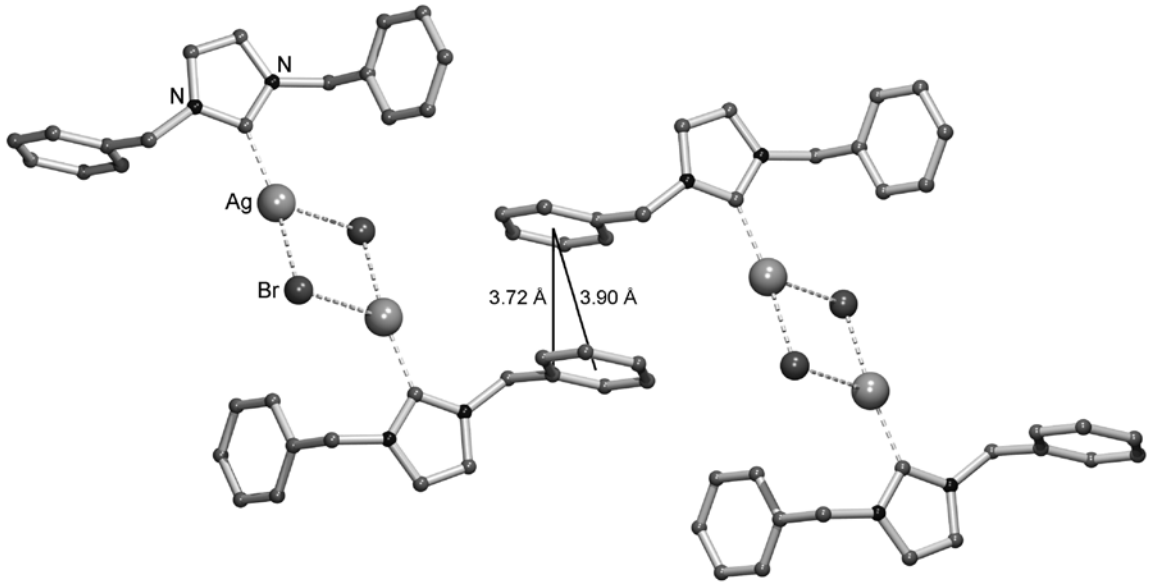

Figure 2.2. Stacking interaction in the solid-state structure of **3**.

Ag-Br distances in **3** and it was suggested that **2** is better described as ionic complex $[(NHC)_2Ag]^+Br^-$.[7] A silver chloride complex containing the ligand 1,3-bis(2-pyridylmethyl)imidazol-2-ylidene does indeed yield the ionic complex $[L_2Ag]^+Cl^-$ in which two silver ions are in close contact (Ag–Ag = 3.65 Å).[9]

2.2.3 NMR studies

Two distinct solid-state structures of silver halide complexes with the ligand Bn_2Im were described in the previous section. It was decided to investigate the structures of these compounds in solution. An attempt was undertaken to monitor the formation of the silver complex in solution. Thus, a 2:1 mixture of **1** and Ag_2O was taken into deuterated dichloromethane and the NMR spectrum of the mixture was recorded within 5 minutes. This spectrum already showed full conversion of the ligand precursor to the silver complex. Repeating this procedure with spectra measured at 243 K allowed for the reaction to be monitored. However, no peaks other than those of the precursor and a single silver complex could be observed in the ^1H and ^{13}C NMR spectra (the latter shown in Figure 2.3). After full conversion was reached, the ^1H and ^{13}C NMR spectra were found to be identical to spectra of

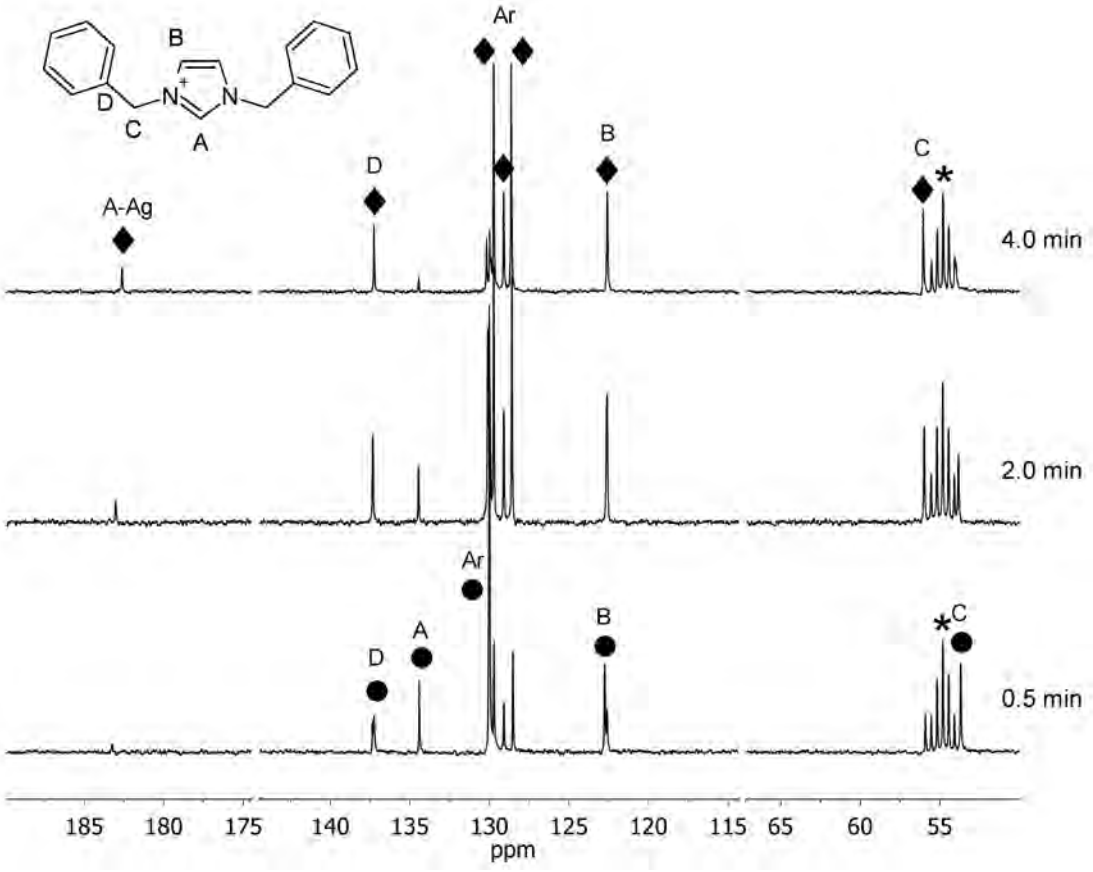

Figure 2.3. Synthesis of **3** in CD_2Cl_2, followed by ^{13}C NMR spectroscopy at 243 K. The time indicated is the reaction time at room temperature. Peaks have been assigned as the starting material (●), the product (♦) and the residual solvent (*).

complex **3**. After standing in the dark for several hours, colorless crystals formed in the NMR tube. Elemental analysis of these crystals revealed a 1:1 ligand to silver ratio, consistent with **3**. Some of the crystals were redissolved in CD_2Cl_2, and the NMR spectra confirmed that the crystals are identical to the bulk compound in solution. Repetition of the NMR experiment in deuterated DMSO yielded comparable ^{1}H and ^{13}C NMR spectra.

A silver complex with the non-coordinating anion tetraphenylborate (BPh_4^-) was also prepared. The required ligand precursor $Bn_2Im{\cdot}HBPh_4$ (**5**) was obtained by anion exchange of $Bn_2Im{\cdot}HCl$ and $NaBPh_4$ in dichloromethane. It is presumed that the ionic complex $[(Bn_2Im)_2Ag]BPh_4$ (**6**) is formed by subsequent reaction of **5** with Ag_2O. This complex was prepared in hot DMSO, as the reaction did not proceed well in dichloromethane. The ^{13}C NMR spectrum shows an unresolved doublet at 180 ppm, with a separation of about 190 Hz, consistent with coupling constants reported for other ionic Ag(I) NHC complexes.[10] The fact that this ionic species exhibits Ag–C coupling, while compound **3** does not, is in agreement with compound **3** being a non-ionic species in solution.

The ^{13}C NMR spectrum of the chloride complex **4** is reported to show an Ag–C resonance at 151 ppm.[7] However, repeating the kinetic NMR study described above for the reaction between $Bn_2Im{\cdot}HCl$ and Ag_2O, the Ag–C signal was observed as a singlet at 181 ppm. Therefore it is concluded that, in our experiments, the solution structures of silver complexes obtained from $Bn_2Im{\cdot}HCl$ and $Bn_2Im{\cdot}HBr$ are very similar, in contrast to what has been reported earlier.

The mass spectra of **3** and the crystals obtained from the NMR experiment described above both show one peak at *m*/*z* 605, indicating a $[(Bn_2Im)_2Ag]^+$ moiety. It has been shown, however, that mass spectrometry cannot be used to unambiguously distinguish (ligand)AgX from $[Ag(ligand)_2]^+$,[11] as is confirmed by the present studies.

2.2.4 Structural considerations

In a recent review seven types of solid-state structures obtained from the reaction between Ag_2O and monodentate azolium salts have been described.[2] For the current discussion, another classification is proposed, shown in Figure 2.4.[12]

Structure types **A** and $\mathbf{A_n}$ (n = 2, 3, …) are characterized by a 1:1 ligand to silver ratio and coordination of both the ligand and the halide to the same metal center. Structure types **B** and $\mathbf{B_2}$ show the same ratio; however, in this case two ligands and two halides are bound separately over two metal centers. Structure types **C**, **C′** and $\mathbf{C'_2}$ have a ligand to silver ratio of 2:1.

The solid-state structure of a silver NHC complex will depend heavily on the nature of the ligand (type of NHC, bulk of ligand and functional groups), the halide, the solvent and the temperature. For instance, imidazole- and benzimidazole-based

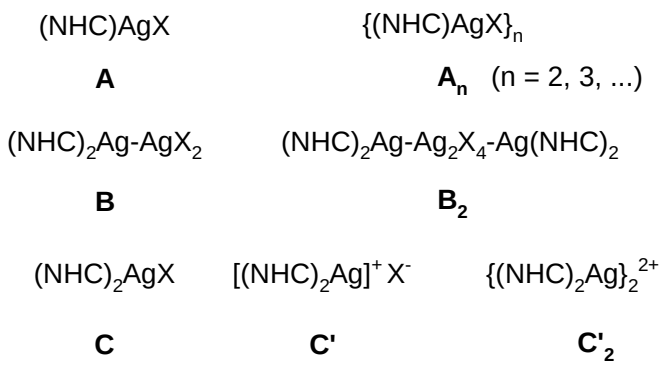

Figure 2.4. Classification of various silver NHC species discussed in this chapter.

carbenes with short alkyl-chain substituents yield complexes of type **B** in the solid state,[6, 13] while those bearing long alkyl chains often result in complexes of type $\mathbf{A_2}$.[14] The exact geometry of this dimer $\mathbf{A_2}$ can vary and a number of different structures has been reported, including the Ag_2X_2 4-membered ring of **3** and **4** and a dimer formed by Ag-Ag interaction.[8, 15] A study to determine the influence of the solvent showed that an increase in solvent polarity shifts the solution equilibrium from **A** to **B** for (IMes)AgCl (IMes = 1,3-bis(2,4,6-trimethylphenyl)imidazol-2-ylidene).[8] Coordination polymers derived from **A** ($\mathbf{A_n}$, n > 3) and dimers derived from **B** ($\mathbf{B_2}$) have been reported in the solid state, but in solution they are most likely in equilibrium with **A** and **B**.[3, 13, 16, 17] The 1,3-bis(2-pyridylmethyl)imidazol-2-ylidene silver complex mentioned above, is an example of a type $\mathbf{C'_2}$ structure.[9]

The current classification does not include complexes with non-coordinating anions that will adopt a type **C′** structure,[18-20] or silver clusters.[9, 16, 21] One example is known with a $[\{(NHC)_2Ag\}_3I]^{2+}2I^-$ structure, in which the NHC has pendant pyridine groups, that may be considered intermediate between structure **C** and **C′**.[22] Chelating NHC ligands are not included explicitly, but are expected to form similar species.

Type **C′** is not likely to be a major product in the solid state with potentially coordinating halides and only few solid-state structures of this type have been reported with bulky ligands.[4] It is argued that in the structure reported by Wang *et al.* (CCDC code: PENJIC) the iodide counter ion may be considered weakly bound to the silver center at 3.36 Å, as this is shorter than the sum of the van der Waals radii of silver and iodine of 3.70 Å.[23]

Even though kinetic evidence was not found, it is assumed that structure **A** is the direct outcome of the reaction between the azolium salt and Ag_2O in solution. This notion is corroborated by recent quantum chemical calculations.[24] The other structures are most likely generated subsequently, due to the fluxional behavior between the ionic and neutral complexes observed in solution for most of the Ag-NHC compounds (Scheme 2.2), and the known equilibrium between AgX_2^- and AgX + X^-.[2] The fact that with the ligand Bn_2Im both type $\mathbf{A_2}$ (**3** and **4**) and type **C** (**2**) structures have been characterized in the solid state, demonstrates that the ligand and the halide are not the only factors determining the solid state structure. The only

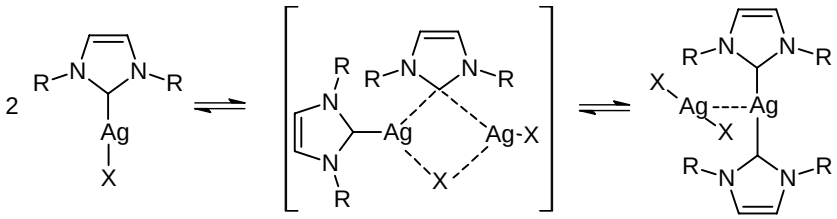

Scheme 2.2. Fluxional behavior of Ag-NHC complexes in solution.[6]

distinction in the reaction conditions of the syntheses of **2** and **3** is the reaction time. Whereas **3** was obtained after 2 hours, compound **2** was isolated after 15 hours of stirring. This seems to suggest that the dimeric **3** is the kinetic product, while three-coordinate **2** is thermodynamically favored under the conditions used. However, repeating the synthesis with 18 hours stirring yielded a solid which again analyzed as complex **3**. Therefore, the fact that it was possible to isolate **3** in crystalline form is ascribed to a subtle difference in crystallization conditions. The observation that different crystallization conditions may lead to different crystal structures of Ag(I) NHC complexes has been noted before.[14] In addition, very recently another example of a type **C** solid-state structure was reported, obtained from a tetra-ether substituted imidazolium bromide.[25] In that case, however, the parent silver complex analyzed as a 1:1 complex and AgBr is reported to be formed at the bottom of the crystallization tube upon crystallization by slow evaporation of a dichloromethane solution. Unfortunately, no NMR data are given for the crystalline compound.

Several attempts to obtain the 2:1 complex by using different crystallization conditions were undertaken, including the use of different solvents, the absence and presence of light and a low temperature. In all cases, however, crystals that formed analyzed (by elemental analysis) as the 1:1 complex. Moreover, stirring a sample of **3** in THF at 70 °C for 14 hours, followed by precipitation with diethyl ether, did not change the composition of the compound. In conclusion, it appears that the isolation of **2** with the type **C** structure should be regarded as serendipitous.

2.2.5 Transmetalation

The Ag NHC complexes are widely used as carbene transfer reagent. Indeed, both **3** and its chloride-analogue **4** have been used in the synthesis of (Bn_2Im)Rh(COD)Cl.[26-28] In this study it was chosen to attempt the transfer of the ligand to a nickel center. Several nickel(II) complexes bearing monodentate NHC ligands have been reported. To date, the two routes employed to obtain these complexes, *i.e.* heating a mixture of imidazolium salt with nickel acetate,[29, 30] and the reaction of the free carbene with a suitable nickel source,[31] have limitations in stability and application. Transmetalation from the silver salt may be an attractive alternative.

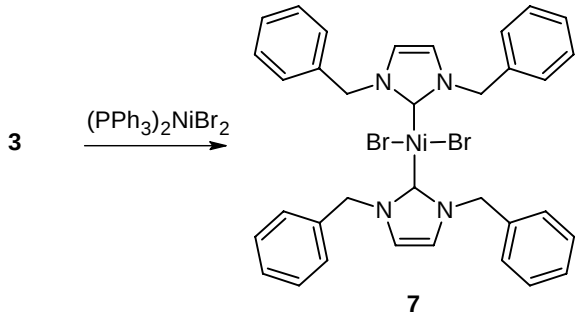

Scheme 2.3. Transmetalation of (Bn_2Im) from silver to nickel.

When a freshly prepared solution of **3** in dichloromethane was added to a solution of $(PPh_3)_2NiBr_2$ in the same solvent, a rapid color change from green to red was observed (Scheme 2.3). Additional stirring led to an off-white precipitate in a red solution. Filtration and concentration *in vacuo* gave a red, diamagnetic precipitate which was isolated by filtration. The color of compound **7** is consistent with square-planar *trans*-$[(Bn_2Im)_2NiBr_2]$.[29, 30] The ^1H and ^{13}C NMR spectra of **7** are similar to those of silver complex **3**, with small shifts due to the difference in electronegativity between the two metal fragments. The carbene C resonance is shifted to 169 ppm in the ^{13}C NMR spectrum, comparable to the values found for other nickel NHC complexes.[30] The catalytic properties of this nickel compound are discussed in Chapter 3.

2.3 Conclusion

In summary, an Ag(I) NHC complex was synthesized starting from 1,3-dibenzylimidazolium bromide, following a common procedure. This complex displays a solid-state structure that is significantly different from a structure that was reported by others. It appears that the difference originates from the crystallization procedure and it is believed that the 1:1 ligand to silver complex is the major product after the first isolation. With this in mind, it is recommended to use elemental analysis, rather than mass spectrometry, for the determination of the composition of the crude product. In addition, NMR experiments indicate that the formation of the silver complex is fast and evidence was found that in solution the complex is present as a neutral species. Furthermore, a novel classification of the solid-state structures of monodentate NHC silver complexes is introduced.

The silver compound was successfully used in a transmetalation reaction to obtain the novel compound *trans*-dibromidobis(1,3-dibenzylimidazol-2-ylidene)nickel(II).

2.4 Experimental Section

General procedures. All chemicals were obtained from commercial sources and used as received. Solvents were reagent grade and used without further purification, except for 1,4-dioxane which was distilled from CaH_2 and stored on molecular sieves under argon. NMR spectra were obtained on a Bruker DPX300 spectrometer and are referenced against TMS. IR spectra were recorded on a Perkin-Elmer Paragon 1000 FT-IR spectrophotometer. C,H,N determinations were performed on a Perkin–Elmer 2400 Series II analyzer. Electrospray mass spectra were recorded on a Finnigan TSQ-quantum instrument using an electrospray ionization technique (ESI-MS), using water/acetonitrile solutions. $(PPh_3)_2NiBr_2$,[32] and 1,3-dibenzylimidazolium chloride,[33] were synthesized according to literature procedures. Imidazolium bromide **1** has been prepared before;[7, 34, 35] however, a full characterization was never reported.

1,3-Dibenzylimidazolium bromide (1). Under argon, a mixture of *N*-benzylimidazole (3.96 g, 25 mmol) and benzyl bromide (5.13 g, 30 mmol) in 30 mL dry 1,4-dioxane was stirred at 100 °C for 4 hours. The resulting two-phase system was cooled and the layers were separated. The bottom layer was washed two times with 1,4-dioxane and once with diethyl ether. Drying *in vacuo* yielded a clear, colorless oil that crystallized very slowly. Yield: 7.6 g (92%). ^{1}H NMR (300 MHz, DMSO-d_6, 300K): δ = 9.51 (s, 1H, NCHN), 7.85 (d, *J* = 2 Hz, 2H, NCH), 7.42 (m, 10H, Ar-H), 5.45 (s, 4H, CH_2). ^{13}C NMR (300 MHz, DMSO-d_6, 300K): δ = 136.2 (NCHN), 134.7 (C_q), 129.0 (C_{Ar}), 128.7 (C_{Ar}), 128.3 (C_{Ar}), 122.8 (NCH), 52.0 (CH_2). IR (neat): ν = 3028 (w), 1557 (m), 1496 (w), 1458 (w), 1350 (w), 1210 (w), 1148 (m), 819 (w), 720 (s), 707 (s), 638 (s), 570 (w), 482 (m) cm^{-1}. MS (ESI): *m*/*z* 249 ([M – Br]$^+$, 100%). Anal. Calc. for $C_{17}H_{17}BrN_2$: C, 62.02; H, 5.20; N, 8.51. Found: C, 61.21; H, 5.23; N, 8.44%.

Bis(μ-bromido(1,3-dibenzylimidazol-2-ylidene)silver(I)) (3). 1,3-Dibenzylimidazolium bromide (0.32 g, 1.0 mmol) and silver(I) oxide (0.14 g, 0.5 mmol) were mixed in dichloromethane (10 mL) and stirred in the absence of light at room temperature for 2 h. The resulting solution was filtered with the aid of a membrane filter and concentrated *in vacuo*. Addition of diethyl ether gave an off-white precipitate which was isolated by filtration, washed with diethyl ether and dried *in vacuo*. Single crystals suitable for X-ray diffraction were grown by slow diffusion of diethyl ether into a chloroform solution at room temperature. Yield: 0.65 g (75%). ^{1}H NMR (300 MHz, $CDCl_3$, 300K): δ = 7.36 (m, 6H, Ar-H), 7.23 (m, 4H, Ar-H), 6.92 (s, 2H, NCH), 5.30 (s, 4H, NCH_2). ^{13}C NMR (300 MHz, $CDCl_3$, 300K): δ = 181.9 (Ag-C), 135.4 (C_q) 129.1 (C_{Ar}), 128.7 (C_{Ar}), 127.9 (C_{Ar}), 121.4 (NCH), 55.8 (NCH_2). IR (neat): ν = 3127 (w), 1492 (w), 1452 (m), 1356 (w), 1226 (m), 1152 (w), 1027 (w), 752 (s), 700 (s), 662 (m), 582 (m) cm^{-1}. MS (ESI): *m*/*z* 605 ([L_2Ag]$^+$, 100%). Anal. Calc. for $C_{17}H_{16}AgBrN_2$: C, 46.82; H, 3.70; N, 6.42, Found: C, 46.85; H, 3.70; N, 6.48%.

Synthesis of 3, followed by NMR spectroscopy at 243 K. In an NMR tube, 1,3-dibenzylimidazolium bromide (0.2 mmol, 57 mg) and silver(I) oxide (0.1 mmol, 23 mg) were dissolved/suspended in 0.75 mL deuterated dichloromethane. The solution was immediately frozen in liquid nitrogen and transferred to an NMR apparatus, cooled to 243 K. After recording the ^{1}H and ^{13}C NMR spectra, the tube was removed from the NMR apparatus and shaken manually for 30 seconds. Then, the next ^{1}H and ^{13}C spectra were recorded and this procedure was repeated until no change in the spectra could be observed anymore.

1,3-Dibenzylimidazolium tetraphenylborate (5). 1,3-Dibenzylimidazolium chloride (0.28 g, 1.0 mmol) and $NaBPh_4$ (0.37 g, 1.1 mmol) were dissolved in 15 mL dichloromethane and vigorously stirred for 3 h. The solution was filtered with a membrane filter to separate the NaCl byproduct. The filtrate was evaporated to dryness. The remaining oil crystallized slowly and was dried *in vacuo* to yield a colorless solid. Yield: 0.48 g (84%). ^{1}H NMR (300 MHz, DMSO-*d*6, 300K): δ 9.35 (s, 1H, NCHN), 7.79 (d, *J* = 1.6 Hz, 2H, NCH), 7.40 (m, 10H, Ar-H), 7.18 (m, 8H, Ar-H), 6.92 (t, *J* = 7.2 Hz, 8H, Ar-H (BPh_4^-)), 6.78 (t, *J* = 7.2 Hz, 4H, Ar-H (BPh_4^-)), 5.40 (s, 4H, NCH_2). ^{13}C NMR (75 MHz, DMSO-*d*6, 300K): δ 163.3 (q, J_{B-C} = 49 Hz, B-C_q), 136.3 (NCHN), 135.5 (C_{BPh4}), 134.7 (C_q), 129.1 (C_{Bn}), 128.8 (C_{Bn}), 128.3 (C_{Bn}), 125.3 (C_{BPh4}), 122.9 (NCH), 121.5 (C_{BPh4}), 52.1 (NCH_2). Anal. calcd for $C_{41}H_{37}BN_2$: C, 86.61; H, 6.56; N, 4.93. Found: C, 86.26; H, 6.55; N, 5.03%.

***In situ* synthesis of [($Bn_2Im)_2Ag]BPh_4$ (6).** In a 10 mL round bottom flask, $Bn_2Im{\cdot}HBPh_4$ (57 mg, 0.2 mmol) and Ag_2O (12 mg, 0.1 mmol) were dissolved/suspended in 0.5 mL DMSO-d_6 and stirred for 14 h at 70 °C. After cooling, the mixture was transferred into a NMR tube and the ^{1}H and ^{13}C NMR spectra were recorded. No attempts were made to isolate the solid product.

Trans-dibromidobis(1,3-dibenzylimidazol-2-ylidene)nickel(II) (7). 1,3-Dibenzylimidazolium bromide (0.23 g, 1.0 mmol) and silver(I) oxide (0.14 g, 0.5 mmol) were mixed in dichloromethane (10 mL) and stirred in the absence of light at room temperature for 2 h. The resulting solution was filtered with the aid of a membrane filter and added to a solution of $(PPh_3)_2NiBr_2$ (0.34 g, 0.5 mmol) in dichloromethane. A rapid color change from green to red occurred and stirring was continued for 30 minutes. The off-white precipitate that had formed was removed by filtration to give an orange solution, which was concentrated *in vacuo* until a red solid started to precipitate. After filtration and washing with hexane the red product was recrystallized from DMF/diethyl ether. Yield: 0.15 g (42%). ^{1}H NMR (300 MHz, DMSO-*d*6, 300K): δ = 7.55 (d, *J* = 4Hz, 4 H, Ar-H), 7.29 (m, 16H, Ar-H), 6.94 (s, 4H, NCH), 6.09 (s, 8H, NCH_2). ^{13}C NMR (75 MHz, DMSO-*d*6, 300K): δ = 169.0 (Ni-C), 136.9 (C_q), 128.5 (C_{Ar}), 128.4 (C_{Ar}), 127.7 (C_{Ar}), 122.0 (NCH), 53.3 (NCH_2). IR (neat): ν = 3134 (w), 2930 (w), 1494 (w), 1452 (m), 1417 (m), 1342 (w), 1228 (m), 1150 (w), 1028 (w), 769 (w), 728 (m), 692 (s), 594 (m) cm^{-1}. MS (ESI): *m*/*z* 676 ($[M - Br + MeCN]^+$, 100%). Anal. Calc. for $C_{34}H_{32}Br_2N_4Ni{\cdot}0.25DMF$: C, 56.91; H, 4.64; N, 8.12. Found: C, 57.01; H, 5.06; N, 8.07%.

X-ray crystallographic structure determination of 3. $C_{34}H_{32}Ag_2Br_2N_4$, triclinic, space group *P-1*, a = 8.1258(10) Å, b = 10.0156(10) Å, c = 10.5681(10) Å, α = 89.427(12)°, β = 68.000(16)°, γ = 85.19(2)°, V = 794.43(17) $Å^3$, Z = 2, MW = 872.18, D(calc) = 1.8231(4) Mg m^{-3}. X-ray data were collected with a Nonius KappaCCD diffractometer on rotating anode (T = 150 K, MoKα radiation, λ = 0.71073 Å, θ(max) = 27.5°, 19982 reflections measured). The structure was solved by Patterson methods (DIRDIF)[36] and refined with SHELXL-97.[37] Hydrogen atoms were introduced at calculated positions and refined riding on their carrier atoms. Convergence was reached at R = 0.0236 for 3474 reflections with I > 2 σ(I), wR2 = 0.0628 for 3625 reflections, S = 1.045. Illustrations and structure validation were done with PLATON.[38]

2.5 References

(1) Herrmann, W. A. *Angew. Chem. Int. Ed.* **2002**, *41*, 1291.
(2) Lin, I. J. B.; Vasam, C. S. *Coord. Chem. Rev.* **2007**, *251*, 642.
(3) Ramirez, J.; Corberan, R.; Sanau, M.; Peris, E.; Fernandez, E. *Chem. Commun.* **2005**, 3056.
(4) Samantaray, M. K.; Katiyar, V.; Pang, K. L.; Nanavati, H.; Ghosh, P. *J. Organomet. Chem.* **2007**, *692*, 1672.
(5) Kascatan-Nebioglu, A.; Panzner, M. J.; Tessier, C. A.; Cannon, C. L.; Youngs, W. J. *Coord. Chem. Rev.* **2007**, *251*, 884.
(6) Wang, H. M. J.; Lin, I. J. B. *Organometallics* **1998**, *17*, 972.
(7) Newman, C. P.; Clarkson, G. J.; Rourke, J. P. *J. Organomet. Chem.* **2007**, *692*, 4962.
(8) de Fremont, P.; Scott, N. M.; Stevens, E. D.; Ramnial, T.; Lightbody, O. C.; Macdonald, C. L. B.; Clyburne, J. A. C.; Abernethy, C. D.; Nolan, S. P. *Organometallics* **2005**, *24*, 6301.
(9) Catalano, V. J.; Malwitz, M. A. *Inorg. Chem.* **2003**, *42*, 5483.
(10) Iglesias, M.; Beetstra, D. J.; Knight, J. C.; Ooi, L. L.; Stasch, A.; Coles, S.; Male, L.; Hursthouse, M. B.; Cavell, K. J.; Dervisi, A.; Fallis, I. A. *Organometallics* **2008**, *27*, 3279.
(11) Tulloch, A. A. D.; Danopoulos, A. A.; Winston, S.; Kleinhenz, S.; Eastham, G. *J. Chem. Soc.-Dalton Trans.* **2000**, 4499.
(12) Relation of our structures A-C' with the review in ref. 2: Type-1 = B, Type-2 = A, Type-3 = A_2, Type-4 = B_2, Type-7 = C'. Type-5 and Type 6 do not correspond to any of the types described here. Type A_n, C and C'_2 were not described as a common type in the review.
(13) Lee, K. M.; Wang, H. M. J.; Lin, I. J. B. *J. Chem. Soc.-Dalton Trans.* **2002**, 2852.
(14) Lee, C. K.; Vasam, C. S.; Huang, T. W.; Wang, H. M. J.; Yang, R. Y.; Lee, C. S.; Lin, I. J. B. *Organometallics* **2006**, *25*, 3768.
(15) Ray, L.; Shaikh, M. M.; Ghosh, P. *Inorg. Chem.* **2008**, *47*, 230.
(16) Chen, W. Z.; Liu, F. H. *J. Organomet. Chem.* **2003**, *673*, 5.
(17) Burling, S.; Mahon, M. F.; Reade, S. P.; Whittlesey, M. K. *Organometallics* **2006**, *25*, 3761.
(18) Wan, X. J.; Xu, F. B.; Li, Q. S.; Song, H. B.; Zhang, Z. Z. *Organometallics* **2005**, *24*, 6066.
(19) Wang, J. W.; Song, H. B.; Li, Q. S.; Xu, F. B.; Zhang, Z. Z. *Inorg. Chim. Acta* **2005**, *358*, 3653.
(20) Catalano, V. J.; Moore, A. L. *Inorg. Chem.* **2005**, *44*, 6558.
(21) McKie, R.; Murphy, J. A.; Park, S. R.; Spicer, M. D.; Zhou, S. Z. *Angew. Chem. Int. Ed.* **2007**, *46*, 6525.
(22) Wang, X.; Liu, S.; Weng, L. H.; Jin, G. X. *Organometallics* **2006**, *25*, 3565.
(23) Wang, C. Y.; Liu, Y. H.; Peng, S. M.; Liu, S. T. *J. Organomet. Chem.* **2006**, *691*, 4012.
(24) Hayes, J. M.; Viciano, M.; Peris, E.; Ujaque, G.; Lledos, A. *Organometallics* **2007**, *26*, 6170.
(25) Yang, W. H.; Lee, C. S.; Pal, S.; Chen, Y. N.; Hwang, W. S.; Lin, I. J. B.; Wang, J. C. *J. Organomet. Chem* **2008**, *693*, 3729.
(26) Fujihara, T.; Obora, Y.; Tokunaga, M.; Sato, H.; Tsuji, Y. *Chem. Commun.* **2005**, 4526.
(27) Rivera, G.; Crabtree, R. H. *J. Mol. Catal. A-Chem.* **2004**, *222*, 59.
(28) Bittermann, A.; Harter, P.; Herdtweck, E.; Hoffmann, S. D.; Herrmann, W. A. *J. Organomet. Chem.* **2008**, *693*, 2079.
(29) Huynh, H. V.; Holtgrewe, C.; Pape, T.; Koh, L. L.; Hahn, E. *Organometallics* **2006**, *25*, 245.
(30) McGuinness, D. S.; Mueller, W.; Wasserscheid, P.; Cavell, K. J.; Skelton, B. W.; White, A. H.; Englert, U. *Organometallics* **2002**, *21*, 175.
(31) Matsubara, K.; Ueno, K.; Shibata, Y. *Organometallics* **2006**, *25*, 3422.
(32) Venanzi, L. M. *J. Chem. Soc.* **1958**, 719.
(33) Starikova, O. V.; Dolgushin, G. V.; Larina, L. I.; Ushakov, P. E.; Komarova, T. N.; Lopyrev, V. A. *Russ. J. Organ. Chem.* **2003**, *39*, 1467.
(34) Staab, H. A.; Schwalbach, G. *Liebigs Ann. Chem.* **1968**, *715*, 128.
(35) Kamijo, T.; Yamamoto, R.; Harada, H.; Iizuka, K. *Chem. Pharm. Bull.* **1983**, *31*, 1213.

(36) Beurskens, P. T.; Admiraal, G.; Beurskens, G.; Bosman, W. P.; Garcia-Granda, S.; Gould, R. O.; Smits, J. M. M.; Smykalla, C. *The DIRDIF99 program system*, Technical Report of the Crystallography Laboratory, University of Nijmegen, The Netherlands: 1999.
(37) Sheldrick, G. M. *Acta Crystallogr. Sect. A* **2008**, *64*, 112.
(38) Spek, A. L. *J. Appl. Cryst.* **2003**, *36*, 7.

Chapter 3

$Ni(NHC)_2X_2$ complexes in the hydrosilylation of internal alkynes[†]

Abstract. *A number of nickel(II) dihalide complexes with small monodentate N-heterocyclic carbene ligands was synthesized and tested for their catalytic activity in the hydrosilylation of internal alkynes. The nickel(0) active species was obtained from the starting nickel(II) complex by reduction with diethylzinc. In all cases the catalytic reaction yielded the syn product selectively. The fastest catalysts reached full conversion in 60 min at 50 °C, with 5 mol% catalyst loading. The active catalyst was demonstrated to be a homogeneous species.*

[†] Based on J. Berding, J. A. van Paridon, V. H. S. van Rixel and E. Bouwman, *in preparation*.

3.1 Introduction

N-Heterocyclic carbenes (NHCs) have been shown to be versatile ligands in organometallic chemistry and catalysis.[1] The bonding properties of these ligands are often compared to those of well-known trialkylphosphanes, and they may even be better σ-donors than these phosphanes. This makes them good candidates for the stabilization of transition-metal catalysts in various oxidation states during the catalytic cycle. In addition, the shape and size of NHCs may easily be modified by the introduction of various substituents on the heterocycle.

The hydrosilylation of C–C double and triple bonds is one of the most important methods for the formation of C–Si bonds and may be used to functionalize organic molecules.[2] Vinyl silanes, obtained from the reaction between a silane and an alkyne, are useful reagents in organic synthesis.[3] A large issue in the direct hydrosilylation of alkynes is the problem of stereoselectivity and regioselectivity, as the use of a terminal alkyne can result in three isomeric vinyl silanes:[4] the *α*-silyl product and the β-(*E*)- and the β-(*Z*)-stereoisomers (Scheme 3.1). Internal alkynes can give rise to regioisomers and (*E*)- and (*Z*)-isomers. The selectivity towards any of these products depends upon several factors, such as the substituents on the alkyne and the silane, the catalyst, and the reaction conditions. The hydrosilylation of alkynes may be catalyzed by a number of different metal complexes, including rhodium,[5-7] iridium,[6, 8] ruthenium[9, 10] and platinum.[11-13] Complexes of the less precious metals nickel,[14] cobalt,[15] and titanium[16] have also been reported to catalyze this reaction. In general, the hydrosilylation of internal alkynes is less explored than the hydrosilylation of terminal alkynes.[15]

A mechanism for the hydrosilylation of olefins, catalyzed by transition metals was proposed by Chalk and Harrod in 1965.[17] This mechanism, adapted for alkynes, is depicted in Scheme 3.2.[2] Later, several modified mechanisms were proposed, differing in the migration of either the hydride or the silyl group.

Recently, Chaulagain *et al*. reported that a catalyst derived from $Ni(COD)_2$ (COD = cycloocta-1,5-diene), a bulky 1,3-diarylimidazolium salt and KO^tBu is effective in the hydrosilylation of alkynes.[18] The active catalyst is assumed to form *in situ* by deprotonation of the imidazolium salt and formation of the Ni(0) NHC complex. In contrast, a mixture of $Ni(COD)_2$ and tributylphosphane was inactive under the same conditions. In order to further investigate the nickel-NHC complex catalyzed reaction in the present study it was decided to prepare a larger range of ligands, and to develop a protocol starting from a nickel(II) complex to avoid the

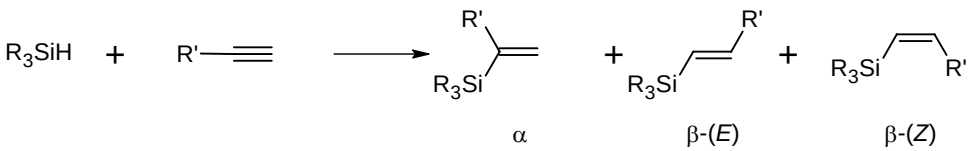

Scheme 3.1. Products in the hydrosilylation of terminal alkynes.

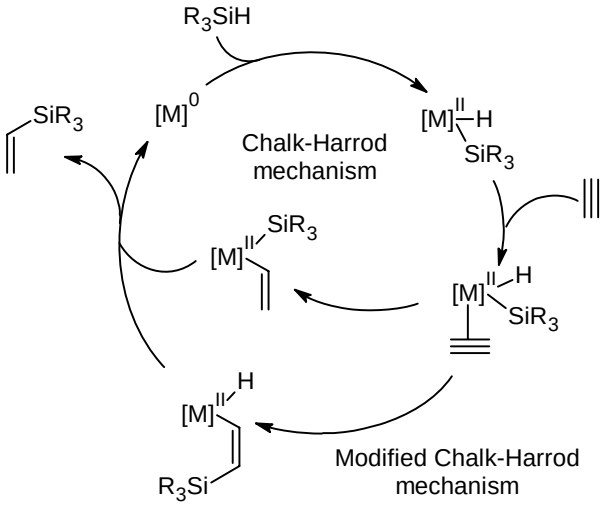

Scheme 3.2. Proposed catalytic cycles for the hydrosilylation of alkynes. Adapted from ref. 2.

handling of the reactive $Ni(COD)_2$.

In this chapter the preparation is described of a variety of nickel(II) complexes bearing two monodentate NHC ligands and two halide anions, based on literature syntheses.[19, 20] These complexes are used in the catalytic hydrosilylation of internal alkynes.

3.2 Results and Discussion

3.2.1 Ligand synthesis

An overview of ligand precursors used in this study is shown in Figure 3.1. The (benz)imidazolium salts were prepared by the direct alkylation of a number of N-substituted imidazoles and benzimidazoles. These quaternization reactions are commonly performed in refluxing THF or acetonitrile. However, to reduce reaction times the higher boiling 1,4-dioxane was used in a number of cases. The salts were obtained in good yields as white to off-white solids and most were found to be hygroscopic. These carbene precursors were characterized by ^{1}H and ^{13}C NMR and IR spectroscopy, elemental analysis and mass spectrometry (ESI-MS). The NMR spectra of the (benz)imidazolium salts in deuterated DMSO showed a downfield shifted signal at around 10 ppm and 140 ppm, characteristic of the imidazolium NCHN proton and carbon, respectively.[21]

	R^1	R^2	X
1a	Me	Me	I
1b	Me	Et	I
1c	Me	Pr	I
1d	Me	iPr	I
1e	Me	Ph	I
1f	Bn	Bn	Br

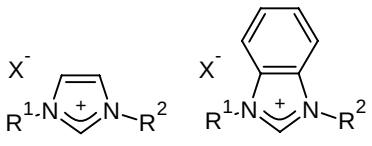

1 **2**

	R^1	R^2	X
2a	Me	Me	I
2b	Me	iPr	Br
2c	Me	iPr	I
2d	Me	Ph	I
2e	iPr	iPr	I
2f	Bn	Bn	Br

Figure 3.1. Overview of ligand precursors used in this study.

3.2.2 Synthesis of nickel(II) complexes bearing two monodentate NHC ligands

Following literature procedures,[20] the (benz)imidazolium salts, with the exception of **1f**, were reacted at high temperatures with $Ni(OAc)_2$ to yield the $Ni(NHC)_2X_2$ complexes depicted in Figure 3.2. In the cases in which the melting point of the imidazolium salt was too high for the reaction to occur successfully an additional low-melting salt, tetrabutylammonium halide, was added as a solvent, in an adaptation of the original procedure reported by Huynh *et al*.[19] After aqueous work-up and purification, the $Ni(NHC)_2X_2$ complexes were obtained as stable, orange-red to purple powders. Complexes **3c**, **3d**, **4a** and **4f** have been synthesized before, following these literature procedures.[19, 20, 22] Complex **3a** has been synthesized before, by an analogous reaction in nitromethane.[23] Complex **3f** was obtained from the corresponding silver(I) complex, as described in Chapter 2.

The ^1H NMR spectra of all nickel complexes lacked the characteristic imidazolium NC*H*N resonance at around 10 ppm, indicating successful carbene generation. The other peaks present in the NMR spectra of the starting imidazolium salts could successfully be identified, albeit shifted slightly from their original position. The carbene carbon atom of the novel complexes **3e** and **4b** is observed in their ^{13}C NMR spectra at 174.7 and 188.0 ppm, respectively. The carbene carbon atoms of complexes **3b**, **4d** and **4e** could not be observed, probably due to peak broadening. Due to its poor solubility in common solvents, a ^{13}C NMR spectrum could not be recorded of complex **4e**. The NMR spectra of **3b**, **3e**, **4b**, **4c** and **4d** showed splitting of a number of resonances, indicating the presence of two rotamers in solution, due to restricted rotation about the Ni–C bond. This behavior has been reported before for complex **3d**.[20] The NMR spectra of **4b** and **4c**, which only differ in halide, are quite similar, as expected. Interestingly, however, the isopropyl-CH and the NCH_3 resonances are shifted more downfield in the case of the bromide complex **4b**. The isopropyl-CH resonances of **4b** are obscured by resonances of the aromatic protons, but could be assigned with the aid of a ^1H COSY NMR spectrum. Moreover, the isopropyl-CH resonances of iodide complex **4e** are shifted less downfield than those reported for the bromide analogue,[22] indicating a trend in the electronic

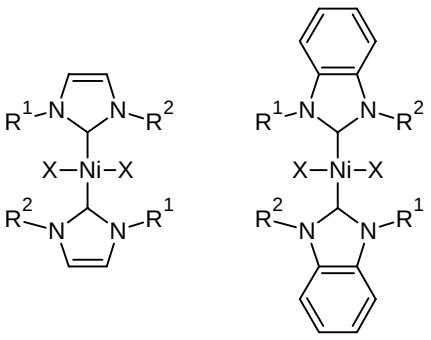

3a-f **4a-f**

Figure 3.2. Nickel complexes prepared in this study. R^1, R^2 and X are as given in Figure 3.1 for **1** and **2**, respectively.

properties of the complexes, depending on the halide. A similar trend was observed in analogous palladium complexes.[24]

3.2.3 Catalytic studies

General

Complexes **3a-f** and **4a-f** were tested for their catalytic activity in the hydrosilylation of internal alkynes with triethylsilane. As a benchmark, the symmetric 3-hexyne was chosen as the internal alkyne. A typical example of the evolution of the substrate and the product in time is shown in Figure 3.3. The results are given in Tables 3.1 and 3.2. The activity is reported as the time needed to consume all alkyne substrate (T_{full}). As full conversion is reached asymptotically, exact determination of T_{full} is difficult, and therefore the time at which 50% of the alkyne was consumed (T_{50}) is reported as well.

Two different isomers of the product may be obtained from the hydrosilylation of 3-hexyne (Figure 3.4), *i.e.* the (*E*)- and the (*Z*)-isomer. In the current experiments, however, only one isomer was observed. Isolation and characterization revealed it was the (*E*)-isomer, in which the H and the $SiEt_3$-group are located on the same face of the double bond, in agreement with the results of other nickel catalysts.[12] In contrast, the Lewis acid-catalyzed hydrosilylation of alkynes has been reported to yield the (*Z*)-isomer selectively.[25]

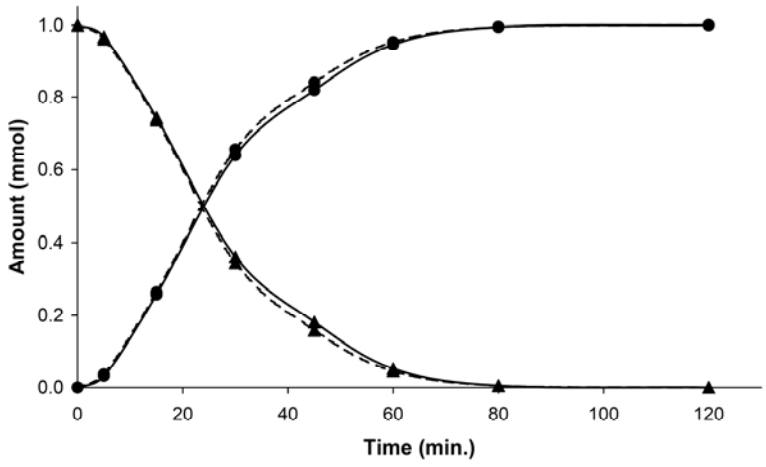

Figure 3.3. Typical example of the consumption of the substrate 3-hexyne (▲) and the evolution of the product (●) in time using complex **4f** (Table 3.2, entry 12). Solid line: regular run; dashed line: with 100 eq. Hg added after 30 min.

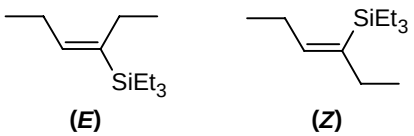

Figure 3.4. Possible isomers of the product of the hydrosilylation of 3-hexyne.

Catalyst activation

The starting point of the catalytic cycle of the hydrosilylation of alkynes is a nickel(0) species. It has been shown that nickel(II) complexes may be activated by reaction with an appropriate silane, however, this process requires high temperatures.[26] As an alternative reducing agent butyllithium was considered, although it was unclear whether this reagent could be used to activate nickel(II) complexes, rather than nickel(II) salts.[27-29] In addition, triethylaluminium, diethylzinc and phenylmagnesium chloride were evaluated. Trialkylaluminium compounds are known for the activation of $Ni(acac)_2$ in Ziegler-type catalysts, the zinc reagent is anticipated to have similar alkylating properties,[30] and the Grignard reagent is used for the activation of nickel dihalide complexes in the Kumada coupling reaction.[31, 32] The results of the catalytic hydrosilylation of 3-hexyne with triethylsilane using complex **3a** in combination with these activators are summarized in Table 3.1.

Initially, in the butyllithium-activated experiments, the activator was added to the nickel(II) complex at 0 °C, which caused a rapid color change of the solution from red to yellow. As it was suspected that this activation method was too vigorous, and the catalytic results were difficult to reproduce, it was decided to moderate the activation, by adding the butyllithium at –78 °C, and allowing the reaction mixture to slowly warm up to room temperature. This modified procedure greatly improved the reproducibility of the catalytic experiments. In the case of the activation using $AlEt_3$, PhMgCl or $ZnEt_2$, no rapid color change was observed during the addition of the activator to the solution of the nickel(II) complex at room temperature, and cooling was not employed in these experiments. Unfortunately, no catalytic activity was observed after the addition of $AlEt_3$, and even an excess of PhMgCl gave only partial activation.

In the catalytic experiments in which butyllithium was employed as activating agent, small amounts of two sideproducts were observed. These were identified as

Table 3.1. The use of different compounds for the activation of complex **3a** in the hydrosilylation of 3-hexyne.[a]

Entry	Activator [b]	Amount [c]	T_{50} (min) [d]	T_{full} (min) [e]
1	BuLi (0 °C) [f]	2	10 – 50	30 – 250
2	BuLi (–78 °C)	2	40	140
3	PhMgCl [g]	4	-	-
4	PhMgCl	10	200	n.d.
5	$AlEt_3$ [g]	8	-	-
6	$ZnEt_2$	2	70	240
7	$ZnEt_2$	4	40	140

[a] Reagents and conditions: 0.05 mmol **3a**, 1.0 mmol 3-hexyne, activator, 2.0 mmol triethylsilane, 5 mL THF, 50 °C. All catalytic runs were performed in duplicate. The (E)-product is obtained selectively; [b] Activator was added at room temperature, unless noted otherwise; [c] Equivalents of activator relative to nickel; [d] Time needed to reach 50% conversion of 3-hexyne; [e] Time needed to reach full conversion; [f] The experiment was difficult to reproduce, and was performed 4 times. In one run no activation occurred; [g] No conversion was observed after 5 h.

Figure 3.5. Side products observed in the BuLi activated catalytic experiments.

butyltriethylsilane and ethoxytriethylsilane (Figure 3.5).[33] The first may be formed by a reaction between butyllithium and triethylsilane, while the latter is most likely derived from butyllithium, triethylsilane and ethanol used in the work-up procedure. In addition, it was observed that the use of a larger excess of butyllithium resulted in larger amounts of these side products. As both side products are derived from the silane reagent, which is used in excess, they are not taken into consideration for the calculation of the selectivity of the catalyst, which is based on conversion of the alkyne.

The catalyst activation with butyllithium at low temperature and the activation with 4 equivalents diethylzinc yielded a catalyst of equal activity. Because of the formation of side products and the laborious activation (cooling to –78 °C) when using butyllithium, and the insufficient activating properties of phenylmagnesium chloride and triethyl aluminium, it was decided to use 4 equivalents of diethylzinc as activator for the remainder of catalytic experiments.

The results of the diethylzinc-activated, nickel-catalyzed hydrosilylation of 3-hexyne using complexes **3a-f** and **4a-f** are summarized in Table 3.2. In all cases the catalytic reaction was performed using the following procedure: the nickel complex

Table 3.2. Nickel-catalyzed hydrosilylation of 3-hexyne using complexes **3** and **4**.[a]

		Standard procedure [b]		With prior activation [c]	
Entry	Catalyst	T_{50} (min) [d]	T_{full} (min) [e]	T_{50} (min) [d]	T_{full} (min) [e]
1	**3a**	40	140	40	160
2	**3b**	40	120	45	150
3	**3c**	40	100	35	120
4	**3d**	60	150	40	140
5	**3e**	40	120	14	60
6	**3f**	25	70	22	80
7	**4a**	40	160	45	180
8	**4b**	20	60	25	80
9	**4c**	60	130	25	80
10	**4d**	50	140	25	120
11	**4e**	300	n.d.	200 (45) [f]	n.d. (150) [f]
12	**4f**	25	80	20	60
13	– [g]	–	–		

[a] Reagents and conditions: 0.05 mmol Ni, 5 mL THF, 0.2 mmol $ZnEt_2$, 1.0 mmol 3-hexyne, 2.0 mmol triethylsilane, 50 °C. All catalytic runs were performed in duplicate. The (E)-product is obtained selectively; [b] All reagents were mixed at room temperature, before heating to 50 °C; [c] Reaction mixture was stirred 10 min at 50 °C, before the alkyne and the silane were added; [d] Time needed to reach 50% conversion; [e] Time needed to reach full conversion; [f] Reaction mixture was stirred 30 min at 50 °C, before the alkyne and the silane were added; [g] No nickel complex was added. No conversion was observed after 5 h in the presence of 0.2 mmol $ZnEt_2$.

is dissolved/suspended in THF and 3-hexyne is added, followed by diethylzinc. Next, the silane is added and the reaction vessel is immediately placed in a preheated oil bath. All nickel complexes bearing monodentate N-heterocyclic carbenes tested in this study are active hydrosilylation catalysts after activation with diethylzinc.

The T_{50} and T_{full} values given in Table 3.2 are an indication the activity of the catalyst. However, if the activation is a slow process, the nickel complex is not activated immediately after the starting point of the catalytic run and the true activity of the catalyst may be underestimated. Therefore, the *overall* activity of the catalyst is dependent on the activation of the initial nickel(II) complex. The activation of the catalyst may be influenced by (a) the halide ion and (b) the solubility of the starting complex.

It is often assumed that the activity of a complex is independent on the halide of the starting compound, as this halide is removed during the activation process. However, it is clear (Table 3.2, entries 8 and 9) that the halide does have an effect on the overall activity, as the substrate is consumed faster when starting from the bromide complex **4b**, than from the iodide complex **4c**. This indicates that in the case of the iodide complexes the activation is rather sluggish. Complexes **4a**, **4c**, and especially **4e** are poorly soluble in THF, which may cause slow catalyst activation. Indeed, in a number of cases an induction time of 5 to 10 minutes is observed before full catalytic activity starts and with complex **4e** no conversion is observed in the first 45 minutes.

To eliminate the influence of the slow activation on the overall activity, all catalytic runs were repeated with an alternative procedure in which the nickel(II) complex is activated prior to the addition of the two reagents. Preactivation is accomplished by stirring the mixture of the nickel complex with diethylzinc at 50 °C for 10 minutes, before the alkyne and the silane are added. The results obtained with this alternative procedure are included in Table 3.2.

In a number of cases the preactivation of the nickel(II) complex significantly decreases the time needed to bring the reaction to full conversion. For instance, using complex **3e** with pre-activation the time needed to reach full conversion is halved compared to the regular procedure. Nickel iodide complexes with isopropyl- and phenyl-substituted ligands appear to benefit the most from the preactivation procedure. In some runs the catalytic activity appears to have decreased slightly, possibly due to catalyst decomposition in the absence of substrate, although this may be within experimental error. However, as expected, the halide of the nickel(II) starting complex no longer has an influence on the catalytic activity, as it is now removed at the activation step before the catalytic reaction starts (Table 3.2, entries 8 and 9). Unfortunately, complex **4e** is highly insoluble and even after preactivation for 30 minutes, some undissolved starting complex is still present in the reaction mixture. Therefore, the results shown for this complex are an underestimation of the true catalytic activity of the nickel(0) species.

Catalytic activity

The catalytic activity of the various nickel complexes ise dependent on the ligand substituents. For instance, an increase in the length of the alkyl chain from methyl to propyl in complexes **3a – 3c**, leads to a decrease in the time needed to reach full conversion, although the more bulky isopropyl substituent leads to a less active catalyst in the case of the imidazole-based carbene ligands. In the case of the benzimidazole-based carbene ligands, an increase in bulk around the metal center clearly leads to enhanced catalytic activity, although this is not apparent for complex **4e**, which was only partly activated.

The most active catalysts found in this study are the N-methyl-N′-phenyl-substituted imidazole-based complex **3e** and N,N′-dibenzyl-substituted benzimidazole-based complex **4f**, which both reach full conversion within 60 minutes. The highest turnover frequency was observed with complex **3e**, as it reached 50% conversion in 14 minutes, which is equal to 43 mol·(mol cat)$^{-1}$·h^{-1}. In the case that no catalyst preactivation is performed, the bromide complexes (**3f**, **4b** and **4f**) are the most active.

To confirm that the nickel complex is the source of the catalytic activity, one experiment was performed without addition of the nickel complex. As expected, after 5 h of stirring at 50 °C no product could be observed (Table 3.2, entry 13).

In addition to the benchmark substrate 3-hexyne, the more sterically hindered diphenylacetylene was used as the internal alkyne in the catalytic studies. Using complex **3a** under the standard conditions, the hydrosilylated product 1,2-diphenyl-1-triethylsilyl-*cis*-ethene was obtained quantitatively in 150 minutes.

The hydrosilylation of 3-hexyne with triethylsilane has been reported a number of times in the literature. For instance, 0.5 mol% of a cationic rhodium complex in an aqueous micellar system yielded 53% of the (*E*)-product in 3 h at room temperature.[34] A cobalt(I) complex was shown to yield 71% of the (*E*)-product in 10 h, using 5 mol% catalyst loading at 40 °C.[15] However, using heterogeneous platinum on carbon, the same product could be obtained in 95% yield in 3 h using only 0.02 mol% Pt at 80 °C.[12] Although the latter catalyst is clearly the most efficient, the nickel catalyst under study may be an economically attractive alternative.

Homogeneous vs heterogeneous catalysis

A continuing discussion in homogeneous catalysis involving zero-valent transition-metal intermediate species is the question whether the active catalyst is indeed the homogeneous zero-valent metal complex, or that heterogeneous metal nanoparticles or clusters are catalytically active. This is of importance, especially since nanoparticles have been shown to be catalytically active in a number of related nickel-catalyzed reactions, such as hydrogenation[35] and the Heck reaction.[36]

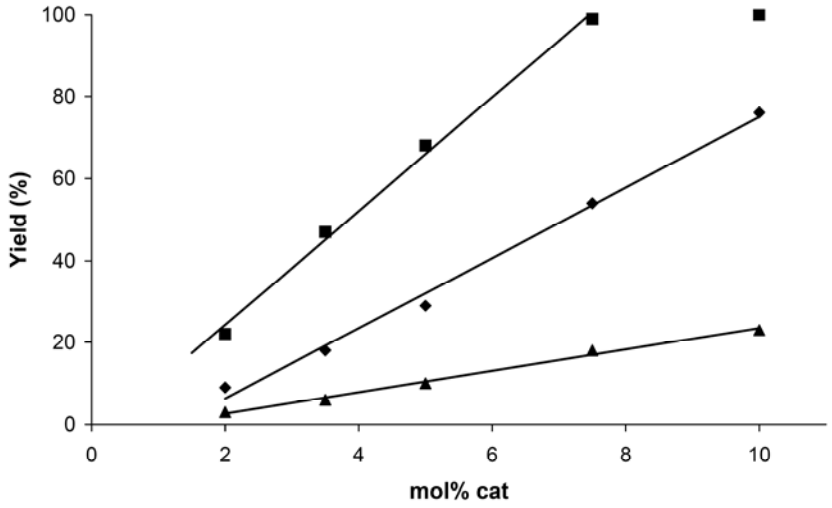

Figure 3.6. Product yield as a function of catalyst concentration after a fixed time: (■) 60 min.; (♦) 30 min.; (▲) 15 min.

One method for excluding the observed catalytic activity to be due to nickel nanoparticles is the so called 'mercury test'. During the catalytic run a drop of metallic mercury is added to the reaction mixture, which, in the case of nickel nanoparticles, should quench the reaction due to the formation of an $HgNi_3$ or $HgNi_4$ amalgam.[37] If, on the other hand, the reaction continues, it is generally accepted that the catalyst must be a homogeneous species. In the present study, 100 equivalents of mercury on nickel were added after 30 minutes of reaction time. To ensure a large contact surface, the reaction mixtures were stirred vigorously to create small mercury droplets. To exclude the possibility of an unintended active heterogeneous catalyst being present, the mercury test was performed with all catalysts. In all cases the addition of mercury had no noticeable effect on the outcome of the catalytic reaction, in terms of rate or selectivity. A comparative example of the evolution of 3-hexyne and the product in time during the mercury test is included in Figure 3.3.

Although the mercury test is a fast and easy-to-perform method for distinguishing homogeneous and heterogeneous catalysts, it is not always conclusive.[38] For instance, poisoning may be incomplete if the contact between the mercury drop and the catalyst solution is not sufficient, the mercury may cause side reactions, or there simply may not be enough mercury present to bind all nanoparticles.[39] Therefore, it was decided to perform a kinetic study on selected catalytic systems. In theory, in the case of a homogeneous catalyst an increase in catalyst concentration should lead to a proportional increase in the overall rate of the reaction, while for heterogeneous catalysts this is not necessarily the case, due to the formation of different sizes of metal clusters. The results of this kinetic study using complex **3e** are shown in Figure 3.6. Using different catalyst concentrations, the product yield was determined after 15, 30 and 60 minutes. Clearly, an increase in catalyst concentration gives a linear increase in the conversion within experimental error and thus it may be concluded that the $ZnEt_2$-activated catalyst is truly homogeneous. Comparable results were obtained using complex **3a**.

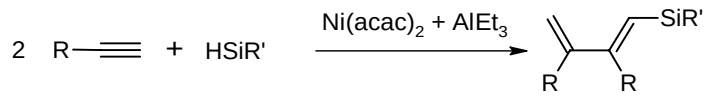

Scheme 3.3. Hydrosilylation and dimerization of terminal alkynes with a Ziegler-type catalyst.[42]

As a final check for homogeneity it was attempted to deliberately prepare a heterogeneous catalyst and to test its activity in the hydrosilylation of internal alkynes. The heterogeneous nickel-catalyzed hydrosilylation of terminal olefins has been reported.[40] However, to the best of our knowledge, no internal alkynes have been used in these studies, except one: Lappert *et al.* reported that $Ni(acac)_2$, reduced by $AlEt_3$, was inactive for the hydrosilylation of 2-hexyne and 4-octyne,[41] although with terminal alkynes a 2:1 adduct could be obtained (Scheme 3.3).[42] Indeed, using $Ni(acac)_2$ and $AlEt_3$ under the conditions of the present study did not result in any conversion of 3-hexyne. Therefore, it is concluded that the activity observed with complexes **3a-f** and **4a-f** must arise from a homogeneous catalyst.

Mechanistic considerations

Chaulagain *et al.*[18] reported that a mixture of 10 mol% $Ni(COD)_2$, 10 mol% of a bulky N,N′-diarylimidazolium salt, such as N,N′-dimesitylimidazolium chloride, and 10 mol% KO^{t}Bu in THF is active in the hydrosilylation of internal alkynes, when using 2 equivalents of silane at room temperature. However, slow addition of the alkyne was required to obtain the 1:1 adduct in good yield. Fast addition of the alkyne led to the formation of a 2:1 adduct (Scheme 3.4). In contrast, the system under investigation in the current study is less active, and requires elevated temperatures in order to proceed at an appreciable rate. However, only the (*E*)-alkene product is observed and can be isolated quantitatively.

The differences between the two systems may be explained by the different ligand-to-metal ratio. In the case of the 1:1 ligand-to-metal catalyst, the nickel center is highly coordinatively unsaturated, which enables the coordination of two alkynes and one silane substrate, leading to the 2:1 adduct. The lack of bulk around the metal center may also account for the high reactivity. In contrast, in the 2:1 ligand-to-metal catalyst only one alkyne and one silane may be bound to the nickel center, leading only to the 1:1 adduct.

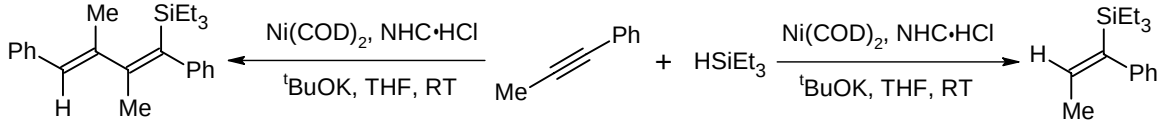

50%, 6:1 isomeric mixture
(alkyne added in 1 minute)

74%,
(alkyne added in 20 minutes)

Scheme 3.4. Hydrosilylation of an internal alkyne using $Ni(COD)_2$ and a bulky imidazolium salt (NHC·HCl = N,N′-dimesitylimidazolium chloride).[18]

3.3 Conclusion

In conclusion, the synthesis and characterization of a number of monodentate N-heterocyclic carbene complexes of nickel(II) and their activity in the catalytic hydrosilylation of internal alkynes is reported. Four activating agents were evaluated, from which diethylzinc was selected as the most efficient. Using a procedure in which the nickel catalyst is preactivated, N-methyl-N'-phenyl-substituted complex **3e** and N,N'-dibenzyl substituted complex **4f** show the highest activity in the hydrosilylation of 3-hexyne with triethylsilane, giving the desired (*E*)-product in quantitative yield within 60 minutes at 5 mol% catalyst loading.

Using the mercury test and kinetic studies, it was unambiguously shown that the active catalyst is a homogeneous species.

3.4 Experimental

General considerations. All experiments were performed under air and moisture-free conditions under an argon atmosphere, unless indicated otherwise. All chemicals were obtained from commercial sources and used as received. THF and 1,4-dioxane were distilled under an argon atmosphere from CaH_2 and stored on molecular sieves. Dry $Ni(OAc)_2$ was obtained by heating the hydrate at 165 °C under a stream of argon. Triethylsilane and 3-hexyne were degassed and stored under argon on activated molecular sieves. N-isopropylimidazole,[21] N-phenylimidazole,[43] N-isopropylbenzimidazole,[21] N-phenylbenzimidazole,[44] **1a**,[45] **1b**,[46] **2e**,[24] **3c**,[20] **3d**,[20] **4a**,[19] and **4f**[22] were synthesized according to literature procedures. The synthesis of **3f** is described in Chapter 2.

^1H and ^{13}C NMR spectra were recorded on a Bruker DPX300. Chemical shifts are reported as referenced against residual solvent signals and quoted in ppm relative to tetramethylsilane. IR spectra were recorded with a Perkin-Elmer FT-IR Paragon 1000 spectrophotometer equipped with a golden-gate ATR device, using the reflectance technique. C, H, N determinations were performed on a Perkin–Elmer 2400 Series II analyzer. Electrospray mass spectra were recorded on a Finnigan TSQ-quantum instrument using an electrospray ionization technique (ESI-MS). GC measurements were performed on a Varian CP-3800 with a 25 m WCOT fused silica column and an autosampler, using heptane as internal standard. Peaks were identified by comparison with the pure compound (3-hexyne, Et_3SiH, 3-triethylsilyl-*cis*-hex-3-ene, butyltriethylsilane,[33] ethoxytriethylsilane,[33] 1,2-diphenyl-1-triethylsilyl-*cis*-ethene) and by GC-MS analysis (butyltriethylsilane, ethoxytriethylsilane). Diethylzinc was added as a 1.0 M solution in hexanes, n-butyllithium was added as a 1.6 M solution in hexanes, triethylaluminium was added as a 0.6 M solution in heptane and phenylmagnesium chloride was added as a 25 wt% solution in THF.

General reaction for the synthesis of (benz)imidazolium salts. A solution of N-substituted (benz)imidazole and about 1.1 equivalents of haloalkane in dry THF or 1,4-dioxane was placed under an argon atmosphere and stirred at 80 or 100 °C, respectively, for 24 h. When using iodomethane as alkylating agent, the reaction mixture was stirred at room temperature. The off-white precipitate was collected by filtration and recrystallized from methanol/diethyl ether to yield a white solid, which was dried *in vacuo*.

N-methyl-N′-phenylimidazolium iodide (1e). The synthesis was performed according to the general procedure, starting from 2.16 g N-phenylimidazole (15 mmol) and 2.42 g iodomethane (17 mmol) in 20 mL THF. Yield: 4.21 g (98%). ^{1}H NMR (300 MHz, 300 K, DMSO-d_6): δ 9.80 (s, 1H, NCHN), 8.31 (s, 1H, NCH), 7.98 (s, 1H, NCH), 7.79 (m, 2H, ArH), 7.68-7.58 (m, 3H, ArH), 3.96 (s, 3H, NCH_3). ^{13}C NMR (75 MHz, 300 K, DMSO-d_6): δ 137.2 (NCHN), 136.0 (C_q), 131.5 (C_{Ar}), 131.0 (C_{Ar}), 125.7 (NCH), 123.1 (C_{Ar}), 122.2 (NCH), 37.6 (NCH_3). IR (neat): 3447 (m), 3371 (m), 3094 (m), 3029 (m), 1599 (w), 1576 (m), 1553 (m), 1496 (m), 1423 (w), 1222 (m), 1068 (m), 813 (w), 758 (s), 682 (s), 611 (s) cm^{-1}. Anal. Calcd for $C_{10}H_{11}IN_2 \cdot 0.5H_2O$: C, 40.70; H, 4.10; N, 9.49. Found: C, 40.69; H, 4.01; N, 9.48. MS (ESI): *m*/*z* 159 ([M – I]$^+$, 100%).

N-methyl-N′-isopropylbenzimidazolium bromide (2b). Following the general procedure, the compound was obtained from 1.06 g N-methylbenzimidazole (8.0 mmol) and 1.23 g 2-bromopropane (10.0 mmol) in 30 mL 1,4-dioxane and isolated as a white solid. Yield: 1.41 g (69%). ^{1}H NMR (300 MHz, 300 K, DMSO-d_6): δ 9.93 (s, 1H, NCHN), 8.12 (m, 1H, Ar-H), 8.03 (m, 1H, Ar-H), 7.69 (m, 2H, Ar-H), 5.06 (septet, 1H, *J* = 7 Hz, NCH), 4.07 (s, 3H, NCH_3), 1.60 (d, 6H, *J* = 7 Hz, CH_3). ^{13}C NMR (75 MHz, 300 K, DMSO-d_6): δ 141.1 (NCHN), 132.0 (C_q), 130.3 (C_q), 126.4 (C_{Bim}), 126.3 (C_{Bim}), 113.8 (C_{Bim}), 113.6 (C_{Bim}), 50.3 (NCH_3), 33.2 (NCH), 21.6 (CH_3). IR (neat): 3080 (w), 2978 (w), 1564 (m), 1456 (m), 1436 (m), 1349 (m), 1262 (m), 1216 (m), 1100 (m), 1016 (w), 830 (w), 759 (s), 615 (m), 552 (m) cm^{-1}. Anal. Calcd for $C_{11}H_{15}BrN_2$: C, 51.78; H, 5.93; N, 10.98. Found: C, 51.98; H, 6.15; N, 10.85. MS (ESI): *m*/*z* 175 ([M – Br]$^+$, 100%), 133 ([M – Br – C_3H_7 + H]$^+$).

N-methyl-N′-isopropylbenzimidazolium iodide (2c). According to the general synthesis, 2.64 g N-methylbenzimidazole (20 mmol) was reacted with 4.25 g 2-iodopropane (25 mmol) in 25 mL THF. The compound was obtained as a white solid. Yield: 3.87 g (64%). ^{1}H NMR (300 MHz, 300 K, DMSO-d_6): δ 9.81 (s, 1H, NCHN), 8.12 (m, 1H, Ar-H), 8.02 (m, 1H, Ar-H), 7.69 (m, 2H, Ar-H), 5.05 (septet, 1H, *J* = 7 Hz, NCH), 4.06 (s, 3H, NCH_3), 1.60 (d, 6H, *J* = 7 Hz, CH_3). ^{13}C NMR (75 MHz, 300 K, DMSO-d_6): δ 141.2 (NCHN), 131.9 (C_q), 130.3 (C_q), 126.4 (C_{Bim}), 126.3 (C_{Bim}), 113.7 (C_{Bim}), 113.6 (C_{Bim}), 50.3 (NCH_3), 33.3 (NCH), 21.6 (CH_3). IR (neat): 3022 (w), 2979 (w), 1610 (w), 1567 (m), 1456 (m), 1431 (m), 1352 (w), 1260 (m), 1215 (m), 1135 (m), 760 (s), 618 (m), 603 (m), 425 (m) cm^{-1}. Anal. Calcd for $C_{11}H_{15}IN_2$: C, 43.73; H, 5.00; N, 9.27. Found: C, 43.88; H, 5.39; N, 9.37. MS (ESI): *m*/*z* 175 ([M – I]$^+$, 100%), 133 ([M – I – C_3H_7 + H]$^+$).

N-methyl-N′-phenylbenzimidazolium iodide (2d). Following the general procedure, the compound was obtained as a white solid from 1.17 g N-phenylbenzimidazole (6.0 mmol) and 0.85 g iodomethane (7.0 mmol) in 15 mL THF. Yield: 1.67 g (83%). ^{1}H NMR (300 MHz, 300 K, DMSO-d_6): δ 10.12 (s, 1H, NCHN), 8.15 (m, 1H, Ar-H), 7.87-7.68 (m, 8H, Ar-H), 4.17 (s, 3H, NCH_3). ^{13}C NMR (75 MHz, 300 K, DMSO-d_6): δ 143.1 (NCHN), 133.1 (C_q), 131.8 (C_q), 130.8 (C_q), 130.4 (2 × C_{Ph}), 127.4 (C_{Bim}), 126.9 (C_{Bim}), 125.1 (C_{Ph}), 113.9 (C_{Bim}), 113.3 (C_{Bim}), 33.5 (NCH_3). IR (neat): 3021 (w), 1563 (m), 1557 (s), 1487 (m), 1424 (w), 1308 (w), 1263 (m), 1239 (m), 1161 (m), 1133 (m), 1080 (m), 828 (m), 785 (m), 747 (s), 697 (s), 600 (s), 484 (m) cm^{-1}. Anal. Calcd for $C_{14}H_{13}IN_2$: C, 50.02; H, 3.90; N, 8.33. Found: C, 50.11; H, 3.92; N, 8.39. MS (ESI): *m*/*z* 209 ([M – I]$^+$, 100%).

General procedure for the synthesis of nickel complexes. A mixture of (benz)imidazolium halide, 0.5 equivalents anhydrous Ni(II) acetate and about 50% of the combined weight of the two reagents of the corresponding tetrabutylammonium halide was dried *in vacuo* at 60 °C

for 1 h. The temperature was then raised to 130 °C (bromide salts) or 155 °C (iodide salts) and kept at this temperature *in vacuo* for several hours. After cooling, water was added and the mixture was triturated thoroughly. After isolation of the crude product by filtration, the pure compound was obtained either by repeated washing of a dichloromethane solution of the crude product with water, evaporation of the solvent and precipitation with diethyl ether (compounds **3a,b,e** and **4b**), or by recrystallization from hot DMF (compounds **4c,d**,**e**), and were isolated as red-orange to purple solids.

Bis(N,N′-dimethylimidazol-2-ylidene)diiodidonickel(II) (3a). Following the general procedure, the complex was obtained from 1.12 g imidazolium iodide **1a** (5.0 mmol) and 0.44 g nickel(II) acetate (2.5 mmol), without the addition of tetrabutylammonium iodide, at 155 °C. Yield: 0.69 g (55%). NMR spectra are identical to those reported in the literature.[23]

Bis(N-ethyl-N′-methylimidazol-2-ylidene)diiodidonickel(II) (3b). Following the general procedure, 1.19 g imidazolium iodide **1b** (5.0 mmol) and 0.44 g nickel(II) acetate (2.5 mmol) were reacted in 0.8 g tetrabutylammonium iodide at 155 °C. Yield: 0.47 g (35%). ^{1}H NMR (300 MHz, 300 K, $CDCl_3$): δ 6.77 (m, 4H, NCH), 4.84 (2 × q, 4H, *J* = 7 Hz, NCH_2), 4.26 (s, 6H, NCH_3), 1.69 (2 × t, 6H, *J* = 7 Hz, CH_3). ^{13}C NMR (75 MHz, 300 K, $CDCl_3$): δ 123.2 (NCH), 120.5 (NCH), 45.6 (NCH_2), 37.9 (NCH_3), 15.2 (CH_3). IR (neat): 3098 (w), 2972 (w), 1558 (w), 1455 (m), 1401 (m), 1256 (m), 1219 (s), 1085 (m), 954 (m), 796 (m), 732 (s), 697 (s) cm^{-1}. Anal. Calcd for $C_{12}H_{20}I_2N_4Ni$: C, 27.05; H, 3.78; N, 10.52. Found: C, 27.27; H, 3.49; N, 10.44. MS (ESI): *m*/*z* 446 ([M – I + MeCN]$^+$, 100%).

Bis(N-methyl-N′-phenylimidazol-2-ylidene)diiodidonickel(II) (3e). Following the general procedure, the compounds was obtained starting from 2.28 g imidazolium salt **1e** (8.0 mmol) and 0.71 g nickel(II) acetate (4.0 mmol) in 1.5 g tetrabutylammonium iodide at 155 °C. Yield: 0.73 g (29%). ^{1}H NMR (300 MHz, 300 K, $CDCl_3$): δ 8.28 (d, 4H, *J* = 8 Hz, Ar-H), 7.61 (t, 4H, *J* = 8 Hz, Ar-H), 7.49 (t, 2H, *J* = 8 Hz, Ar-H), 7.00 (d, 2H, *J* = 2 Hz, NCH), 6.84 (d, 2H, *J* = 2 Hz, NCH), 4.01 (s, 6H, NCH_3). ^{13}C NMR (75 MHz, 300 K, $CDCl_3$): δ 174.7 (Ni-C), 140.8 (C_q), 128.8 (C_{Ar}), 128.1 (C_{Ar}), 126.4 (C_{Ar}), 123.6 (NCH), 122.6 (NCH), 38.2 (NCH_3). IR (neat): 3129 (w), 1598 (w), 1497 (s), 1444 (m), 1403 (w), 1229 (m), 1069 (m), 915 (m), 759 (m), 724 (m), 690 (s), 623 (m), 547 (m) cm^{-1}. Anal. Calcd for $C_{20}H_{20}I_2N_4Ni$: C, 38.20; H, 3.21; N, 8.91. Found: C, 38.23; H, 3.00; N, 8.86. MS (ESI): *m*/*z* 542 ([M – I + MeCN]$^+$), 501 ([M – I]$^+$, 100%), 228 ([M – 2I + MeCN]$^{2+}$).

Bis(N-methyl-N′-isopropylbenzimidazol-2-ylidene)dibromidonickel(II) (4b). Following the general synthsis, the complex was obtained from 1.28 g benzimidazolium bromide **2b** (5.0 mmol) and 0.44 g nickel(II) acetate (2.50 mmol) in 0.8 g tetrabutylammonium bromide at 130 °C. Yield: 0.57 g (40%). ^{1}H NMR (300 MHz, 300 K, $CDCl_3$): δ 7.50 (m, 2H, Ar-H), 7.33-7.14 (m, 8H, Ar-H + NCH), 4.72 (2 × s, 6H, NCH_3), 1.95 (2 × d, 12H, *J* = 7 Hz, CH_3). ^{13}C NMR (75 MHz, 300 K, $CDCl_3$): δ 183 (Ni-C), 136.7 (C_q), 132.7 (C_q), 122.0 (C_{Ar}), 121.8 (C_{Ar}), 111.7 (C_{Ar}), 109.7 (C_{Ar}), 54.0 (NCH_3), 34.2 (NCH), 21.2 (CH_3). IR (neat): 2974 (w), 1484 (m), 1435 (m), 1386 (m), 1344 (m), 1293 (m), 1135 (m), 1092 (m), 780 (w), 744 (s), 564 (m) cm^{-1}. Anal. Calcd for $C_{22}H_{28}Br_2N_4Ni$: C, 46.60; H, 4.98; N, 9.88. Found: C, 46.55; H, 4.97; N, 9.79. MS (ESI): *m*/*z* 528 ([M – Br + MeCN]$^+$, 100%).

Bis(N-methyl-N′-isopropylbenzimidazol-2-ylidene)diiodidonickel(II) (4c). This complex was obtained following the general synthesis, starting from 0.50 g benzimidazolium salt **2c** (1.65 mmol) and 0.14 g nickel(II) acetate (0.82 mmol) in 0.4 g tetrabutylammonium iodide at 155 °C. Yield: 0.25 g (46%). ^{1}H NMR (300 MHz, 300 K, $CDCl_3$): δ 7.48 (m, 2H, Ar-H), 7.31 (m,

2H, Ar-H), 7.18 (m, 4H, Ar-H), 6.90 (m, 2H, NCH), 4.47 (2 × s, 6H, NCH_3), 1.91 (d, 12H, J = 7 Hz, CH_3). ^{13}C NMR (75 MHz, 300 K, $CDCl_3$): δ 188.0 (Ni-C), 137.4 (C_q), 133.1 (C_q), 121.8 (C_{Ar}), 121.7 (C_{Ar}), 111.7 (C_{Ar}), 109.5 (C_{Ar}), 54.0 (NCH_3), 34.4 (NCH), 20.4 (CH_3). IR (neat): 2975 (w), 1483 (w), 1436 (w), 1392 (m), 1351 (m), 1294 (m), 1137 (w), 1090 (m), 744 (s), 563 (m), 427 (m) cm^{-1}. Anal. Calcd for $C_{22}H_{28}I_2N_4Ni$: C, 39.98; H, 4.27; N, 8.48. Found: C, 39.85; H, 4.36; N, 8.26. MS (ESI): *m*/*z* 574 ([M – I + MeCN]$^+$, 100%).

Bis(N-methyl-N′-phenylbenzimidazol-2-ylidene)diiodidonickel(II) (4d). This complex was obtained following the general complex synthesis, starting from 0.20 g benzimidazolium salt **2d** (0.6 mmol) and 53 mg nickel(II) acetate (0.3 mmol) in 0.2 g tetrabutylammonium iodide at 155 °C. Yield: 0.14 g (63%). ^1H NMR (300 MHz, 300 K, $CDCl_3$): δ 8.17 (m, 4H, CH_{Ph}), 7.75 (m, 4H, CH_{Ph}), 7.67 (m, 2H, CH_{Ph}), 7.21 (m, 4H, CH_{Bim}), 7.13 (m, 4H, CH_{Bim}), 4.06 (s, 6H, NCH_3). ^{13}C NMR (75 MHz, 300 K, $CDCl_3$): δ 138.2 (C_q), 136.8 (C_q), 136.7 (C_q), 129.1 (C_{Ph}), 128.8 (C_{Ph}), 127.9 (C_{Ph}), 122.5 (C_{Bim}), 122.4 (C_{Bim}), 110.2 (C_{Bim}), 109.1 (C_{Bim}), 34.5 (NCH_3). IR (neat): 3054 (w), 1597 (w), 1500 (m), 1435 (m), 1389 (m), 1339 (m), 1231 (m), 1090 (m), 917 (w), 750 (s), 695 (s), 613 (m), 554 (m), 490 (m) cm^{-1}. Anal. Calcd for $C_{28}H_{24}I_2N_4Ni$: C, 46.13; H, 3.32; N, 7.69. Found: C, 46.07; H, 3.46; N, 7.72. ESI (MS): *m*/*z* 642 ([M – I + MeCN]$^+$, 100%).

Bis(N,N′-diisopropylbenzimidazol-2-ylidene)diiodidonickel(II) (4e). The compound was prepared following the general procedure, from 3.90 g N,N′-diisopropylbenzimidazolium iodide (11.8 mmol) and 1.04 g nickel(II) acetate (5.9 mmol) in 2.0 g tetrabutylammonium iodide at 155 °C. Yield: 1.26 g (30%). ^1H NMR (300 MHz, 300 K, $CDCl_3$): δ 7.48 (m, 4H, Ar-H), 7.12 (m, 4H, Ar-H), 6.93 (septet, 4H, J = 7 Hz, NCH), 1.88 (d, 24H, J = 7 Hz, CH_3). Due to the poor solubility, no ^{13}C NMR spectrum was recorded. IR (neat): 2976 (w), 1472 (m), 1417 (m), 1385 (m), 1343 (m), 1306 (m), 1139 (m), 1095 (m), 745 (s), 551 (m) cm^{-1}. Anal. Calcd for $C_{26}H_{36}I_2N_4Ni{\cdot}2H_2O$: C, 41.46; H, 5.35; N, 7.44. Found: C, 41.45; H, 5.01; N, 7.55. ESI (MS): *m*/*z* 630 ([M – I + MeCN]$^+$, 100%).

Typical procedure for the nickel-catalyzed hydrosilylation of internal alkynes. In a Schlenk tube at room temperature, 0.050 mmol nickel complex **3a** (25.2 mg) was dissolved/suspended in 5.0 mL dry THF and 1.0 mmol 3-hexyne (82.1 mg) was added. Then, 0.20 mmol diethylzinc (1.0 M in hexanes, 0.20 mL) was added with stirring, followed by 2.0 mmol triethylsilane (232.5 mg). The tube was then placed in an oil bath, preheated to 50 °C and the mixture was kept at this temperature. The reaction was followed by taking samples at regular intervals, which were quenched by the addition of ethanol and which were analyzed by GC. To isolate the product after full conversion was reached, water was added to the reaction mixture and the product was extracted using ethyl acetate. After drying of the organic layer with magnesium sulfate, and removal of the solvents *in vacuo*, the residue was purified by column chromatography (silica gel, hexanes) to give the product, which analyzed as 3-triethylsilyl-*cis*-hex-3-ene, as a colorless oil.[12] Yield: 186 mg (94%). In the hydrosilylation of diphenylacetylene, the product was purified by column chromatography (silica gel, petroleum ether), and obtained as a colorless oil, which analyzed as 1,2-diphenyl-1-triethylsilyl-*cis*-ethene.[12] Yield: 283 mg (96%). The mercury test was performed by the addition of 5.0 mmol mercury (1.0 g) to the reaction mixture, 30 minutes after the tube was transferred to the oil bath.

3.5 References

(1) Herrmann, W. A. *Angew. Chem.-Int. Edit.* **2002**, *41*, 1291.
(2) Marciniec, B. *Silicon Chem.* **2002**, *1*, 155.
(3) Langkopf, E.; Schinzer, D. *Chem. Rev.* **1995**, *95*, 1375.
(4) Trost, B. M.; Ball, Z. T. *Synthesis* **2005**, 853.
(5) Mori, A.; Takahisa, E.; Yamamura, Y.; Kato, T.; Mudalige, A. P.; Kajiro, H.; Hirabayashi, K.; Nishihara, Y.; Hiyama, T. *Organometallics* **2004**, *23*, 1755.
(6) Mas-Marza, E.; Poyatos, M.; Sanau, M.; Peris, E. *Inorg. Chem.* **2004**, *43*, 2213.
(7) Jimenez, M. V.; Perez-Torrente, J. J.; Bartolome, M. I.; Gierz, V.; Lahoz, F. J.; Oro, L. A. *Organometallics* **2008**, *27*, 224.
(8) Sridevi, V. S.; Fan, W. Y.; Leong, W. K. *Organometallics* **2007**, *26*, 1157.
(9) Kawanami, Y.; Sonoda, Y.; Mori, T.; Yamamoto, K. *Org. Lett.* **2002**, *4*, 2825.
(10) Trost, B. M.; Ball, Z. T. *J. Am. Chem. Soc.* **2005**, *127*, 17644.
(11) Tsipis, C. A. *J. Organomet. Chem.* **1980**, *188*, 53.
(12) Chauhan, M.; Hauck, B. J.; Keller, L. P.; Boudjouk, P. *J. Organomet. Chem.* **2002**, *645*, 1.
(13) De Bo, G.; Berthon-Gelloz, G.; Tinant, B.; Marko, I. E. *Organometallics* **2006**, *25*, 1881.
(14) Tillack, A.; Pulst, S.; Baumann, W.; Baudisch, H.; Kortus, K.; Rosenthal, U. *J. Organomet. Chem.* **1997**, *532*, 117.
(15) Yong, L.; Kirleis, K.; Butenschon, H. *Adv. Synth. Catal.* **2006**, *348*, 833.
(16) Takahashi, T.; Bao, F. Y.; Gao, G. H.; Ogasawara, M. *Org. Lett.* **2003**, *5*, 3479.
(17) Chalk, A. J.; Harrod, J. F. *J. Am. Chem. Soc.* **1965**, *87*, 16.
(18) Chaulagain, M. R.; Mahandru, G. M.; Montgomery, J. *Tetrahedron* **2006**, *62*, 7560.
(19) Huynh, H. V.; Holtgrewe, C.; Pape, T.; Koh, L. L.; Hahn, E. *Organometallics* **2006**, *25*, 245.
(20) McGuinness, D. S.; Mueller, W.; Wasserscheid, P.; Cavell, K. J.; Skelton, B. W.; White, A. H.; Englert, U. *Organometallics* **2002**, *21*, 175.
(21) Starikova, O. V.; Dolgushin, G. V.; Larina, L. I.; Ushakov, P. E.; Komarova, T. N.; Lopyrev, V. A. *Russ. J. Organ. Chem.* **2003**, *39*, 1467.
(22) Huynh, H. V.; Wong, L. R.; Ng, P. S. *Organometallics* **2008**, *27*, 2231.
(23) Herrmann, W. A.; Gerstberger, G.; Spiegler, M. *Organometallics* **1997**, *16*, 2209.
(24) Han, Y.; Huynh, H. V.; Koh, L. L. *J. Organomet. Chem.* **2007**, *692*, 3606.
(25) Asao, N.; Sudo, T.; Yamamoto, Y. *J. Org. Chem.* **1996**, *61*, 7654.
(26) Kiso, Y.; Kumada, M.; Maeda, K.; Sumitani, K.; Tamao, K. *J. Organomet. Chem.* **1973**, *50*, 311.
(27) Blakey, S. B.; MacMillan, D. W. C. *J. Am. Chem. Soc.* **2003**, *125*, 6046.
(28) Sato, Y.; Sawaki, R.; Mori, M. *Organometallics* **2001**, *20*, 5510.
(29) Tekavec, T. N.; Zuo, G.; Simon, K.; Louie, J. *J. Org. Chem.* **2006**, *71*, 5834.
(30) Benson, S.; Payne, B.; Waymouth, R. M. *J. Polym. Sci. Pol. Chem.* **2007**, *45*, 3637.
(31) Corriu, J. P.; Masse, J. P. *J. Chem. Soc.-Chem. Commun.* **1972**, 144.
(32) Tamao, K.; Sumitani, K.; Kumada, M. *J. Am. Chem. Soc.* **1972**, *94*, 4374.
(33) Meals, R. N. *J. Am. Chem. Soc.* **1946**, *68*, 1880.
(34) Sato, A.; Kinoshita, H.; Shinokubo, H.; Oshima, K. *Org. Lett.* **2004**, *6*, 2217.
(35) Alonso, F.; Osante, I.; Yus, M. *Tetrahedron* **2007**, *63*, 93.
(36) Houdayer, A.; Schneider, R.; Billaud, D.; Ghanbaja, J.; Lambert, J. *Synth. Met.* **2005**, *151*, 165.
(37) Whitesides, G. M.; Hackett, M.; Brainard, R. L.; Lavalleye, J.; Sowinski, A. F.; Izumi, A. N.; Moore, S. S.; Brown, D. W.; Staudt, E. M. *Organometallics* **1985**, *4*, 1819.
(38) Widegren, J. A.; Finke, R. G. *J. Mol. Catal. A-Chem.* **2003**, *198*, 317.
(39) Weddle, K. S.; Aiken, J. D.; Finke, R. G. *J. Am. Chem. Soc.* **1998**, *120*, 5653.
(40) Boudjouk, P.; Han, B. H.; Jacobsen, J. R.; Hauck, B. J. *J. Chem. Soc.-Chem. Commun.* **1991**, 1424.
(41) Lappert, M. F.; Takahashi, S. *J. Chem. Soc.-Chem. Commun.* **1972**, 1272.
(42) Lappert, M. F.; Nile, T. A.; Takahashi, S. *J. Organomet. Chem.* **1974**, *72*, 425.
(43) Huang, Y. Z.; Miao, H.; Zhang, Q. H.; Chen, C.; Xu, J. *Catal. Lett.* **2008**, *122*, 344.

(44) Phillips, M. A. *J. Chem. Soc.* **1929**, *131*, 2820.
(45) Kondo, Y.; Izawa, S.; Kusabayashi, S. *J. Chem. Soc.-Perkin Trans. 2* **1988**, 1925.
(46) Lancaster, N. L.; Salter, P. A.; Welton, T.; Young, G. B. *J. Org. Chem.* **2002**, *67*, 8855.

Chapter 4

Synthesis of novel chelating benzimidazole-based carbenes and their nickel(II) complexes; activity in the Kumada coupling reaction†

Abstract. *Nickel(II) halide complexes of novel chelating bidentate benzimidazole-based N-heterocyclic carbenes have been prepared from $Ni(OAc)_2$ and bisbenzimidazolium salts. Single-crystal X-ray structure determination on four complexes revealed a cis-geometry on a square-planar nickel center. The complexes are active catalysts for the Kumada coupling of 4-chloroanisole and 4-bromoanisole with phenylmagnesium chloride. The most active catalyst gives a complete conversion of 4-bromoanisole within 75 minutes with a selectivity to 4-methoxybiphenyl of 82% and a complete conversion of 4-chloroanisole in less than 14 hours with a selectivity to 4-methoxybiphenyl of 99%.*

† Based on J. Berding, M. Lutz, A. L. Spek, E. Bouwman, *Organometallics*, **2009**, *28*, 1845.

4.1 Introduction

Since the first isolation of a stable, free N-heterocyclic carbene (NHC) by Arduengo in 1991,[1] complexes with NHC ligands have found application in a wide variety of homogeneous catalysts. The strong σ-donating properties of carbenes have often been compared to those of phosphane ligands, which are known to stabilize various oxidation states of a transition metal in a catalytic cycle. Ligand dissociation, a known occurrence in phosphane complexes, is less likely to take place when NHCs are used instead.[2, 3] Some excellent reviews have been published on the development and use of NHCs.[4-6] Research has been focused mainly on replacing phosphane ligands in known catalytic systems; well known is the second generation Grubbs' catalyst with one NHC and one phosphane ligand, which showed a large improvement in reactivity and stability compared to the first-generation catalyst bearing two phosphane ligands.[7] Recently, in our group, nickel complexes with bidentate phosphane ligands were found to be active homogeneous catalysts in alkene hydrogenation.[8, 9] Inspired by this discovery, it was decided to investigate the catalytic activity of nickel complexes with bidentate carbene ligands.

Carbon-carbon bond formation is one of the most important transition-metal catalyzed reactions in organic synthesis. Cross-coupling reactions between aryl halides or aryl triflates and aryl–M (M = $B(OR)_2$, SnR_3, SiR_3, MgX) leading to the formation of biaryl derivatives have been investigated extensively.[10-12] Palladium often yields the most efficient catalyst, showing good activity in a variety of C–C coupling reactions. Some nickel complexes are known to be efficient C–C coupling catalysts as well, both with monodentate and chelating phosphane ligands.[13-17] However, only a few nickel complexes with N-heterocyclic carbene ligands have been reported as catalysts in aryl-aryl coupling reactions.[18-21] It was decided to focus on the coupling of Grignard reagents with aryl halides, a reaction that was reported independently by both Kumada and Corriu in 1972.[13, 22] Aryl-aryl coupling reactions utilizing aryl boronic acids, stannanes and silicon and zinc derivatives have a better functional group tolerance and have been studied in more detail. However, often their starting compounds are less reactive and have to be prepared from the Grignard or organolithium precursor. The advantage of the Kumada reaction is therefore the elimination of one synthetic step. Two systems based on nickel compounds in combination with imidazolium salts have been reported to catalyze the Kumada reaction. The nickel NHC complex is presumed to be formed *in situ*;[23-25] other systems make use of preformed nickel complexes.[26-29]

The study described in this chapter focused on nickel complexes of the type (bisNHC)NiX_2, in which bisNHC is a *chelating* bidentate bis(imidazol-2-ylidene) ligand. In literature a number of attempts to obtain this type of complex with two halide anions has been reported to be unsuccessful, leading only to intractable reaction mixtures,[30] or to homoleptic $[(bisNHC)_2Ni]^{2+}$ complexes.[31, 32] A successful attempt by Baker *et al.* resulted in the synthesis of a nickel complex (**I**) derived from an imidazolium-linked *ortho*-cyclophane (Figure 4.1).[33] Douthwaite *et al*. were able to prepare two types of bisNHC nickel complexes; one bearing an additional PMe_3 ligand,[34] the other a bisNHC nickel

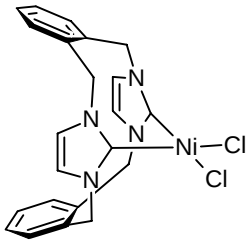

I

Figure 4.1. *cis*-(BisNHC) nickel complex prepared by Baker *et al.*[33]

complex with two methyl ligands.[30] One bisNHC dihalido complex has been reported with a very long bridging moiety leading to a *trans* geometry.[35]

Recently, Hahn *et al.*, who described the first benzimidazole-based free carbene in 1999,[36] reported the successful synthesis of a dihalido nickel complex bearing two monodentate bis(benzimidazol-2-ylidene) ligands.[37] In this chapter the synthesis and characterization of new dihalido nickel complexes of novel chelating bisNHC ligands are described. These compounds are efficient catalysts for the Kumada coupling reaction of aryl chlorides and bromides with aryl magnesium chloride under mild conditions.

4.2 Results and Discussion

4.2.1 Preparation of Alkyl-Bridged Bisbenzimidazolium Salts

Bisbenzimidazolium salts are relatively unknown, compared to the widely used alkyl-bridged bisimidazolium salts. Both may be obtained by quaternization of an

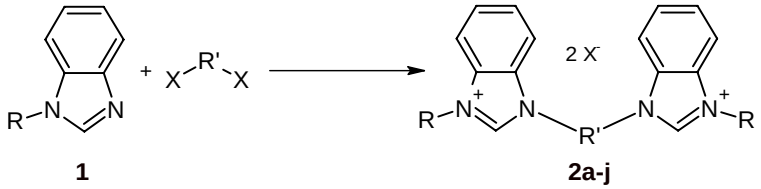

1 **2a-j**

2a R = Me, R' = 1,3-propyl, X = Br
2b R = Me, R' = 1,3-propyl, X = Cl
2c R = Pr, R' = 1,3-propyl, X = Br
2d R = ^{i}Pr, R' = 1,3-propyl, X = Br
2e R = Bn, R' = 1,3-propyl, X = Br
2f R = Ph, R' = 1,3-propyl, X = Br
2g R = Me, R' = 1,4-butyl, X = Br
2h R = Me, R' = 1,4-butyl, X = Cl
2i R = Me, R' = 1,1'-$SiMe_4$, X = Cl
2j R = Me, R' = α,α'-*o*-xylyl, X = Br

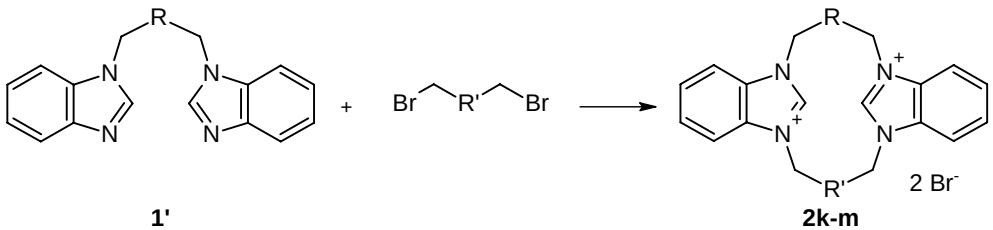

1' **2k-m**

2k R = R' = *o*-C_6H_4
2l R = *o*-C_6H_4, R' = C_2H_4
2m R = *m*-C_6H_4, R' = C_2H_4

Scheme 4.1. Bisbenzimidazolium salts described in this chapter.

N-substituted (benz)imidazole with a dihaloalkane,[38] or by reacting a bridged di(benz)imidazole with two equivalents of an alkyl halide.[39] In this study dihaloalkanes were reacted with an excess of N-substituted benzimidazoles **1** in hot 1,4-dioxane to furnish the bridged bisbenzimidazolium salts **2a-j** shown in Scheme 4.1. 1,4-Dioxane was chosen as a solvent instead of the more commonly used THF, because it can be used at higher temperatures, thus reducing reaction times. The white bisbenzimidazolium salts **2a-j** were obtained in good yields and high purity. Cyclic salts **2k** and **2l** were prepared according to literature procedures by reaction of 1,1′-(α,α′-*o*-xyxyl)dibenzimidazole with α,α′-dibromo-*o*-xylene, or 1,4-dibromobutane, respectively.[39, 40] Similarly, **2m** was obtained by treating 1,1′-(α,α′-*m*-xylyl)dibenzimidazole with excess 1,4-dibromobutane under high dilution conditions.

The ^{1}H and ^{13}C NMR spectra of the bisbenzimidazolium salts in DMSO-d_6 show the characteristic resonances of the benzimidazolium N*CH*N proton and carbon downfield at around 10 and 140 ppm, respectively.[41] The iodide salts of **2a**,[42] **2g**,**h**,**j**,[39] and the chloride salt of **2e**,[43] are known in literature and our findings are consistent with the reported NMR data.

4.2.2 Preparation of Nickel Complexes.

McGuinness *et al.*[44] developed a method in which imidazolium iodides bearing small N-substituents were melted and reacted directly with $Ni(OAc)_2$ *in vacuo* to yield the corresponding $Ni(NHC)_2I_2$ complexes. The melting points of the larger azolium salts,

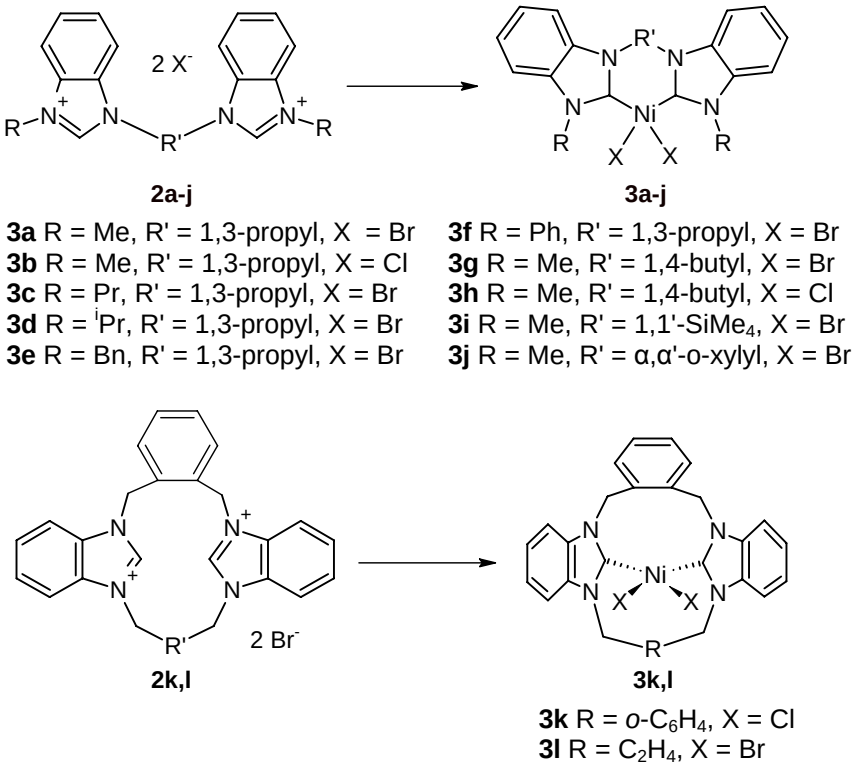

Scheme 4.2. Nickel(II) bisNHC complexes prepared in this study.

however, are too high for this procedure, resulting in decomposition. This problem was overcome for the benzimidazolium salts by adding another non-reactive, low-melting salt (tetrabutylammonium iodide or bromide) to the reaction mixture as an ionic liquid solvent.[37] This allowed the use of lower reaction temperatures (120 °C) and afforded the nickel complexes in good yield. The latter method has been used in this study to obtain dihalidonickel complexes with chelating bisbenzimidazol-2-ylidene ligands (**3a-j**,**3l**, Scheme 4.2).

Nickel complexes **3a-j** and **3l** were obtained as yellow solids after trituration of the reaction mixture with water to remove the tetrabutylammonium salt and unreacted starting material. Further purification was accomplished by dissolving the crude product in dichloromethane and washing with water and brine. Unfortunately, treatment of **2m** with $Ni(OAc)_2$ under the same conditions did not yield any isolable complex. Compound **3h** is soluble in water and work-up was performed omitting the filtration after trituration with water. All complexes are stable towards air and moisture and are soluble in dichloromethane, acetonitrile and DMSO, sparingly soluble in THF and insoluble in diethyl ether and hexane. In the synthesis of **3g** and **3h** a more diluted reaction mixture was used to avoid the formation of polynuclear species. The reaction of **2i** with nickel acetate in tetrabutylammonium chloride did not give a stable isolable product. Alternatively, it was reacted in tetrabutylammonium bromide with potassium bromide added to ensure the presence of a large excess of bromide anions. From this mixture the nickel bromide complex **3i** could be obtained. Treatment of cyclic bisbenzimidazolium salt **2k** with KPF_6 in methanol furnished the corresponding hexafluoridophosphate salt which was subsequently reacted with $NiCl_2$ and NaOAc in DMF, following the synthetic procedure reported by Baker *et al*. for cyclophane-based nickel complex **I**.[33] This yielded the corresponding dichloridonickel complex **3k** as a yellow solid.

Initially, a satisfactory elemental analysis could not be obtained for a number of dibromide complexes. Potentiometric titration of a solution of the analytical samples of two of these complexes with silver nitrate revealed that during the washing with brine the bromide anions were replaced by chlorides. The elemental analyses were consistent with the Cl : Br ratios thus found. Therefore, in stead of the final washing with brine, the dichloromethane solutions of the bromide complexes were washed with a sodium bromide solution. The elemental analyses of the complexes thus obtained were consistent with a dibromido formulation. The elemental analyses of complexes obtained before the extraction were unsatisfactory due to the presence of varying amounts of tetrabutylammonium salts.

The square-planar low-spin nickel complexes are diamagnetic and give rise to clear ^{1}H and ^{13}C NMR spectra. With the exception of shifts of the signals of the bridging moieties, there are only minor changes in the ^{1}H NMR spectra compared to the benzimidazolium salts. The benzimidazolium NC*H*N is absent in the ^{1}H NMR spectra of the complexes, confirming carbene generation. A representative example, the ^{1}H NMR spectra of bisbenzimidazolium salt **2a** and nickel complex **3a**, is depicted in Figure 4.2. Due to conformational constraints and possibly interaction with the nickel center the

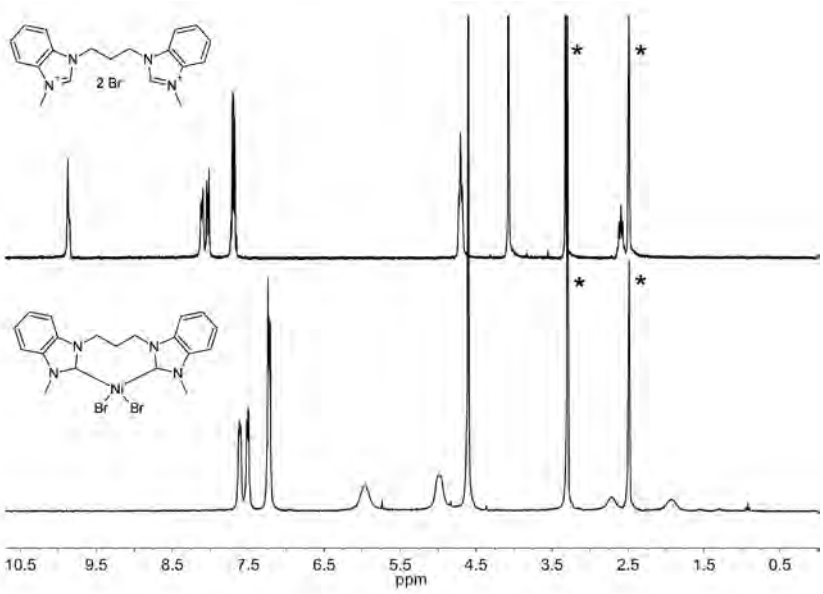

Figure 4.2. ^{1}H NMR spectra of bisbenzimidazolium salt **2a** and complex **3a**. Peaks marked with (*) are solvent signals.

resonances of the bridging moieties are split over a range up to 2.1 ppm for the o-xylyl bridged complex **3j**. The splitting of the resonances of bridges of the cyclic bisNHC ligands are even larger; for **3k** the splitting is about 2.6 ppm (as was observed for **I**)[33], while for **3l** this is also 2.1 ppm. As an example, the ^{1}H COSY NMR spectrum of **3l**, which was used to assign the resonances of the bridges, is shown in Figure 4.3. Unfortunately, due to peak broadening the carbene–C resonance could not be observed in the ^{13}C NMR spectra for all complexes.

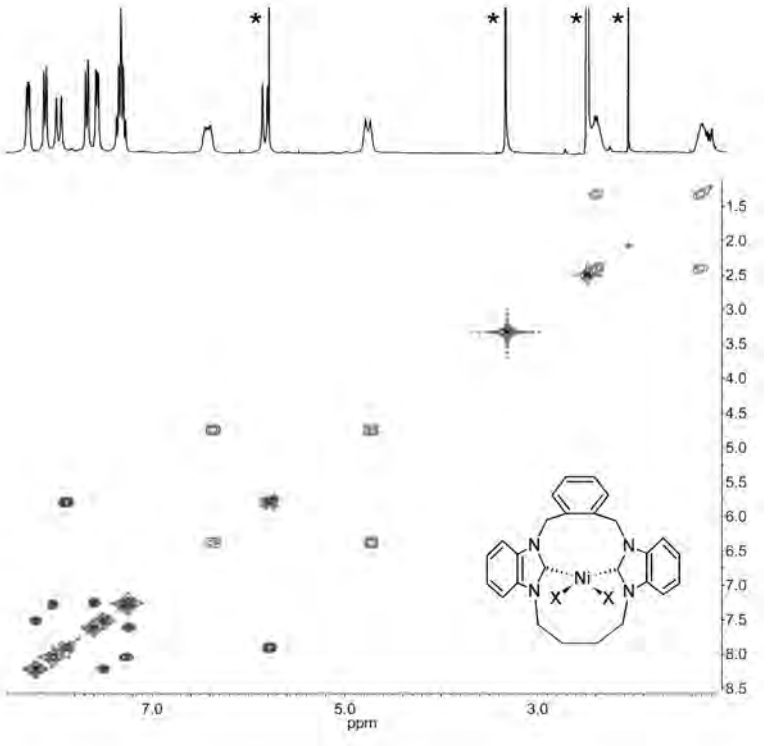

Figure 4.3. ^{1}H COSY NMR spectrum of complex **3l**. Peaks marked with (*) are solvent signals.

4.2.3 Description of the structures

Dark yellow single crystals of **3a**, **3e**, **3g** and **3i** were obtained from dichloromethane/acetonitrile or dichloromethane/diethyl ether solutions by slow evaporation, and their molecular structures were determined by X-ray diffraction. Molecular plots of **3a**, **3e**, **3g** and **3i** are shown in Figure 4.4 and selected bond distances and angles are collected in Table 4.1. All complexes show a *cis*-geometry around a slightly distorted square-planar nickel center, with the two bromide ions twisted out of the C_2Ni plane by 5.3(3) to 9.9(2) degrees. The coordination bond lengths in the four complexes are rather similar and the Ni-C distances are only slightly shorter than those reported for the related *trans*-[Ni(NHC)$_2$Br$_2$] (NHC = 1,3-dipropylbenzimidazol-2-ylidene).[37] The C12–Ni–C22 bite angle changes slightly upon lengthening of the bridging moiety, from 85.8(2)° for the propyl bridge to 91.0(2)° for the butyl bridge. Compared to the chelating phosphanes, where every additional carbon in the chain leads to an increase in bite angle of 8 – 10°, this is a relatively small difference.[34] This smaller effect in the bite angle is due to the angle at which the benzimidazole rings are twisted relative to the coordination plane (Table 4.1). On average, the ligands with a longer bridge have their benzimidazole rings closer to a plane perpendicular to the plane of coordination, as was observed in a palladium analogue,[45] and a rhodium di(imidazol-2-ylidene) complex with

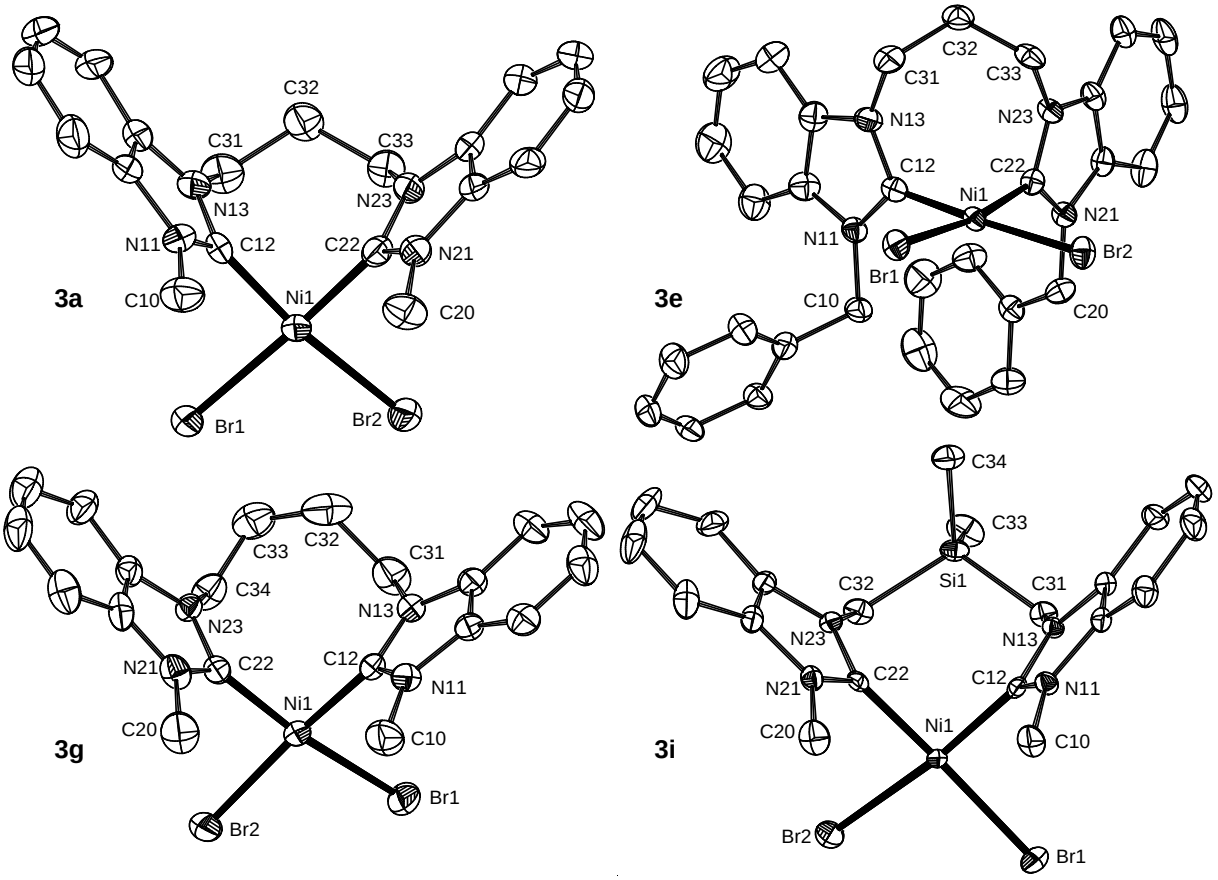

Figure 4.4. Displacement ellipsoid plots of **3a**, **3e**, **3g** and **3i** at the 50% probability level. Hydrogen atoms and solvent molecules are omitted for clarity.

Table 4.1. Selected Bond Lengths (Å) and Angles (deg) for complexes **3a**, **3e**, **3g** and **3i**

	3a	**3e**	**3g**	**3i**
Ni–Br1	2.3545(10)	2.3400(9)	2.3491(8)	2.3383(4)
Ni–Br2	2.3568(10)	2.3447(10)	2.3384(8)	2.3516(4)
Ni–C12	1.859(6)	1.863(6)	1.867(5)	1.872(2)
Ni–C22	1.859(6)	1.861(6)	1.860(5)	1.865(2)
N11–C12	1.369(8)	1.346(8)	1.350(6)	1.353(3)
N13–C12	1.343(8)	1.367(8)	1.346(6)	1.355(3)
N21–C22	1.368(8)	1.368(8)	1.359(6)	1.354(3)
N23–C22	1.341(8)	1.345(8)	1.364(6)	1.354(3)
Br1–Ni–Br2	95.95(4)	95.09(4)	94.26(3)	95.039(14)
C12–Ni–C22	85.8(2)	85.9(3)	91.0(2)	89.51(10)
C12–Ni–Br1	90.27(17)	90.50(17)	85.32(14)	90.47(7)
C22–Ni–Br2	88.20(18)	88.54(18)	90.28(14)	85.37(7)
N11–C12–N13	106.6(5)	106.9(5)	106.6(4)	106.5(2)
N21–C22–N23	106.9(5)	106.4(5)	105.5(4)	106.9(2)
NiC_2 / carbene	84.4(4)	81.7(4)	88.1(3)	85.80(14)
dihedral angle[a]	83.5(5)	84.5(3)	86.8(3)	85.82(15)
T_d twist[b]	5.3(3)	8.8(3)	9.9(2)	6.76(11)

[a] NiC_2 / Carbene dihedral angle = angle between LS planes; one through the imidazole ring; one through Ni–C12–C22; [b] T_d twist = angle between LS planes through Br1–Ni–Br2 and C12–Ni–C22.

bridges of varying lengths.[46]

Although a plane of symmetry is present in the free ligands, in all cases the complexes crystallized asymmetrically due to packing effects. The benzimidazole moieties are twisted out of the plane perpendicular to the C_2Ni plane by a few degrees, as mentioned before. These are, however, twisted to a different degree, leading to two values for the NiC_2 / carbene dihedral angle as shown in Table 4.1.

In the crystal structure of complex **3g** the C_4 bridge is asymmetric, as exemplified by the difference in torsion angles around the C31–C32 (eclipsed, –124.0(5)°) and the C34–C33 (staggered, 51.6(7)°) bonds. This leads to a weak anagostic interaction between the nickel and one of the NCH_2 hydrogens (d(H–M) = 2.65 Å, θ(C–H–M) = 117°).[47] A similar asymmetry is also observed in the structure of a related palladium complex (1,1'-dimethyl-3,3'-(1,4-butanediyl)diimidazol-2,2'-diylidene)palladium(II) chloride.[48] The bridges in **3a, 3e** and **3i** show staggered conformations along their C31–C32, C33–C32 and C31–Si1, C31–Si1 bonds, as expected.

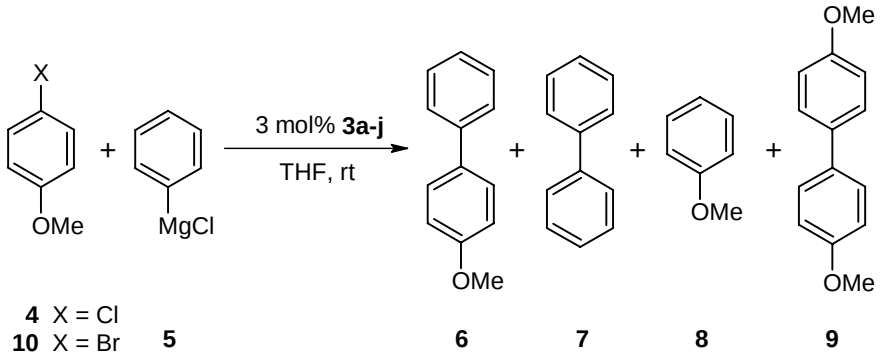

Scheme 4.3. Nickel-catalyzed Kumada coupling of 4-haloanisole and phenylmagnesium chloride.

4.2.4 Catalytic studies

Complexes **3a-j** were tested as catalysts in the coupling of 4-chloro- and 4-bromoanisole with phenylmagnesium chloride (Scheme 4.3). Apart from the desired product 4-methoxybiphenyl (**6**), varying amounts of biphenyl (**7**), anisole (**8**) and bisanisole (**9**) are observed in the reaction mixtures. The activity for the different catalysts – given as the time needed to consume all starting aryl halide – and the yields (in mmol) of the various products are summarized in Table 4.2 and Table 4.3. The total amount of product varies, due to the excess of Grignard reagent used and the fact that unreacted Grignard reagent could not be detected by GC analysis. The total amount of **6** and **8** plus twice the amount of **9** should be equal to 1 mmol; the amount of **7** should not exceed half the amount of Grignard reagent that was not used in the formation of **6**, which is equal to 0.5 × (1.5 mmol – the amount of **6**). Within experimental error, both requirements are met in all catalytic runs. As an example, a plot of the evolution in time of the substrate and products in a typical catalytic experiment starting from 4-bromoanisole and using **3j** as catalyst is shown in Figure 4.5. In this case the reaction starts immediately, whereas with some of the catalysts a short induction time is observed. The amounts of the byproducts

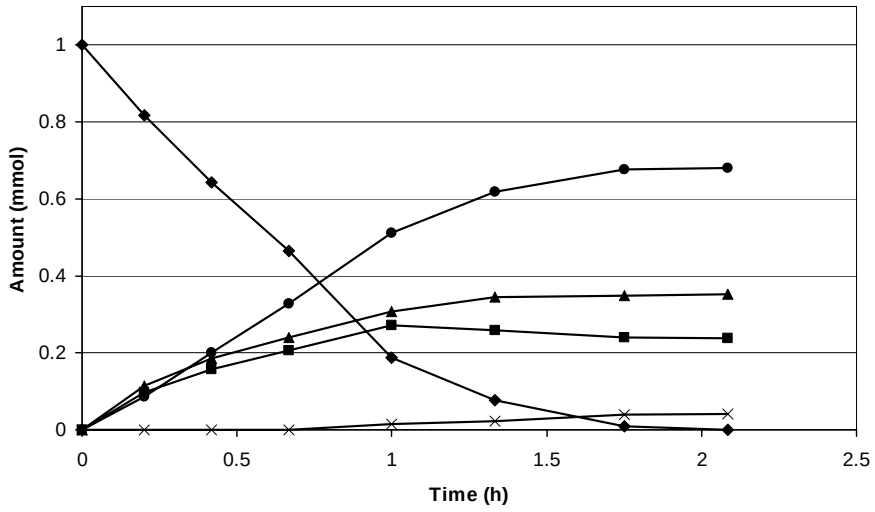

Figure 4.5. Evolution of the products in time of a typical catalytic experiment (Table 4.3, entry 3). (♦) 4-bromoanisole; (●) 4-methoxybiphenyl; (▲) biphenyl; (■) anisole; (×) bisanisole.

Table 4.2. Nickel-catalyzed Kumada cross-coupling of 4-chloroanisole and phenylmagnesium chloride at room temperature.[a]

Entry	Complex	Time to completion (h)	Yield (10^{-2} mmol) [b]			
			6	**7**	**8**	**9**
1	**3a**	37	85	18	3	6
2	**3b**	35	83	16	3	7
3	**3c**	18	88	13	6	3
4	**3d**	15	82	25	1	7
5	**3e**	<14	99 (93)	4	0	0
6	**3f**	18	75	37	13	8
7	**3g**	16	99 (91)	7	0	0
8	**3h**	18	99	8	0	0
9	**3i**	25	92	18	3	3
10	**3j**	15	80	27	6	7
11	$Ni(acac)_2$ + IPr·HCl [c]	18	71	16	1	9
12	(C^P)$NiBr_3$ [d]	18	95	19	0	1

[a] Reaction conditions: 1.0 mmol 4-chloroanisole, 1.5 mmol phenylmagnesium chloride (25 w% in THF), 0.03 mmol catalyst, 1 mL THF, room temperature; [b] GC yields, average of two runs. Isolated yield in parentheses; [c] 81% conversion after 18 h, ref. 23; [d] 96% conversion after 18 h, ref. 24.

biphenyl and anisole increase in the first hour, but then stabilize to the final composition, while the conversion of the substrates to the desired product continues. Bisanisole is not detected in the first 45 minutes of the reaction.

All the new complexes **3a-j** are able to catalyze the coupling of 4-chloroanisole with phenylmagnesium chloride (Table 4.2); however, the rate and the selectivity depend to a large extent on the complex used. Full conversion is achieved in less than 14 hours (entry 5) up to 37 hours (entry 2), furnishing the desired product in 75% (entry 6) to nearly quantitative yields (entries 5, 7 and 8). The halide anion present in the starting nickel complex does not have an effect on the rate and the selectivity of the reaction, as **3a** and **3b** (entries 1 and 2) give the same results, within experimental error, as do **3g** and **3h** (entries 7 and 8). The various N-substituents of the ligands do have an effect on the rate and selectivity of the catalysts (entries 1 and 3-6). The rate of the reaction decreases in the order Bn > ^{i}Pr > Pr = Ph > Me. The selectivity towards the desired product 4-methoxybiphenyl decreases in the order Bn > Pr > Me ≥ ^{i}Pr > Ph. The influence of the bridging moiety can be established from a comparison of the results of complexes **3a,h-j** (entries 1 and 7-10) as these complexes only differ in the bridging part. For this series of complexes the time necessary to complete the reaction increases in the order o-Xy < Bu < Si < Pr. The selectivity towards 4-methoxybiphenyl decreases in the order Bu > Si > Pr > o-Xy. The most efficient catalyst for the coupling of 4-chloroanisole and phenylmagnesium chloride thus found in this study is complex **3e**, which has both the highest rate and the highest selectivity towards the desired product. The observed influence of the substituents of the ligand on the rate of the reaction seems to correlate with the bulkiness

Table 4.3. Nickel-catalyzed Kumada cross-coupling of 4-bromoanisole and phenylmagnesium chloride at room temperature.[a]

Entry	Complex	Time to completion (h)	Yield (10^{-2} mmol) [b]			
			6	**7**	**8**	**9**
1	**3a**	1.25	72	39	19	3
2	**3b**	1.25	68	39	25	4
3	**3c**	1.5	70	35	23	4
4	**3d**	4.5	71	33	23	4
5	**3e**	1.25	82	27	12	4
6	**3f**	1.5	76	38	13	5
7	**3g**	6.5	70	37	19	6
8	**3h**	8	69	35	20	5
9	**3i**	1.5	76	34	16	5
10	**3j**	1.25	76	38	12	5
11	**3k** [c]	50	33	33	10	1
12	**3l** [d]	90	59	41	15	1
13	**I** [e]	68	80	25	4	2

[a] Reaction conditions: 1.0 mmol 4-bromoanisole, 1.5 mmol phenylmagnesium chloride (25 w% in THF), 0.03 mmol catalyst, 1 mL THF, room temperature; [b] GC yields, average of two runs; [c] 43% conversion after 50 h; [d] 74% conversion after 90 h; [e] 88% conversion after 68 h.

of the side group. It appears that the side groups having more bulk close to the nickel center favor the rate of the reaction. A possible added effect of the benzyl side groups of complex **3e** may be that these may have a stacking interaction with the reagents. This effect is not observed with the phenyl substituents of complex **3f** because these point away from the nickel center and are not flexible enough to move closer to the reaction center. The order observed in the influence of the bridging moiety on the rate shows that the reaction rate benefits from longer and more rigid bridges.

The complexes **3a-j** are also active catalysts in the coupling of 4-bromoanisole; the effect of the better leaving group is reflected in the higher rates as compared to the reaction with the aryl chloride (Table 4.3). Again, the rate of the reaction and the composition of the final mixture differ depending on the ligand structure, whereas the influence of the halide anion in the starting complex is negligible. Seven of the complexes are able to complete the reaction within 90 minutes. Only the isopropyl-substituted complex **3d** and the butyl-bridged complexes **3g**,**h** require more time to bring the reaction to completion. The selectivity towards the desired product **6** ranges from 68 to 82%. A comparison of different ligands shows that the N-substituents of the carbene ligands do not have a large influence on the course of the reaction; all yield roughly the same selectivity around 70%, with the benzyl group as a positive exception with 82% (entry 5). The bridging group does not appear to have a large influence on the selectivity. The positive exception here is the Si-bridged complex **3i**, with a selectivity of 76% (entry 9).

It appears that in the case of 4-bromoanisole the rate decreases when bulkier side

groups and longer bridges are used. For example, the lower rate of **3d** (Table 4.3, entry 4) may be attributed to the steric bulk of the isopropyl substituents on the ligand, which makes it more difficult for the reagents to approach the metal center. The high rate observed with complex **3e** may again be explained by stacking interaction of the benzyl substituents with the reagents. The slowest reaction is observed with complexes **3g** and **3h** (entries 7 and 8), which both contain the butyl-bridged ligand. Here, the lower rate may be a consequence of a difference in bite angle, even though the solid-state structure of **3g** has a bite angle that is only slightly larger compared to the other complexes. During the catalytic cycle, however, it is probable that the complex with the longer bridge adopts a conformation that could hinder the reaction. The bridge of **3j** is based on a four-carbon chain as well; however, the rigidity of the xylyl group may prevent the proposed unfavorable conformation.

A preliminary study showed that a reaction using the even more reactive 4-iodoanisole under the same conditions is completed in less than 10 minutes.

In addition to the bisNHC complexes described in catalysis above, nickel(II) complexes with macrocyclic bisNHC ligands (**3k**, **3l**) and the nickel cyclophane compound **I** reported by Baker *et al.*,[33] were tested in the Kumada coupling of 4-bromoanisole, with the conditions used with the other bisNHC complexes. The results are included in Table 4.3. Unfortunately, these macrocyclic complexes are remarkably inactive in this reaction. For instance, complex **I** gave only 88% conversion of the starting aryl bromide to the desired product after 68 hours.

Numerous reports in literature describe the cross coupling of aryl halides and aryl Grignard reagents.[49-54] Unfortunately, making a comparison of the results is difficult, because of the various reaction conditions employed and the use of aryl halides and aryl Grignards with different substituents. In this study the reaction conditions used by Böhm *et al***.** and Wolf *et al*. are followed, making it possible to compare our results to theirs.[23-25] Böhm *et al*.[23] obtained the highest rate and selectivity with $Ni(acac)_2$ *in situ* combined with the monodentate, bulky imidazolium salt N,N'-bis(2,6-diisopropyl-phenyl)imidazolium chloride (IPr·HCl). Wolf *et al*.[24, 25] used zwitterionic nickel(II) complexes with a phosphane ligand linked to an imidazolium group ((C^P)$NiBr_3$). The results of the most efficient catalysts of both reports are included in Table 4.2 (entries 11 and 12). Unfortunately, only the compositions of the reaction mixtures after 18 hours are reported, even though kinetic studies performed by Wolf *et al.* show that a conversion of 95% was reached within two hours. It appears therefore that our fastest catalysts (**3e** and **3j**, Table 4.2, entry 5 and 10) are more active than the Böhm system and less active than the fastest catalyst reported by Wolf. However, the most efficient catalyst in our work, **3e** (Table 4.2, entry 5) shows a higher selectivity for the desired cross-coupling product.

To test the stability of our catalyst type, a catalyst of average performance was chosen. Complex **3i** was used as catalyst for the coupling of 4-bromoanisole and phenylmagnesium chloride as in the other catalytic reactions. After GC analysis had shown full consumption of 4-bromoanisole, new substrates (1.0 mmol 4-bromanisole and

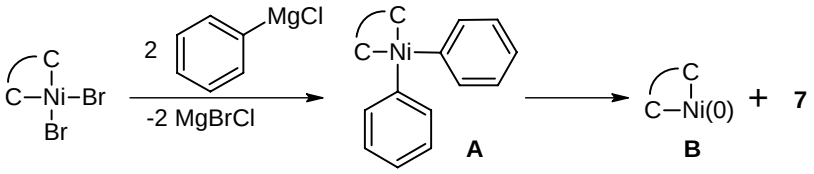

Scheme 4.4. Activation of catalyst precursor **3**.

1.5 mmol Grignard reagent in 0.78 mL THF) were added. This was repeated 7 times over a period of 140 hours. The catalyst was found to be able to complete the reaction every time, indicating excellent stability. This resulted in a total turnover number of 230 mol [mol cat]$^{-1}$, although the final batch took 10 hours to reach complete conversion. This lowering of the rate is most likely due to the accumulation of large amounts of product and magnesium salts, causing a substantial change in polarity and concentration of the reaction mixture.

4.2.5 Mechanistic considerations

While monitoring the reaction of 4-chloroanisole with phenylmagnesium chloride by GC, it was observed that most of the biphenyl present at the end of the reaction had formed within the first ten minutes. This is in agreement with the mechanism leading to the active Ni(0) species as proposed by Kumada,[55] which results in biphenyl as a byproduct.[56] The proposed mechanism, adapted to the present catalytic system, is shown in Scheme 4.4. In the first step the two bromide ions of the precatalyst are replaced by phenyl groups of the Grignard reagent by transmetalation, yielding species **A**, which in the second step yields the active Ni(0) species **B** and biphenyl by reductive elimination. After activation the catalytic cycle (shown in Scheme 4.5) is followed as proposed in literature:[55] Oxidative addition of the 4-haloanisole yields species **C**, which undergoes a transmetalation step with the Grignard reagent to give bisaryl species **D**. Reductive elimination of 4-methoxybiphenyl **6** regenerates the nickel(0) species.

The results obtained for the catalysis with 4-chloroanisole (Table 4.2) show an increase in the rate of the reaction with more bulkiness of the ligand. This implies that the reductive elimination step from **D** to product **6** is rate determining, as the oxidative addition and the transmetalation would be hampered by a bulky ligand. For 4-bromoanisole the reaction is slowed down by a bulky ligand (Table 4.3), which implies that for this substrate either the oxidative addition or the transmetalation step is rate

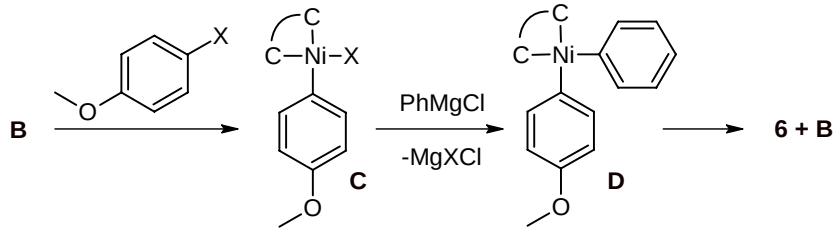

Scheme 4.5**.** Transient species in the catalytic cycle of the Kumada coupling.

determining. Oxidative addition of aryl halides to analogous $Pd(0)(PR_3)_2$ species has been calculated to be relatively easy,[57] and the strong σ–electron donating ability of the carbene ligands should make the oxidative addition more facile.[11] This leaves the transmetalation step to be rate limiting. Attempts to clarify this dependence of the rate-determining step on the halide and to elucidate the origin of the side products using density functional theory calculations are presented in Chapter 6. The relation between the shape and the bulk of the other ligands and the selectivity towards the various products with respect to the proposed mechanism remains uncertain.

4.3 Conclusion

In summary, several members of a novel class of Ni(II) dihalide complexes with chelating bis(benzimidazol-2-ylidene) ligands have been synthesized and structurally characterized. In the complexes the biscarbene ligand is coordinated in a *cis*-configuration on a square-planar nickel center. The complexes are precursors for active catalysts for the Kumada coupling reaction of aryl bromides and chlorides with aryl Grignard reagents. The highest rate and selectivity are achieved using a benzyl-substituted, 1,3-propanediyl bridged biscarbene system. The trends observed in catalysis appear to indicate a change in the rate-determining step for the two different substrates.

4.4 Experimental Section

General Procedures. All syntheses were performed in air, unless noted otherwise. 1,4-Dioxane was dried by distillation from CaH_2 and stored on molecular sieves under argon. N-phenylbenzimidazole,[58] N-n-propylbenzimidazole, N-isopropylbenzimidazole, N-benzylbenzimidazole,[41] α,α′-di(1-benzimidazolyl)-*o*-xylene,[39] α,α′-di(1-benzimidazolyl)-*m*-xylene,[59] bisbenzimidazolium salt **2k**[33] and bisbenzimidazolium salt **2l**,[39] were prepared according to literature procedures. Dehydrated $Ni(OAc)_2$ was obtained by heating $Ni(OAc)_2{\cdot}4H_2O$ at 165 °C under a stream of argon. Other chemicals were obtained commercially and used as received. ^1H NMR and ^{13}C NMR spectra were recorded on a Bruker DPX300. Chemical shifts are reported as referenced against the residual solvent signals and quoted in ppm relative to tetramethylsilane (TMS). IR spectra were recorded with a Perkin-Elmer FT-IR Paragon 1000 spectrophotometer equipped with a golden-gate ATR device, using the reflectance technique (4000-300 cm^{-1}; resolution 4 cm^{-1}). Elemental analyses were carried out with a Perkin-Elmer series II CHNS/O analyzer 2400. Halide contents were determined by potentiometric titration with silver nitrate according to the Volhard method. Electrospray mass spectra were recorded on a Finnigan TSQ-quantum instrument using an electrospray ionization technique (ESI-MS), using a water/acetonitrile or water/methanol mixture as solvent. GC measurements were performed on a Varian CP-3800 gas chromatograph equipped with an autosampler. Retention times were compared to commercially obtained compounds. Diethyleneglycol di-*n*-butyl ether was used as an internal standard.

General Procedure for the Synthesis of 1,1′-substituted bisbenzimidazolium salts (2). In a Schlenk flask 1 equivalent of dihaloalkane and 2.1–2.2 equivalents of N-substituted

benzimidazole were dissolved in dry 1,4-dioxane under an argon atmosphere. The mixture was stirred at 100 °C for 16–24 h (for bromide salts) or 48 h (chloride salts), at which point the formation of a white precipitate was observed. The reaction mixture was cooled, filtered, washed thoroughly with THF and diethyl ether and dried *in vacuo*. The product was obtained as a white powder. The compound was further purified by recrystallization from MeOH/diethyl ether.

1,1′-Dimethyl-3,3′-(1,3-propanediyl)bisbenzimidazolium dibromide (2a). This ligand precursor was prepared as described in the general procedure, starting from 1,3-dibromopropane (1.22 mL, 12 mmol) and 1-methylbenzimidazole (3.44 g, 26 mmol) in 30 mL dry 1,4-dioxane. Yield: 4.45 g (80%). ^{1}H NMR (300 MHz, DMSO-d_6, 300 K): δ 9.88 (s, 2H, NCHN), 8.10 (m, 2H, Ar-H), 8.05 (m, 2H, Ar-H), 7.71 (m, 4H, Ar-H), 4.71 (t, 4H, *J* = 7 Hz, NCH_2), 4.07 (s, 6H, CH_3), 2.59 (t, 2H, *J* = 7 Hz, CH_2). ^{13}C NMR (75 MHz, DMSO-d_6, 300 K): δ 142.9 (NCHN), 131.8 (C_q), 130.8 (C_q), 126.5 (Ar), 126.4 (Ar), 113.6 (Ar), 113.6 (Ar), 43.8 (NCH_2), 33.3 (NCH_3), 28.1 (CH_2). IR (neat): 3014 (w), 1569 (m), 1488 (m), 1456 (m), 1353 (m), 1266 (m), 1202 (m), 1128 (m), 1008 (w), 764 (s), 600 (m) cm^{-1}. Anal. Calcd for $C_{19}H_{22}Br_2N_4 \cdot 0.5H_2O$: C, 48.02; H, 4.88; N, 11.79. Found: C, 48.02; H, 4.87; N, 12.10. ESI-MS: *m*/*z* 385 ([M – Br]$^+$), 305 ([M – 2Br – H]$^+$), 153 ([M – 2Br]$^{2+}$, 100%).

1,1′-Dimethyl-3,3′-(1,3-propanediyl)bisbenzimidazolium dichloride (2b). The compound was obtained following the general procedure, starting from N-methylbenzimidazole (2.91 g, 22 mmol) and 1,3 dichloropropane (0.95 mL, 10 mmol) in 30 mL dry 1,4-dioxane. Yield: 2.15 g (57%). ^{1}H NMR (300 MHz, DMSO-d_6, 300 K): δ 10.18 (s, 2H, NCHN), 8.13 (m, 2H, Ar-H), 8.02 (m, 2H, Ar-H), 7.68 (m, 4H, Ar-H), 4.73 (t, 4H, *J* = 7 Hz, NCH_2), 4.08 (s, 6H, CH_3), 2.60 (t, 2H, *J* = 7 Hz, CH_2). ^{13}C NMR (75 MHz, DMSO-d_6, 300 K): δ 143.1 (NCHN), 131.8 (C_q), 130.8 (C_q), 126.5 (Ar), 126.4 (Ar), 113.6 (Ar), 113.6 (Ar), 43.7 (NCH_2), 33.2 (NCH_3), 28.1 (CH_2). IR (neat): 2939 (w), 1564 (m), 1462 (m), 1414 (m), 1354 (m), 1198 (m), 1010 (m), 756 (s), 432 (m) cm^{-1}. Anal. Calcd for $C_{19}H_{22}Cl_2N_4 \cdot 2H_2O$: C, 55.21; H, 6.34; N, 13.55. Found: C, 55.45; H, 6.47; N, 13.79. ESI-MS: *m*/*z* 341 ([M – Cl]$^+$), 205 ([M – 2Cl – H]$^+$), 153 ([M – 2Cl]$^{2+}$, 100%).

1,1′-Di-n-propyl-3,3′-(1,3-propanediyl)bisbenzimidazolium dibromide (2c). The compound was obtained following the general procedure, starting from 1-isopropylbenzimidazole (4.49 g, 28 mmol) and 1,3-dibromopropane (2.42 g, 12 mmol) in 25 mL dry dioxane. The product is obtained as a white powder. Yield: 4.42 g (71%). ^{1}H NMR (300 MHz, DMSO-d_6, 300 K): δ 10.08 (s, 2H, NCHN), 8.13 (m, 4H, Ar-H), 7.70 (m, 4H, Ar-H), 4.74 (t, 4H, *J* = 7 Hz, NCH_2), 4.50 (t, 4H, *J* = 7 Hz, NCH_2), 2.65 (quint, 2H, *J* = 7 Hz, CH_2), 1.89 (hex, 4H, *J* = 7 Hz, NCH_2CH_2), 0.92 (t, 6H, *J* = 7 Hz, CH_3). ^{13}C NMR (75 MHz, DMSO-d_6, 300 K): δ 142.1 (NCHN), 131.1 (2 × C_q), 126.5 (Ar), 126.4 (Ar), 113.6 (2 × Ar), 48.1 (NCH_2), 43.9 (NCH_2), 27.9 (CH_2), 21.9 (CH_2), 10.6 (CH_3). IR (neat): 3016 (w), 1564 (s), 1457 (m), 1431 (m), 1352 (w), 1211 (m), 1018 (w), 877 (w), 760 (s), 611 (m), 426 (m) cm^{-1}. Anal. Calcd for $C_{23}H_{30}Br_2N_4 \cdot 0.5H_2O$: C, 51.99; H, 5.88; N, 10.54. Found: C: 51.62; H, 5.80; N, 10.57. ESI-MS: *m*/*z* 443 ([M – Br]$^+$), 361 ([M – 2Br – H]$^+$), 319 ([M – 2Br – Pr]$^+$), 201 ([M – 2Br – PrBim]$^+$), 181 ([M – 2Br]$^{2+}$, 100%).

1,1′-Diisopropyl-3,3′-(1,3-propanediyl)bisbenzimidazolium dibromide (2d). The compound was prepared following the general procedure, starting from 1-propylbenzimidazole (3.52 g, 22 mmol) and 1,3-dibromopropane (2.02 g, 10 mmol) in 25 mL dry dioxane. The product is obtained as a white powder. Yield: 4.49 g (86%). ^{1}H NMR (300 MHz, DMSO-d_6, 300 K): δ 10.07 (s, 2H, NCHN), 8.16 (m, 4H, Ar-H), 7.68 (m, 4H, Ar-H), 5.06 (sept, 2H, *J* = 7 Hz, $NCH(CH_3)_2$), 4.72 (t, 4H, *J* = 7 Hz, NCH_2), 2.70 (quint, 2H, *J* = 7Hz, CH_2), 1.62 (d, 12H, *J* = 7Hz, CH_3). ^{13}C NMR (75 MHz, DMSO-d_6, 300 K): δ 140.9 (NCHN), 131.3 (C_q), 130.5 (C_q), 126.6 (Ar), 126.5 (Ar), 114.0 (Ar), 113.8 (Ar), 50.6 (NCH), 44.0 (NCH_2), 28.1 (CH_2), 21.6 (CH_3). IR (neat): 3020 (w), 2980 (w), 1557 (m), 1436

(m), 1241 (m), 1213 (m), 1098 (m), 835 (w), 761 (s), 748 (s), 615 (s), 421 (s) cm^{-1}. Anal. Calcd for $C_{23}H_{30}Br_2N_4 \cdot 0.5H_2O$: C, 51.99; H, 5.88; N, 10.54. Found: C, 51.77; H, 5.52; N, 10.59. ESI-MS: *m*/*z* 443 ($[M - Br]^+$), 361 ($[M - 2Br - H]^+$), 319 ($[M - 2Br - i\text{-}Pr]^+$), 201 ($[M - 2Br - i\text{-}PrBim]^+$), 181 ($[M - 2Br]^{2+}$, 100%).

1,1′-Dibenzyl-3,3′-(1,3-propanediyl)bisbenzimidazolium dibromide (2e). The compound was obtained following the general procedure, starting from 3 mmol 1,3-dibromopropane (0.31 mL, 3 mmol) and 1-benzylbenzimidazole (1.29 g, 6.2 mmol) in 10 mL dry 1,4-dioxane. Yield: 1.20 g (65%). ^{1}H NMR (300 MHz, DMSO-d_6, 300 K): δ 10.07 (s, 2H, NCHN), 8.15 (m, 2H, Ar-H), 7.96 (m, 2H, Ar-H), 7.68 (m, 4H, Ar-H), 7.54 (m, 4H, Ar-H), 7.41 (m, 6H, Ar-H), 5.79 (s, 4H, $PhCH_2N$), 4.73 (t, 4H, *J* = 7 Hz, NCH_2), 2.66 (t, 2H, *J* = 7 Hz, CH_2). ^{13}C NMR (75 MHz, DMSO-d_6, 300 K): δ 142.3 (NCHN), 135.1 (C_q), 132.6 (C_q), 132.1 (C_q), 130.2 (Ar), 130.0 (Ar), 129.6 (Ar), 128.0 (Ar), 127.9 (Ar), 115.2 (Ar), 115.1 (Ar), 51.2 (CH_2), 45.4 (CH_2), 28.0 (CH_2). IR (neat): 3026 (w), 1559 (s), 1456 (m), 1344 (m), 1184 (m), 1020 (w), 753 (s), 702 (s) cm^{-1}. Anal. Calcd for $C_{31}H_{30}Br_2N_4$: C, 60.21; H, 4.89; N, 9.06. Found: C, 59.97; H, 4.51; N, 9.06. ESI-MS: *m*/*z* 538 ($[M - Br]^+$), 456 ($[M - 2Br - H]^+$), 367 ($[M - BnBimPr]^+$), 250 ($[M - 2Br - BnBim]^+$), 299 ($[M - 2Br]^{2+}$, 100%).

1,1′-Diphenyl-3,3′-(propanediyl)dibenzimidazolium dibromide (2f). The compound was prepared following the general procedure starting, from 1-phenylbenzimidazole (2.33 g, 12 mmol) and 1,3-dibromopropane (1.01 g, 5 mmol) in 15 mL dry dioxane. Yield: 2.12 g (72%). ^{1}H NMR (300 MHz, DMSO-d_6, 300 K): δ 10.34 (s, 2H, NCHN), 8.27 (d, 2H, 8Hz, Ar-H), 7.90-7.70 (m, 16H, Ar-H), 4.87 (t, 4H, *J* = 7 Hz, NCH_2), 2.83 (t, 2H, *J* = 7 Hz, CH_2). ^{13}C NMR (75 MHz, DMSO-d_6, 300 K): δ 141.0 (NCHN), 133.1 (C_q), 131.3 (C_q), 131.1 (C_q), 130.5 (Ar), 130.4 (Ar), 127.6 (Ar), 127.0 (Ar), 125.1 (Ar), 114.1 (Ar), 113.6 (Ar), 44.3 (NCH_2), 27.6 (CH_2). IR (neat): 3005 (w), 1559 (m), 1421 (w), 1236 (m), 1118 (w), 872 (m), 764 (s), 745 (s), 696 (s), 592 (m) cm^{-1}. Anal. Calcd for $C_{29}H_{26}Br_2N_4 \cdot 2CH_3OH$: C, 56.89; H, 5.24; N, 8.56. Found: C, 56.66; H, 4.93; N, 8.89. ESI-MS: *m*/*z* 511 ($[M - Br]^+$), 429 ($[M - 2Br - H]^+$), 215 ($[M - 2Br]^{2+}$, 100%).

1,1′-Dimethyl-3,3′-(1,4-butanediyl)bisbenzimidazolium dibromide (2g). The compound was prepared following the general procedure, starting from of 1,4-dibromobutane (1.20 mL, 10 mmol) and 1-benzylbenzimidazole (3.17 g, 24 mmol) in 20 mL dry 1,4-dioxane. Yield: 4.02 g (84%). ^{1}H NMR (300 MHz, DMSO-d_6, 300 K): δ 9.84 (s, 2H, NCHN), 8.10 (m, 2H, Ar-H), 8.02 (m, 2H, Ar-H), 7.69 (m, 4H, Ar-H), 4.57 (s, 4H, NCH_2), 4.07 (s, 6H, NCH_3), 1.99 (s, 4H, CH_2). ^{13}C NMR (75 MHz, DMSO-d_6, 300 K): δ 144.0 (NCHN), 133.0 (C_q), 132.1 (C_q), 127.7 (Ar), 114.9 (Ar), 114.8 (Ar), 47.2 (NCH_2), 34.6 (NCH_3), 26.8 (CH_2). IR (neat): 2961 (m), 1620 (w), 1568 (m), 1460 (m), 1355 (m), 1221 (m), 759 (s), 567 (m), 426 (m) cm^{-1}. Anal. Calcd for $C_{20}H_{24}Br_2N_4 \cdot H_2O$: C, 48.21; H, 5.26; N, 11.24. Found: C, 48.06; H, 5.36; N, 11.20. ESI-MS: *m*/*z* 399 ($[M - Br]^+$), 319 ($[M - 2Br - H]^+$), 160 ($[M - 2Br]^{2+}$, 100%).

1,1′-Dimethyl-3,3′-(1,4-butanediyl)bisbenzimidazolium dichloride (2h). The compound was prepared following the general procedure, starting from of 1,4-dichlorobutane (1.46 g, 11.5 mmol) and 1-benzylbenzimidazole (3.5 g, 26.5 mmol) in 20 mL dry 1,4-dioxane. Yield: 2.40 g (61%). ^{1}H NMR (300 MHz, DMSO-d_6, 300 K): δ 10.12 (NCHN), 8.10 (m, 2H, Ar-H), 8.01 (m, 2H, Ar-H), 7.66 (m, 4H, Ar-H), 4.61 (t, 4H, *J* = 7H, NCH_2), 4.08 (s, 6H, NCH_3), 2.01 (t, 4H, *J* = 7Hz, CH_2). ^{13}C NMR (75 MHz, DMSO-d_6, 300 K): δ 143.0 (NCHN), 131.8 (C_q) , 130.9 (C_q), 126.4 (2 × Ar), 113.6 (Ar), 113.5 (Ar), 45.8 (NCH_2), 33.2 (NCH_3), 25.3 (CH_2). IR (neat): 3397(m), 3030 (m), 1622 (w), 1568 (s), 1464 (m), 1354 (m), 1219 (m), 1144 (w), 764 (s), 652 (m), 601 (m), 557 (m), 424 (s) cm^{-1}. Anal. Calcd for $C_{20}H_{24}Cl_2N_4 \cdot 2H_2O$: C, 56.21; H, 6.60; N, 13.11. Found: C, 56.47; H, 6.44; N, 13.13. ESI-MS: *m*/*z* 355 ($[M - Cl]^+$), 319 ($[M - 2Cl - H]^+$), 160 ($[M - 2Cl]^{2+}$, 100%).

1,1′-Dimethyl-3,3′-(α,α′-tetramethylsilane)bisbenzimidazolium dichloride (2i). The compound was prepared following the general procedure, starting from bis(chloromethyl)dimethylsilane (1.45 mL, 10 mmol) and 1-methylbenzimidazole (2.91 g, 22 mmol) in 15 mL of dry 1,4-dioxane. Yield: 3.58 g (85%). ^{1}H NMR (300 MHz, DMSO-d_6, 300 K): δ 10.03 (s, 2H, NCHN), 8.16 (m, 2H, Ar-H), 8.01 (m, 2H, Ar-H), 7.66 (m, 4H, Ar-H), 4.53 (s, 4H, NCH_2Si), 4.10 (s, 6H, NCH_3), 0.19 (s, 6H, $Si(CH_3)_2$). ^{13}C NMR (75 MHz, DMSO-d_6, 300 K): δ 142.1 (NCHN), 131.8 (2 × C_q), 126.3 (Ar), 126.1 (Ar), 113.7 (Ar), 113.4 (Ar), 35.4 (NCH_2Si), 33.2 (NCH_3), –5.0 ($Si(CH_3)_2$). IR (neat): 3018 (m), 2957 (m), 1613 (w), 1560 (m), 1470 (m), 1357 (m), 1147 (m), 857 (s), 818 (m), 766 (s) cm^{-1}. Anal. Calcd for $C_{20}H_{26}Cl_2N_4Si{\cdot}H_2O$: C, 54.66; H, 6.42; N, 12.75. Found: C, 54.58; H, 6.51; N, 12.68. ESI-MS: *m*/*z* 385 ([M – Cl]$^+$), 221 ([M – 2Cl – MeBim]$^+$, 100%), 175 ([M – 2Cl]$^{2+}$), 147 ([Me_2Bim]$^+$).

1,1′-Dimethyl-3,3′-(α,α′-o-xylylene)bisbenzimidazolium dibromide (2j). The compound was prepared following the general procedure, starting from N-methylbenzimidazole (12 mmol, 1.59 g) and α,α′-dibromo-o-xylene (5 mmol, 1.32 g) in 20 mL dry 1,4-dioxane. Yield: 2.62 g (81%). ^{1}H NMR (300 MHz, DMSO-d_6, 300 K): δ 9.71 (s, 2H, NCHN), 8.04 (s, 2H, *J* = 8 Hz, Ar-H), 7.93 (d, 2H, *J* = 8 Hz, Ar-H), 7.67 (m, 4H, Ar-H), 7.42 (m, 4H, Ar-H), 7.24 (m, 4H, Ar-H), 6.05 (s, 4H, NCH_2Ph), 4.06 (s, 6H, CH_3). ^{13}C NMR (75 MHz, DMSO-d_6, 300 K): δ 144.3 (NCHN), 133.3 (C_q), 133.2 (C_q), 132.1 (C_q), 130.7 (Ar), 130.2 (Ar), 128.0 (Ar), 127.9 (Ar), 115.0 (2 Ar), 48.7 (NCH_2Ph), 34.7 (CH_3). IR (neat): 3011 (m), 1568 (s), 1456 (m), 1381 (w), 1203 (m), 1093 (w), 1021 (w), 757 (s), 744 (s), 667 (w), 606 (w), 570 (m), 421 (m) cm^{-1}. Anal. Calcd for $C_{24}H_{24}Br_2N_4{\cdot}H_2O$: C, 52.77; H, 4.86; N, 10.26. Found: C, 52.74; H, 4.87; N, 10.35. ESI-MS: *m*/*z* 449 ([M – Br]$^+$), 367 ([M – 2Br – H]$^+$), 184 ([M – 2Br]$^{2+}$, 100%).

1,1′-(1,4-butanediyl)-3,3′-(α,α′-m-xylylene)dibenzimidazolium bromide (2m). To a solution of α,α′-di(1-benzimidazolyl)-*m*-xylene (0.60 g, 1.78 mmol) in 400 mL degassed acetonitrile was added 1,4-dibromobutane (5.2 g, 24 mmol) and the resulting mixture was refluxed for 4 days. The volume was then reduced *in vacuo* to 25 mL and cooled. The white precipitated that formed was collected by filtration and washed with acetonitrile and diethyl ether. Yield: 0.74 g (75%). ^{1}H NMR (300 MHz, DMSO-d_6, 300 K): δ 9.70 (s, 2H, NCHN), 8.20 (m, 4H, Ar-H), 7.72 (m, 6H, Ar-H), 7.53 (t, 1H, *J* = 8 Hz, Ar-H), 7.08 (s, 1H, Ar-H), 5.75 (s, 4H, CH_2Xy), 4.53 (broad s, 4H, NCH_2), 1.77 (broad s, 4H, CH_2). ^{13}C NMR (75 MHz, DMSO-d_6, 300 K): δ 141.8 (NCHN), 135.7 (C_q), 132.2 (C_q), 131.0 (C_q), 129.4 (Ar-C), 129.3 (Ar-C), 126.8 (Ar-C), 126.7 (Ar-C), 125.8 (Ar-C), 113.6 (Ar-C), 113.5 (Ar-C), 49.2 (NCH_2), 45.1 (NCH_2), 26.8 (CH_2). IR (neat): 2959 (w), 1558 (s), 1448 (m), 1423 (m), 1376 (m), 1189 (s), 1015 (m), 821 (m), 798 (m), 752 (s), 427 (s) cm^{-1}. ESI-MS: *m*/*z* 197 ([M – 2Br]$^{2+}$, 100%), 218 ([M – 2Br + MeCN]$^{2+}$), 393 ([M – 2Br – H]$^+$), 475 ([M – Br]$^+$). Anal. Calcd for $C_{26}H_{26}Br_2N_4{\cdot}1.5H_2O$: C, 53.72; H, 5.03; N, 9.64. Found: C, 54.01; H, 5.30; N, 9.83.

General procedure for the synthesis of nickel complexes (3). Bisbenzimidazolium salt **2**, nickel(II) acetate and tetrabutylammonium halide were mixed and heated under vacuum in a 10 mL flask at 60 °C for 1 h, followed by heating under vacuum at 128 °C for 3 – 4 h. After cooling, the reaction mixture was triturated with water; the resulting solid was collected by filtration and washed with water. The complexes were further purified by dissolving the crude product in dichloromethane and washing the solution with water and saturated sodium halide solution. After the organic phase was dried with magnesium sulfate, the solution was concentrated *in vacuo* and the complex was precipitated with diethyl ether, filtered and dried *in vacuo*.

Dibromido-(1,1′-dimethyl-3,3′-(1,3-propanediyl)dibenzimidazol-2,2′-diylidene)nickel(II) (3a). The complex was obtained as a yellow solid following the general procedure, starting from 0.47 g (1.0 mmol) bisbenzimidazolium salt **2a**, 1.0 mmol $Ni(OAc)_2$ (0.18 g) and 2.0 g

tetrabutylammonium bromide. Yield: 0.35 g (67%). ^{1}H NMR (300 MHz, DMSO-d_6, 300 K): δ 7.61 (m, 2H, Ar-H), 7.49 (m, 2H, Ar-H), 7.22 (m, 4H, Ar-H), 5.96 (broad s, 2H, NCH_2), 5.00 (broad d, 2H, J = 11 Hz, NCH_2), 4.60 (s, 6H, CH_3), 2.72 (broad s, 1H, CH_2), 1.93 (broad s, 1H, CH_2). ^{13}C NMR (75 MHz, DMSO-d_6, 300 K): δ 134.3 (C_q), 134.0 (C_q), 122.8 (Ar), 122.7 (Ar), 110.2 (Ar), 109.8 (Ar), 48.4 (NCH_2), 35.0 (CH_3), 28.0 (CH_2). Ni-C could not be observed due to peak broadening. IR (neat): 3504 (w), 3037 (w), 2957 (w), 1457 (m), 1442 (m), 1394 (m), 1370 (m), 1340 (m), 1231 (w), 1134 (w), 1036 (w), 966 (w), 795 (w), 744 (s), 701 (m), 558 (m), 432 (m) cm^{-1}. Anal. Calcd for $C_{19}H_{20}Br_2N_4Ni$: C, 43.64; H, 3.85; N, 10.71. Found: C, 43.91; H, 3.95; N, 11.06. ESI-MS: m/z 483 ([M – Br + MeCN]$^+$, 100%), 340 ([M – 2Br + OH]$^+$). Crystals suitable for X-ray crystal structure determination were obtained by slow evaporation of a solution of the crude complex in dichloromethane/diethyl ether.

Dichlorido-(1,1′-dimethyl-3,3′-(1,3-propanediyl)dibenzimidazol-2,2′-diylidene)nickel(II) (3b). The complex was obtained as a yellow solid following the general procedure, starting from bisbenzimidazolium salt **2b** (0.28 g, 0.75 mmol), $Ni(OAc)_2$ (0.13 g, 0.75 mmol) and 2.0 g tetrabutylammonium chloride. Yield: 0.19 g (58%). ^{1}H NMR (300 MHz, DMSO-d_6, 300 K): δ 7.61 (m, 2H, Ar-H), 7.50 (m, 2H, Ar-H), 7.21 (m, 4H, Ar-H), 5.97 (broad s, 2H, NCH_2), 4.97 (broad d, 2H, J = 11 Hz, NCH_2), 4.60 (s, 6H, CH_3), 2.72 (broad s, 1H, CH_2), 1.90 (broad s, 1H, CH_2). ^{13}C NMR (75 MHz, DMSO-d_6, 300 K): δ 134.3 (C_q), 134.0 (C_q), 122.8 (Ar), 122.7 (Ar), 110.2 (Ar), 109.7 (Ar), 48.3 (NCH_2), 35.0 (CH_3), 28.0 (CH_2). Ni-*C* could not be observed due to peak broadening. IR (neat): 2923 (m), 2854 (m), 1611 (w), 1462 (s), 1437 (s), 1393 (s), 1370 (s), 1338 (m), 1230 (w), 1127 (m), 1091 (m), 1034 (m), 967 (w), 859 (w), 795 (w), 736 (s), 560 (m), 435 (m) cm^{-1}. Anal. Calcd. For $C_{19}H_{20}Cl_2N_4Ni{\cdot}H_2O$: C, 50.49; H, 4.91; N, 12.39. Found: C, 50.69; H, 5.18; N, 12.55. ESI-MS: m/z 438 ([M – Cl + MeCN]$^+$, 100%), 340 ([M – 2Cl + OH]$^+$).

Dibromido-(1,1′-di-n-propyl-3,3′-(1,3-propanediyl)dibenzimidazol-2,2′-diylidene)nickel(II) (3c). The complex was obtained as a yellow solid following the general procedure, starting from bisbenzimidazolium salt **2c** (0.52 g, 1.0 mmol), $Ni(OAc)_2$ (0.18 g, 1.0 mmol) and 2.0 g tetrabutylammonium bromide. Yield: 0.37 g (64%). ^{1}H NMR (300 MHz, DMSO-d_6, 300 K): δ 7.60 (m, 4H, Ar-H), 7.21 (m, 4H, Ar-H), 6.05 (bs, 2H, NCH_2), 5.41 (m, 2H, NCH_2), 4.98 (m, 2H, NCH_2), 4.86 (m, 2H, NCH_2), 2.71 (m, 1H, CH_2), 2.06 (m, 3H, CH_2), 1.84 (m, 2H, CH_2), 1.15 (t, 6H, J = 7 Hz, CH_3). ^{13}C NMR (75 MHz, DMSO-d_6, 300 K): δ 134.5 (C_q), 133.3 (C_q), 122.9 (Ar), 122.7 (Ar), 110.9 (Ar), 110.1 (Ar), 50.3 (NCH_2), 48.55 (NCH_2), 30.4 (CH_2), 22.04 (CH_2), 11.2 (CH_3). IR (neat): 2960 (w), 1479 (m), 1455 (m), 1400 (s), 1214 (m), 1135 (m), 1044 (m), 1019 (m), 968 (w), 857 (w), 760 (s), 742 (s), 578 (w), 435 (m) cm^{-1}. Anal. Calcd for $C_{23}H_{28}Br_2N_4Ni{\cdot}0.1CH_2Cl_2$: C, 47.23; H, 4.84; N, 9.54. Found: C, 47.11; H, 4.79; N, 9.60. ESI-MS: m/z 540 ([M – Br + MeCN]$^+$, 100%), 435 ([M – 2Br + OH]$^+$).

Dibromido-(1,1′-diisopropyl-3,3′-(1,3-propanediyl)dibenzimidazol-2,2′-diylidene)nickel(II) (3d). The complex was obtained as a yellow solid following the general procedure, starting from bisbenzimidazolium salt **2d** (0.52 g, 1.0 mmol), $Ni(OAc)_2$ (0.18 g, 1.0 mmol) and 2.0 g tetrabutylammonium bromide. Yield: 0.34 g (59%). ^{1}H NMR (300 MHz, DMSO-d_6, 300 K): δ 7.60 (m, 4H, Ar-H), 7.24 (m, 4H, Ar-H), 6.68 (m, 1H, NCH or NCH_2), 6.05 (m, 1H, NCH or NCH_2), 5.75 (m, 1H, NCH or NCH_2), 5.35 (m, 1H, NCH or NCH_2), 5.01 (m, 2H, NCH or NCH_2), 2.72 (m, 1H, CH_2), 2.05 (m, 1H, CH_2), 1.87 (m, 6H, CH_3), 1.66 (m, 6H, CH_3). Due to the poor solubility in regular solvents, no ^{13}C NMR spectrum was obtained. IR (neat): 3385 (w), 2978 (w), 1463 (m), 1403 (s), 1294 (m), 1137 (m), 1092 (m), 742 (s), 556 (m), 432 (m) cm^{-1}. Anal. Calcd for

$C_{23}H_{28}Br_2N_4Ni{\cdot}0.5CH_2Cl_2$: C, 45.42; H, 4.70; N, 9.02. Found: C, 45.59; H, 4.45; N, 9.21. ESI-MS: *m*/*z* 496 ($[M - Br]^+$, 100%).

Dibromido-(1,1′-dibenzyl-3,3′-(1,3-propanediyl)dibenzimidazol-2,2′-diylidene)nickel(II) (3e). The complex was obtained as a yellow solid following the general procedure, starting from bisbenzimidazolium salt **2e** (0.46 g, 0.75 mmol), $Ni(OAc)_2$ (0.13 g, 0.75 mmol) and 2.0 g tetrabutylammonium bromide. Yield: 0.31 g (41%). ^{1}H NMR (300 MHz, DMSO-d_6, 300 K): δ 7.67 (d, 2H, *J* = 8 Hz, Ar-H), 7.30-6.75 (m, 18H, Ar-H + $PhCH_2N$), 6.20 (bs, 2H, $PhCH_2N$), 5.57 (bs, 2H, NCH_2), 5.08 (bs, 2H, NCH_2), 2.79 (bs, 1H, $CH_2CH_2CH_2$), 2.15 (bs, 1H, $CH_2CH_2CH_2$). ^{13}C NMR (75 MHz, DMSO-d_6, 300 K): δ 135.5 (C_q), 134.8 (C_q), 133.1 (C_q), 128.5 (Ar), 127.8 (Ar), 127.4 (Ar), 122.9 (Ar), 122.7 (Ar), 111.1 (Ar), 110.3 (Ar), 51.9 (CH_2), 48.7 (CH_2), 28.6 (CH_2). Ni-*C* could not be observed due to peak broadening. IR (neat): 2960 (m), 2872 (m), 1607 (w), 1458 (m), 1404 (s), 1361 (m), 1203 (m), 1034 (m), 739 (s), 699 (m), 434 (m) cm^{-1}. Anal. Calcd for $C_{31}H_{28}Br_2N_4Ni{\cdot}0.1CH_2Cl_2$: C, 54.64; H, 4.16; N, 8.20. Found: C, 54.65; H, 3.90; N, 8.39. ESI-MS: *m*/*z* 532 ($[M - 2Br + OH]^+$), 592 ($[M - Br]^+$, 100%). Crystals suitable for X-ray crystal structure determination were obtained by slow evaporation of a solution of the crude complex in dichloromethane/diethyl ether.

Dibromido-(1,1′-diphenyl-3,3′-(1,3-propanediyl)dibenzimidazol-2,2′-diylidene)nickel(II) (3f). The complex was obtained as a yellow solid following the general procedure, starting from bisbenzimidazolium salt **2f** (0.59 g, 1.0 mmol), $Ni(OAc)_2$ (0.18 g, 1.0 mmol) and 2.5 g tetrabutylammonium bromide. Yield: 0.38 g (59%). ^{1}H NMR (300 MHz, DMSO-d_6, 300 K): δ 7.99 – 7.77 (m, 6H, Ar-H), 7.55 – 7.13 (m, 12H, Ar-H), 6.63 (bs, 2H, NCH_2), 5.20 (m, 2H, NCH_2), 2.96 (bs, 1H, CH_2), 2.28 (bs, 1H, CH_2). ^{13}C NMR (75 MHz, DMSO-d_6, 300 K): δ 137.2 (C_q), 135.6 (2 × C_q) 130.7 (Ar), 129.7 (Ar), 127.1 (Ar), 124.9 (Ar), 124.5 (Ar), 112.0 (Ar), 111.5 (Ar), 50.2 (NCH_2), 26.4 (CH_2). IR (neat): 2961 (m), 1597 (w), 1502 (m), 1474 (m), 1402 (m), 1369 (m), 1221 (w), 1091 (w), 1026 (w), 810 (w), 750 (s), 696 (s) 4901 (w), 438 (w) cm^{-1}. Anal. Calcd for $C_{29}H_{24}Br_2N_4Ni{\cdot}0.2Et_2O$: C, 54.08; H, 3.96; N, 8.46. Found: C, 53.96; H, 4.15; N, 8.45. ESI-MS: *m*/*z* 607 ($[M - Br + ACN]^+$, 100%).

Dibromido-(1,1′-dimethyl-3,3′-(1,4-butanediyl)dibenzimidazol-2,2′-diylidene)nickel(II) (3g). The complex was obtained as a yellow solid following the general procedure, starting from bisbenzimidazolium salt **2g** (0.24 g, 0.5 mmol), $Ni(OAc)_2$ (0.09 g, 0.5 mmol) and 3.0 g tetrabutylammonium bromide. Yield: 0.12 g (45%). ^{1}H NMR (300 MHz, DMSO-d_6, 300 K): δ 7.63 (m, 2H, Ar-H), 7.55 (m, 2H, Ar-H), 7.25 (m, 4H, Ar-H), 6.30 (m, 2H, NCH_2), 4.71 (m, 2H, NCH_2), 4.61 (s, 6H, NCH_3), 2.36 (m, 2H, CH_2), 1.31 (m, 2H, CH_2). ^{13}C NMR (75 MHz, DMSO-d_6, 300 K): δ 135.2 (C_q), 133.6 (C_q), 122.9 (Ar), 122.8 (Ar), 110.4 (Ar), 110.2 (Ar), 43.3 (NCH_2), 35.3 (NCH_3), 24.1 (CH_2). Ni-*C* could not be observed due to peak broadening. IR (neat): 2940 (w), 1612 (w), 1464 (m), 1439 (m), 1393 (m), 1342 (m), 1189 (m), 745 (s), 440 (m) cm^{-1}. Anal. Calcd for $C_{20}H_{22}Br_2N_4Ni{\cdot}0.75CH_2Cl_2$: C, 41.49; H, 3.94; N, 9.33. Found: C, 41.41; H, 3.66; N, 9.34. ESI-MS: *m*/*z* 394 ($[M - 2Br + OH]^+$), 498 ($[M - Br + MeCN]^+$, 100%). Crystals suitable for X-ray crystal structure determination were obtained by slow evaporation of a solution of the crude complex in dichloromethane/acetonitrile.

Dichlorido-(1,1′-dimethyl-3,3′-(1,4-butanediyl)dibenzimidazol-2,2′-diylidene)nickel(II) (3h). The complex was obtained as a yellow solid following the general procedure, starting from bisbenzimidazolium salt **2h** (0.39 g, 1.0 mmol), $Ni(OAc)_2$ (0.18 g, 1.0 mmol) and 3.0 g tetrabutylammonium chloride. This complex is soluble in water and therefore the purification step after the trituration with water was omitted. Yield: 0.34 g (77%). ^{1}H NMR (300 MHz, DMSO-d_6, 300 K): δ 7.61 (m, 2H, Ar-H), 7.55 (m, 2H, Ar-H), 7.23 (m, 4H, Ar-H), 6.34 (m, 2H, NCH_2), 4.75 (m, 2H, NCH_2), 4.62 (s, 6H, NCH_3), 2.36 (m, 2H, CH_2), 1.29 (m, 2H, CH_2). ^{13}C NMR (75

MHz, DMSO-d_6, 300 K): δ 134.9 (C_q), 133.4 (C_q), 122.8 (Ar), 122.7 (Ar), 110.2 (Ar), 110.1 (Ar), 43.2 (NCH_2), 35.1 (NCH_3), 24.1 (CH_2). Ni-*C* could not be observed due to peak broadening. IR (neat): 3403 (w), 2961 (w), 1471 (m), 1444 (m), 1395 (s), 1343 (m), 1192 (m), 1127 (w), 1008 (w), 808 (w), 752 (s), 745 (s), 580 (w), 445 (m) cm^{-1}. Anal. Calcd for $C_{20}H_{22}Cl_2N_4Ni \cdot H_2O \cdot 0.2Bu_4NCl$: C, 53.42; H, 6.03; N, 11.28. Found: C, 53.56; H, 6.18; N, 11.59. ESI-MS: *m*/*z* 452 ($[M - Cl + MeCN]^+$, 100%).

Dibromido-(1,1′-dimethyl-3,3′-(α,α′-tetramethylsilane)dibenzimidazol-2,2′-diylidene)nickel(II) (3i). The complex was obtained as a yellow solid following the general procedure, starting from bisbenzimidazolium salt **2i** (0.32 g, 0.75 mmol), $Ni(OAc)_2$ (0.13 g, 0.75 mmol), potassium bromide (0.5 g) and 2.0 g tetrabutylammonium bromide. Yield: 0.29 g (68%). ^{1}H NMR (300 MHz, DMSO-d_6, 300 K): δ 7.71 (m, 2H, Ar-H), 7.50 (m, 2H, Ar-H), 7.22 (m, 4H, Ar-H), 5.47 (d, 2H, *J* = 16 Hz, NCH_2Si), 4.67 (s, 6H, NCH_3), 4.35 (d, 2H, *J* = 16 Hz, NCH_2Si), 0.66 (s, 3H, $SiCH_3$), –0.49 (s, 3H, $SiCH_3$). ^{13}C NMR (75 MHz, DMSO-d_6, 300 K): δ 135.0 (C_q), 134.4 (C_q), 122.6 (Ar), 122.4 (Ar), 110.2 (2 Ar), 38.2 (NCH_2Si), 35.5 (NCH_3), –5.4 ($SiCH_3$), –7.6 ($SiCH_3$). Ni-*C* could not be observed due to peak broadening. IR (neat): 3048 (w), 2955 (w), 1609 (w), 1438 (m), 1385 (m), 1249 (w), 863 (m), 741 (s), 695 (w), 439 (m) cm^{-1}. Anal. Calcd for $C_{20}H_{24}Br_2N_4NiSi \cdot 0.7Et_2O$: C, 44.25; H, 5.05; N, 9.05. Found: C, 44.55; H, 4.99; N, 9.87. ESI-MS: *m*/*z* 423 ($[M - 2Br + OH]^+$), 484 ($[M - Br]^+$, 100%). Crystals suitable for X-ray crystal structure determination were obtained by slow evaporation of a solution of the crude complex in dichloromethane/acetonitrile.

Dibromido-(1,1′-dimethyl-3,3′-(α,α′-o-xylylene)dibenzimidazol-2,2′-diylidene)nickel(II) (3j). The complex was obtained as a yellow solid following the general procedure, starting from bisbenzimidazolium salt **2j** (0.53 g, 1.0 mmol), $Ni(OAc)_2$ (0.18 g, 1.0 mmol) and 2.0 g tetrabutylammonium bromide. Yield: 0.42 g (72%). ^{1}H NMR (300 MHz, DMSO-d_6, 300 K): δ 8.20 (m, 2H, Ar-H), 8.07 (d, 2H, *J* = 8 Hz, Ar-H), 7.88 (d, 2H, *J* = 15 Hz, NCH_2), 7.50 (m, 4H, Ar-H), 7.28 (m, 4H, Ar-H), 5.78 (d, 2H, *J* = 15 Hz, NCH_2), 4.67 (s, 6H, NCH_3). ^{13}C NMR (75 MHz, DMSO-d_6, 300 K): δ 135.3 (C_q), 135.1 (C_q), 133.9 (C_q), 133.6 (Ar), 129.2 (Ar), 123.0 (Ar), 122.9 (Ar), 111.3 (Ar), 110.5 (Ar), 50.0 (CH_2), 35.7 (CH_3). Ni-*C* could not be observed due to peak broadening. IR (neat): 3062 (w), 1616 (w), 1463 (m), 1436 (m), 1395 (m), 1340 (m), 1214 (w), 1194 (w), 1095 (w), 1016 (w), 788 (m), 740 (s), 700 (w), 668 (w), 580 (w), 549 (w), 436 (m) cm^{-1}. Anal. Calcd for $C_{24}H_{22}Br_2N_4Ni \cdot 0.5CH_2Cl_2$: C, 46.90; H, 3.69; N, 8.93. Found: C, 47.08; H, 3.70; N, 8.99. ESI-MS: *m*/*z* 442 ($[M - 2Br + OH]^+$), 502 ($[M - Br]^+$, 100%).

Dichlorido-(1,1′-3,3′-bis(α,α′-o-xylylene)dibenzimidazol-2,2′-diylidene)nickel(II) (3k). Following an adaptation of the procedure reported for the synthesis of **I** by Baker *et al.*[33] a solution of benzimidazolium bromide **2k** (1.0 g, 1.7 mmol) in 25 mL methanol was added to a solution of KPF_6 (1,5 g, 8.1 mmol) in 25 mL of the same solvent and stirred at room temperature for several hours. The white precipitate that formed was isolated by filtration and dried *in vacuo*. A solution of this PF_6 salt (0.36 g, 0.50 mmol), NaOAc (0.09 g, 1.10 mmol) and $NiCl_2$ (65 mg, 0.50 mmol) in 12 mL of degassed DMF was stirred for 72 h at 90 °C. The resulting mixture was evaporated to dryness, dissolved in 200 mL dichloromethane and washed twice with water and once with brine. After drying with magnesium sulfate, most of the solvent was remove *in vacuo* and the product was precipitated by addition of diethyl ether, filtered and dried *in vacuo*. The compound was obtained as a yellow solid and was further purified by recrystallization from dichloromethane/diethyl ether. Yield: 0.16 g (55%). ^{1}H NMR (300 MHz, $CDCl_3$, 300 K): δ 7.88 (d, 4H, *J* = 15 Hz, CH_2), 7.68 (m, 4H, Ar-H), 7.41 (m, 4H, Ar-H), 7.19 (m, 4H, Ar-H), 6.91 (m, 4H, Ar-H), 5.28 (d, 4H, *J* = 15 Hz, CH_2). ^{13}C NMR (75 MHz, DMSO-d_6, 300 K): δ 134.8 (2 × C_q), 133.9 (C_{Ar}), 129.8 (C_{Ar}), 123.2 (C_{Ar}), 110.8 (C_{Ar}), 51.9 (CH_2). IR (neat): 3063 (w), 1475 (w), 1458 (w), 1413 (m),

1336 (w), 1020 (w), 834 (s), 736 (s), 556 (s) cm^{-1}. Anal. Calcd. For $C_{30}H_{24}Cl_2N_4Ni \cdot 2.5H_2O$: C, 58.57; H, 4.75; N, 9.11. Found: C, 58.65; H, 4.51; N, 9.32. ESI-MS: *m*/*z* 533 ($[M - Cl]^+$, 100%).

Dibromido-(1,1′-(1,4-butanediyl)-3,3′-(α,α′-o-xylylene)dibenzimidazol-2,2′-diylidene)nickel(II) (3l). This compound was prepared according to the general procedure, starting from macrocyclic bisbenzimidazolium bromide **2l** (0.30 g, 0.54 mmol), $Ni(OAc)_2$ (96 mg, 0.54 mmol) and 1.0 g of tetrabutylammonium bromide and obtained as a yellow solid. Yield: 0.14 g (42%). ^{1}H NMR (300 MHz, DMSO-d_6, 300 K): δ 8.21 (m, 2H, Xy-H), 8.03 (d, 2H, *J* = 7 Hz, Bim-H), 7.89 (d, 2H, *J* = 15 Hz, $XyCH_2$), 7.61 (d, 2H, *J* = 7 Hz, Bim-H), 7.50 (m, 2H, Xy-H), 7.26 (m, 4H, Bim-H), 6.37 (m, 2H, NCH_2), 5.79 (d, 2H, *J* = 15 Hz, $XyCH_2$), 4.72 (d, 2H, NCH_2), 2.40 (m, 2H, CH_2), 1.24 (m, 2H, CH_2). ^{13}C NMR (75 MHz, DMSO-d_6, 300 K): δ 135.1 (C_q), 134.1 (Ar-C), 134.0 (2 × C_q), 129.3 (Ar-C), 123.2 (Ar-C), 123.0 (Ar-C), 111.6 (Ar-C), 110.6 (Ar-C), 50.2 (NCH_2), 43.5 (NCH_2), 24.5 (CH_2). IR (neat): 2942 (s), 1478 (m), 1409 (s), 1338 (m), 1178 (m), 1008 (w), 786 (m), 742 (s), 668 (m), 428 (m) cm^{-1}. Anal. Calcd. for $C_{26}H_{24}Br_2N_4Ni \cdot 0.4CH_2Cl_2$: C, 49.16; H, 3.88; N, 8.69. Found: C, 49.07; H, 3.99; N, 8.47. ESI-MS: *m*/*z* 571 ($[M - Br + MeCN]^+$, 100%).

General procedure for the Kumada reaction. At room temperature, 1.0 mmol of the appropriate 4-haloanisole was added to a solution or suspension of 0.03 mmol nickel complex in 1 mL dry THF under an argon atmosphere. A 25 wt% solution of phenylmagnesium chloride in THF (0.78 mL, 1.5 mmol) was added drop wise with stirring, changing the reaction mixture into a clear, brown solution. At regular intervals aliquots were taken, dissolved in aqueous ethanol and analyzed by gas chromatography. Samples were taken until full conversion was reached. All catalytic reactions were performed in duplicate and were found to be consistent.

To obtain the desired coupling product, water was added and the reaction mixture was extracted into ethyl acetate (3 × 20 mL). The organic fractions were combined, dried with magnesium sulfate and evaporated to dryness. Purification by column chromatography on silica gel (95:5 hexane:dichloromethane) yielded 4-methoxybiphenyl as a colorless solid. ^{1}H NMR and ^{13}C NMR spectra were in agreement with the proposed structure,[26] and the GC retention time corresponded to that of a commercial sample.

X-ray crystal structure determinations. X-ray reflections were measured with Mo-K_α radiation (λ = 0.71073 Å) on a Nonius KappaCCD diffractometer with rotating anode at a temperature of 150 K. Integration of the reflections was performed with EvalCCD.[60] The structures were solved with automated Patterson methods (program DIRDIF-99[61] for **3a** and **3g**) or Direct Methods (program SIR-97 for **3e**;[62] SHELXS-97 for **3i**).[63] Refinement was performed with SHELXL-97 against F^2 of all reflections.[63] Non hydrogen atoms were refined with anisotropic displacement parameters. All hydrogen atoms were introduced in calculated positions and refined with a riding model. Geometry calculations and checking for higher symmetry were performed with the PLATON program.[64]

The crystal of **3a** was non-merohedrally twinned with a twofold rotation about *hkl* (001) as twin operation. This twin law was taken into account during intensity integration and the HKLF5 structure refinement.[65] The twin fraction refined to 0.5053(11).

The crystal of **3e** contained large voids (648.6 Å^3 / unit cell) filled with disordered solvent molecules. Their contribution to the structure factors was secured by back-Fourier transformation using the routine SQUEEZE of the program PLATON resulting in 228.8 electrons / unit cell.[64]

In the crystal structure of **3i** the methyl group at C33 was rotationally disordered.

Further details concerning the crystal structure determinations are given in Table 4.4.

Table 4.4. Selected crystallographic data for complexes **3a**, **3e**, **3g**, and **3i**.

	3a	**3e**	**3g**	**3i**
formula	$C_{19}H_{20}Br_2N_4Ni \cdot CH_2Cl_2$	$C_{31}H_{28}Br_2N_4Ni \cdot CH_2Cl_2$ + disordered solvent	$C_{20}H_{22}Br_2N_4Ni$	$C_{20}H_{24}Br_2N_4NiSi$
Fw	607.85	760.03 [a]	536.95	567.05
crystal color	yellow	yellow	yellow	dark yellow
crystal size [mm^3]	0.42x0.15x0.13	0.45x0.27x0.15	0.66x0.12x0.06	0.42x0.31x0.27
crystal system	monoclinic	monoclinic	monoclinic	monoclinic
space group	$P2_1/c$ (no. 14)	$P2_1/c$ (no. 14)	$P2_1/c$ (no. 14)	$P2_1/c$ (no. 14)
a [Å]	10.885(2)	9.7277(4)	10.00749(19)	8.5452(2)
b [Å]	19.126(4)	15.0886(6)	14.1631(2)	17.5481(3)
c [Å]	15.216(3)	25.4183(9)	15.0239(2)	14.7896(3)
β [°]	133.513(4)	106.788(2)	106.392(1)	97.951(2)
V [Å^3]	2297.3(8)	3571.8(2)	2042.89(6)	2196.42(8)
Z	4	4	4	4
D_x [g/cm^3]	1.757	1.413 [a]	1.746	1.715
$(\sin\theta/\lambda)_{max}$ [Å^{-1}]	0.61	0.61	0.65	0.65
refl. meas./unique	41727 / 7247	54246 / 6591	34303 / 4693	45494
μ [mm^{-1}]	4.570	2.955 [a]	4.874	4.590
abs. corr.	analytical	multi-scan	analytical	multi-scan
abs. corr. range	0.28-0.76	0.29-0.64	0.12-0.82	0.13-0.29
param./restraints	265 / 0	370 / 0	246 / 0	257 / 0
R1/wR2 [I>2σ(I)]	0.0637 / 0.1553	0.0579 / 0.1472	0.0514 / 0.1023	0.0275 / 0.0655
R1/wR2 [all refl.]	0.0849 / 0.1681	0.0673 / 0.1508	0.0686 / 0.1085	0.0372 / 0.0691
S	1.153	1.083	1.140	1.084
res. density [e/Å^3]	-1.59 / 2.20	-0.77 / 1.59	-1.25 / 1.46	-1.00 / 0.43

[a] Derived parameters do not contain the contribution of the disordered solvent.

4.5 References

(1) Arduengo, A. J.; Harlow, R. L.; Kline, M. *J. Am. Chem. Soc.* **1991**, *113*, 361.
(2) Lee, M. T.; Hu, C. H. *Organometallics* **2004**, *23*, 976.
(3) Weskamp, T.; Kohl, F. J.; Hieringer, W.; Gleich, D.; Herrmann, W. A. *Angew. Chem. Int. Ed.* **1999**, *38*, 2416.
(4) Herrmann, W. A. *Angew. Chem. Int. Ed.* **2002**, *41*, 1291.
(5) Weskamp, T.; Bohm, V. P. W.; Herrmann, W. A. *J. Organomet. Chem.* **2000**, *600*, 12.
(6) Hahn, F. E.; Jahnke, M. C. *Angew. Chem. Int. Ed.* **2008**, *47*, 3122.
(7) Scholl, M.; Ding, S.; Lee, C. W.; Grubbs, R. H. *Org. Lett.* **1999**, *1*, 953.
(8) Angulo, I. M.; Bouwman, E.; Lutz, M.; Mul, W. P.; Spek, A. L. *Inorg. Chem.* **2001**, *40*, 2073.
(9) Angulo, I. M.; Bouwman, E.; van Gorkum, R.; Lok, S. M.; Lutz, M.; Spek, A. L. *J. Mol. Catal. A-Chem.* **2003**, *202*, 97.
(10) Hassan, J.; Sevignon, M.; Gozzi, C.; Schulz, E.; Lemaire, M. *Chem. Rev.* **2002**, *102*, 1359.
(11) Kantchev, E. A. B.; O'Brien, C. J.; Organ, M. G. *Angew. Chem. Int. Ed.* **2007**, *46*, 2768.
(12) Hillier, A. C.; Grasa, G. A.; Viciu, M. S.; Lee, H. M.; Yang, C. L.; Nolan, S. P. *J. Organomet. Chem.* **2002**, *653*, 69.
(13) Tamao, K.; Sumitani, K.; Kumada, M. *J. Am. Chem. Soc.* **1972**, *94*, 4374.
(14) Percec, V.; Golding, G. M.; Smidrkal, J.; Weichold, O. *J. Org. Chem.* **2004**, *69*, 3447.
(15) Wolf, C.; Xu, H. H. *J. Org. Chem.* **2008**, *73*, 162.
(16) Consiglio, G.; Morandini, F.; Piccolo, O. *Tetrahedron* **1983**, *39*, 2699.
(17) Babudri, F.; Florio, S.; Ronzini, L.; Aresta, M. *Tetrahedron* **1983**, *39*, 1515.
(18) McGuinness, D. S.; Cavell, K. J.; Skelton, B. W.; White, A. H. *Organometallics* **1999**, *18*, 1596.
(19) Lee, C. C.; Ke, W. C.; Chan, K. T.; Lai, C. L.; Hu, C. H.; Lee, H. M. *Chem.-Eur. J.* **2007**, *13*, 582.
(20) Xi, Z. X.; Zhang, X. M.; Chen, W. Z.; Fu, S. Z.; Wang, D. Q. *Organometallics* **2007**, *26*, 6636.
(21) Liao, C. Y.; Chan, K. T.; Chang, Y. C.; Chen, C. Y.; Tu, C. Y.; Hu, C. H.; Lee, H. M. *Organometallics* **2007**, *26*, 5826.
(22) Corriu, J. P.; Masse, J. P. *J. Chem. Soc.-Chem. Commun.* **1972**, 144.
(23) Bohm, V. P. W.; Weskamp, T.; Gstottmayr, C. W. K.; Herrmann, W. A. *Angew. Chem. Int. Ed.* **2000**, *39*, 1602.
(24) Wolf, J.; Labande, A.; Daran, J. C.; Poli, R. *J. Organomet. Chem.* **2006**, *691*, 433.
(25) Wolf, J.; Labande, A.; Natella, M.; Daran, J. C.; Poli, R. *J. Mol. Catal. A-Chem.* **2006**, *259*, 205.
(26) Inamoto, K.; Kuroda, J.; Sakamoto, T.; Hiroya, K. *Synthesis* **2007**, 2853.
(27) Matsubara, K.; Ueno, K.; Shibata, Y. *Organometallics* **2006**, *25*, 3422.
(28) Xi, Z.; Liu, B.; Chen, W. *J. Org. Chem.* **2008**, *73*, 3954.
(29) Zhou, Y. B.; Xi, Z. X.; Chen, W. Z.; Wang, D. Q. *Organometallics* **2008**, *27*, 5911.
(30) Douthwaite, R. E.; Green, M. L. H.; Silcock, P. J.; Gomes, P. T. *Organometallics* **2001**, *20*, 2611.
(31) Herrmann, W. A.; Schwarz, J.; Gardiner, M. G.; Spiegler, M. *J. Organomet. Chem.* **1999**, *575*, 80.
(32) Herrmann, W. A.; Schwarz, J.; Gardiner, M. G. *Organometallics* **1999**, *18*, 4082.
(33) Baker, M. V.; Skelton, B. W.; White, A. H.; Williams, C. C. *J. Chem. Soc.-Dalton Trans.* **2001**, 111.
(34) Douthwaite, R. E.; Haussinger, D.; Green, M. L. H.; Silcock, P. J.; Gomes, P. T.; Martins, A. M.; Danopoulos, A. A. *Organometallics* **1999**, *18*, 4584.
(35) Clyne, D. S.; Jin, J.; Genest, E.; Gallucci, J. C.; RajanBabu, T. V. *Org. Lett.* **2000**, *2*, 1125.
(36) Hahn, F. E.; Wittenbecher, L.; Boese, R.; Blaser, D. *Chem.-Eur. J.* **1999**, *5*, 1931.
(37) Huynh, H. V.; Holtgrewe, C.; Pape, T.; Koh, L. L.; Hahn, E. *Organometallics* **2006**, *25*, 245.
(38) Lee, H. M.; Lu, C. Y.; Chen, C. Y.; Chen, W. L.; Lin, H. C.; Chiu, P. L.; Cheng, P. Y. *Tetrahedron* **2004**, *60*, 5807.
(39) Shi, Z.; Thummel, R. P. *J. Org. Chem.* **1995**, *60*, 5935.
(40) Baker, M. V.; Bosnich, M. J.; Brown, D. H.; Byrne, L. T.; Hesler, V. J.; Skelton, B. W.; White, A. H.; Williams, C. C. *J. Org. Chem.* **2004**, *69*, 7640.

(41) Starikova, O. V.; Dolgushin, G. V.; Larina, L. I.; Ushakov, P. E.; Komarova, T. N.; Lopyrev, V. A. *Russ. J. Organ. Chem.* **2003**, *39*, 1467.
(42) Murphy, J. A.; Khan, T. A.; Zhou, S. Z.; Thomson, D. W.; Mahesh, M. *Angew. Chem. Int. Ed.* **2005**, *44*, 1356.
(43) Kucukbay, H.; Cetinkaya, E.; Durmaz, R. *Arzneimittel-Forsch.* **1995**, *45-2*, 1331.
(44) McGuinness, D. S.; Mueller, W.; Wasserscheid, P.; Cavell, K. J.; Skelton, B. W.; White, A. H.; Englert, U. *Organometallics* **2002**, *21*, 175.
(45) Hahn, F. E.; von Fehren, T.; Lugger, T. *Inorg. Chim. Acta* **2005**, *358*, 4137.
(46) Mata, J. A.; Chianese, A. R.; Miecznikowski, J. R.; Poyatos, M.; Peris, E.; Faller, J. W.; Crabtree, R. H. *Organometallics* **2004**, *23*, 1253.
(47) Brookhart, M.; Green, M. L. H.; Parkin, G. *Proc. Natl. Acad. Sci. U. S. A.* **2007**, *104*, 6908.
(48) Ahrens, S.; Zeller, A.; Taige, M.; Strassner, T. *Organometallics* **2006**, *25*, 5409.
(49) Haswell, S. J.; O'Sullivan, B.; Styring, P. *Lab Chip* **2001**, *1*, 164.
(50) Huang, J. K.; Nolan, S. P. *J. Am. Chem. Soc.* **1999**, *121*, 9889.
(51) Lipshutz, B. H.; Tomioka, T.; Blomgren, P. A.; Sclafani, J. A. *Inorg. Chim. Acta* **1999**, *296*, 164.
(52) Martin, R.; Buchwald, S. L. *J. Am. Chem. Soc.* **2007**, *129*, 3844.
(53) Tsai, F. Y.; Lin, B. N.; Chen, M. J.; Mou, C. Y.; Liu, S. T. *Tetrahedron* **2007**, *63*, 4304.
(54) Wang, Z. X.; Wang, L. *Chem. Commun.* **2007**, 2423.
(55) Tamao, K.; Sumitani, K.; Kiso, Y.; Zembayashi, M.; Fujioka, A.; Kodama, S.; Nakajima, I.; Minato, A.; Kumada, M. *Bull. Chem. Soc. Jpn.* **1976**, *49*, 1958.
(56) Tasler, S.; Lipshutz, B. H. *J. Org. Chem.* **2002**, *68*, 1190.
(57) Ariafard, A.; Lin, Z. Y. *Organometallics* **2006**, *25*, 4030.
(58) Phillips, M. A. *J. Chem. Soc.* **1929**, *131*, 2820.
(59) Raehm, L.; Mimassi, L.; Guyard-Duhayon, C.; Amouri, H.; Rager, M. N. *Inorg. Chem.* **2003**, *42*, 5654.
(60) Duisenberg, A. J. M.; Kroon-Batenburg, L. M. J.; Schreurs, A. M. M. *J. Appl. Crystallogr.* **2003**, *36*, 220.
(61) Beurskens, P. T.; Admiraal, G.; Beurskens, G.; Bosman, W. P.; Garcia-Granda, S.; Gould, R. O.; Smits, J. M. M.; Smykalla, C. *The DIRDIF99 program system*, Technical Report of the Crystallography Laboratory, University of Nijmegen, The Netherlands: 1999.
(62) Altomare, A.; Burla, M. C.; Camalli, M.; Cascarano, G. L.; Giacovazzo, C.; Guagliardi, A.; Moliterni, A. G. G.; Polidori, G.; Spagna, R. *J. Appl. Crystallogr.* **1999**, *32*, 115.
(63) Sheldrick, G. M. *Acta Crystallogr. Sect. A* **2008**, *64*, 112.
(64) Spek, A. L. *J. Appl. Cryst.* **2003**, *36*, 7.
(65) Herbst-Irmer, R.; Sheldrick, G. M. *Acta Crystallogr. Sect. B-Struct. Sci.* **1998**, *54*, 443.

Chapter 5

N-donor functionalized N-heterocyclic carbene nickel(II) complexes in the Kumada coupling[†]

Abstract. *The synthesis and characterization of novel nickel(II) complexes bearing two bidentate N-heterocyclic carbene ligands functionalized with anionic N-donor moieties are described. Two different N-donor groups are employed, namely amido and benzimidazolato moieties. The solid-state structures of three of these complexes have been determined by X-ray crystallography. The amido-functionalized low-spin, square-planar Ni(II) complexes exhibit a cis-geometry around the metal center, while the benzimidazolato-functionalized complex crystallizes as the trans isomer. The activity of these novel complexes in the Kumada cross-coupling of phenylmagnesium chloride with 4-chloroanisole and 4-fluoroanisole was investigated. One of the benzimidazolato-functionalized complexes shows the highest activity in this reaction reported to date, yielding the desired product in quantitative yields within 30 minutes (4-chloroanisole), or 150 minutes (4-fluoroanisole) with only 1 mol% catalyst.*

[†] Based on: J. Berding, T. F. van Dijkman, M. Lutz, A. L. Spek, E. Bouwman, *Dalton Trans.*, **2009**, 6948

5.1 Introduction

The study and application of N-heterocyclic carbenes (NHCs) have increased rapidly in recent years, most notably for their use as spectator ligands in homogeneous catalysis.[1-4] For example, palladium NHC complexes have been used as versatile catalysts for a number of C–C couplings reactions, such as the Heck, Stille, Suzuki and Sonogashira reactions, which are of great importance for organic chemistry.[5] Though not as popular as their palladium analogues, nickel NHC complexes have also been investigated for a number of C–C couplings reactions. One reaction in which nickel complexes perform particularly well, compared to palladium, is the Kumada cross-coupling of aryl halides with aryl Grignard reagents. This reaction, discovered simultaneously by two groups in 1972,[6, 7] may be an economically attractive alternative to other cross-coupling reactions, as it uses cheap starting materials and only has magnesium salts as by-products, even though it lacks the functional group tolerance.

An early report of the use of N-heterocyclic carbenes in the nickel-catalyzed Kumada coupling from the group of Herrmann revealed that imidazolium salts with bulky N-substituents in combination with $Ni(acac)_2$ generates an active catalyst for the coupling of aryl chlorides with aryl Grignard reagents.[8] The results on the Kumada coupling with nickel complexes of chelating benzimidazole-based dicarbenes is described in Chapter 4. Other groups investigated chelating ligands or ligand precursors consisting of one (or more) NHC and one (or more) hemi-labile group for the same reaction.[9-12] In most cases these chelating ligands are neutral, leading to either cationic Ni(II) complexes or complexes with coordinated counterions, such as halides. A recent review describing donor-functionalized NHC complexes of group 9 and 10 metals, reveals that NHC ligands with anionic side groups are quite uncommon.[4] A number of nickel(II) complexes of chelating ligands with N-heterocyclic carbenes and amido functionalities has recently been reported to form active catalysts in the Suzuki cross-coupling.[13] The present chapter describes the Kumada coupling using nickel complexes of NHC ligands with various pendant anionic N-donor moieties.

5.2 Results and Discussion

5.2.1 Synthesis of ligand precursors

An overview of the ligand precursors used in this study is shown in Figure 5.1. Ligand precursors **1** and **2** were synthesized following an adaptation of literature procedures,[14] by reacting N-substituted (benz)imidazoles with 2-chloro-N-phenylacetamide. Novel ligand precursors **3** and **4** were obtained in good yield by a facile quaternization of N-benzyl(benz)imidazole with 2-chloromethylbenzimidazole in hot 1,4-dioxane. The ^{1}H and ^{13}C NMR spectra of **1 – 4** show the characteristic

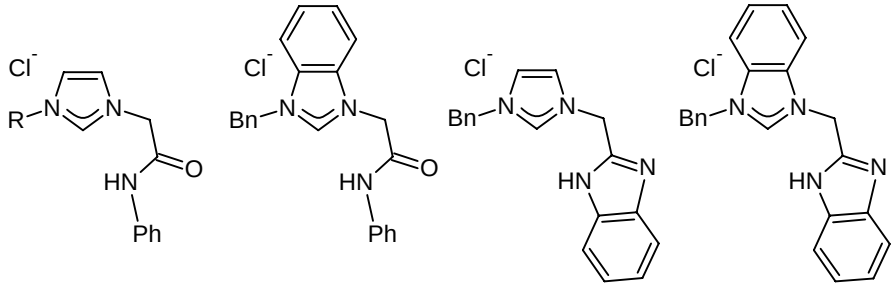

Figure 5.1. Overview of the ligand precursors used in this study.

imidazolium NCHN resonances around 9.5 and 140 ppm, respectively. The formation of **1** – **4** was further confirmed with ESI-MS, the spectra showing the parent peak for the respective $[M - Cl]^+$ fragments.

5.2.2 Synthesis and characterization of the nickel complexes

Treatment of ligand precursors **1** – **4** with potassium carbonate in the presence of nickel(II) chloride in hot DMF yields yellow, diamagnetic complexes **5** – **8**, shown in Figure 5.2. All complexes are air- and moisture stable and could be isolated after treatment with water in air. In principle such complexes can be obtained as either the *cis* or the *trans* isomer. It was shown for complex **5b** that the ratio of the two isomers depends on the polarity of the solvent: more polar solvents yield a higher amount of the *cis* complex, while in apolar solvents the complex isomerizes to the *trans* isomer.[13]

In accordance with the square-planar geometry of the nickel(II) complexes, the ^{1}H NMR spectra of all complexes show sharp signals in the diamagnetic region. The characteristic NCHN signals of the precursors are absent from the NMR spectra of these complexes, indicating carbene generation. In addition, the NH signals are no

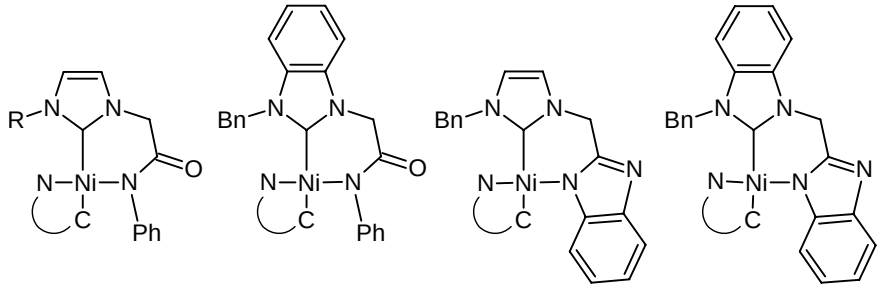

Figure 5.2. Schematic representation of the nickel complexes 5-8. Only the *trans* isomer is drawn.

longer present in the spectra of the complexes, reflecting bidentate coordination of the ligand. The ^{1}H NMR spectrum of **7** in DMSO-d_6 is indicative of a 0.6:0.4 mixture of *trans* and *cis* isomers (Figure 5.3). No attempts were made to assign the peaks to

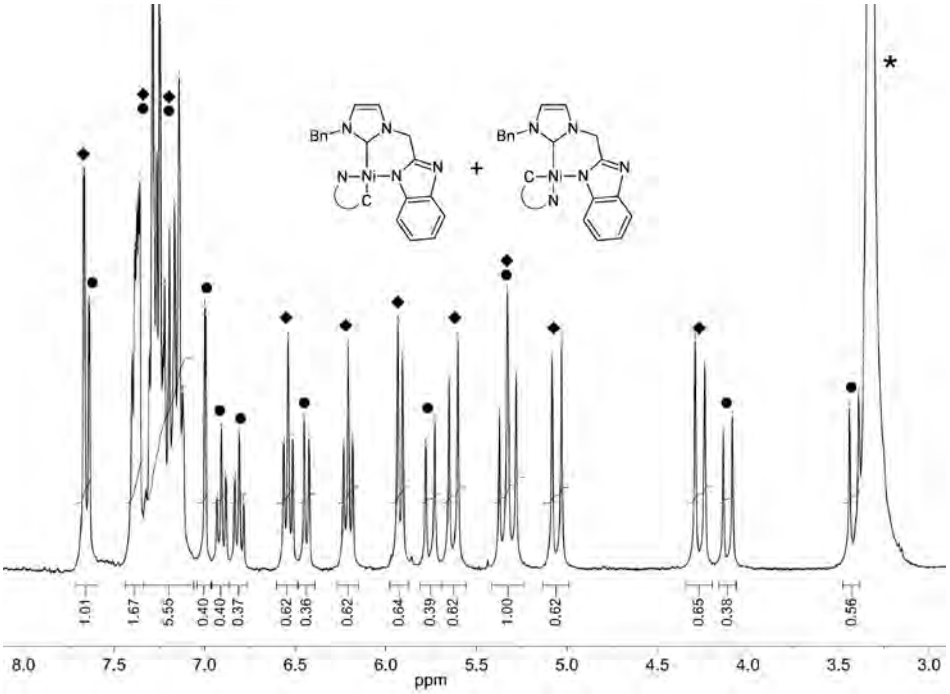

Figure 5.3. ^{1}H NMR spectrum of complex **7** in DMSO. The peaks of two different isomers are marked with (♦) and (●). The residual water peak is marked with (*).

their respective isomers. In $CDCl_3$ only one isomer of **7** is present, presumably with the *trans* configuration. The other nickel compounds appear to be present as a single isomer in DMSO-d_6. The ^{1}H NMR spectra of all complexes show splitting of the

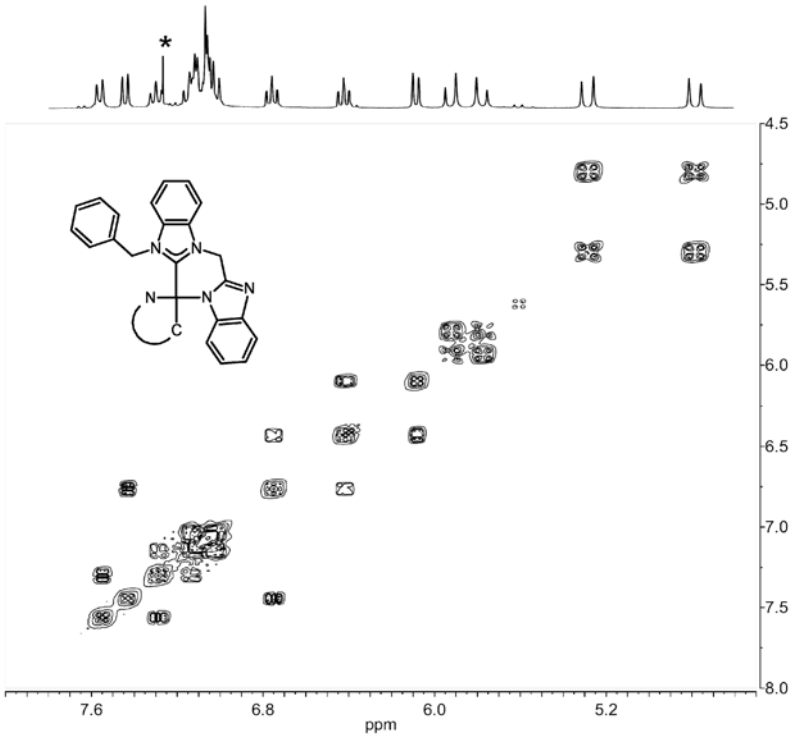

Figure 5.4. ^{1}H COSY NMR spectrum of complex **8** in $CDCl_3$. The residual solvent peak is marked with (*).

backbone-CH_2 resonances, apparently caused by the rigidity of the structure in solution. The resonances of the benzimidazolato group of complex **8** are split over a range of 1.5 ppm and could be assigned with the aid of COSY NMR spectroscopy (Figure 5.4). The ESI-MS spectra of the complexes show the $[M + H]^+$ parent peak for all complexes.

5.2.3 Description of the structures

Single crystals suitable for X-ray crystal structure determination were obtained from methanol (**5a**), by slow diffusion of hexane into a concentrated solution of the compound in dichloromethane (**6**), or by slow diffusion of diethyl ether into a concentrated solution of the compound in chloroform (**8**). Molecular plots of **5a** and **6** are shown in Figure 5.5, selected bond lengths, angles and torsion angles are given in Table 5.1.

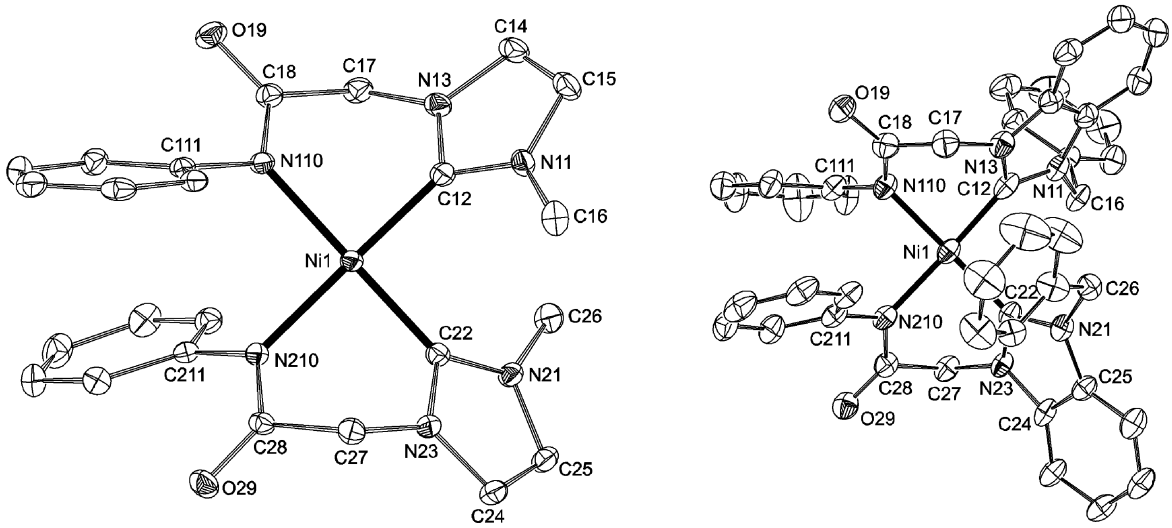

5a **6**

Figure 5.5. Displacement ellipsoid plots (30% probability level) of **5a** and **6** in the crystal. In **5a** only one of two independent metal units is shown. In both cases, hydrogen atoms and solvent molecules are omitted for clarity.

The two independent metal entities of **5a**, as well as complex **6**, have an approximate twofold symmetry, which is only broken by slightly different conformations of the phenyl rings. The nickel ions in these complexes are in a slightly distorted square-planar geometry with *cis*-angles that range between 85.60(14) and 94.71(15)°. The ligands are bound in a *cis* configuration. The Ni–C and Ni–N bond distances are within the expected range.[13] The carbene (benz)imidazol-2-ylidene rings are twisted with respect to the coordination plane by 45.08(11) – 53.5(2)°. The six-membered chelate rings adopt a boat conformation in all cases.

Table 5.1. Selected bond lengths (Å), angles, and torsion angles (°) for **5a** and **6**. [Second independent molecule of **5a** in brackets] and parameters for the hydrogen bonding in **5a**.

	5a	**6**
Ni1 – N110	1.9524(18) [1.9338(18)]	1.926(3)
Ni1 – N210	1.9511(18) [1.9582(18)]	1.952(3)
Ni1 – C12	1.849(2) [1.845(2)]	1.852(4)
Ni1 – C22	1.867(2) [1.849(2)]	1.875(3)
C14 – C15	1.337(4) [1.340(4)]	1.387(5)
C24 – C25	1.341(3) [1.349(3)]	1.400(5)
N110 – Ni1 – N210	92.57(8) [94.12(8)]	91.89(12)
N110 – Ni1 – C12	88.44(9) [88.14(9)]	85.60(14)
N210 – Ni1 – C22	88.05(9) [87.87(8)]	87.69(14)
C12 – Ni1 – C22	91.02(10) [89.92(9)]	94.71(15)
N11 – C12 – N13	105.2(2) [104.98(19)]	105.8(3)
N21 – C22 – N23	104.74(19) [104.47(19)]	106.3(3)
N110 – Ni1 – C12 – N13	–43.82(18) [–46.37(17)]	53.0(3)
N210 – Ni1 – C22 – N23	–42.76(18) [–43.98(19)]	42.0(3)

5a	D-H [Å]	H···A [Å]	D···A [Å]	D-H···A [°]
O5-H5O···O19	0.96	1.80	2.740(2)	168
O6-H6O···O29	0.93	1.75	2.675(2)	173
O7-H7O···O49	0.89	1.86	2.731(3)	166
O8-H8O···O19	1.05	1.70	2.737(3)	169
O9-H9A···O8	1.02	1.98	2.934(3)	154
O9-H9B···O39	0.96	1.94	2.797(3)	175

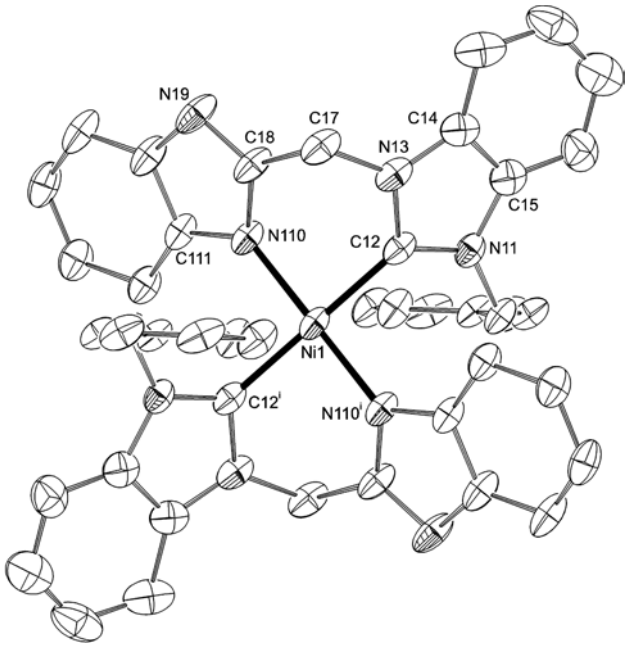

Figure 5.6. Displacement ellipsoid plot (30% probability level) of **8**. Only one of the independent metal complexes is shown. Hydrogen atoms and solvent molecules are omitted for clarity. Symmetry operation i: –x, –y, –z.

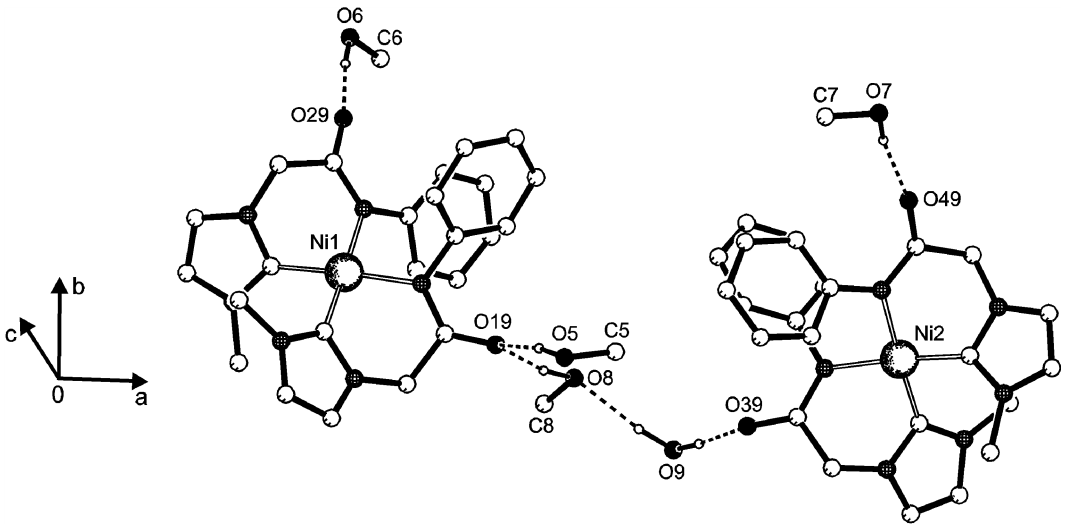

Figure 5.7. Discrete hydrogen-bonded aggregate of metal complexes, methanol and water molecules in the asymmetric unit of **5a**. C-H hydrogen atoms are omitted for clarity. Geometrical characterizations of the hydrogen bonds are provided in Table 5.1.

The asymmetric unit of **5a** contains two independent metal complexes, four methanol and one water molecule, which are connected by O-H···O hydrogen bonds (Figure 5.7). In particular, hydrogen bonding occurs through the carbonyl functionalities of the ligands. Oxygen O29 is acceptor of a hydrogen bond from a methanol molecule, while oxygen O19 interacts with two methanol molecules, one of which is linked to the water molecule. The latter connects to the other nickel complex through oxygen O39. Finally, oxygen O49 is a hydrogen bond acceptor of the fourth methanol molecule.

Two independent metal complexes are present in the crystal structure of **8**, which are both located on inversion centers. The asymmetric unit thus contains two

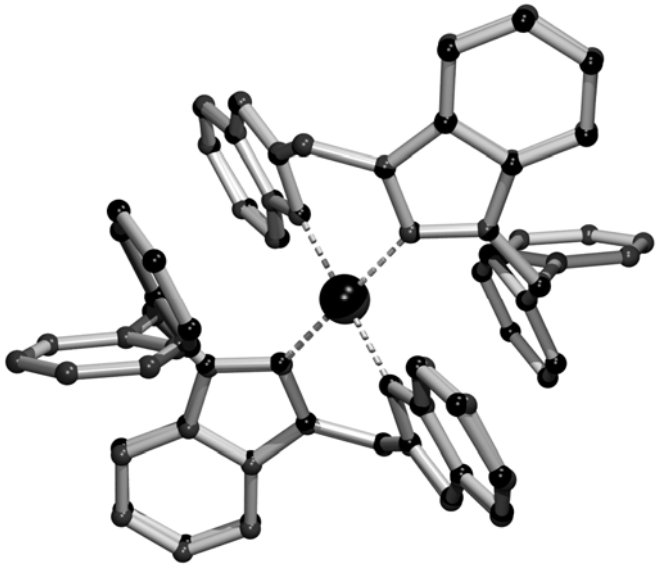

Figure 5.8. Quaternion fit of the two independent metal complexes in the crystal structure of **8**, based on the six-membered chelate ring. Both independent molecules are located on an inversion center. The calculation was performed with the program PLATON.

Table 5.2. Selected bond lengths (Å), angles, and torsion angles (°) for **8**. [Second independent molecule in brackets].

Ni1 – N110	1.8840(13) [1.8776(12)]
Ni1 – C12	1.9133(19) [1.9070(15)]
C14 – C15	1.370(3) [1.389(2)]
N110 – Ni1 – C12	86.41(7) [86.59(6)]
N110 – Ni1 – C12^{i}	93.59(7) [93.41(6)]
N11 – C12 – N13	105.58(16) [106.33(13)]
N110 – Ni1 – C12 – N13	42.19(14) [43.54(12)]

different half molecules. A molecular plot is shown in Figure 5.6 and a selection of bond lengths, angles and torsion angles is listed in Table 5.2.

Due to the inversion symmetry of the metal complexes, a *trans* ligand geometry is present. The nickel ion has an almost square-planar geometry, with Ni–C bond lengths of 1.9070(15) – 1.9133(19) Å. These distances are significantly longer than the Ni–C distances found for the *cis* complexes **5a** and **6** and are slightly longer than those found in *trans*-[(NHC)$_2$NiI$_2$] complexes, in which NHC is a monodentate benzimidazole-based N-heterocyclic carbene.[15] The Ni–N$^-$ bond lengths of compound **8** of 1.8776(12) – 1.8840(13) Å are shorter than in other Ni complexes with a N-deprotonated benzimidazole ligand, with distances of 1.9004(14)[16] and 2.0724(16) Å.[17] The carbene rings are twisted with respect to the NiC$_2$N$_2$ coordination plane by 45.46(9) and 46.01(7)°, while the N-coordinated benzimidazole rings are twisted by 42.46(11) and 44.39(8)°. The six-membered chelate rings adopt boat conformations. The two independent complexes in the asymmetric unit have roughly the same coordination environment around the nickel center. However, a significant difference is observed in the orientation of the benzyl side group. A superposition of the two molecules showing this difference is given in Figure 5.8. One of the orientations brings the benzyl aromatic ring in proximity of the nickel center, resulting in an

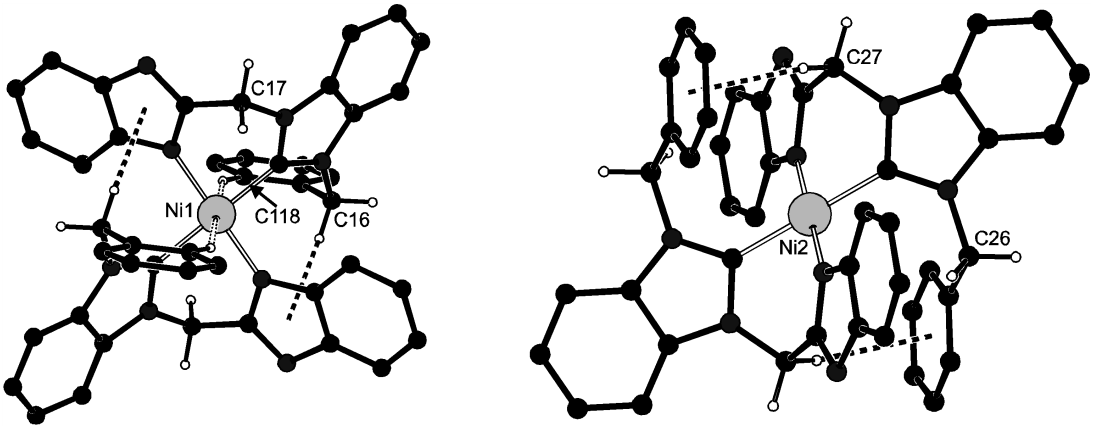

Figure 5.9. C-H···Ni and C-H···π interactions in the two independent molecules of **8**. H118···Ni1, 2.72 Å; C118···Ni1, 3.579(2) Å; C118-H118···Ni1, 151°; H16A···Cg, 2.54 Å; C16···Cg, 3.485(2) Å; C16-H16A···Cg, 161°; H27B···Cg, 2.65 Å; C27···Cg, 3.5420(19); C27-H27B···Cg, 150°.

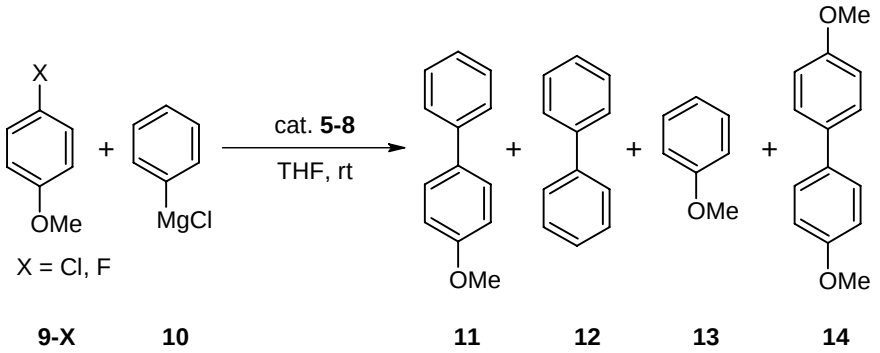

Scheme 5.1. Products of the nickel-catalyzed Kumada cross-coupling of 4-haloanisole and phenylmagnesium chloride.

anagostic interaction between one *ortho* proton and the nickel ion (d(Ni···H = 2.72 Å, ∠(C-H···Ni) = 151°).[18] Similar observations were reported recently for square-planar nickel complexes containing phenylimidazole as a ligand.[19] The other orientation in the second independent metal complex allows a C-H···π interaction between one of the CH_2-bridges as donor and the benzyl aromatic ring as acceptor (Figure 5.9).

5.2.4 Catalytic studies

Complexes **5** – **8** were tested as catalysts in the Kumada coupling of 4-chloroanisole (**9-Cl**) with phenylmagnesium chloride (**10**) at room temperature (Scheme 5.1). The results of the catalytic experiments are summarized in Table 5.3. The reaction was monitored by taking samples at regular intervals and analysis by gas chromatography. A number of side products was identified. Apart from the desired product 4-methoxybiphenyl (**11**), varying amounts of biphenyl (**12**), anisole

Table 5.3. Nickel-catalyzed Kumada cross-coupling of 4-haloanisole and phenylmagnesium chloride at room temperature.[a]

		Time [b]	Yield (10^{-2} mmol) [c]			
Entry	Catalyst	(min)	**11**	**12**	**13**	**14**
1	**5a**	150	85	10	1	6
2	**5b**	75	87	13	3	4
3	**6**	150	90	15	2	3
4	**7**	20	99 (95)	3	0	0
5	**8**	12	97	6	0	2
6	**8** [d]	30	99	3	0	0
7	**8** [d,e]	150	98	5	0	1
8	(C^C)NiBr$_2$ [f]	< 840	99	6	0	0

[a] Reaction conditions: 0.03 mmol cat., 1.0 mmol 4-chloroanisole, 1.5 mmol phenylmagnesium chloride (25 wt% in THF), 1.0 mL THF, RT; [b] Time needed for full consumption of 4-haloanisole; [c] Yields determined by GC, average of two runs. Yields in parentheses are isolated yields; [d] 0.01 mmol cat.; [e] 4-fluoroanisole was used a substrate; [f] Dibromido-1,1′-dibenzyl-3,3′-(1,3-propanediyl)dibenzimidazol-2,2′-diylidenenickel(II), see Chapter 4.

(**13**) and bisanisole (**14**) were found to be present in the reaction mixtures.

Initially, the catalytic reactions were performed using commonly used conditions, *i.e.* a 0.03 : 1 : 1.5 ratio of nickel complex, 4-chloroanisole, and phenylmagnesium chloride in THF at room temperature (Table 5.3, entry 1 – 5).[8, 9, 20] Additionally, complex **8** was used at a lower catalyst loading of 1.0 mol% (entry 6) and it was used to couple 4-fluoroanisole (**9-F**) with phenylmagnesium chloride at the same low catalyst loading (entry 7).

The results of the catalytic reactions are summarized in Table 5.3 as the time needed to quantitatively consume the 4-haloanisole with the yields (in mmol) of the desired product and the side products. As the Grignard reagent was used in excess, and unreacted Grignard reagent cannot be detected on GC, the following constraints should apply (see Chapter 4): The sum of the amounts of **11**, **13** and twice the amount of **14** should be equal to 1 mmol, while the amount of **12** should not exceed half the amount of Grignard reagent that did not react to form **11**, which is equal to 0.5 × (1.5 mmol – the amount of **11**). Both requirements are met in all catalytic experiments.

All complexes **5** – **8** are catalytically active in the coupling of 4-chloroanisole with phenylmagnesium chloride. The time needed to consume all starting aryl halide and the selectivity, however, are strongly dependent on the ligand used. The catalysts **5** and **6** with the amide-substituted ligands need 75 to 150 minutes to complete the reaction, yielding the desired product in 85 to 90% yield. The complexes **7** and **8** with benzimidazole-substituted ligands are highly active, furnishing the product **11** in nearly quantitative yields in less than 20 minutes. A plot of the development of reagents and products in the reaction mixture in time using compound **8** (Table 5.3, entry 6) is shown in Figure 5.10. In this case side products **13** and **14** are not detected in the reaction mixture. A short induction time is observed.

Used at a lower catalyst concentration, compound **8** was able to couple the two reagents quantitatively within 30 minutes at room temperature, corresponding to an average turnover frequency of 200 mol·(mol cat.)$^{-1}$·h^{-1}. Moreover, even the less reactive 4-fluoroanisole could be coupled efficiently and nearly quantitatively in 150 minutes at the same 1 mol% catalyst concentration.

Compared to the catalytic results obtained with nickel catalysts with bidentate bisNHC ligands (Chapter 4), the new complexes with anionic (C^N$^-$) ligands perform remarkably well. The best performing bisNHC nickel catalyst reported in Chapter 4 was also able to reach quantitative conversion of the aryl chloride to the desired product; however, it required about 14 hours to complete the reaction (Table 5.3, entry 8).[21]

Several reports have been published on the nickel NHC catalyzed Kumada coupling of 4-chloroanisole (**9-Cl**) with phenylmagnesium chloride.[8-12, 20-23] As different conditions were used in different studies and furthermore, in most cases only the conversion and selectivity after a fixed time are given, comparison is difficult. The best performing nickel NHC complexes to date are the following. A

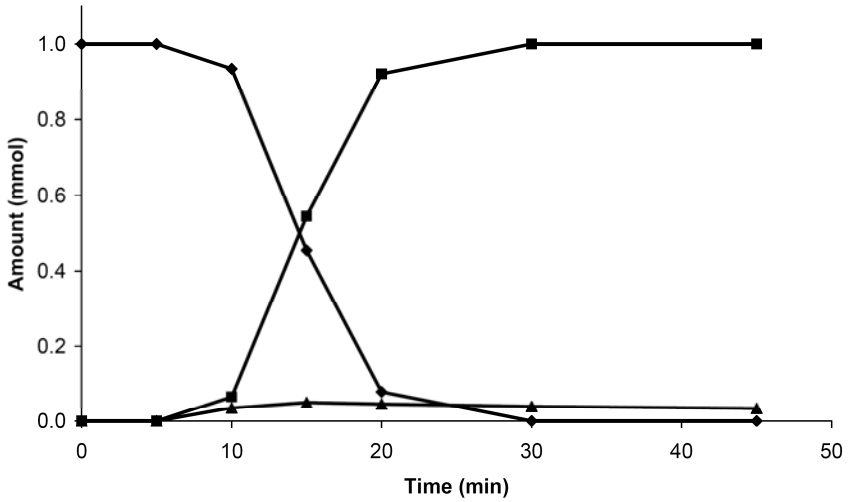

Figure 5.10. Evolution of the products in time of a typical catalytic experiment (Table 5.3, entry 6): (♦) 4-chloroanisole; (■) 4-methoxybiphenyl; (▲) biphenyl.

nickel complex bearing a phosphane-NHC (C^P) bidentate ligand, gave **11** in 95% yield after 18 h, although a kinetic study on one of the complexes revealed that the reaction was actually completed within one hour.[9, 20] In addition, using 0.5 mol% $Ni(IPr)(PPh_3)Cl_2$ (IPr = 1,3-bis(2,6-diisopropylphenyl)imidazol-2-ylidene) product **11** could be obtained in 39% yield in 30 minutes,[22] while a dinuclear nickel complex was reported to couple 4-chloroanisole with phenylmagnesium bromide in 91% yield in 12 h at the same catalyst loading.[12]

The best performing nickel NHC catalyst for the Kumada coupling of 4-fluoroanisole (**9-F**) with phenylmagnesium bromide reported to date consists of a 1:1 mixture of $Ni(acac)_2$ and a bulky imidazolium salt, leading to 58% conversion to **11** in 18 h with 5 mol% nickel.[24] Evidently, complex **8** is an extremely efficient catalyst, in terms of both reaction rate and selectivity.

The reactivity of complex **5b** has been reported for the Suzuki coupling of phenylboronic acid with 4-chloroanisole, amongst others.[13] This yielded 4-methoxybiphenyl in 92% yield after 18h, using 3 mol% of catalyst, 6 mol% of PPh_3 and stoichiometric amounts of K_3PO_4 as additional base, at 80 °C in toluene. Clearly, to obtain the desired coupling product the Kumada coupling is more efficient and economical.

5.2.5 Mechanistic considerations

As the present catalysts are the only ones described for the Kumada coupling using a ligand with an anionic pendant arm, it is believed that the relatively high rates in the catalytic runs must be due to the presence of these anionic side groups. The commonly accepted mechanism for the Kumada coupling consists of three consecutive steps: (1) oxidative addition of the aryl halide to a Ni(0) active species,

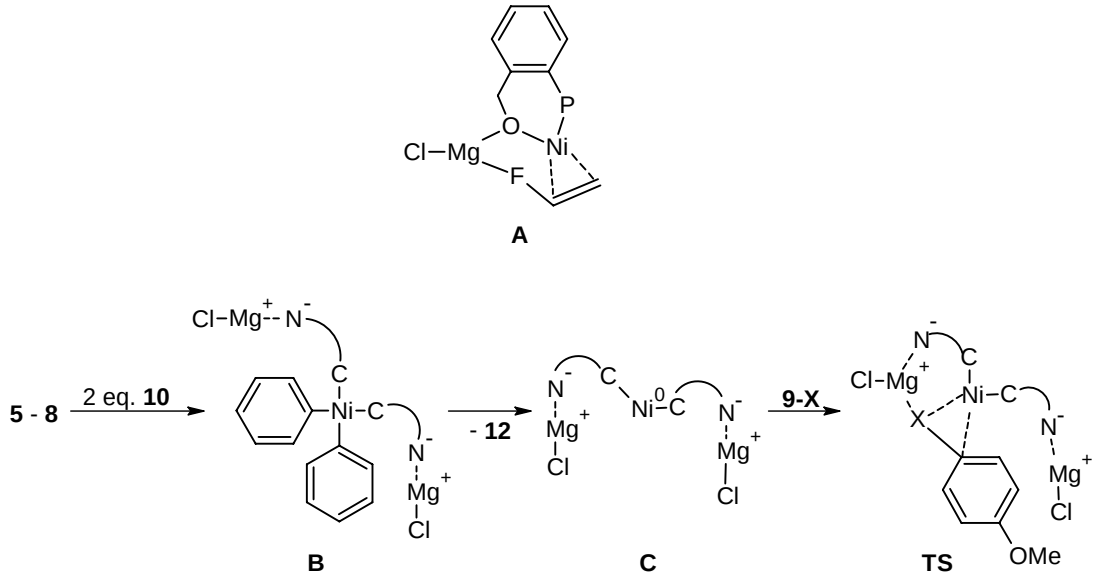

Scheme 5.2. Transition state proposed by Yoshikai *et al.*[26] (**A**) and proposed mechanism for the activation of the pre-catalyst and the transition state for carbon-halide bond activation for the system described in this chapter (**B** – **TS**).

(2) exchange of the halide on the nickel ion with the aryl group of the Grignard reagent (transmetalation) and (3) reductive elimination of the biaryl product, furnishing the coupling product and the starting Ni(0) species.[25] The Ni(0) species is believed to be obtained from the starting Ni(II) complex by two consecutive transmetalation steps, followed by a reductive elimination of biphenyl.

In the present case this implies that the two anionic N-donor moieties must be replaced by two phenyl groups, yielding a pendant anionic N-donor group, coordinated to the liberated $[MgCl]^+$ species (Scheme 5.2, **C**). These magnesium cations may then aid in the oxidative addition of the aryl halide, similar to a mechanism proposed by Yoshikai *et al.* (Scheme 5.2, **A**).[26] Based on a theoretical model, they designed a phosphane ligand with a benzylalcoholate pendant arm, which accelerated the Kumada coupling of aryl fluorides assumedly by a nickel/magnesium bimetallic cooperation. A transition state for the oxidative addition of the C–F bond was calculated, showing how a magnesium ion coordinated to the phenolato group assisted in the bond activation. The activation barrier was calculated to be only 6.4 kcal/mol instead of the 35.5 kcal/mol needed for the activation in the absence of the magnesium center. The high rate of our catalytic system may therefore also be explained by bimetallic cooperation, *i.e.* through a similar transition state (Scheme 5.1, **TS**).

5.3 Conclusions

A number of nickel complexes of chelating anionic ($C^\wedge N^-$) ligands have been prepared and characterized. Two new compounds are based on known amido-functionalized N-heterocyclic carbene ligands, two other nickel complexes are

obtained with novel anionic benzimidazole-functionalized carbene ligands. Unexpectedly, these compounds are highly active as homogeneous catalysts in the Kumada coupling of phenylmagnesium chloride with 4-chloroanisole. The highest rate and selectivity were obtained using a benzimidazole-functionalized NHC, yielding the desired product in quantitative yields with a TOF of 200 mol·(mol cat.)$^{-1}$·h^{-1}. Moreover, coupling of 4-fluoroanisole proceeded efficiently. The high rate of the reaction is explained by a possible nickel/magnesium bimetallic cooperation.

5.4 Experimental Section

General Procedures. All reactions were performed under an atmosphere of dry argon using standard Schlenk techniques. N-benzylbenzimidazole[27] and 2-chloro-N-phenylacetamide[14] were prepared according to literature procedures. All other chemicals were obtained from commercial sources and used as received. Solvents were reagent grade and used without further purification, except for THF and 1,4-dioxane, which were distilled from CaH_2 and stored on molecular sieves under argon. DMF was degassed prior to use. Nickel complex **5b** was prepared following a reported procedure.[13] ^{1}H and ^{13}C NMR spectra were recorded on a Bruker DPX-300 spectrometer and are referenced against tetramethylsilane. IR spectra were obtained on a Perkin-Elmer Paragon 1000 FT-IR spectrophotometer. C,H,N determinations were performed on a Perkin-Elmer 2400 Series II analyzer. Electrospray mass spectra were recorded on a Finnigan TSQ-quantum instrument using an electrospray ionization technique (ESI-MS), using water/acetonitrile solutions. GC measurements were performed on a Varian CP-3800 gas chromatograph equipped with an autosampler. Retention times were compared to commercially obtained compounds. Diethyleneglycol-di-*n*-butylether was used as an internal standard.

1-Methyl-3-(N-phenylaminocarbonylmethyl)imidazolium chloride (1a). A mixture of 1.0 g 2-chloro-N-phenylacetamide (5.9 mmol) and 0.49 g N-methylimidazole (6.0 mmol) in 15 mL dry THF was stirred at 75 °C for 48 h. The colourless precipitate was isolated by filtration, washed with THF and diethyl ether and dried *in vacuo*. Recrystallization from methanol/diethyl ether afforded the pure compound. Yield: 1.46 g (98%). ^{1}H NMR (300 MHz, DMSO-d_6, 300 K) δ 11.29 (s, 1H, NH), 9.25 (s, 1H, NCHN), 7.79 (s, 1H, NCH), 7.74 (s, 1H, NCH), 7.66 (d, J = 8 Hz, 2H, Ar-H), 7.31 (t, J = 8 Hz, 2H, Ar-H), 7.06 (t, J = 8 Hz, 1H, Ar-H), 5.31 (s, 2H, CH_2), 3.91 (s, 3H, CH_3). ^{13}C NMR (75 MHz, DMSO-d_6, 300 K) δ 163.7 (C=O), 138.5 (C_q), 137.8 (NCHN), 128.8 (Ar), 123.8 (NCH), 123.7 (Ar), 123.0 (NCH), 119.1 (Ar), 51.2 (CH_2), 35.8 (CH_3). IR (neat): 2979 (m), 1690 (s), 1553 (s), 1498 (m), 1444 (m), 1312 (m), 1254 (m), 1181 (s), 1108 (w), 942 (w), 784 (w), 752 (s), 695 (m), 622 (s) cm^{-1}. ESI-MS: *m*/*z* 216 ([M – Cl]$^+$, 100%). Anal. Calcd for $C_{12}H_{14}ClN_3O$: C, 57.26; H, 5.61; N, 16.69. Found: C, 57.58; H, 5.75; N, 17.08.

1-Benzyl-3-(N-phenylaminocarbonylmethyl)benzimidazolium chloride (2). This compound was synthesized following the procedure described for **1a**, starting from 1.70 g 2-chloro-N-phenylacetamide (10 mmol) and 2.08 g N-benzylbenzimidazole (10 mmol). Yield: 2.94 g (78%). ^{1}H NMR (300 MHz, DMSO-d_6, 300 K): δ 11.15 (s, 1H, NH), 10.05 (s, 1H, NCHN), 8.00 (m, 2H, Ar-H), 7.64-7.27 (m, 10H, Ar-H), 7.08 (m, 1H, Ar-H), 5.86 (s, 2H, CH_2), 5.63 (s, 2H, CH_2). ^{13}C NMR (75 MHz, DMSO-d_6, 300 K): δ 164.7 (C=O), 144.9 (NCHN), 139.5 (C_q), 135.1 (C_q), 133.1 (C_q), 131.6 (C_q), 130.3 (Ar), 130.2, (Ar), 130.1 (Ar), 129.5 (2 × Ar), 128.2 (Ar),

128.0 (Ar), 125.3 (Ar), 120.5 (Ar), 115.1 (Ar), 51.2 (CH_2), 50.4 (CH_2). IR (neat): 3023 (w), 2973 (w), 1685 (m), 1602 (m), 1560 (s), 1492 (m), 1447 (m), 1351 (m), 1311 (m), 1261 (m), 1188 (m), 949 (w), 753 (s), 692 (s), 640 (m) cm^{-1}. ESI-MS: *m*/*z* 341 ($[M - Cl]^+$, 100%). Anal. Calcd for $C_{22}H_{20}ClN_3O$: C, 69.93; H, 5.33; N, 11.12. Found: C, 69.77; H, 5.50; N, 11.04.

1-(Benzimidazol-2-ylmethyl)-3-benzylimidazolium chloride (3). A mixture of 2.37 g N-benzylimidazole (15.0 mmol) and 2.50 g 2-chloromethylbenzimidazole (15.0 mmol) in 20 mL dry 1,4-dioxane was stirred at 100 °C for 48 h. The reaction mixture was cooled and the off-white precipitate that had formed was collected by filtration, washed with THF and diethyl ether and dried *in vacuo*. The compound was further purified by recrystallization from MeOH/diethyl ether. Yield: 4.13 g (85%). ^{1}H NMR (300 MHz, D_2O, 300 K): δ 9.63 (s, 1H, NCHN), 7.97 (s, 1H, CH_{Im}), 7.90 (s, 1H, CH_{Im}), 7.58 (m, 2H, CH_{Bim}), 7.50-7.35 (m, 5H, Ar-H), 7.24 (m, 2H, CH_{Bim}), 5.85 (s, 2H, CH_2), 5.52 (s, 2H, CH_2). ^{13}C NMR (75 MHz, D_2O, 300 K): δ 147.8 (N=*C*(CH_2)N), 137.3 (NCHN), 134.7 (2 × C_q), 129.0 (Ar), 128.7 (Ar), 128.4 (Ar), 123.7 (?), 122.6 (?), 52.0 (CH_2), 46.2 (CH_2). IR (neat): 3050 (w), 2459 (w), 1559 (m) 1426 (m), 1331 (w), 1270 (w), 1218 (w), 1161 (m), 1012 (w), 839 (w), 797 (m), 741 (s), 700 (s), 635 (m), 618 (m) cm^{-1}. ESI-MS: *m*/*z* 289 ($[M - Cl]^+$, 100%). Anal. Calcd for $C_{18}H_{16}ClN_4 \cdot 2H_2O$: C, 60.08; H, 5.60; N, 15.57. Found: C, 59.95; H, 5.51; N, 15.55.

1-(Benzimidazol-2-ylmethyl)-3-benzylbenzimidazolium chloride (4). This ligand precursor was prepared following the procedure given for imidazolium salt **3**, starting from 2.08 g N-benzylbenzimidazole (10 mmol) and 1.67 g 2-chloromethylbenzimidazole (10 mmol) in 15 mL dry 1,4-dioxane. Yield: 1.95 g (52%). ^{1}H NMR (300 MHz, D_2O, 300 K): δ 9.79 (s, 1H, NCHN), 7.92 (m, 1H, Ar-H), 7.70 (m, 5H, Ar-H), 7.54 (m, 7H, Ar-H), 6.36 (s, 2H, CH_2), 5.80 (s, 2H, CH_2). The N*H* was not observed. ^{13}C NMR (75 MHz, D_2O, 300 K): δ 146.3 (N*C*(CH_2)N, 143.6 (NCHN), 133.7 (C_q), 133.3 (C_q), 132.2 (2 × C_q), 130.5 (Ar), 129.7 (Ar), 129.1 (Ar), 128.8 (Ar), 127.2 (Ar), 115.6 (Ar), 115.3 (2 × Ar), 113.7 (Ar), 52.2 (CH_2), 43.9 (CH_2). IR (neat): 2969 (w), 2485 (w), 1617 (w), 1555 (m), 1458 (w), 1428 (w), 1376 (w), 1220 (w), 1181 (m), 1027 (w), 880 (m), 754 (s), 710 (s), 619 (m), 597 (m) cm^{-1}. ESI-MS: *m*/*z* 339 ($[M - Cl]^+$, 100%). Anal. Calcd for $C_{22}H_{19}ClN_4 \cdot 1.8H_2O$: C, 64.88; H, 5.59; N, 13.76. Found: C, 64.86; H, 5.58; N, 13.95.

Bis(1-methyl-3-(N-phenylamidocarbonylmethyl)imidazol-2-ylidene)nickel(II) (5a). Based on the procedure given by Liao *et al.*,[13] a mixture of 0.38 g imidazolium salt **1a** (1.5 mmol), 97 mg dry $NiCl_2$ (0.75 mmol) and 0.62 g potassium carbonate (4.5 mmol) were heated in DMF at 130 °C for 16 h. After cooling, the yellow solution was filtered and the filtrate was evaporated to dryness *in vacuo*. The remaining solid was dissolved in dichloromethane and washed with water and brine. After drying with magnesium sulfate, the solvent was reduced in volume to 10 mL. Addition of diethyl ether yielded a bright yellow precipitate which was collected by filtration, washed with diethyl ether and dried *in vacuo*. The complex was purified by repeated recrystallization from methanol/hexane. Yield: 0.27 g (73%). ^{1}H NMR (300 MHz, DMSO-d_6, 300 K) δ 7.52 (d, *J* = 1.5 Hz, 2H, NCH), 7.25 (d, *J* = 7.5 Hz, 4H, Ar-H), 7.21 (d, *J* = 1.5 Hz, 2H, NCH), 6.91 (t, *J* = 7.5 Hz, 4H, Ar-H), 6.75 (t, *J* = 7.5 Hz, 2H, Ar-H), 5.71 (d, *J* = 14.5 Hz, 2H, CH_2), 4.31 (d, *J* = 14.5 Hz, 2H, CH_2), 3.13 (s, 6H, CH_3). ^{13}C NMR (75 MHz, DMSO-d_6, 300 K) δ 166.8 (C_q), 165.5 (C_q), 147.2 (C_q), 126.5 (Ar), 125.6 (Ar), 122.6 (NCH), 122.2 (NCH), 120.8 (Ar), 56.8 (CH_2), 35.2 (CH_3). IR (neat): 3152 (w), 1601 (s), 1580 (s), 1558 (s), 1486 (m), 1445 (m), 1374 (s), 1296 (m), 1235 (m), 1075 (m), 754 (s), 693 (s), 534 (m), 502 (m) cm^{-1}. ESI-MS: *m*/*z* 487 ($[M + H]^+$, 100%), 216 ($[ligand]^+$). Anal. Calcd for $C_{24}H_{24}N_6NiO_2 \cdot H_2O$: C, 57.06; H, 5.19; N, 16.63. Found: C, 56.80; H, 5.51; N, 16.39.

Bis(1-benzyl-3-(N-phenylamidocarbonylmethyl)benzimidazol-2-ylidene)nickel(II) (6). This compound was synthesized according to the procedure given for **5a**, starting from 1.13 g benzimidazolium salt **2** (3.0 mmol), 1.23 g potassium carbonate (9.0 mmol) and 0.19 g dry $NiCl_2$ (1.5 mmol) in 40 mL DMF. The complex was purified by repeated recrystallization from dichloromethane/diethyl ether. Yield: 0.78 g (70%). ^{1}H NMR (300 MHz, DMSO-d_6, 300 K) δ 7.94 (d, *J* = 8 Hz, 2H, Ar-H), 7.53 (d, *J* = 8 Hz, 2H, Ar-H), 7.40 (t, *J* = 8 Hz, 2H, Ar-H), 7.29 (t, *J* = 8 Hz, 2H, Ar-H), 7.21 (m, 6H, Ar-H), 6.95-6.70 (m, 14H, Ar-H), 5.61 (m, 4H, CH_2), 4.85 (d, *J* = 16 Hz, 2H, CH_2), 4.58 (d, *J* = 16 Hz, 2H, CH_2). ^{13}C NMR (75 MHz, DMSO-d_6, 300 K) δ 179.5 (Ni-C), 166.4 (C=O), 146.4 (C_q), 136.2 (C_q), 134.5 (C_q), 133.8 (C_q), 128.7 (Ar), 127.7 (Ar), 126.2 (Ar), 126.1 (Ar), 125.7 (Ar), 123.8 (Ar), 123.4 (Ar), 121.2 (Ar), 111.4 (Ar), 110.6 (Ar), 53.9 (CH_2), 49.8 (CH_2). IR (neat): 3131 (w), 1603 (s), 1581 (s), 1570 (s), 1486 (m), 1446 (s), 1362 (s), 1220 (m), 1078 (m), 1026 (m), 970 (w), 754 (m), 739 (s), 722 (m), 693 (s) cm^{-1}. ESI-MS: *m*/*z* 739 ([M + H]$^+$, 100%). Anal. Calcd for $C_{44}H_{36}N_6NiO_2 \cdot 1.5H_2O$: C, 68.94; H, 5.13; N, 10.96. Found: C, 69.09; H, 5.08; N, 10.94.

Bis(1-(benzimidazolato-2-ylmethyl)-3-benzylimidazol-2-ylidene)nickel(II) (7). This complex was obtained following the procedure given for complex **5a**, starting from 0.97 g imidazolium salt **3** (3.0 mmol), 1.23 g potassium carbonate (9.0 mmol) and 0.19 g dry $NiCl_2$ (1.5 mmol) in 40 mL DMF. The complex was purified by recrystallization from dichloromethane/diethyl ether. Yield: 0.74 g (78%). ^{1}H NMR (300 MHz, $CDCl_3$, 300 K): δ 7.68 (d, *J* = 8 Hz, 2H, Ar-H), 7.45-7.05 (m, 12H, Ar-H), 6.93 (t, *J* = 8 Hz, 2H, Ar-H), 6.78 (m, 3H, Ar-H), 6.42 (m, 3H, Ar-H), 5.66 (d, *J* = 15 Hz, 2H, CH_2), 5.19 (d, *J* = 15 Hz, 2H, CH_2), 3.93 (d, *J* = 16 Hz, 2H, CH_2), 3.80 (d, *J* = 16 Hz, 2H, CH_2). ^{13}C NMR (75 MHz, $CDCl_3$, 300 K): δ 171.2 (Ni-C), 155.5 (C_q), 146.2 (C_q), 144.1 (C_q), 136.3 (C_q), 128.8 (Ar), 127.9 (Ar), 127.3 (Ar), 121.6 (Ar), 121.1 (Ar), 120.2 (Im-C), 120.0 (Im-C), 118.8 (Ar), 113.4 (Ar), 52.5 (CH_2), 50.7 (CH_2). IR (neat): 3060 (w), 1605 (w), 1446 (m), 1393 (m), 1304 (w), 1270 (m), 1338 (w), 1158 (w), 857 (w), 741 (s), 726 (s), 702 (s) cm^{-1}. ESI-MS: *m*/*z* 633 ([M + H]$^+$, 100%). Anal. Calcd for $C_{36}H_{30}N_8Ni \cdot H_2O$: C, 66.38; H, 4.95; N, 17.20. Found: C, 66.43; H, 5.23; N, 17.43.

Bis(1-(benzimidazolato-2-ylmethyl)-3-benzylbenzimidazol-2-ylidene)nickel(II) (8). This compound was synthesized following the procedure given for complex **5a**, starting from 1.13 g benzimidazolium salt **4** (3.0 mmol), 0.19 g dry $NiCl_2$ (1.5 mmol), 1.23 g potassium carbonate (9.0 mmol) in 40 mL DMF. Recrystallization from chloroform/diethyl ether yielded the pure compound. Yield: 0.67 g (61%). ^{1}H NMR (300 MHz, $CDCl_3$, 300 K): δ 7.55 (d, 2H, *J* = 8 Hz, Ar-H_{Bim}), 7.43 (d, 2H, *J* = 8 Hz, Ar-H_{Bim}-), 7.29 (t, 2H, *J* = 8 Hz, Ar-H_{Bim}), 7.25 – 7.05 (m, 14H, Ar-H), 6.75 (dt, 2H, *J* = 1 Hz, *J* = 8 Hz, Ar-H_{Bim}-), 6.42 (dt, 2H, *J* = 1 Hz, *J* = 8 Hz, Ar-H_{Bim}-), 6.08 (d, 2H, *J* = 8 Hz, Ar-H_{Bim}-), 5.92 (d, 2H, *J* = 14 Hz, NCH_2CN_2), 5.81 (d, 2H, *J* = 14 Hz, NCH_2CN_2), 5.28 (d, 2H, *J* = 16 Hz, CH_2Ph), 4.79 (d, 2H, *J* = 16 Hz, CH_2Ph). ^{13}C NMR (75 MHz, $CDCl_3$, 300 K): δ 181.2 (Ni-C), 153.5 (C_q NiN*C*=N(CH_2)), 143.6 (C_q benzyl), 134.1 (3 × C_q benzimidazole), 134.0 (C_q benzimidazole), 129.0 (Ar benzyl), 128.4 (Ar), 125.7 (Ar benzyl), 124.4 (Ar), 123.8 (Ar), 120.1 (Ar), 119.8 (Ar), 117.6 (Ar), 114.6 (Ar), 110.5 (2 × Ar), 50.7 (CH_2), 47.5 (CH_2). IR (neat): 3059 (w), 1606 (w), 1476 (w), 1446 (m), 1394 (m), 1340 (w), 1310 (w), 1269 (m), 1211 (w), 1182 (w), 735 (s), 702 (m) cm^{-1}. ESI-MS: *m*/*z* 733 ([M + H]$^+$, 100%). Anal. Calcd for $C_{44}H_{34}N_8Ni \cdot 0.25CHCl_3$: C, 69.62; H, 4.52; N, 14.68. Found: C, 69.44; H, 4.86; N, 15.00.

General procedure for the Kumada coupling. At room temperature, 0.03 mmol nickel complex was dissolved/suspended in 1.0 mL THF, followed by the addition of 1.0 mmol of the 4-haloanisole. The reaction was started with the addition of 1.5 mmol phenylmagnesium

chloride (25 wt% in THF, 0.78 mL) and monitored by taking samples at regular intervals until GC analysis showed full consumption of the 4-haloanisole. All catalytic reactions were performed in duplicate and were found to give consistent results. To isolate the desired coupling product, water was added to the reaction mixture, followed by extraction into ethyl acetate (3 × 20 mL). The organic fractions were combined, dried with magnesium sulfate and evaporated to dryness. Purification by column chromatography on silica gel (95:5 hexane:dichloromethane) yielded 4-methoxybiphenyl as a colorless solid. ^{1}H NMR and ^{13}C NMR spectra were in agreement with the proposed structure,[11] and the GC retention time corresponded to that of a commercial reference sample.

X-ray crystal structure determinations. X-ray reflections were measured with Mo-Kα radiation (λ = 0.71073 Å) on a Nonius KappaCCD diffractometer with rotating anode at a temperature of 150 K. The intensities were integrated using HKL2000.[28] Absorption correction, scaling and merging was performed with SORTAV.[29] The structures were solved with Direct Methods (program SIR-97[30] for **5a** and **6**, program SHELXS-97[31] for **8**). Refinement was performed with SHELXL-97[31] against F^2 of all reflections. Non hydrogen

Table 5.4. Details of the X-ray crystal structure determinations

	5a	**6**	**8**
formula	$C_{24}H_{24}N_6NiO_2 \cdot 2CH_3OH \cdot 0.5H_2O$	$C_{44}H_{36}N_6NiO_2$ + disordered solvent	$C_{44}H_{34}N_8Ni$ + disordered solvent
FW	560.29	739.50 [a]	733.50 [a]
Crystal colour	Yellow	yellow	yellow
crystal size [mm^3]	0.60x0.24x0.09	0.30x0.30x0.20	0.30x0.30x0.20
Crystal system	Monoclinic	monoclinic	triclinic
Space group	$P2_1/c$ (no. 14)	$P2_1/c$ (no. 14)	$P\bar{1}$ (no. 2)
a [Å]	20.7321(3)	11.3697(2)	12.5841(1)
b [Å]	8.5908(1)	16.9361(4)	13.4533(2)
c [Å]	33.5771(6)	24.0007(6)	15.7310(2)
α [°]	-	-	109.7758(8)
β [°]	117.8263(8)	115.0097(13)	103.2347(6)
γ [°]	-	-	95.7404(5)
V [Å^3]	5288.74(14)	4188.20(16)	2393.36(5)
Z	8	4	2
D_x [g/cm^3]	1.407	1.173 [a]	1.018 [a]
$(\sin\theta/\lambda)_{max}$ [Å^{-1}]	0.65	0.60	0.65
refl. meas./unique	41023 / 11971	33596 / 7579	44462 / 10861
μ [mm^{-1}]	0.78	0.50 [a]	0.44 [a]
abs. corr.	multi-scan	multi-scan	multi-scan
abs. corr. range	0.84-0.94	0.75-0.90	0.76-0.92
param./restraints	684 / 0	478 / 0	481 / 0
R1/wR2 [I>2σ(I)]	0.0420 / 0.1007	0.0608 / 0.1601	0.0404 / 0.1009
R1/wR2 [all refl.]	0.0661 / 0.1144	0.0893 / 0.1730	0.0534 / 0.1050
R(int)	0.0549	0.0672	0.0514
S	1.065	1.059	1.061
Res. density [e/Å^3]	-0.43 / 0.90	-0.43 / 1.03	-0.39 / 0.33

[a] Derived values do not contain the contribution of the disordered solvent.

atoms were refined with anisotropic displacement parameters. In **5a** all hydrogen atoms were located in difference Fourier maps. O-H hydrogen atoms were kept fixed at their located position; C-H hydrogen atoms were refined with a riding model. In **6** and **8**, all hydrogen atoms were introduced in calculated positions and refined with a riding model. Geometry calculations and checking for higher symmetry was performed with the PLATON program.[32] Further details are given in Table 5.4.

Crystal structures **6** and **8** contain large solvent-accessible voids (880 Å^3/unit cell in **6**, 852 Å^3/unit cell in **8**) filled with disordered solvent molecules. Their contribution to the structure factors was secured by back-Fourier transformation using the SQUEEZE routine of PLATON,[32] resulting in 199 electrons/unit cell for **6** and 367 electrons/unit cell for **8**.

5.5 References

(1) Herrmann, W. A. *Angew. Chem. Int. Ed.* **2002**, *41*, 1291.
(2) Dragutan, V.; Dragutan, I.; Delaude, L.; Demonceau, A. *Coord. Chem. Rev.* **2007**, *251*, 765.
(3) Hahn, F. E.; Jahnke, M. C. *Angew. Chem. Int. Ed.* **2008**, *47*, 3122.
(4) Normand, A. T.; Cavell, K. J. *Eur. J. Inorg. Chem.* **2008**, 2781.
(5) Kantchev, E. A. B.; O'Brien, C. J.; Organ, M. G. *Angew. Chem. Int. Ed.* **2007**, *46*, 2768.
(6) Corriu, J. P.; Masse, J. P. *J. Chem. Soc.-Chem. Commun.* **1972**, 144.
(7) Tamao, K.; Sumitani, K.; Kumada, M. *J. Am. Chem. Soc.* **1972**, *94*, 4374.
(8) Bohm, V. P. W.; Weskamp, T.; Gstottmayr, C. W. K.; Herrmann, W. A. *Angew. Chem. Int. Ed.* **2000**, *39*, 1602.
(9) Wolf, J.; Labande, A.; Natella, M.; Daran, J. C.; Poli, R. *J. Mol. Catal. A-Chem.* **2006**, *259*, 205.
(10) Xi, Z.; Liu, B.; Chen, W. *J. Org. Chem.* **2008**, *73*, 3954.
(11) Inamoto, K.; Kuroda, J.; Sakamoto, T.; Hiroya, K. *Synthesis* **2007**, 2853.
(12) Zhou, Y. B.; Xi, Z. X.; Chen, W. Z.; Wang, D. Q. *Organometallics* **2008**, *27*, 5911.
(13) Liao, C. Y.; Chan, K. T.; Chang, Y. C.; Chen, C. Y.; Tu, C. Y.; Hu, C. H.; Lee, H. M. *Organometallics* **2007**, *26*, 5826.
(14) Liao, C. Y.; Chan, K. T.; Zeng, J. Y.; Hu, C. H.; Tu, C. Y.; Lee, H. M. *Organometallics* **2007**, *26*, 1692.
(15) Huynh, H. V.; Holtgrewe, C.; Pape, T.; Koh, L. L.; Hahn, E. *Organometallics* **2006**, *25*, 245.
(16) Bishop, M. M.; Lee, A. H. W.; Lindoy, L. F.; Turner, P. *Polyhedron* **2003**, *22*, 735.
(17) He, Y.; Kou, H. Z.; Zhou, B. C.; Xiong, M.; Wang, R. J.; Li, Y. D. *Acta Crystallogr. Sect. E.-Struct Rep. Online* **2002**, *58*, m389.
(18) Brookhart, M.; Green, M. L. H.; Parkin, G. *Proc. Natl. Acad. Sci. U. S. A.* **2007**, *104*, 6908.
(19) Mukhopadhyay, A.; Pal, S. *Eur. J. Inorg. Chem.* **2006**, 4879.
(20) Wolf, J.; Labande, A.; Daran, J. C.; Poli, R. *J. Organomet. Chem.* **2006**, *691*, 433.
(21) Berding, J.; Lutz, M.; Spek, A. L.; Bouwman, E. *Organometallics* **2009**, *28*, 1845.
(22) Matsubara, K.; Ueno, K.; Shibata, Y. *Organometallics* **2006**, *25*, 3422.
(23) Schneider, S. K.; Rentzsch, C. F.; Krueger, A.; Raubenheimer, H. G.; Herrmann, W. A. *J. Mol. Catal. A-Chem.* **2007**, *265*, 50.
(24) Bohm, V. P. W.; Gstottmayr, C. W. K.; Weskamp, T.; Herrmann, W. A. *Angew. Chem. Int. Ed.* **2001**, *40*, 3387.
(25) Tamao, K. *J. Organomet. Chem.* **2002**, *653*, 23.
(26) Yoshikai, N.; Mashima, H.; Nakamura, E. *J. Am. Chem. Soc.* **2005**, *127*, 17978.
(27) Starikova, O. V.; Dolgushin, G. V.; Larina, L. I.; Ushakov, P. E.; Komarova, T. N.; Lopyrev, V. A. *Russ. J. Organ. Chem.* **2003**, *39*, 1467.
(28) Otwinowski, Z.; Minor, W., *Methods in Enzymology*. Academic Press: 1997; Vol. 276, p 307.
(29) Blessing, R. H. *Acta Crystallogr. Sect. A* **1995**, *51*, 33.

(30) Altomare, A.; Burla, M. C.; Camalli, M.; Cascarano, G. L.; Giacovazzo, C.; Guagliardi, A.; Moliterni, A. G. G.; Polidori, G.; Spagna, R. *J. Appl. Crystallogr.* **1999**, *32*, 115.
(31) Sheldrick, G. M. *Acta Crystallogr. Sect. A* **2008**, *64*, 112.
(32) Spek, A. L. *J. Appl. Cryst.* **2003**, *36*, 7.

Chapter 6

Theoretical study on the Kumada coupling catalyzed by bisNHC nickel complexes[†]

Abstract. *The complete catalytic cycle of the Kumada coupling of aryl halides with aryl Grignard reagents using a nickel complex with a chelating bis(N-heterocyclic carbene) ligand has been calculated using density functional theory. The results indicate that the three steps of the catalytic cycle have barriers of similar magnitude, in agreement with the experimentally observed change in the rate-limiting step with a change of the leaving group. Moreover, the route towards the various experimentally-observed side products was calculated to originate from an aryl-exchange pathway that arises during the transmetalation step.*

[†] Based on: J. Berding, F. Buda, A. W. Ehlers, E. Bouwman, *J. Organomet. Chem.*, *in preparation*.

6.1 Introduction

Transition-metal catalyzed cross-coupling reactions, such as the Suzuki and Stille reactions have become important tools in modern organic synthesis.[1, 2] A substantial number of papers has been focused on the elucidation of the mechanism of these cross-coupling reactions, often aided by calculations based on density functional theory (DFT). Most of these investigations are dealing with palladium catalysts bearing phosphane ligands. Especially the oxidative addition of aryl halides to Pd(0) complexes received much attention.[3-6]

Even though the Kumada coupling was discovered more than 35 years ago,[7, 8] only few attempts have been made to investigate its proposed mechanism (Scheme 6.1)[9] using theoretical calculations. The main reason for this appears to be the fact that soon after the Kumada coupling was discovered many other types of catalytic aryl-aryl couplings were found. These other reactions proved to be more versatile, had better functional group tolerance, and have been studied in more detail. Still, often their starting compounds are less reactive and have to be prepared from a Grignard reagent. The advantage of the Kumada coupling is therefore that it eliminates one synthetic step, as it uses the Grignard reagent in the catalytic reaction.

The work on the nickel-catalyzed Kumada coupling of aryl halides with aryl Grignard reagents is described in Chapter 4.[10] The catalysts used in that study are based on nickel(II) dihalide complexes, bearing bidentate bis(N-heterocyclic carbene) (bisNHC) ligands (Figure 6.1, **I**),[10] which were used to catalytically couple 4-haloanisoles (**i_X**, X = Cl, Br) with phenylmagnesium chloride (**ii**) (Scheme 6.2). This yielded 4-methoxybiphenyl (**iii**) in varying yields and at varying rates, depending on the leaving group of the reagent (**i_X**) and the side groups and bridging moiety of the ligand of the nickel catalyst. In addition, a number of side products could be identified, *i. e.* biphenyl (**iv**), anisole (**v**), and 4,4-dimethoxy-biphenyl (**vi**).

It was observed that the rate of the reaction strongly depends on the bulk of the ligand used. The coupling of 4-chloroanisole proceeds at a higher rate when larger side-groups are present on the ligand, while starting from 4-bromoanisole the

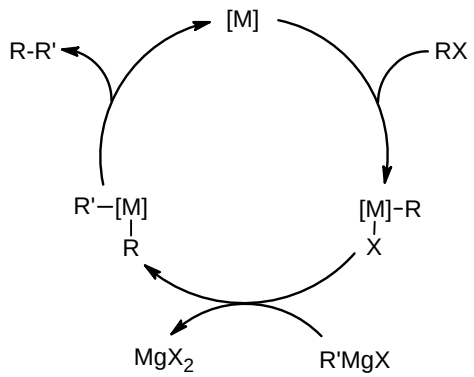

Scheme 6.1. Proposed catalytic cycle of the Kumada coupling (adapted from ref. 9).

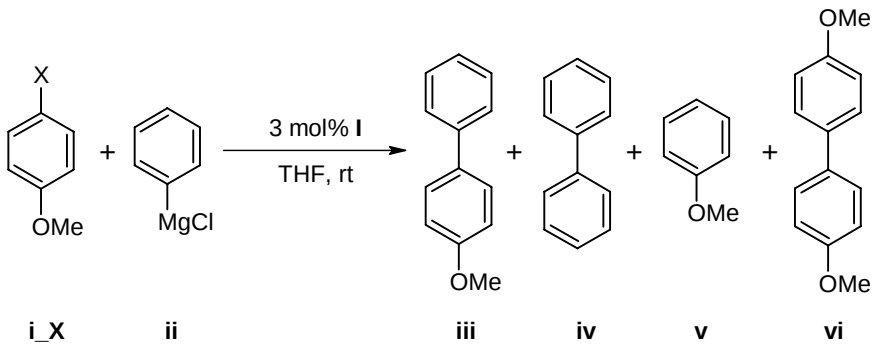

Scheme 6.2. Products of the nickel-catalyzed Kumada coupling as experimentally observed.

opposite is observed. This difference was tentatively ascribed to a change in the rate-determining step; for the chloride-containing reagent the reductive elimination is most likely to be rate-determining, while for the bromide-containing reagent it should be either the oxidative addition or the transmetalation step.[10]

To the best of our knowledge, so far no attempts have been made to calculate the complete catalytic cycle of the Kumada coupling by quantum mechanical calculations. Only recently, Yoshikai *et al.* reported their studies of the Kumada coupling of 2-halotoluene catalyzed by a nickel diphosphane complex, making use of an analysis of kinetic isotope effects (KIEs) and DFT calculations.[11]

N-Heterocyclic carbene complexes have been investigated by quantum-mechanical computational tools a number of times. For instance, the nature of the NHC-metal bond has been studied in detail,[12, 13] and some reports deal with NHC ligands in catalysis.[14]

In this chapter, the results of quantum-chemical calculations of the complete catalytic cycle of the Kumada coupling (Scheme 6.1) with a nickel bisNHC complex are reported, and the data are used to rationalize the trends observed in catalytic experiments.[10] In addition, a possible route has been calculated that may explain the formation of the various side products that are observed experimentally.

6.2 Computational Details

All calculations were performed using the Amsterdam Density Functional (ADF) 2006.01 program packages.[15-17] The density functional calculations (DFT) with the BLYP functional[18, 19] employed a basis set of triple-ζ quality, which is denoted TZP in ADF. Geometries were fully optimized, normally without symmetry constraints. Analytical frequency calculations were performed at the same level of theory and used to identify stationary points (no imaginary frequencies) and transition states (one large imaginary frequency, corresponding to the nuclear motion along the reaction coordinate under study). Furthermore, the frequency calculations were used to determine zero-point energy (ZPE) corrected bonding energies and the Gibbs free energy at 298 K.

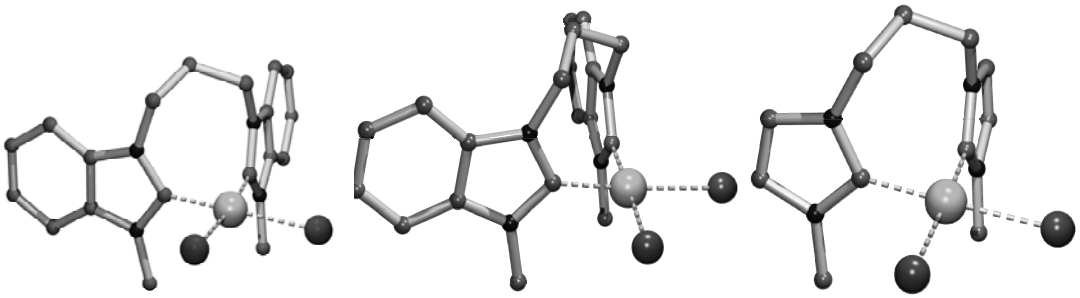

Figure 6.1. Geometry comparison of the solid state structure of full complex **I** (R = Me, R' = 1,3-propanediyl), calculated full complex **I** and the calculated structure of the smaller system **II** at the BLYP/TZP level of theory used in this chapter.

Solvent effects were taken into account for all of the systems under study through single-point calculations at each optimized geometry using the conductor-like screening model (COSMO)[20, 21]. In this model the molecule under investigation is placed in a cavity, which has the shape of this molecule.[22] Outside this cavity, the solvent is calculated as a homogeneous dielectric medium, which is polarized by the charge distribution. The response of the medium is described by the generation of screening charges on the cavity surface. The electrostatic interaction between the molecule and the solvent is calculated through the solvent-induced cavity surface charges. In this study the solvent (tetrahydrofuran) had the following parameters: dielectric constant = 7.58, radius = 3.18 Å.

6.3 Results and Discussion

6.3.1 Model and test calculations

To limit the computational workload, a slightly modified, simplified system was used in the DFT calculations. The bisNHC ligand was reduced in size by replacing the benzimidazole moieties by imidazoles (Figure 6.1, **II**). Even though the free imidazol-2-ylidene and benzimidazol-2-ylidenes are known to behave differently in solution,[23] their properties as ligands are expected to be comparable. As bridging moiety the $(CH_2)_3$-chain was selected, which was calculated completely, as it exerts strain on the *cis* chelating ligand. The methyl substituents were maintained for steric and electronic reasons, even though some reports use H-substituted NHCs in calculations.[13] The methoxy group of the 4-haloanisole reagent used in the catalytic reaction was not included in the calculations, as it was included in catalysis mainly to discriminate between product and side products and is not considered to be essential for the reaction. Furthermore, the influence of the methoxy group on the oxidative addition to a palladium phosphane complex was calculated to be small in comparison to a system without this substituent.[3]

To justify executing calculations at the BLYP/TZP level of theory and the use of the smaller imidazole-based ligand instead of the full benzimidazole moiety, the structure of the full starting complex **I** (R = Me, R' = 1,3-propanediyl) and the smaller complex $LNiBr_2$ (**II**), (L is 1,1'-dimethyl-3,3'-(1,3-propanediyl)-bisimidazol-2,2'-diylidene), were calculated and compared to the known solid-state structure of **I** (Figure 6.1).[10] Selected structural parameters are listed in Table 6.1. The calculated parameters for complex **I** correspond well to the experimental data. The Ni–Br distance is slightly overestimated, as is the C–C bite angle; however, as packing effects are not included in the calculations and as these calculations place the structures in a vacuum, some deviations are to be expected. The bond distances and angles calculated for the trimmed-down complex **II** are in line with those found for the larger complex **I**. As expected, the C–C backbone of the imidazole ring is shorter, as it is now a double bond and not part of an aromatic benzene ring. The absence of the aromatic rings in complex **II** causes a slight lengthening of the Ni–C bond from 1.88 to 1.90 Å.

Because of the high bond-dissociation energy of metal-carbene bonds observed experimentally,[24] the possibility of dissociation of the NHC ligand was not taken into consideration and indeed during the calculations lengthening of the Ni–C_{NHC} bond indicating dissociation was not observed. Furthermore, the possibility of *cis*/*trans* isomerization of the bidentate ligand was not taken into account. For monodentate ligands this is expected to occur during the catalytic cycle, however, due to the bridging moiety the ligand C donors should remain in *cis* positions.

In addition to the gas-phase calculations, the conductor-like screening model (COSMO) was used to estimate the implicit effect of the solvent (THF) on the

Table 6.1. Selected bond lengths (Å) and angles (°) of the solid–state structure of compound **I** (R = Me, R' = 1,3-propanediyl), calculated compound **I**, and calculated compound **II** (X = Br).

	$\mathbf{I}_{Exp.}$ (avgd.)	$\mathbf{I}_{Calc.}$ (avgd.)	$\mathbf{II}_{Calc.}$
Ni–Br	2.36	2.43	2.43
Ni–C	1.86	1.88	1.90
C-C backbone	1.38	1.41	1.36
Br1–Ni–Br2	96.0	96.5	95.4
C12–Ni–C22	85.8	90.8	91.4
NCN	106.8	106.1	104.5
NiC_2 / carbene dihedral angle[a]	84.0	80.1	78.1

[a] NiC_2 / Carbene dihedral angle = angle between LS planes; one through the imidazole ring; one through the NiC_2-coordination plane.

Table 6.2. Energies (kcal mol^{-1}) related to the coordination of THF to magnesium compounds.

[Mg] + n THF → [Mg](THF)$_n$

	ΔE_{ZPE}			ΔG_{gas}			ΔG_{THF}		
n	$MgCl_2$	MgBrCl	PhMgCl	$MgCl_2$	MgBrCl	PhMgCl	$MgCl_2$	MgBrCl	PhMgCl
1	–21.2	–23.6	–17.2	–9.5	–10.0	–6.2	–5.9	–7.1	–2.6
2	–39.0	–41.2	–30.7	–16.6	–16.9	–7.2	–9.7	–10.7	–1.1
3	–42.1	–43.9		–5.8	–7.1		5.2	3.0	
4[a]	–45.4	–47.1		2.8	3.1		16.6	15.6	

[a] Only the *trans* complex was calculated

reaction free energy of all structures. Explicit solvent interactions were taken into account for two coordinatively unsaturated metal centers. The coordination of THF to coordinatively unsaturated Ni(0) complex **1** (see below) was calculated to be slightly endothermic and entropically unfavorable (ΔE_{ZPE} = 3.7 kcal mol^{-1} , ΔG_{THF} = 18.8 kcal mol^{-1}). The interaction of THF and other ethers with Grignard reagents and other magnesium salts has been investigated experimentally,[25, 26] and computationally[27, 28] several times. Even though these reports are not always in agreement, it is clear that solvent interaction is important. Therefore, it was decided to calculate the structures and energies of all magnesium starting materials and products with explicit THF coordination.

The energies (Table 6.2) related to the coordination of varying equivalents of THF to $MgCl_2$, MgBrCl and phenylmagnesium chloride, and the structures (the chloride compounds are depicted in Figure 6.2) of the adducts MgXCl(THF)$_n$ (n = 1 – 4) and PhMgCl(THF)$_n$ (n = 1, 2) were calculated at the BLYP/TZP level of theory. In agreement with previous results,[28] the coordination of two molecules of THF was energetically most favourable for magnesium dihalide salts, when implicit solvent corrections are taken into account (ΔG_{THF} = –9.7 kcal mol^{-1} for $MgCl_2$, –10.7 kcal mol^{-1} for MgBrCl). The present calculations reveal that the most stable THF adduct of phenylmagnesium chloride has only one THF coordinated to it (ΔG_{THF} = –2.6 kcal mol^{-1} for PhMgCl), however, with only a small energy difference, compared to the coordination of two THF molecules.

The overall reaction (1) was calculated to be highly exothermic and exergonic: ΔE_{ZPE} = –73.4 kcal mol^{-1}, ΔG_{THF} = –59.9 for X = Cl and ΔE_{ZPE} = –74.5 kcal mol^{-1}, ΔG_{THF} = –59.6 kcal mol^{-1}, for X = Br.[29]

$$PhX + PhMgCl(THF) + THF \rightarrow PhPh + MgXCl(THF)_2 \qquad (1)$$

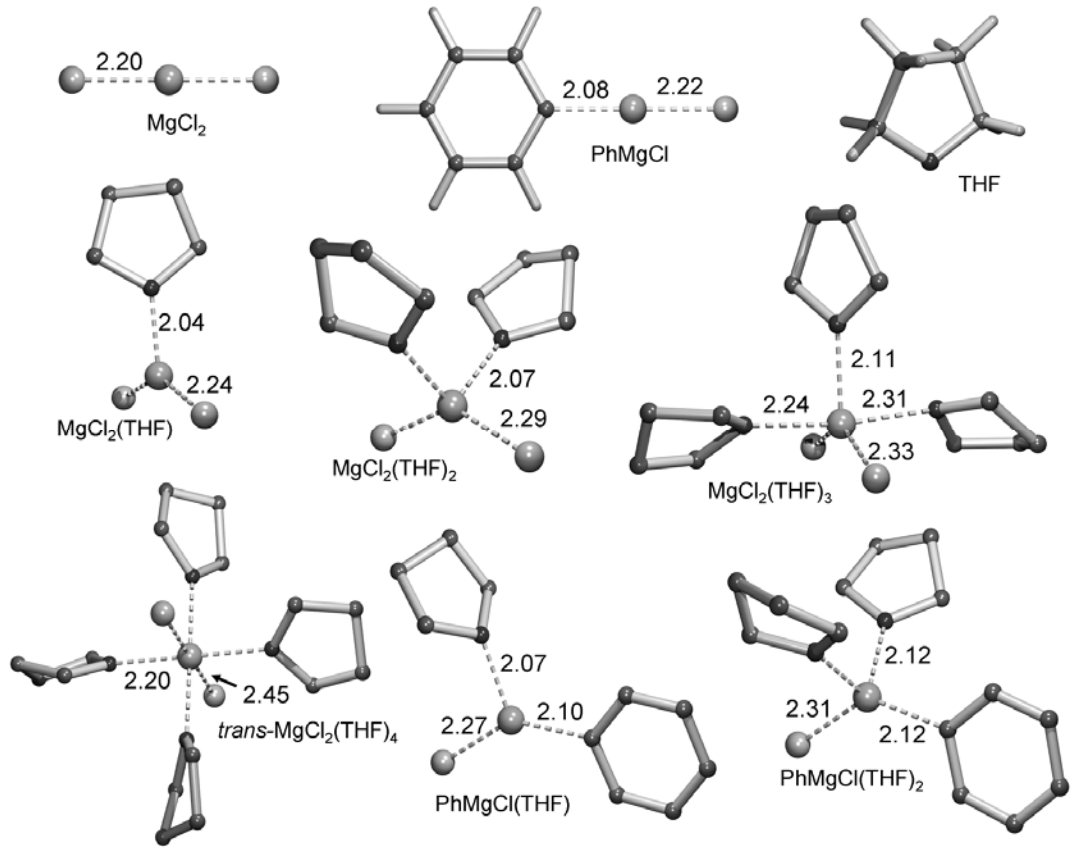

Figure 6.2. Calculated structures of the species involved in the coordination of THF to magnesium compounds. Selected bond lengths are given in Å. Hydrogen atoms are omitted from the THF adducts for clarity.

6.3.2 The catalytic cycle

General

The generally accepted mechanism for the nickel-catalyzed Kumada coupling, schematically shown in Scheme 6.1, consists of three consecutive steps: oxidative addition of the aryl halide, transmetalation of the aryl moiety of the Grignard reagent to the nickel center and finally reductive elimination of the biaryl product. These three steps are discussed separately below. The starting point of the catalytic cycle is a nickel(0) complex. Under experimental conditions this species is obtained from the starting nickel(II) complex **I** by a transmetalation of both halides (see below), followed by reductive elimination of biphenyl.

The relative enthalpies with zero-point energy correction (ΔE_{ZPE}), the gas-phase Gibbs free energies (ΔG_{gas}) and the relative Gibbs free energies with COSMO solvent correction (ΔG_{THF}) for all calculated species are listed in Table 6.3. The following discussion is mainly focused on the solvent-corrected relative Gibbs free energies, ΔG_{THF}.

Table 6.3. Relative total energies (kcal mol^{-1}) with zero-point correction, gas-phase Gibbs free energies and COSMO–THF corrected Gibbs free energies for the species along the oxidative addition, transmetalation, aryl exchange and reductive elimination steps.[a]

	X = Cl			X = Br		
Structure	ΔE_{ZPE}	ΔG_{gas}	ΔG_{THF}	ΔE_{ZPE}	ΔG_{gas}	ΔG_{THF}
1 + PhX	0.0	0.0	0.0	0.0	0.0	0.0
2_X	–10.6	1.7	1.3	–12.9	–0.4	–2.0
TS$_{23}$X	8.3	21.6	24.1	7.4	21.1	24.7
3_X	–38.8	–26.4	–41.1	–42.2	–29.3	–43.1
3_X + PhMgCl(THF) + THF	0.0	0.0	0.0	0.0	0.0	0.0
4_X + 2 THF	–4.8	–3.0	6.3	–2.2	1.3	9.5
TS$_{45}$X + 2 THF	5.3	10.7	20.9	7.5	12.0	21.2
5_X + 2 THF	–8.6	–2.1	4.5	–6.2	–0.2	7.1
6 + MgXCl(THF)$_2$	–31.2	–16.9	–9.8	–28.8	–14.9	–7.5
6	0.0	0.0	0.0			
TS$_{67}$	14.7	16.1	20.9			
7	–2.3	–0.9	9.8			
8	–11.4	–11.4	–1.9			
1 + PhPh	–3.5	–15.3	–9.0			

[a] For every step the energies are reported relative to the first species of that step.

Oxidative addition

Theoretical investigations into the insertion of zerovalent group-10 transition metals, most notably palladium, into carbon-halide bonds has been the subject of a number of recent papers.[3-6] The reason for this interest is that this process is often the rate-determining step in a catalytic cycle. In a number of papers the oxidative addition is proposed to take place starting from an η^2-coordinated aryl halide.[30, 31] In addition, evidence is available that the metal may coordinate to different C–C bonds in sequence before the actual oxidative addition takes place, *i.e.* in a ring-walking

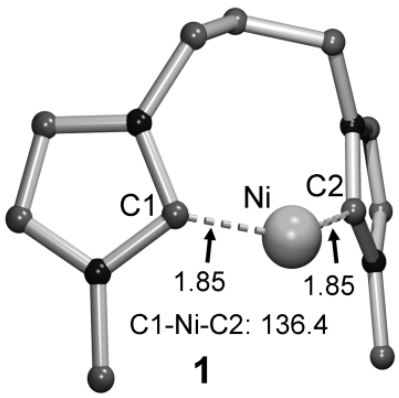

Figure 6.3. Geometry of starting nickel(0) species **1** with calculated bond distances (Å) and angles (°). Hydrogen atoms are omitted for clarity.

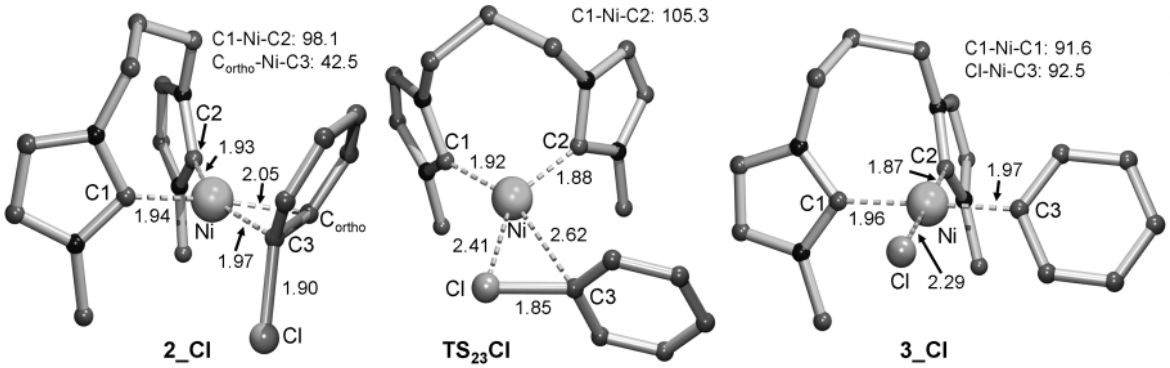

Figure 6.4. Geometries of the species in the oxidative addition step with calculated bond distances (Å) and angles (°) for the chloride compounds. Hydrogen atoms are omitted for clarity.

mechanism. Such ring-walking calculations were not performed for the present system, as the barriers have been calculated to be small for the nickel bisphosphane complex.[11]

The bisNHC ligand in the starting nickel(0) species **1** (Figure 6.3) was calculated to have a bite angle of 136.4°. It is known from experimental data that nickel(0) species bearing two monodentate NHC ligands adopt a linear geometry,[32] however, the propylene bridging group keeps the two carbene rings closer to each other. The Ni–C bonds are relatively short, compared to the nickel(II) species **II** (1.85 and 1.90 Å, respectively), and are comparable to other calculated Ni(0)-NHC distances.[13]

The calculated structures for the oxidative addition sequence with selected structural parameters (for the chloride compounds) are depicted in Figure 6.4 and the relative energies are plotted in Scheme 6.3. The aryl halide coordinates to the nickel(0) species **1** in a η^2 fashion to form the pre-reactive π-complex **2_X**. The Ni–C3

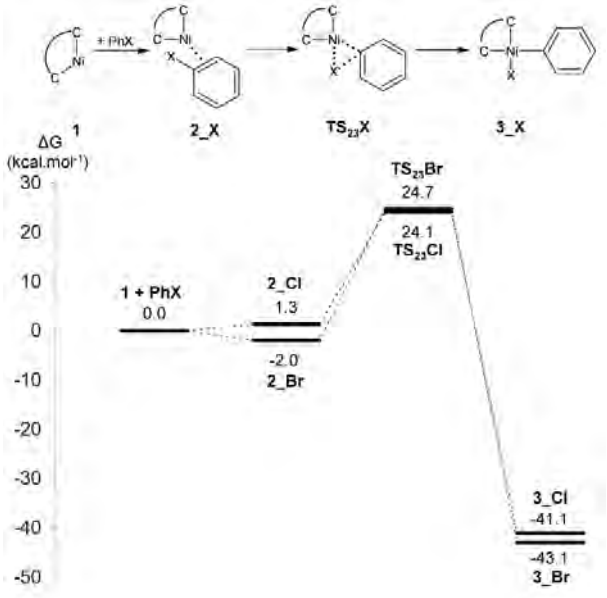

Scheme 6.3. Energy diagram for the oxidative addition step. Energies are given as Gibbs free energy in solution (THF, COSMO) relative to **1** + PhX.

bond is slightly longer than the Ni–C_{ortho} bond, due to the electronegative halide on C3. The bidentate ligand is reoriented, resulting in a trigonal geometry around the nickel center, with a bite-angle of 98.1° and 97.9° for X = Cl and Br, respectively.

The coordination of the aryl halide is favored by total energy (ΔE_{ZPE} = –10.6 and –12.9 kcal mol^{-1} for X = Cl and Br, respectively), but is entropically disfavored, giving a total solvent-corrected free energy of 1.3 and –2.0 kcal mol^{-1} for X = Cl and Br, respectively.

The π-complex is transformed into a three-center transition state **TS_{23}_X**, with an imaginary frequency corresponding to a cleavage of the C3–X bond. This leads to an increase of the free energy of 22.7 and 26.7 kcal mol^{-1} for X = Cl and Br, respectively, and a widening of the bisNHC bite angle to 105.3° and 113.7°. The C3–X bond is slightly shortened, while the Ni–C3 bond is significantly longer than in species **2_X**. The shorter C3–X bond suggests that another intermediate, with coordination of the nickel center to the C3–X bond, should be present; however, attempts to locate this intermediate were unsuccessful.

The transition state leads to a cleavage of the C–X bond yielding the nickel(II) species **3_X**, with the halide and the phenyl ring in *cis* positions. Due to the strong *trans* effect of the phenyl ring, the Ni–C1 bond is significantly longer than the Ni–C2 bond. As the Ni–X and Ni–C3 bonds are now fully formed, they are shorter than those in transition state **TS_{23}X**. Overall, starting from complex **1** and phenyl halide, the oxidative addition is highly exothermic. The total gain in solvent-corrected free energy is 41.1 and 43.1 kcal mol^{-1}, for X = Cl and Br, respectively. The oxidative addition of chlorobenzene to $Ni(PH_3)_2$ was calculated to have a barrier of 8.9 kcal mol^{-1} and a total gain in energy of 19.1 kcal mol^{-1}.[33] The difference between the present NHC system and the phosphane species may be due to the fact that NHCs are more electron donating than phosphanes.

Transmetalation

Even though the transmetalation steps of a number of C–C cross coupling reactions have been investigated theoretically,[34] in the case of the Kumada coupling this step has not received a lot of attention. Generally, a 4-membered cyclic transition state is assumed for the exchange of the halide of the transition metal and the organic moiety on the donating fragment.[35] The intermediates and transition state calculated for the transmetalation steps are shown in Figure 6.5 (for the chloride compounds),[36] the corresponding relative free energies are plotted in Scheme 6.4.

The transmetalation sequence starts with the formation of adduct **4_X** from complex **3_X** and phenylmagnesium chloride, accompanied by a loss of the THF molecule which was coordinated to the latter. The magnesium ion is located between the halide and the aryl ring of the nickel complex thus forming a 4-membered ring, and adopts a distorted tetrahedral geometry. The nickel halide and nickel phenyl

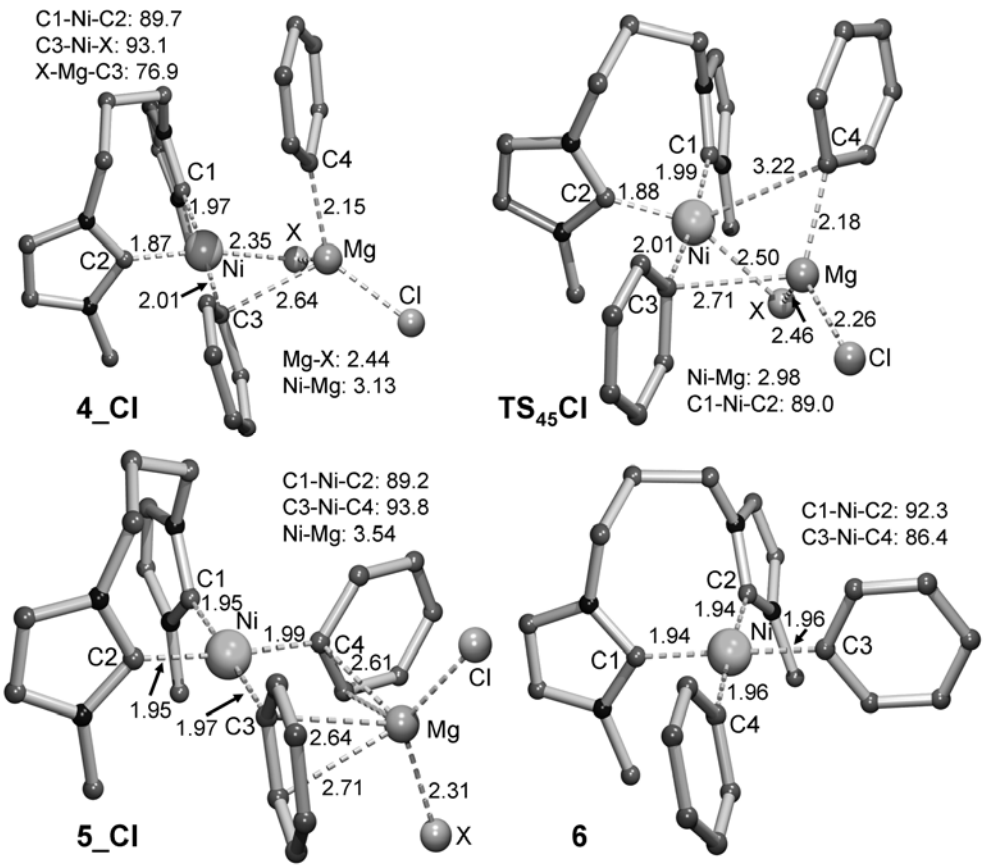

Figure 6.5. Geometries of the species in the transmetalation step (X = Cl) with calculated bond distances (Å) and angles (°). Hydrogen atoms are omitted for clarity.

bonds are slightly elongated. In addition to this geometry, another, less stable structure was calculated in which the magnesium ion is only coordinated to the nickel halide. Possibly, this alternative structure is an intermediate for the formation of **4_X**, however, no transition state between the two could be located. The formation of adduct **4_X** is endothermic, with ΔG_{THF} = 6.3 and 9.5 kcal mol^{-1} for X = Cl and Br, respectively, of which 2.6 kcal mol^{-1} is due to the dissociation of the THF molecule.

The following transition state **TS$_{45}$X**, which has an imaginary vibration equivalent to a rotation around the Mg–C3 bond, brings the magnesium-bound phenyl ring closer to the nickel center, while the halide is moved away from the nickel center. The magnesium ion remains in a tetrahedral geometry, including a weak interaction with the non-reactive nickel-bound phenyl ring. The Ni–C4–Mg–X 4-membered ring is highly distorted, with a short Ni–Mg distance of 2.98 and 3.07 Å, for X = Cl and Br, respectively.

The transition state is 20.9 and 21.2 kcal mol^{-1} for X = Cl and Br, respectively, higher in energy than the starting complex **3_X** and PhMgCl(THF) and leads to intermediate **5_X**, in which an MgXCl moiety is located between the two nickel-bound phenyl rings, with π coordination to both rings. The free energies of **4_X** and **5_X** are of comparable magnitude. The subsequent release of MgXCl from complex **5_X** yields complex **6**; simultaneous coordination of two THF solvent molecules to

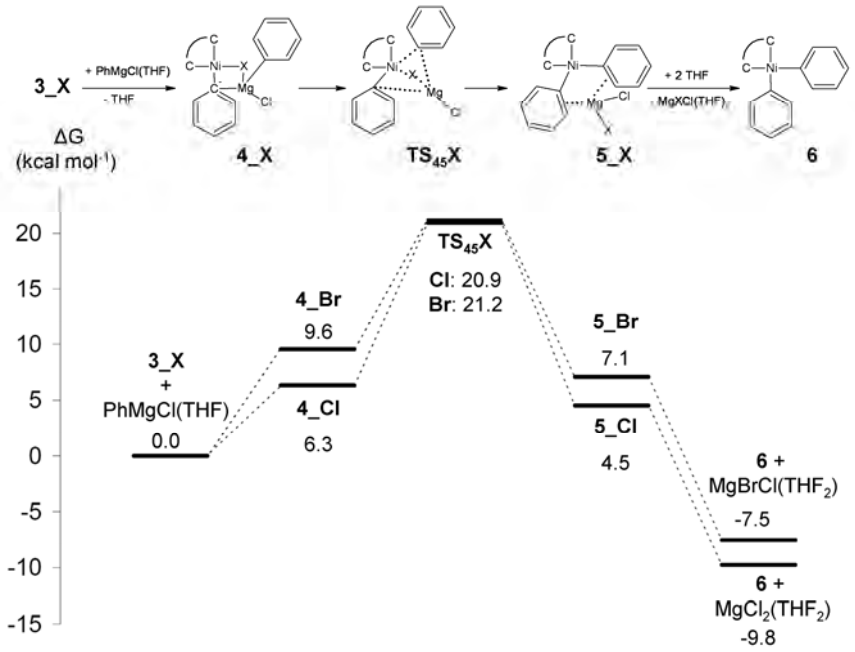

Scheme 6.4. Energy diagram for the transmetalation step. Energy is given as Gibbs free energy in solution (THF, COSMO) relative to **3_X** + PhMgCl(THF) + THF.

MgXCl lowers the free energy by 14.3 and 14.6 kcal mol^{-1}, for X = Cl and Br, respectively, of which 9.7 and 10.7 kcal mol^{-1} is due to the solvent coordination. Species **6** has a slightly distorted square-planar C_4 coordination sphere, with both phenyl rings perpendicular to the coordination plane.

In addition to the structures depicted in Figure 6.5, alternative structures in which the phenylmagnesium chloride is initially coordinated with the phenyl ring and the chloride anion located on exchanged positions on the magnesium ion were considered. However, initial calculations showed only small energy differences compared to those reported above, and these alternative structures not taken into account.

Reductive elimination

The last step in the catalytic cycle is the reductive elimination of the product. In this process the nickel center is formally reduced from the 2+ to the 0 oxidation state, while two Ni–C bonds are broken and a new C–C bond is formed. This step is well known for sp^3 carbons, however, few theoretical studies are available for unsaturated carbon ligands.[37, 38] The species involved in the reductive elimination are depicted in Figure 6.6. The relative energies of these species are plotted in Scheme 6.5.

The two phenyl rings of **6** approach each other to give a new C–C bond, via transition state **TS$_{67}$**. At the same time, the Ni–C3 and Ni–C4 bond lengths are elongated and the biphenyl moiety that is forming is rotated slightly with respect to the coordination plane. The energy difference is quite large, with ΔE_{ZPE} = 14.7 and ΔG_{THF} = 20.9 kcal mol^{-1}. Then, the phenyl rings move closer to complete the C–C bond

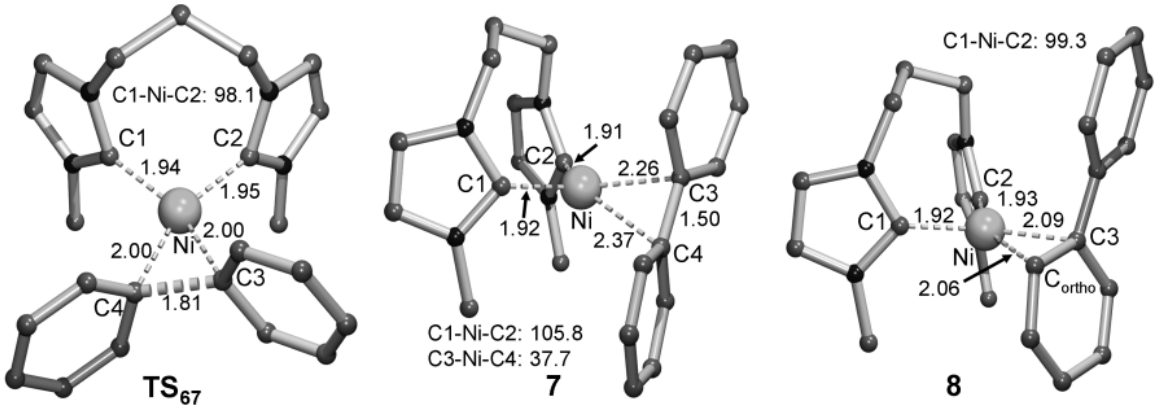

Figure 6.6. Geometries of the species involved in the reductive elimination, with calculated bond distances (Å) and angles (°). Hydrogen atoms are omitted for clarity.

formation, with the biphenyl moiety rotated more out of the coordination plane to give adduct **7**. As the structure approaches the Ni(0) species, the bisNHC bite angle widens to 105.8°, while the Ni–C1 and Ni–C2 bonds shorten slightly. Species **7** easily releases the biphenyl adduct to give the starting Ni(0) species **1**, which may participate in another catalytic cycle. The overall reductive elimination process is exothermic by 9.0 kcal mol^{-1}.

In addition to the η^2 adduct **7** complex **8** could be located with the nickel center bound to C3–C_{ortho}. In this case the biphenyl moiety is more tightly bound to the nickel center and the two phenyl rings are more rotated away from coplanarity. Species **8** has a free energy between that of **7** and the final Ni(0) species (ΔG_{THF} = –1.9 kcal mol^{-1}, relative to **6**). The fact that this stable complex could be identified may indicate that a ring walking mechanism is available for the product, as was the case before the oxidative addition step. No attempts were made to find transition states for this ring walk, as its barriers are probably low and the structures not important for the complete mechanism.

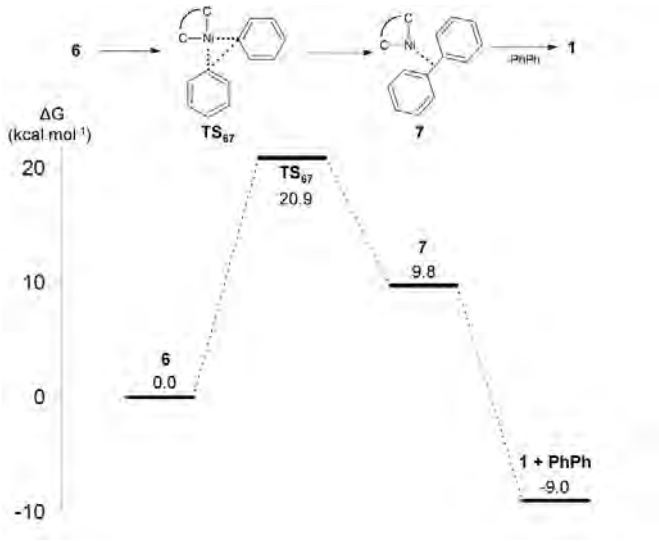

Scheme 6.5. Energy diagram for the reductive elimination step. Energy is given as Gibbs free energy in solution (THF, COSMO) relative to **6**.

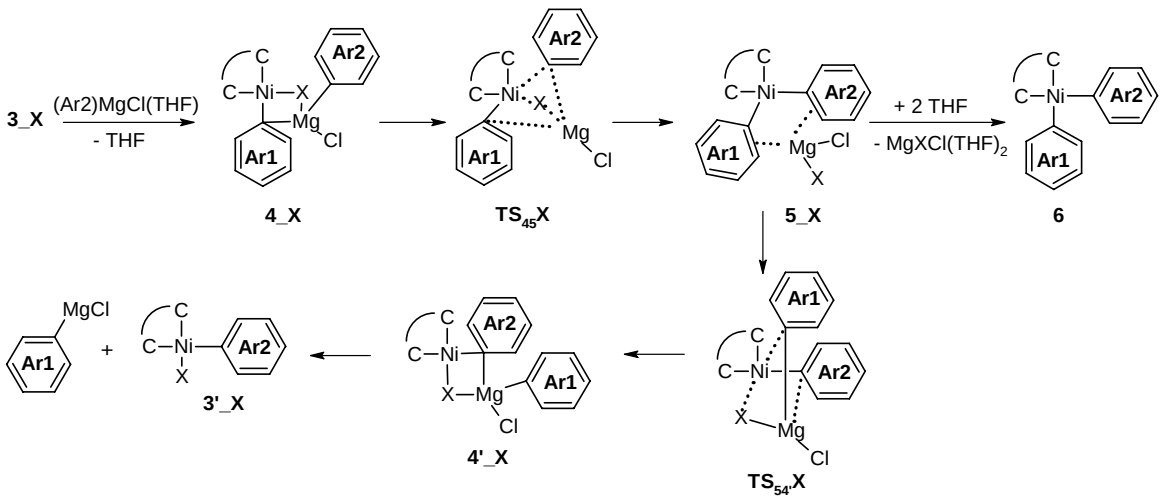

Scheme 6.6. Overview of the proposed aryl-exchange pathway. The two aryl rings are numbered according to their starting position (ring Ar1 originates from **3_X**, ring Ar2 originates from the Grignard reagent).

Aryl exchange

During the catalytic studies of the nickel-catalyzed Kumada coupling, a number of side products was observed.[10, 39] In particular, varying amounts of anisole, biphenyl and 4,4'-dimethoxybiphenyl could be detected (Scheme 6.2). Recently, it has been proposed that these side products are formed during the transmetalation step by exchange of the aromatic moieties on the nickel species and the Grignard reagent.[40] To incorporate this hypothesis in the present DFT study, it is proposed that the exchange takes place according to the route depicted in Scheme 6.6. The pathway calculated for the transmetalation sequence (**3_X** to **6**) if followed until intermediate **5_X**. From this intermediate the reaction may continue to give the desired diaryl complex **6**, or a reverse transmetalation may occur in which aryl ring Ar1 is replaced with the magnesium-bound halide. For this step a transition state **TS$_{54'}$X** is proposed which is the mirror image of transition state **TS$_{45}$X**, with a barrier of equal height. Dissociation of the newly formed phenylmagnesium chloride from intermediate **4'_X** effectively leads to an exchange of aryl rings between the nickel center and the magnesium ion.

In addition to the aryl exchange route depicted in Scheme 6.6, an alternative route starting from intermediate **4_X** was also considered. Whereas rotation about the Mg–C3 bond leads to transmetalation of the halide and the aryl ring, rotation about the Mg–X bond would lead to an exchange of aryl rings between the magnesium ion and the nickel center. Unfortunately, the transition state describing this movement could not be located.

Mechanistic considerations

In principle, the step in the catalytic cycle with the largest energy barrier to the transition state is rate determining. Taking into account the three steps of the

catalytic cycle and the energy barriers calculated for these steps, it is clear that all three steps have barriers of comparable magnitude of 20 – 25 kcal mol^{-1}. Therefore, the actual rate-determining step may be determined by subtle differences in the catalyst and the substrate. In the experimental catalytic studies (Chapter 4) it was observed that the rate of the reaction with 4-chloroanisole increases with the bulk of the side groups on the ligand, while with 4-bromoanisole the rate decreases with bulk.[10] Based on these observations, it was proposed that in the case of the aryl chloride the reductive elimination step must be rate determining, while with the aryl bromide substrate it must be either the transmetalation or the oxidative addition step. In agreement with these experimental observations, the barriers for the oxidative addition and the transmetalation of the bromo compounds were calculated to be slightly larger than the barriers for the oxidative addition and transmetalation of the chloro compounds.

The energy profiles for the complete catalytic cycle starting from chlorobenzene and bromobenzene are remarkably similar. The experimentally observed distinct reactivity of the two aryl halide substrates must therefore originate from rather small energy differences. The higher reactivity of aryl bromides compared to aryl chlorides may be explained by the initial coordination of the aryl halide to the nickel(0) species in the oxidative addition step, which was calculated to be slightly exothermic for aryl bromides and endothermic for aryl chlorides.

In Scheme 6.7 the steps are depicted that result from the aryl exchange pathway, under experimental conditions and which lead to the experimentally observed side products. The sequence starts with the exchange of the anisyl moiety on the nickel species (**A**) and the phenyl ring of the Grignard reagent. Subsequent reaction of nickel phenyl intermediate **B** with another Grignard reagent leads to biphenyl **iv**, while the anisyl Grignard reagent **C** eventually leads to the formation of

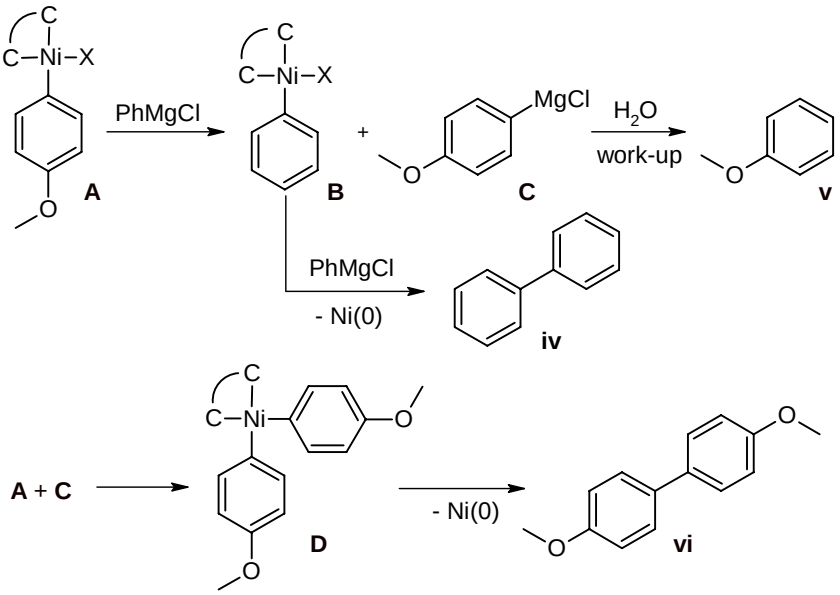

Scheme 6.7. Routes leading to the formation of side products **iv** - **vi**.

the 4,4′-dimethoxybiphenyl **vi** (by reacting with another species **A**) and anisole **v** (during work-up). According to this reaction scheme, the amount of biphenyl formed should be equal to the amount of anisole plus the amount of 4,4′-dimethoxybiphenyl. This correlates well with the experimental results.[10]

It was observed experimentally that a significantly larger amount of side products is formed during the coupling of 4-bromoanisole than with 4-chloroanisole. As both the transmetalation and the aryl exchange pathway have structure **5_X** as an intermediate, the differences observed in selectivity must originate here. Apparently, in the case of X = Br the rate of the reverse transmetalation is higher then with X = Cl. This is in agreement with the calculated energies of **5_X**, as for X = Br the barrier towards **TS$_{54'}$X** is lower than for X = Cl.

6.4 Conclusion

The complete pathway for the Kumada coupling of aryl halides with aryl Grignard reagents catalyzed by nickel complexes bearing a bisNHC ligand has been investigated theoretically at the BLYP/TZP level of theory with explicit solvent coordination and implicit COSMO solvent correction. The present calculations confirm the feasibility of the proposed route, consisting of oxidative addition, transmetalation and reductive elimination. The transmetalation step has been calculated with aryl Grignard reagents for the first time and is found to occur via a four-membered transition state with possible nickel-magnesium interaction. Moreover, the transmetalation sequence and the scrambling of aryl rings, leading to experimentally observed side products, have been proposed to evolve through a single intermediate species.

As the energy profiles calculated for the Kumada coupling of aryl chlorides and aryl bromides are quite similar, and as the rate-determining step could not be located unambiguously, it is difficult to correlate the calculations with experimental results. However, the fact that the barriers for the three steps in the catalytic cycle are calculated to be close in energy is in agreement with the experimentally observed change in rate-determining step when changing the substrate halide.

6.5 References

(1) Littke, A. F.; Fu, G. C. *Angew. Chem.-Int. Edit.* **2002**, *41*, 4176.
(2) Corbet, J. P.; Mignani, G. *Chem. Rev.* **2006**, *106*, 2651.
(3) Ahlquist, M.; Norrby, P. O. *Organometallics* **2007**, *26*, 550.
(4) Ariafard, A.; Lin, Z. Y. *Organometallics* **2006**, *25*, 4030.
(5) Fazaeli, R.; Ariafard, A.; Jamshidi, S.; Tabatabaie, E. S.; Pishro, K. A. *J. Organomet. Chem.* **2007**, *692*, 3984.
(6) Goossen, L. J.; Koley, D.; Hermann, H. L.; Thiel, W. *Organometallics* **2005**, *24*, 2398.
(7) Corriu, J. P.; Masse, J. P. *J. Chem. Soc.-Chem. Commun.* **1972**, 144.
(8) Tamao, K.; Sumitani, K.; Kumada, M. *J. Am. Chem. Soc.* **1972**, *94*, 4374.

(9) Tamao, K. *J. Organomet. Chem.* **2002**, *653*, 23.
(10) Berding, J.; Lutz, M.; Spek, A. L.; Bouwman, E. *Organometallics* **2009**, *28*, 1845.
(11) Yoshikai, N.; Matsuda, H.; Nakamura, E. *J. Am. Chem. Soc.* **2008**, *130*, 15258.
(12) Penka, E. F.; Schlapfer, C. W.; Atanasov, M.; Albrecht, M.; Daul, C. *J. Organomet. Chem.* **2007**, *692*, 5709.
(13) Radius, U.; Bickelhaupt, F. M. *Organometallics* **2008**, *27*, 3410.
(14) Green, J. C.; Herbert, B. J.; Lonsdale, R. *J. Organomet. Chem.* **2005**, *690*, 6054.
(15) ADF2006.01, *SCM, Theoretical Chemistry, Vrije Universiteit, Amsterdam, The Netherlands, http://www.scm.com*.
(16) Fonseca Guerra, C.; Snijders, J. G.; te Velde, G.; Baerends, E. J. *Theor. Chem. Acc.* **1998**, *99*, 391.
(17) Te Velde, G.; Bickelhaupt, F. M.; Baerends, E. J.; Guerra, C. F.; Van Gisbergen, S. J. A.; Snijders, J. G.; Ziegler, T. *J. Comput. Chem.* **2001**, *22*, 931.
(18) Becke, A. D. *Phys. Rev. A* **1988**, *38*, 3098.
(19) Lee, C. T.; Yang, W. T.; Parr, R. G. *Phys. Rev. B* **1988**, *37*, 785.
(20) Klamt, A. *J. Phys. Chem.* **1995**, *99*, 2224.
(21) Klamt, A.; Schuurmann, G. *J. Chem. Soc.-Perkin Trans. 2* **1993**, 799.
(22) Zhu, W. H.; Wu, G. S.; Jiang, Y. S. *Int. J. Quantum Chem.* **2002**, *86*, 347.
(23) Bohm, V. P. W.; Herrmann, W. A. *Angew. Chem.-Int. Edit.* **2000**, *39*, 4036.
(24) Scott, N. M.; Clavier, H.; Mahjoor, P.; Stevens, E. D.; Nolan, S. P. *Organometallics* **2008**, *27*, 3181.
(25) Smith, M. B.; Becker, W. E. *Tetrahedron* **1967**, *23*, 4215.
(26) Holm, T. *Acta Chem. Scand.* **1969**, *23*, 579.
(27) Ehlers, A. W.; van Klink, G. P. M.; van Eis, M. J.; Bickelhaupt, F.; Nederkoorn, P. H. J.; Lammertsma, K. *J. Mol. Model.* **2000**, *6*, 186.
(28) Tammiku-Taul, J.; Burk, P.; Tuulmets, A. *J. Phys. Chem. A* **2004**, *108*, 133.
(29) Without explicit solvent interaction: $\Delta E(ZPE) = -51.6$ kcal/mol, $\Delta G(THF) = -52.8$ kcal/mol for X = Cl, $\Delta E(ZPE) = -50.5$ kcal/mol, $\Delta G(THF) = -51.6$ kcal/mol for X = Br.
(30) Reinhold, M.; McGrady, J. E.; Perutz, R. N. *J. Am. Chem. Soc.* **2004**, *126*, 5268.
(31) Surawatanawong, P.; Fan, Y.; Hall, M. B. *J. Organomet. Chem.* **2008**, *693*, 1552.
(32) Arduengo, A. J.; Gamper, S. F.; Calabrese, J. C.; Davidson, F. *J. Am. Chem. Soc.* **1994**, *116*, 4391.
(33) Lin, B. L.; Liu, L.; Fu, Y.; Luo, S. W.; Chen, Q.; Guo, Q. X. *Organometallics* **2004**, *23*, 2114.
(34) Alvarez, R.; Faza, O. N.; de Lera, A. R.; Cardenas, D. J. *Adv. Synth. Catal.* **2007**, *349*, 887.
(35) Wendt, O. F. *Curr. Org. Chem.* **2007**, *11*, 1417.
(36) Please note that the structures calculated for the transmetalation step are mirrored, compared to those of the other steps. This does not affect the outcome of the energy calculations.
(37) Ananikov, V. P.; Musaev, D. G.; Morokuma, K. *Organometallics* **2005**, *24*, 715.
(38) Huang, Y. L.; Weng, C. M.; Hong, F. E. *Chem.-Eur. J.* **2008**, *14*, 4426.
(39) Wolf, J.; Labande, A.; Daran, J. C.; Poli, R. *J. Organomet. Chem.* **2006**, *691*, 433.
(40) Richardson, J. M.; Jones, C. W. *J. Mol. Catal. A-Chem.* **2009**, *297*, 125.

Chapter 7

Nickel N-heterocyclic carbene complexes in the vinyl polymerization of norbornene[†]

Abstract. *Three types of nickel(II) complexes with N-heterocyclic carbene (NHC) ligands, described in this thesis, have been used in the catalytic vinyl polymerization of norbornene under a range of conditions. Specifically, two nickel complexes bearing a chelating bis(NHC) ligand, two nickel complexes bearing two chelating anionic N-donor functionalized NHC ligands as well as one nickel(II) diiodide complex with two monodentate NHCs were tested. The solid-state structure of bis(1,3-dimethylimidazol-2-ylidene)diiodidonickel(II), as determined by X-ray crystallography, is presented. The highest activity of 2.6 × 10^7 g·(mol cat)$^{-1}$·h^{-1} was observed using the latter nickel complex as catalyst, activated by methylaluminoxane. The norbornene polymers thus obtained are of high molecular weight and narrow polydispersity.*

[†] Based on: J. Berding, M. Lutz, A. L. Spek, E. Bouwman, *in preparation*.

7.1 Introduction

In the last few decades, the polymerization of norbornene (bicyclo[2.2.1]hept-2-ene, **1**) has become a field of active research. Three types of (homo)polymer may be obtained from norbornene, following different mechanisms (Scheme 7.1).[1] The most studied is the ring-opening metathesis polymerization (ROMP), which gives polymers with unsaturated backbones and high solubility in a large range of solvents. ROMP is commonly catalyzed by complexes of molybdenum, tungsten, rhenium or ruthenium.[2] An organic radical or aluminum-initiated mechanism leads to the less well known and less understood cationic or radical polymerization, which usually results in low-molecular weight polymers with 2,7-connectivity.[3, 4] The third type of polymerization, which leads to opening of the π-component of the double bond, leaves the bicyclic unit intact. This is known in literature as addition or vinyl polymerization and this reaction was recently reviewed.[2] Vinyl-polymerized norbornene has some useful properties such as good mechanical strength, optical transparency and heat resistance.[5, 6] Several transition metal complexes have been described in the literature as active catalysts for the vinyl polymerization of norbornene. The most common metals in these catalysts are zirconium, titanium, chromium, and the late transition metals cobalt, nickel and palladium. Generally, these metals need to be activated with a cocatalyst, such as methylaluminoxane (MAO), or $B(C_6F_5)_3/AlEt_3$.[2]

The use of nickel complexes in the vinyl polymerization of norbornene was first described in 1993; the catalysts were obtained by a reaction of the nickel allyl trifluoroacetate dimer with hexafluoro- or hexachloroacetone and did not need any cocatalyst to start the reaction.[7] Other nickel complexes used in this reaction have ligands based on acetylacetonates, carboxylic acids, salen,[8] or other chelating $[N_2]$-,[9-12] $[N_4]$-,[13] [N,O]-,[14, 15] [N,S]-,[16] and [P,N][17]-ligands. Furthermore, some bisphosphane-based ligands have been reported in the nickel catalyzed vinyl polymerization of norbornene.[18] To the best of our knowledge, the use of nickel N-heterocyclic carbene

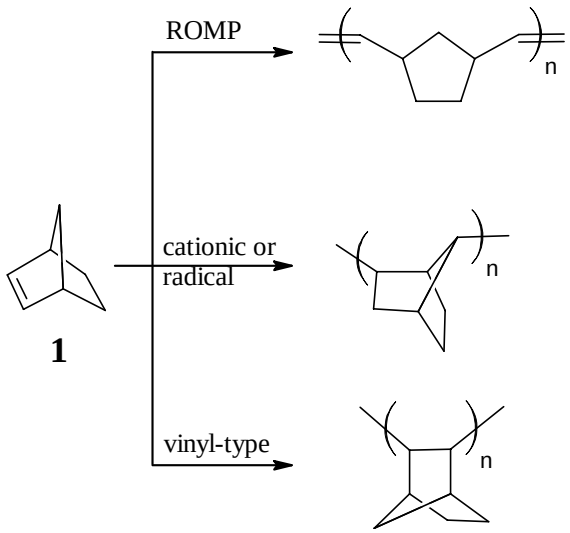

Scheme 7.1 Three types of norbornene polymerization.

complexes in this reaction has only been reported twice. These are a complex with two picolyl-functionalized NHC ligands,[19] and a nickel compound bearing one bulky monodentate NHC and one η^3-coordinated benzyl moiety.[20]

N-Heterocyclic carbenes (NHCs) are increasingly used in homogeneous catalysis as stable, versatile spectator ligands. Some excellent reviews describe a large number of reactions in which these strong σ-donor ligands have been investigated.[21, 22] Because of their electron-donating properties they are often compared to the frequently used and intensively studied tertiary phosphane ligands, even though they have been assumed to have less π-back bonding properties,[23-26] and have a different shape. In some cases, replacing a phosphane ligand by a NHC ligand proved to be beneficial for the catalytic activity.[27] As described in Chapter 4, a number of nickel complexes bearing chelating benzimidazole-based bisNHC ligands has been synthesized.[28] As nickel complexes bearing chelating phosphanes are capable of polymerizing norbornene,[18, 29] it was decided to study the activity of the bisNHC complexes in this polymerization reaction. Given the successful use of N-donor ligands in the catalytic polymerization of norbornene, it was decided to investigate the catalytic properties of two nickel complexes with benzimidazolato-functionalized NHC ligands described in Chapter 6,[30] as well. Furthermore, in order to assess the effect of chelation of the ligand, one complex bearing two monodentate NHC ligands with small substituents (Chapter 3) is tested under the same conditions.

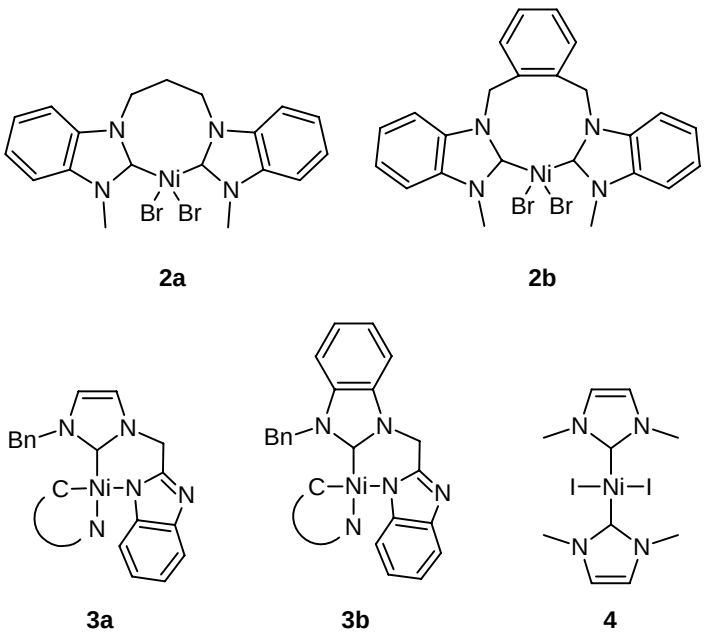

Figure 7.1. Nickel NHC complexes under study.

7.2 Results and Discussion

7.2.1 Nickel complexes

Three types of nickel(II) complexes were tested in the vinylpolymerization of norbornene (depicted in Figure 7.1): nickel dihalide complexes with chelating bisNHC ligands (**2a**, **2b**), nickel complexes bearing two chelating N-donor functionalized NHCs (**3a**, **3b**) and a nickel(II) dihalide complex bearing two monodentate NHC ligands (**4**). The synthesis and characterization of these complexes are described in Chapters 3 – 5.

7.2.2 Description of the crystal structure of complex 4.

Although the compound has been reported previously in the literature,[25] and several other nickel(II) complexes of monodentate NHC ligands have been structurally characterized,[31] the crystal structure of complex **4** was so far not elucidated. Single crystals of **4** were obtained by slow evaporation of a concentrated solution of the compound in THF and the structure was determined using X-ray diffraction. The molecular structure is shown in Figure 7.2. In the crystal structure the molecule has an exact C_{2h} symmetry. The coordination geometry around the nickel(II) center is nearly perfectly square planar, with the coordination of two carbene carbons and two iodides in *trans* positions. Due to symmetry, the I1–Ni1–I1A and the C1–Ni1–C1A bonds are perfectly linear. The Ni–C and Ni–I bond distances are within the range reported for other nickel NHC complexes.[31] The imidazole rings are oriented nearly perpendicular to the coordination plane, with a N1–C1–Ni1–I1 torsion angle of 88.48(19)°.

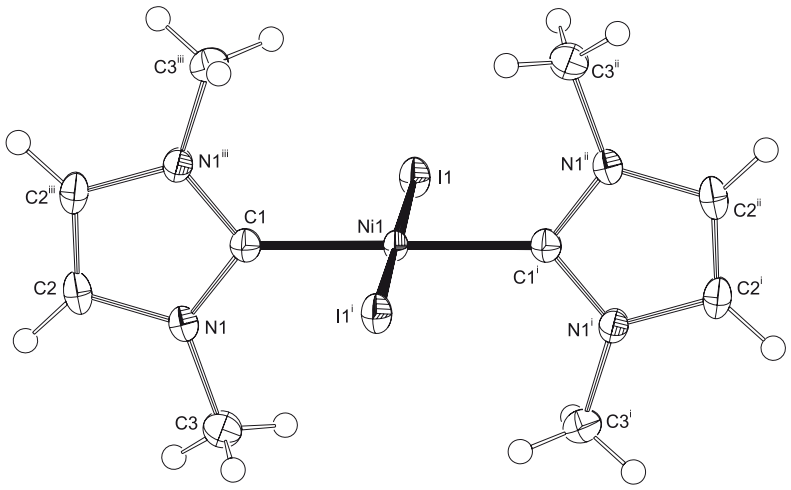

Figure 7.2. Molecular structure of **4** in the crystal showing 50% probability ellipsoids. Selected bond lengths (Å) and angles (°): Ni1–C1 1.905(2), Ni1–I1 2.50729(17), C1–N1 1.349(2), C2–C2^{i} 1.342(2), C1–Ni1–I1 90.01(7), C1–Ni1–I1^{i} 89.99(7), N1–C1–N1^{iii} 104.5(2). Symmetry operations i: –x, y, –z; ii: –x, –y, –z; iii: x, –y, z.

7.2.3 Catalytic studies

Compounds **2** – **4** were tested for their catalytic activity in the vinyl polymerization of norbornene (**1**). The results of the most pertinent polymerization reactions using MAO as cocatalyst are summarized in Table 7.1. In this table the

Table 7.1. Overview of catalytic vinyl polymerization experiments using nickel NHC complexes.[a]

Entry	Cat	**1**/Ni (× 10^3)	Solv [b]	Temp (°C) [c]	Time (min)	Yield (%) [d]	Activity (×10^6 g·(mol cat)$^{-1}$·h^{-1})	M_w (× 10^5 g/mol)	PDI [e]
1 [f]	**2a**	3.3	DCM	RT	5	21	0.8	7.9	3.2
2	**2a**	3.3	DCM	RT	5	71	2.7	9.9	2.1
3 [g]	**2a**	3.3	DCM	RT	5	71	2.7	11.0	2.2
4	**2a**	6.7	DCM	RT	5	72	5.4	11.1	2.3
5	**2a**	3.3	DCE	RT	5	65	2.5	>14	
6	**2a**	3.3	DCE	40	5	68	2.6	>14	
7	**2a**	3.3	DCE	60	5	73	2.7	>14	
8	**2b**	3.3	DCM	RT	5	80	3.0	14.1	2.1
9	**2b**	6.7	DCM	RT	5	50	3.8	7.5	2.0
10	**2b**	10.0	DCM	RT	5	42	4.7	8.4	2.0
11	**2b**	3.3	DCM	0	5	65	2.5	4.0	2.3
12	**2b**	6.7	DCM	0	5	33	2.5	4.3	2.8
13	**3a**	3.3	DCE	RT	5	26	1.0	>14	
14	**3a**	6.7	DCE	RT	5	14	1.0	>14	
15	**3a**	3.3	DCE	60	5	22	0.8	>14	
16	**3a**	3.3	DCE	RT	10	40	0.8	n.d.	
17	**3b**	3.3	DCE	RT	5	10	0.4	>14	
18	**3b**	6.7	DCE	RT	5	5	0.4	n.d.	
19	**3b**	3.3	DCE	60	5	11	0.4	>14	
20	**3b**	3.3	DCE	60	15	22	0.3	n.d.	
21	**4**	3.3	DCM	RT	5	71	2.7	>14	
22	**4**	10.0	DCM	RT	5	41	4.6	>14	
23	**4**	3.3	DCE	RT	2	78	7.4	>14	
24	**4**	6.7	DCE	RT	2	77	14.6	n.d.	
25	**4**	3.3	DCE	60	1	85	16.0	>14	
26	**4**	1.0	DCE	RT	0.2	91	25.8	>14	
27 [h]	**4**	3.3	DCE	RT	3	76	4.8	>14	
28 [i]	**4**	1.0	DCE	RT	5	66	0.7	n.d.	
29 [i]	**4**	3.3	DCE	RT	5	45	1.7	n.d.	
30 [j]	**4**	3.3	DCM	RT	15	0	0		
31 [k]	-	-	DCM	RT	15	0	0		

[a] Unless otherwise noted, a 0.5 M solution of norbornene was used and a 500 : 1 MAO to nickel ratio; [b] solvent, DCM = dichloromethane; DCE = 1,2-dichloroethane; [c] RT = room temperature [d] Isolated yield; [e] Polydispersity index = M_w/M_n; [f] MAO/Ni = 100; [g] MAO/Ni = 1000; [h] 0.17 M norbornene solution; [i] 83 mM norbornene solution; [j] No MAO was added; [k] **1**/MAO = 8.

polymer yields and characteristics, and the catalytic activities of all five nickel complexes under various conditions are presented. Variations were made in the amount of cocatalyst, the catalyst loading, the solvent, the temperature, the norbornene concentration and the reaction time. The polymers were characterized by IR spectroscopy, ^{1}H and ^{13}C NMR spectroscopy and size exclusion chromatography (SEC). The IR spectra of the polymer products are consistent with the spectrum reported for vinyl-polymerized norbornene.[19] Peaks indicative of double bonds (1680 – 1620 cm^{-1}) are not observed, indicating that the product was not obtained *via* ROMP.[18] The ^{1}H and ^{13}C NMR spectra are very similar to those reported and also show no resonances assignable to double bonds.[11, 17] The SEC measurements of several samples indicated that high-molecular weight polymers with a narrow polydispersity are formed. Unfortunately, a large number of polynorbornene samples could not be analyzed by size exclusion chromatography; due to the high molecular weight these polymers could not be dissolved in the commonly used chlorobenzene or 1,3,5-trichlorobenzene, even after stirring at elevated temperatures for several days. It is estimated that the molecular weight of these polymers is at least $1.4 \cdot 10^{6}$ g/mol, the highest molecular weight found for a soluble polymer sample (entry 8). As expected,[32] the polymers are stable up to 390 °C under an argon atmosphere, as shown by TGA studies.

The influence of the Ni:MAO ratio on the efficiency of the reaction may be found from entries 1 to 3. An increase of the amount of MAO from 100 to 500 equivalents gives a large enhancement of polymer yield, whereas a further increase to 1000 equivalents does not improve the yield. The average molecular weight of the polymers appears to increase slightly with a larger amount of MAO. It was decided to use a Ni:MAO ratio of 1:500 in the other catalytic experiments. Although Ni to MAO ratios of 1:100 have been used,[18] often a much larger excess is applied, up to 1:9000.[15]

Initially, the catalytic runs were performed in dichloromethane. This solvent has been used by others for the polymerization of norbornene.[33, 34] However, due to its low boiling point, this solvent cannot be used to test the catalytic performance of the catalysts at elevated temperatures. Therefore, a number of catalytic runs were performed in 1,2-dichloroethane (DCE) as well.[35] The two solvents are of comparable polarity and the change in solvent is not expected to have a large influence on the reactivity of the catalyst. Indeed, a comparison of entries 2 and 5 shows that difference in reactivity of the catalyst in the two solvents is small.

Under standard conditions (MAO/Ni = 500, **1**/Ni = 3.3×10^{3}, 0.5 M norbornene, 5 min at room temperature, entries 2, 8, 13, 17 and 21) the five different catalysts may be compared. Under these conditions, the reactivity of the catalysts increases in the order **3b** < **3a** << **4** ≈ **2a** < **2b**.

The influence of the temperature on the activity of complex **2a** is rather limited. Entries 5 – 7 show only a small increase in the yield of the reaction when going from

room temperature to 60 °C. This was also observed for complex **2b**, which shows a decrease in activity going from room temperature to 0 °C (entries 9 and 12, or 8 and 11). The influence on the molecular weight of the resulting polymer, however, is larger; M_w drops considerably when performing the catalytic reaction at lower temperatures. For catalysts **3a** and **3b** the influence of the temperature on the activity is also limited. The influence of the temperature on the activity of complex **4** appears to be larger, as at room temperature a yield of 78% is reached within two minutes, whereas at 60 °C a yield of 85% is obtained within one minute (entries 23 and 25).

The catalyst loading, expressed as the norbornene:nickel complex ratio, has a large influence on the activity of the catalyst. For instance, using complex **2a** or **4** the average activity more than doubles on using half the amount of catalyst under the same conditions (entries 2 and 4, or 23 and 24), although the effect is less pronounced in the less active catalysts **3a** and **3b**. Probably the reaction using the higher catalyst loading was actually deactivated before complete conversion was reached and the quenching was started, leading to an underestimation of the activity.

As catalysts **3a** and **3b** are not very active catalysts in the vinyl polymerization, compared to the other complexes, some experiments were performed to determine whether the reaction had stopped after the standard 5 minutes, or whether a longer reaction time would lead to a higher yield. Indeed, it is clear (entries 13 and 16, or 19 and 20) that the reaction is not finished after 5 minutes, although the resulting overall activity drops with longer reaction times.

In the initial test complex **4** showed good activity (Table 7.1, entry 21). It then was attempted to get an estimation of the initial rate of the reaction, by quenching the reaction after short reaction times (entries 23 – 26). The highest overall activity thus found is 2.6×10^7 g/(mol cat)·h, which was reached when a reaction of **4** with 1000 equivalents of norbornene at room temperature furnished 91% yield within 12 seconds. This may still be an underestimation of the real catalyst activity, as a thick slurry formed even before all of the catalyst solution had been added. Unfortunately, a shorter reaction time was experimentally unattainable.

In addition, it was attempted to perform the catalytic reaction in more diluted reaction mixtures (entries 27 – 29). This way, the polymerization of norbornene using complex **4** was slowed down, giving only 45% yield in 5 minutes in a solution that was six times diluted, compared to 78% yield in 2 minutes (entry 23). Control experiments (entries 30 and 31) show that complex **4** without MAO does not catalyze the polymerization reaction, nor does MAO alone, as was reported before.[19]

It is clear from the results shown in Table 7.1 that the activity of the catalyst is highly dependent on the type of complex used. For instance, complex **4** is very active, while complexes **3a** and **3b** are not. The differences in reactivity between **2a** and **2b** and the differences between **3a** and **3b** are not very large; however, more experiments are needed to draw a conclusion on the exact influence of the various substituents.

Nickel catalysts for the vinyl polymerization of norbornene have been reported to have activities in the wide range of 10^3 to 10^9 g/(mol cat)·h.[2] The highest activity reported so far of 1.68×10^9 g/(mol cat)·h was achieved with a nickel complex with two benzimidazole ligands.[9]

In the literature, two other types of nickel NHC complexes have been reported to be active the norbornene polymerization catalysts. Wang *et al.*[19] reported activities up to 2.6×10^7 g/(mol cat)·h using a cationic nickel complex bearing two picolyl functionalized NHCs (**1**/Ni = 68000, Al/Ni = 4500, 10 min. at 80 °C in chlorobenzene), with molecular weights up to 4.2×10^6 and polydispersity indices ranging from 1.3 to 3.5. More recently, Sujith *et al.*[20] reported neutral and cationic η^3-benzylnickel(II) complexes bearing one bulky imidazole-based carbene, which were found to be active norbornene polymerization catalyst, even without cocatalyst. The highest activity observed with this type of complex was 3.3×10^5 g/(mol cat)·h (**1**/Ni = 5000, 20 min. at 130 °C in toluene), with molecular weights up to 4.1×10^5 and polydispersity indices ranging from 2.4 to 3.3. Interestingly, analogous complexes with imidazoline-based carbene ligands were not active. Unfortunately, due to the different reaction conditions used, a comparison between these complexes and the complexes of the present study cannot be made.

7.2.4 Mechanistic considerations

The mechanism for the vinyl polymerization of norbornene has been proposed to comprise the steps depicted in Scheme 7.2.[11] A reaction between the catalyst precursor and MAO in the presence of norbornene yields a nickel compound with a methyl ligand and a coordinated norbornene (**A**). The norbornene then inserts into the Ni–CH_3 bond to give the coordinatively unsaturated species **B**. By repeating the coordination and insertion steps the polymer chain grows, until species **E** reacts with a methyl aluminium species resulting in chain transfer and regeneration of nickel species **A**. The aluminium species is hydrolyzed during work-up yielding the free polynorbornene polymer chain.

It is clear from a comparison of the molecular weights of the polymers and the ratio between norbornene and nickel catalyst that only few nickel centers are actually catalytically active. If, for instance (Table 7.1, entry 2), every nickel center that was introduced to the reaction mixture would react, the average polymer would consist of approximately 2360 norbornene monomers, which is equal to a molecular weight of about 2×10^5 g/mol. In the experiments, however, the average molecular weight is significantly higher (1×10^6 g/mol in this example). Apparently, once a nickel catalyst starts the polymerization reaction, the rate of propagation is considerably higher than the rate of elimination. The low polydispersity measured for a number of polymers indicates that the catalyst operates through a single site active species, in line with the proposed mechanism.[18]

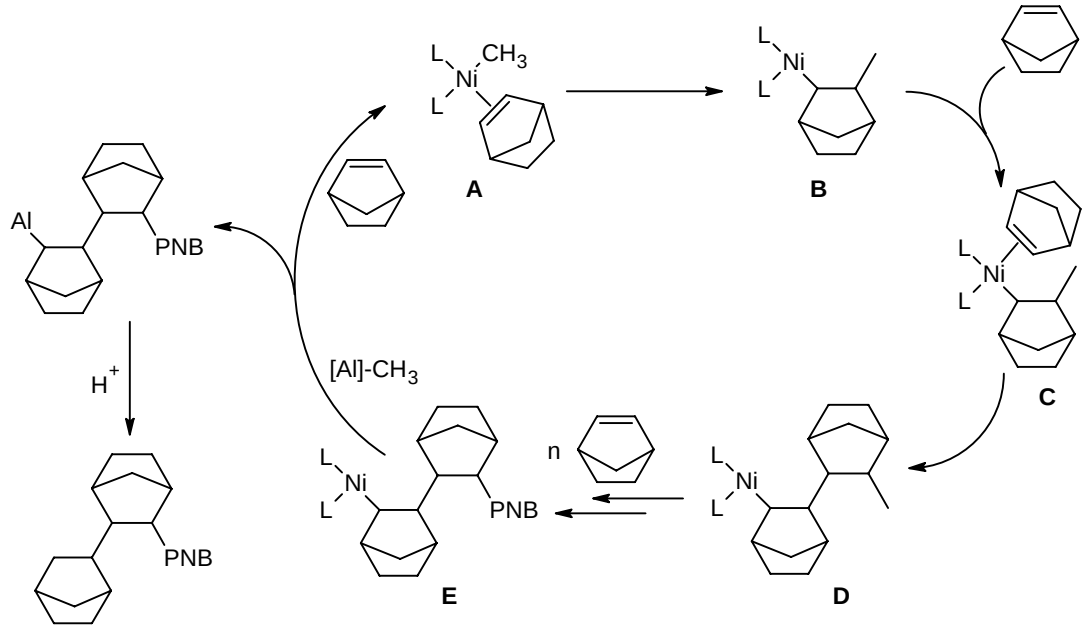

Scheme 7.2. Proposed mechanism for the nickel catalyzed vinyl polymerization of norbornene. (L = carbene ligand; PNB = polynorbornene). Adapted from ref. 11.

The large difference in reactivity between the highly active catalysts **2a**, **2b** and **4**, and the less active **3a** and **3b** may arise from the fact that in the first case a halide anion must be replaced to activate the catalyst, while in the latter case this is a benzimidazolato group. This benzimidazolato moiety remains in the vicinity of the catalyst, which may hinder the chain growth. The small difference in activity between complexes **2a,b** and **4** may indicate that chelation is not of importance for this catalytic reaction. For the polymerization reaction to occur, the monodentate ligands in **4** must adopt *cis* positions, similar to the configuration of complexes **2a,b**.

7.3 Conclusion

Five nickel(II) N-heterocyclic carbene complexes, comprising the three types described in Chapters 3 – 5, have been tested for their catalytic activity in the MAO-activated vinyl polymerization of norbornene over a range of conditions. The small $Ni(NHC)_2I_2$ compound showed the highest activity of 2.6×10^7 g/(mol cat)·h. The poor solubility of most of the polymers thus obtained indicate that these are of high ($>1.4 \times 10^6$) molecular weight. The polymers that are soluble are of low polydispersity.

7.4 Experimental

General considerations. All experiments were performed under an atmosphere of dry argon, using standard Schlenk techniques. Dichloromethane and 1,2-dichloroethane were dried by distillation from calcium hydride and stored over molecular sieves under argon. Norbornene (bicyclo[2.2.1]hept-2-ene) was obtained from Aldrich and distilled under argon from sodium. Methylaluminoxane (MAO, 10 wt% solution in toluene) was obtained from Aldrich and used as received. Complexes **2a,b**,[28] **3a,b**,[30] and **4**,[36] were synthesized following the procedures described in Chapters 3 – 5 and were added from a 3.0 mM stock solution in dichloromethane or 1,2-dichloroethane.

NMR spectra were recorded on a Bruker DPX-300 at 300 MHz (^{1}H NMR) and 75 MHz (^{13}C NMR), in *o*-dichlorobenzene-d_4, referenced against TMS. IR spectra were recorded on a Perkin-Elmer Paragon 1000 FT-IR spectrophotometer. The size-exclusion chromatography (SEC) measurements were carried out with a multiple detection system consisting of an interferometric RI detector (Optilab DSP, Wyatt Technology) in series with a multi-angle laser light scattering detector (Dawn DSP-F, Wyatt Technology). With this configuration absolute molecular weights are obtained on-line. The samples were measurxed on two Styragel columns (300 x 7.5 mm, Waters Associates) in chlorobenzene with a flow of 1 ml/min. The columns were kept at 40 °C. The concentration was 5 mg/ml; sample load was 100 μl. Molecular weights are calculated using dn/dc=0.062 ml/g, calculated from the response of the refractive index detector for injections with known concentration.

General procedure for the vinyl polymerization of norbornene. To a solution of norbornene in dichloromethane to 1,2-dichloroethane was added MAO (10 wt% in toluene). While stirring thoroughly with a magnetic stir bar, a solution of nickel complex in the same solvent was added. The total reaction volume was 20 mL in all cases. The reaction was kept at the required temperature by placing the reaction vessel in an oil bath. After the appropriate reaction period the reaction was quenched by the addition of 5 mL of a 10% HCl solution in ethanol. The reaction mixture was poured into 100 mL 10% HCl in ethanol and stirred for several hours. After filtration and washing with copious amounts of ethanol the colorless residue was dried under vacuum at 50 °C until no further weight loss occurred. IR (neat): 2946 (vs), 2866 (vs), 1474 (m), 1453 (s), 1294 (m), 1258 (w), 1148 (m), 1107 (m), 942 (w), 890 (m) cm^{-1}. ^{1}H NMR (300 MHz, *o*-dichlorobenzene-d_4, 300 K) δ 2.8 – 0.8 (m, with maxima at 2.28, 1.62, 1.39, 1.22, 1.12). ^{13}C NMR (75 MHz, *o*-dichlorobenzene-d_4, 300 K) δ 52 – 26 (broad signals, maxima at 52.0, 47.8, 38.3, 31.4).

X-ray crystal structure determination. $C_{10}H_{16}I_2N_4Ni$, Fw = 504.78, red block, 0.33 x 0.24 x 0.09 mm^3, monoclinic, C2/m (no. 12), a = 13.5582(4), b = 8.5892(2), c = 8.4350(3) Å, β = 128.126(2)°, V = 772.73(4) Å^3, Z = 2, D_x = 2.169 g/cm^3, μ = 5.24 mm^{-1}. 8666 Reflections were measured on a Nonius Kappa CCD diffractometer with rotating anode (graphite monochromator, λ = 0.71073 Å) up to a resolution of $(\sin\theta/\lambda)_{max}$ = 0.65 Å^{-1} at a temperature of 150(2) K. Intensities were integrated with EvalCCD[37] taking into account a large anisotropic mosaicity about the b-axis. An absorption correction based on multiple measured reflections was performed using the program SADABS[38] (correction range 0.16-0.63). 950 Reflections were unique (R_{int} = 0.032), of which 924 were observed [I>2σ(I)]. The structure was solved with automated Patterson methods using the program DIRDIF-99.[39] The structure was refined with SHELXL-97[40] against F^2 of all reflections. Non-hydrogen atoms were refined with anisotropic displacement parameters. All hydrogen atoms were located in difference Fourier maps and

refined freely with isotropic displacement parameters. 60 Parameters were refined with no restraints. R1/wR2 [I > 2σ(I)]: 0.0131 / 0.0317. R1/wR2 [all refl.]: 0.0141 / 0.0320. S = 1.141. Residual electron density between –0.63 and 0.43 e/Å^3. Geometry calculations and checking for higher symmetry was performed with the PLATON program.[41]

7.5 References

(1) Janiak, C.; Lassahn, P. G. *J. Mol. Catal. A-Chem.* **2001**, *166*, 193.
(2) Blank, F.; Janiak, C. *Coord. Chem. Rev.* **2009**, *253*, 827.
(3) Gaylord, N. G.; Deshpande, A. B.; Mandal, B. M.; Martan, M. *J. Macromol. Sci.-Chem.* **1977**, *A11*, 1053.
(4) Myagmarsuren, G.; Lee, K. S.; Jeong, O. Y.; Ihm, S. K. *Polymer* **2004**, *45*, 3227.
(5) Grove, N. R.; Kohl, P. A.; Allen, S. A. B.; Jayaraman, S.; Shick, R. *J. Polym. Sci. Pt. B-Polym. Phys.* **1999**, *37*, 3003.
(6) Haselwander, T. F. A.; Heitz, W.; Krugel, S. A.; Wendorff, J. H. *Macromol. Chem. Phys.* **1996**, *197*, 3435.
(7) Deming, T. J.; Novak, B. M. *Macromolecules* **1993**, *26*, 7089.
(8) Janiak, C.; Lassahn, P. G.; Lozan, V. *Macromol. Symp.* **2006**, *236*, 88.
(9) Tarte, N. H.; Cho, H. Y.; Woo, S. I. *Macromolecules* **2007**, *40*, 8162.
(10) Gao, H. Y.; Pei, L. X.; Li, Y. F.; Zhang, J. K.; Wu, Q. *J. Mol. Catal. A-Chem.* **2008**, *280*, 81.
(11) Li, Y. F.; Gao, M.; Wu, Q. *Appl. Organomet. Chem.* **2007**, *21*, 965.
(12) Patil, A. O.; Zushma, S.; Stibrany, R. T.; Rucker, S. P.; Wheeler, L. M. *J. Polym. Sci. Pol. Chem.* **2003**, *41*, 2095.
(13) Lee, D. H.; Lee, J. Y.; Ryu, J. Y.; Kim, Y.; Kim, C.; Lee, I. M. *Bull. Korean Chem. Soc.* **2006**, *27*, 1031.
(14) Chen, F. T.; Tang, G. R.; Jin, G. X. *J. Organomet. Chem.* **2007**, *692*, 3435.
(15) Tang, G. R.; Lin, Y. J.; Jin, G. X. *J. Polym. Sci. Pol. Chem.* **2008**, *46*, 489.
(16) Huang, Y. B.; Jia, W. G.; Jin, G. X. *J. Organomet. Chem.* **2009**, *694*, 86.
(17) Yang, H. J.; Li, Z. L.; Sun, W. H. *J. Mol. Catal. A-Chem.* **2003**, *206*, 23.
(18) Lassahn, P. G.; Lozan, V.; Wu, B.; Weller, A. S.; Janiak, C. *Dalton Trans.* **2003**, 4437.
(19) Wang, X.; Liu, S.; Jin, G. X. *Organometallics* **2004**, *23*, 6002.
(20) Sujith, S.; Noh, E. K.; Lee, B. Y.; Han, J. W. *J. Organomet. Chem.* **2008**, *693*, 2171.
(21) Herrmann, W. A. *Angew. Chem.-Int. Edit.* **2002**, *41*, 1291.
(22) Weskamp, T.; Bohm, V. P. W.; Herrmann, W. A. *J. Organomet. Chem.* **2000**, *600*, 12.
(23) Lee, M. T.; Hu, C. H. *Organometallics* **2004**, *23*, 976.
(24) Dorta, R.; Stevens, E. D.; Scott, N. M.; Costabile, C.; Cavallo, L.; Hoff, C. D.; Nolan, S. P. *J. Am. Chem. Soc.* **2005**, *127*, 2485.
(25) Herrmann, W. A.; Kocher, C. *Angew. Chem.-Int. Edit.* **1997**, *36*, 2163.
(26) Jacobsen, H.; Correa, A.; Costabile, C.; Cavallo, L. *J. Organomet. Chem.* **2006**, *691*, 4350.
(27) Scholl, M.; Ding, S.; Lee, C. W.; Grubbs, R. H. *Org. Lett.* **1999**, *1*, 953.
(28) Berding, J.; Lutz, M.; Spek, A. L.; Bouwman, E. *Organometallics* **2009**, *28*, 1845.
(29) Sun, Z. G.; Zhu, F. M.; Wu, Q.; Lin, S. A. *Appl. Organomet. Chem.* **2006**, *20*, 175.
(30) Berding, J.; van Dijkman, T. F.; Lutz, M.; Spek, A. L.; Bouwman, E. *Dalton Trans.* **2009**, 6948.
(31) McGuinness, D. S.; Mueller, W.; Wasserscheid, P.; Cavell, K. J.; Skelton, B. W.; White, A. H.; Englert, U. *Organometallics* **2002**, *21*, 175.
(32) Long, J. M.; Gao, H. Y.; Song, K. M.; Liu, F. S.; Hu, H.; Zhang, L.; Zhu, F. M.; Wu, Q. *Eur. J. Inorg. Chem.* **2008**, 4296.
(33) Lozan, V.; Lassahn, P. G.; Zhang, C. G.; Wu, B.; Janiak, C.; Rheinwald, G.; Lang, H. *Z.Naturforsch.(B)* **2003**, *58*, 1152.
(34) Han, F. B.; Zhang, Y. L.; Sun, X. L.; Li, B. G.; Guo, Y. H.; Tang, Y. *Organometallics* **2008**, *27*, 1924.

(35) Barnes, D. A.; Benedikt, G. M.; Goodall, B. L.; Huang, S. S.; Kalamarides, H. A.; Lenhard, S.; McIntosh, L. H.; Selvy, K. T.; Shick, R. A.; Rhodes, L. F. *Macromolecules* **2003**, *36*, 2623.
(36) Herrmann, W. A.; Gerstberger, G.; Spiegler, M. *Organometallics* **1997**, *16*, 2209.
(37) Duisenberg, A. J. M.; Kroon-Batenburg, L. M. J.; Schreurs, A. M. M. *J. Appl. Crystallogr.* **2003**, *36*, 220.
(38) Sheldrick, G. M. *SADABS: Area-Detector Absorption Correction, v2.10*, Universität Göttingen, Germany, **1999**.
(39) Beurskens, P. T.; Admiraal, G.; Beurskens, G.; Bosman, W. P.; Garcia-Granda, S.; Gould, R. O.; Smits, J. M. M.; Smykalla, C. *The DIRDIF99 program system*, Technical Report of the Crystallography Laboratory, University of Nijmegen, The Netherlands, **1999**.
(40) Sheldrick, G. M. *Acta Crystallogr. Sect. A* **2008**, *64*, 112.
(41) Spek, A. L. *J. Appl. Cryst.* **2003**, *36*, 7.

Chapter 8

Summary, general discussion and outlook

8.1 Summary

8.1.1 Introduction

Even though the extraordinary chemistry of N-heterocyclic carbenes (NHCs) has been under investigation for about forty years, only in the past decade the field has come to full development. First regarded as a laboratory peculiarity, NHCs are now known as stable, economically attractive, and highly versatile ligands in a wide range of homogeneous catalytic applications. Although initially NHCs were mostly investigated as phosphane analogues for ruthenium and palladium catalyzed reactions, numerous unprecedented transformations have been disclosed using NHC complexes of these and many other transition metals. In this regard, nickel-NHC complexes have only been used in a relatively small number of catalytic reactions. The aim of the research described in this thesis was to prepare nickel-NHC complexes, with an emphasis on chelating ligands, and to use these complexes in a variety of homogeneous catalytic reactions.

In Chapter 1, first an overview of the electronic and steric properties of N-heterocyclic carbenes and the corresponding transition-metal complexes is given. This is followed by a summary of the various methods for the preparation of NHCs and their complexes. The chapter is concluded with a summary of the catalytic reactions in which transition-metal NHC complexes have played a role, with an emphasis on nickel NHC complexes.

8.1.2 Silver complexes of N-heterocyclic carbene

The transmetalation of NHCs from silver(I) to other transition metals has been shown to be an efficient way for the preparation of transition-metal NHC complexes. For this reason, attempts to obtain silver(I) NHC complexes were undertaken, which ultimately resulted in the determination of the solid-state structure of a dimer of a silver(I) bromide complex of a monodentate NHC, as described in Chapter 2. Surprisingly, using a nearly identical synthetic route, a significantly different crystal structure had been obtained by another research group.[1] In this case the solid-state structure comprised of a mononuclear silver(I) bromide complex with two monodentate NHCs. Several studies, including NMR and crystallization studies, were undertaken to determine the structure of the complex in solution and to elucidate why two different solid state structures could be obtained using nearly identical reaction conditions. It was finally concluded that the isolation of the [$(NHC)_2AgBr$] structure must be serendipitous. Moreover, a new classification of all known solid-state structures of silver NHC complexes was introduced. In addition, the silver(I) NHC complex was used to obtain the corresponding nickel(II) dihalide complex, demonstrating the feasibility of transmetalation of monodentate NHCs from silver(I) to nickel(II).

8.1.3 Nickel N-heterocyclic carbene complexes in homogeneous catalysis

General

A number of nickel-NHC complex-catalyzed reactions was introduced in Chapter 1. The aim of this research was to extend and improve the use of nickel NHC complexes in homogeneous catalytic reactions. Ultimately, the use of nickel NHC complexes was successfully studied for three types of catalysis: the hydrosilylation of internal alkynes, the Kumada cross coupling of aryl halides with an aryl Grignard reagent, and the vinyl polymerization of norbornene.

Monodentate NHC ligands - Hydrosilylation

The synthesis of a variety of nickel(II) dihalide complexes of monodentate N-heterocyclic carbenes bearing small substituents is described in Chapter 3. These complexes were used as catalysts in the hydrosilylation of internal alkynes, which is an important route toward vinylsilanes. The majority of investigations concerning catalytic hydrosilylation reported to date focus on terminal alkynes and often use precious metals as catalyst. In the study described in this thesis, the active catalyst is a nickel(0) species, which is generated *in situ* by a reaction of the nickel(II) NHC precursor complex with diethylzinc. Using a protocol in which the catalyst is activated before the reagents are added, two of the $Ni(NHC)_2I_2$ complexes were found to be active catalysts for the hydrosilylation of 3-hexyne with triethylsilane; full conversion was reached within 60 minutes at 5 mol% catalyst loading at 50 °C. The (*E*)-product, in which the hydrogen and the silane are located on the same face of the double bond, is obtained selectively in all cases.

As the NHCs in this catalytic system are only coordinated as a monodentate ligand, there is a possibility that the ligand dissociates, possibly leading to free nickel metal or nanoparticles. To be sure that the observed catalytic activity is not the result of any heterogeneous nickel species, two tests to distinguish between homogeneous and heterogeneous catalysis were performed. First, all catalytic runs were repeated with 100 equivalents of mercury present, as this is a known poison for heterogeneous catalysts. Second, the catalyst concentration was varied, as in a homogeneous system the catalytic activity should increase linearly with catalyst concentration, while for a heterogeneous system this is not the case. The results of both tests clearly showed that the active catalyst must be a homogeneous species.

Chelating NHC ligands - Kumada cross coupling

Early attempts to isolate *cis*-chelating bisNHC nickel dihalide complexes were unsuccessful and in stead yielded dicationic homoleptic tetracarbene complexes,[2] or intractable mixtures.[3] The only *cis*-$[(bisNHC)NiX_2]$ complex was reported in the literature was prepared from a rigid, cyclic bisimidazolium salt, in which the two

imidazolium rings are connected by two C_4 bridges.[4] The synthesis and characterization of a number of nickel(II) dihalide complexes of bidentate benzimidazole-based bisNHC ligands is described in Chapter 4. The reason why it is possible to obtain these complexes with benzimidazole-based carbenes, while with imidazole-based carbenes the synthesis failed, remains to be elucidated. Nonetheless, the solid-state structures of four of these complexes were determined by single-crystal X-ray diffraction, providing evidence for the proposed square-planar *cis*-geometry. In addition, two nickel complexes with a macrocyclic bisNHC ligand were successfully prepared.

The novel nickel bisNHC complexes were investigated for their catalytic activity in the Kumada cross coupling of aryl chlorides and bromides with phenyl magnesium chloride at room temperature. This reaction is an effective and economically attractive route for the synthesis of C–C coupled diaryls, even though it lacks a high functional group tolerance. With the exception of the complexes bearing cyclic bisNHC ligands, all complexes are moderately to highly active in this reaction. The most efficient catalyst for both aryl halides found in this study is a benzyl-substituted nickel bisNHC complex, giving full conversion of 4-chloroanisole in less then 14 h, with a selectivity of 99% to the desired product 4-methoxybiphenyl with 3 mol% catalyst loading, and full conversion of 4-bromoanisole in 75 min, with a selectivity of 82%, under the same conditions. Furthermore, it was observed that the catalytic activity of the nickel complexes is dependent on the bulk of the substituents on the bisNHC ligand: in the case of the 4-bromoanisole the rate decreased with an increase in bulk, while with 4-chloroanisole the rate increased with more bulky ligands. From this it was concluded that the rate-determining step of the catalytic cycle is dependent on the leaving group of the starting material.

It is interesting to mention that, simultaneous with and independent from the publication of the work on nickel bisNHC complexes in the Kumada coupling described in Chapter 4, the group of Huynh also reported the synthesis, crystal structure and use of the nickel(II) dibromide complex bearing a methyl substituted, propanediyl-bridged bisNHC ligand (**3a**) in the same reaction.[5] In addition, they attempted to obtain the analogous complex using a methylene bridged bisbenzimidazolium salt. In this case, however, a dicationic nickel complex with two chelating bisNHC ligands was obtained, probably due to the smaller chelate ring of the methylene bridged ligand, compared to the propylene bridged one. In contrast to the work described in Chapter 4, in which a range of different complexes is tested with one substrate, Huyhn *et al.* used complex **3a** to cross-couple a variety of aryl halides with phenyl or *p*-tolyl magnesium bromide. Good to excellent yields are obtained of the desired products, using 1 mol% catalyst, after reacting for 12 h at room temperature. In addition, it is reported that the homoleptic bis(bisNHC) nickel complex and a nickel dihalide complex with two monodentate benzimidazole-based NHC ligands are able to catalyze the coupling, although they are less active than complex **3a**. Unfortunately, the evolution of products was not followed in time, and

side products are not reported, so no conclusions about the "true" catalytic activities with these substrates may be drawn.

The continuing search for an efficient Kumada coupling catalyst is described in Chapter 5. It was decided to attempt to synthesize nickel complexes bearing chelating NHC ligands, in which the NHC is functionalized with an anionic donor moiety. Based on the complexes introduced by Liao *et al.*,[6] a number of complexes bearing amido- and benzimidazolato-functionalized NHCs were prepared and characterized by single-crystal X-ray diffraction. Surprisingly, these complexes are highly active in the Kumada coupling of 4-chloroanisole with phenylmagnesium chloride, under the conditions used in Chapter 4. The benzimidazolato-functionalized complex shows the highest activity and efficacy in this reaction reported to date, yielding the desired product in quantitative yields within 30 min, even with only 1 mol% catalyst loading. In addition, the less reactive 4-fluoroanisole could be coupled quantitatively in 150 min, under the same conditions. It is proposed that the high rate of these catalysts may be explained by a cooperative interaction between the anionic N-donor side group, magnesium halide, and the substrate, allowing for faster oxidative addition of the substrate to the nickel center.

DFT studies

To conclude the investigations into the nickel-catalyzed Kumada coupling an attempt was undertaken to rationalize the results of the catalytic experiments described in Chapter 4. Using density functional theory (DFT), the complete catalytic cycle of this reaction using a nickel bisNHC complex was calculated. The results of these quantum-chemical calculations are presented in Chapter 6 and show the feasibility of the generally accepted cycle, which consists of oxidative addition of the aryl halide, transmetalation of the halide and the second aryl with the Grignard reagent, and reductive elimination of the coupling product. The oxidative addition was shown to start with coordination of the aryl halide to the starting Ni(0) species, followed by insertion of the nickel center into the C–X bond to give a *cis*-coordinated nickel(II) species. In the second step, the arylmagnesium chloride is coordinated between the nickel-bound aryl and halide and, following a transition state comprising a 4-membered Ni–C–Mg–X ring, the new aryl group and the halide exchange positions. This leads to an MgXCl moiety, located between two nickel-coordinated aryl rings, which dissociates. In the third step, the two remaining aryl groups form a C–C bond, following a three-membered transition state, and the coupled product dissociated to yield the starting nickel(0) species.

In addition to the cycle leading to the desired product, a route was proposed, starting from an intermediate of the transmetalation sequence, which would effectively lead to scrambling of the aryl rings of the two starting materials. This route excellently explains all sideproducts observed in the experimental studies.

The calculated energy profile of the full catalytic cycle shows barriers of nearly

equal magnitude for all three steps of the cycle, which is consistent with the change in rate-determining step when changing leaving groups. Unfortunately, this also hampers a clear cut conclusion about the exact rate-determining step under experimental conditions.

Vinyl polymerization of norbornene

The last type of homogeneous catalysis under experimental investigation in this research is the vinyl polymerization of norbornene, which is presented in Chapter 7. Due to their good thermal resistance and transparency, polynorbornenes are of interest for a number of optical and electronic applications and their catalytic synthesis has been reported with numerous nickel complexes with N, O, and P-donor ligands. Only two examples of nickel NHC complexes in this reaction are known, and it was decided to investigate the activity of complexes of the three types described in Chapters 3-5, *i.e.* a complex with monodentate NHC ligands, two complexes with a chelating bisNHC ligand, and two complexes with anionic bidentate N-donor functionalized NHC ligands.

Activated by a relatively low 500-fold excess of methylaluminoxane (MAO) the three complex types showed good to high activity, over a range of temperatures in dichloromethane or 1,2-dichloroethane. The polymeric products were shown by IR spectroscopy and NMR spectrometry be of the vinyl-polymerized type and were of high molecular weight and narrow polydispersity (as determined with size exclusion chromatography). Of the three types of catalysis under investigation, the N-donor functionalized complexes were the least active, while the highest activity of 2.6×10^7 g/(mol cat)·h was obtained with the small diiodidobis(1,3-dimethylimidazol-2-ylidene)nickel(II).

8.2 Concluding remarks and outlook

The aim of the research described in this thesis was to design and prepare nickel complexes with N-heterocyclic carbene ligands and to use these complexes in homogeneous catalysis. The fact that three distinct types of nickel-NHC complexes could be obtained and used in three very different types of catalysis is a clear demonstration of the great flexibility of NHCs and the potential of their complexes as versatile, stable and efficient homogeneous catalysts in a wide range of reactions. Even though the present research was mainly curiosity-driven, the results may lead to more efficient, economically attractive, and environmentally friendly catalytic processes. For instance, if the precious metals (Pd, Pt, Rh) generally used in catalysis could be replaced by nickel, if phosphane ligands with their elaborate synthesis could be replaced by NHCs, or if C–C couplings reactions have only magnesium salts as byproducts this would save costs and avoid environmentally unfriendly chemicals.

Research is never finished and many research areas have not been explored in the work described in this thesis. A few subjects involving nickel NHC complexes which may be of interest for future investigations are listed below.

In the hydrosilylation of alkynes described in Chapter 3, only two symmetric alkynes were used as substrates. It should be interesting to see the regioselectivity of the catalyst in the case of an asymmetric internal alkyne. It is expected that the shape and size of the NHC ligand will have a large influence on this selectivity.

In the studies on the Kumada cross coupling described in Chapter 4 and 5, the catalysts have only been tested against 4-haloanisoles. It should be very exciting to see how these catalysts perform with more challenging substrates, especially the highly efficient N-donor functionalized complexes of Chapter 5. Relevant challenges are ortho-substituted aryl halides, heteroaryl halides and Grignard reagents, and polyhalogenated aromatic rings. A major limitation of the Kumada cross coupling is the poor functional-group tolerance, which may be addressed by using highly active nickel NHC complexes. For instance, the coupling to cyanoaryl halides would lead to cyanobiphenyl molecules, which are relevant for drug synthesis. In addition, the cross coupling of alkyl and aryl reagents would worthwhile to investigate.

The nickel-catalyzed vinyl-polymerization studies on norbornene described in Chapter 7, although preliminary, clearly show that next to the often used polydentate N, O and P-donor ligands, mono- and bidentate NHC ligands may be used for this type of reaction as well. The real benefit of nickel NHC complexes should be made clear by testing them against less strained olefins and using them in the preparation of copolymers.

The catalytic processes under investigation in this research have all been reported in the literature before, using other types of catalyst. A larger challenge would be to actually find a novel catalytic process, for which the NHC ligand is an essential component of the catalytic system and for which other ligand types are unsuitable. Especially in catalytic reactions in which the metal center would benefit from elevated electron density, such as those involving an oxidative addition, NHCs may prove to be of importance. In that respect, the use of NHC ligands with anionic side groups should be investigated further. If the mechanism proposed in Chapter 5 is indeed correct, the use of such ligands in catalysis should be very beneficial for all kinds of reactions involving oxidative additions of aryl or alkyl halides, as the anionic side group has interaction with the substrate or leaving group, while the NHC ensures stable coordination of the ligand.

Although not directly applicable to the catalytic reactions under study in this thesis, the use of chiral substituents on the NHC ligands may lead to stereoselective synthesis. Some examples of chiral NHC ligands in homogeneous catalysis have started to emerge, leading to good enantioselectivities in a number of cases.[7]

Even though the field of N-heterocyclic carbenes has only come to full activity in the last decade, a vast amount of exciting and promising applications in

homogeneous catalysis has already been disclosed. The work described in this thesis has extended the field with some highly active catalysts, and has provided insight in the versatile chemistry of nickel N-heterocyclic carbene complexes.

8.3 References

(1) Newman, C. P.; Clarkson, G. J.; Rourke, J. P. *J. Organomet. Chem.* **2007**, *692*, 4962.
(2) Herrmann, W. A.; Schwarz, J.; Gardiner, M. G.; Spiegler, M. *J. Organomet. Chem.* **1999**, *575*, 80.
(3) Douthwaite, R. E.; Green, M. L. H.; Silcock, P. J.; Gomes, P. T. *Organometallics* **2001**, *20*, 2611.
(4) Baker, M. V.; Skelton, B. W.; White, A. H.; Williams, C. C. *J. Chem. Soc.-Dalton Trans.* **2001**, 111.
(5) Huynh, H. V.; Jothibasu, R. *Eur. J. Inorg. Chem.* **2009**, 1926.
(6) Liao, C. Y.; Chan, K. T.; Chang, Y. C.; Chen, C. Y.; Tu, C. Y.; Hu, C. H.; Lee, H. M. *Organometallics* **2007**, *26*, 5826.
(7) Douthwaite, R. E. *Coord. Chem. Rev.* **2007**, *251*, 702.

Appendix A

Synthesis of diimidazolium salts

Abstract. *The syntheses of a number of diimidazolium salts using conventional heating in THF or 1,4-dioxane, as well as using microwave-assisted reactions in toluene are described and evaluated. In total, the synthesis and characterization of nineteen novel (di)imidazolium salts is presented.*

A.1 Introduction

Imidazolium salts have been under investigation for a number of applications. Small N,N′-dialkyl imidazolium salts are a well known class of ionic liquids, and have as such found use as highly versatile solvents in synthesis and catalysis.[1] Polyimidazolium salts, on the other hand, have been studied for their anion receptor properties.[2, 3] Recent interest in imidazolium salts is mainly due the fact that they are excellent precursors for N-heterocyclic carbenes (see Chapter 1).

Generally, imidazolium salts are prepared by a quaternization reaction between an N-substituted imidazole with an alkyl halide or an alkyl chain with another suitable leaving group (Scheme A.1). Often, the reaction is performed in an apolar solvent, such as THF, toluene, or diethyl ether, in which the reagents dissolve and from which the product salt separates. Only in the case of N,N′-diaryl imidazolium salts this synthetic route cannot be followed, as aryl halides are unreactive towards nucleophilic substitution. Usually, these salts are obtained following a ring-closing pathway, in which the imidazole ring is formed *in situ*.[4]

The quaternization reaction, depending on the leaving group, often requires refluxing conditions to proceed at an appreciable rate. In principle, the rate of the reaction may be increased by refluxing in a higher boiling solvent. Alternatively, a lower boiling solvent may be used when performing the reaction in a pressure tube, at temperatures well above the boiling point of the solvent.[5] In addition, the reaction may be heated using microwave radiation. The use of household or laboratory microwave ovens is one of the latest advances in organic synthesis,[6] although there is an ongoing debate whether the success of its use is due to the high temperatures employed, or if there is an added enhancement due to the radiation.[7] In 2001 Varma *et al.* reported the use of a household microwave oven in the solvent-free synthesis of mono- and diimidazolium salts.[8] Later, the method was improved and extended to a scale up to 2 mol, using an open-vessel microwave setup.[9]

In this appendix the synthetic procedures leading toward various imidazolium salts are described. These products were obtained during the research described in Chapters 2-5, however, attempts to synthesize their corresponding nickel N-heterocyclic carbene complexes failed, or were ultimately not attempted. Still, a number of these novel imidazolium salts have not been reported in the literature.

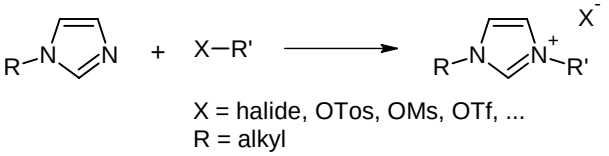

Scheme A.1. General synthetic route toward imidazolium salts.

A.2 Results and discussion

A number of N-substituted imidazoles that could not be obtained commercially were synthesized following various literature procedures or adaptations thereof. In total, eleven different N-substituted imidazoles and benzimidazoles were obtained, shown in Figure A.1. The various products obtained from these N-substituted imidazoles are depicted in Figure A.2 (N.B. Product numbering is as follows: the numeral denotes the type of imidazole or diimidazole; the letter suffix is unique for the N-sidegroup). In principle, diimidazolium salts may be obtained either by reaction of an N-substituted imidazole with a suitable alkyl dihalide,[10] or by reaction of a bridged bisimidazole with two equivalents of an alkyl halide or another alkylating reagent.[11] With the exception of [**6k**]Br_2, all diimidazolium salts were obtained following the first route.

A small survey was undertaken to determine the optimal conditions for the quaternization reaction of these N-substituted imidazoles with 1,2-dibromoethane. The details of the synthetic procedures leading to diimidazolium salts *via* three different methods are summarized in Table A.1. The yield of the different products is given for each method. Method A consists of refluxing a solution of the reagents in THF for 2 – 3 days, as developed by Lee *et al*.[10] In Method B the reagents are dissolved in toluene in a pressure tube and heated in a laboratory microwave to 125 to 140 °C for five to ten minutes. In Method C the reagents are heated in 1,4-dioxane at 100 °C for 16 hours.

Method A gave the salts in relatively high yields in most cases. However, of the three methods, Method A has the lengthiest reaction time and some products contained colored impurities, and therefore the mixture had to be recrystallized. Moreover, imidazoles **1c** and **2a** appeared to be quite unreactive, leading to an inseparable mixture of mono- and dicondensates. It should be noted, however, that products [**5c**]Br_2 and [**7a**]Br_2 have been prepared before and more efficiently, by heating the reagents for 2 days in THF at 130 °C in a pressure tube.[5] Method B, which has the shortest reaction time and fair to good yields, gave colored products which needed recrystallization, as well. Presumably, the coloration is caused by

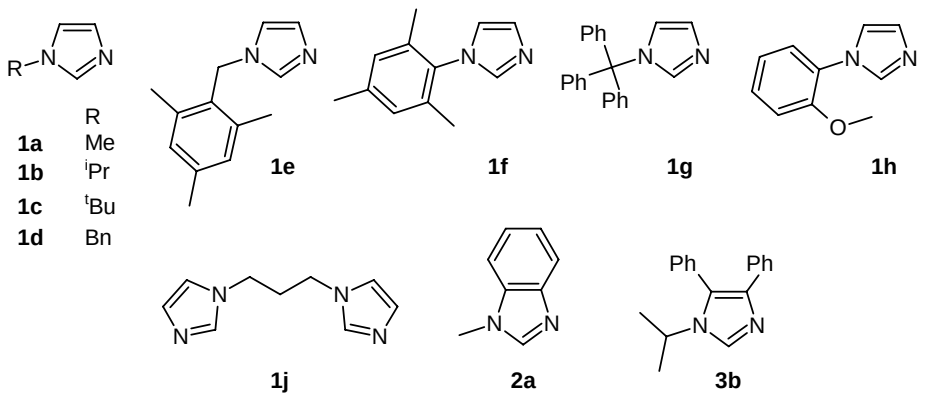

Figure A.1. N-substituted imidazoles used in this study.

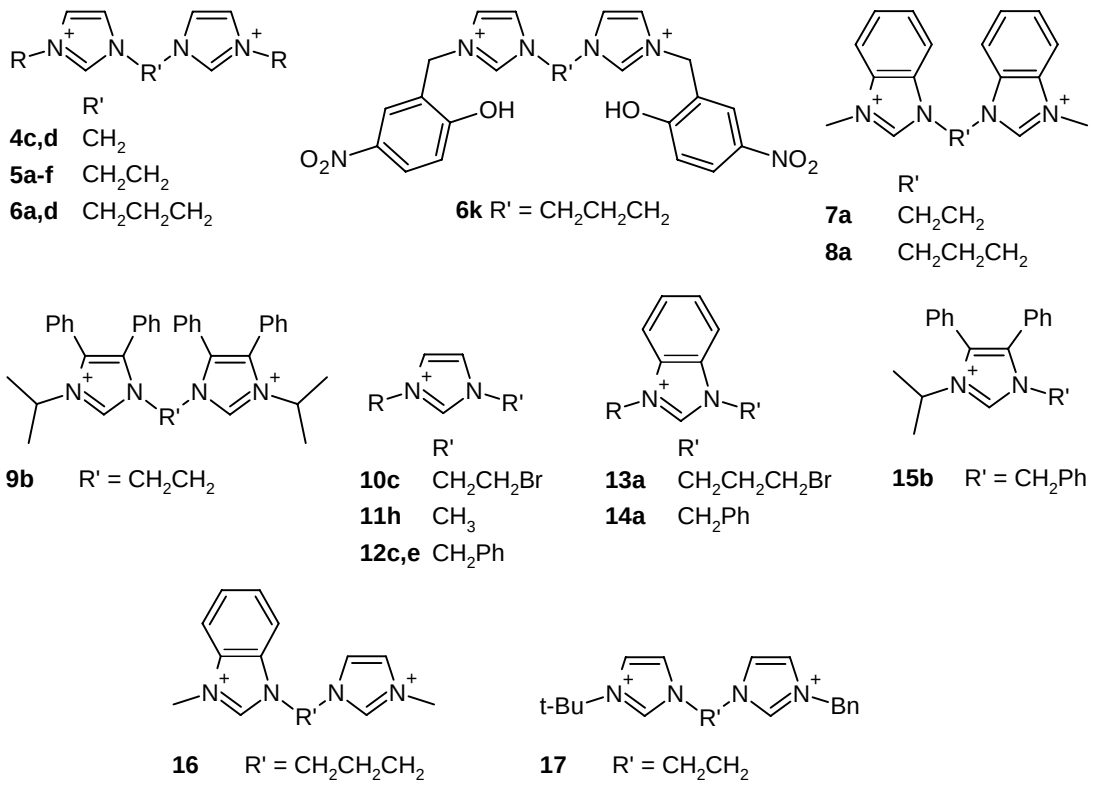

Figure A.2. All imidazolium cations prepared in this study.

decomposition due to the high temperatures employed in the microwave assisted synthesis. Method C gave most products in good to high yields, and in high purity (>99%, judging from the NMR spectra), without further purification being required.

The initial survey included the use of leaving groups other than bromides, i.e. tosylates and mesylates. These leaving groups gave the corresponding products in high yields, except for the microwave assisted synthesis with 1,2-di-O-mesylethane which lead to a mixture of mono- and di-condensates.

Table A.1. Imidazolium salts synthesized and the yield depending on the method used.

Dication	R-Im	X-R'-X R'	X	THF, 80 °C, 2-3 d [a]	Toluene, μW [a]	1,4-Dioxane, 100 °C, 16 h [a]
5a	**1a**	CH_2CH_2	OTos		86	95
5c	**1c**	CH_2CH_2	Br	0 [b] (85) [c]	35	78
5d	**1d**	CH_2CH_2	Br	65 (52) [10]	43	
5d	**1d**	CH_2CH_2	OMs	75	0 [b]	
5e	**1e**	CH_2CH_2	Br		27	66
5f	**1f**	CH_2CH_2	Br	39 (45) [10]	21	70
7a	**2a**	CH_2CH_2	Br	0[b] (68) [c]	37	55

[a] X-R'-X : R-Im = 1 : 2.1-2.5; isolated yield (%), literature values in parentheses; [b] A mixture of inseparable products was obtained; [c] THF, pressure tube, 130 °C, 2 d, ref. 5.

In summary, it is clear from Table A.1 that, even though the microwave-assisted synthesis yields the products in moderate amounts in a very short time, the conventional heating in 1,4-dioxane is the superior synthesis method in terms of isolated yields and, moreover, in terms of product purity. Therefore, the remaining syntheses were performed by conventional heating.

The conditions and yields of the synthesis of an additional variety of diimidazolium salts by conventional heating are summarized in Table A.2. Variations are made in the N-substituent, the length of the bridge and the leaving group. The bromide salts of **4c**, **4d** and **5b** have been reported before in higher yielding reactions, either by heating in a pressure tube to 130 °C in THF,[5] or following a solvent-free method.[10]

In the case of the trityl-substituted imidazolium salts, only a mixture of the mono- and dicondensates could be obtained, probably due to the poor solubility of the starting material, or the low reactivity. Unfortunately, the mixture could not be separated.

Table A.2. Overview of diimidazolium salts obtained by conventional heating.

Dication	R-Im	R′	X	Yield (%) [a]	Solvent and conditions [b]
4c	**1c**	CH_2	Br	42	1,4-dioxane
				79 [5]	THF, 130 °C, 2 d
4d	**1d**	CH_2	Br	30	1,4-dioxane
				81 [10]	Neat, 80 °C, 16 h
5b	**1b**	CH_2CH_2	Br	75	THF
				90 [5]	THF, 130 °C, 2 d
5d	**1d**	CH_2CH_2	OTos	95	THF
5g	**1g**	CH_2CH_2	Br	0 [c]	1,4-dioxane
5h	**1h**	CH_2CH_2	Br	42	THF
6a	**1a**	$(CH_2)_3$	OTos	93	THF
6d	**1d**	$(CH_2)_3$	Br	60	1,4-dioxane
6d	**1d**	$(CH_2)_3$	OTos	93	THF
6k	**1j**	3-(NO_2)-6-(OH)Bn	Br	86	3 : 1 1,4-dioxane-acetonitrile, R-Im : R′-X = 1 : 2.4
8a	**2a**	$(CH_2)_3$	OTos	94	1,4-dioxane
9b	**3b**	CH_2CH_2	Br	53	1,4-dioxane
16	**1a**	**13a**	Br	58	1,4-dioxane, R′-X : R-Im = 1 : 1.7
17	**1d**	**10c**	Br	87	1,4-dioxane, R′-X : R-Im = 1 : 1

[a] Isolated yield (%); [b] Standard conditions: X-R′-X : R-Im = 1 : 2.0-2.5; with THF: 80 °C, 2-3 d; with 1,4-dioxane: 100 °C, 16 h; [c] A mixture of inseparable products was obtained.

Asymmetric diimidazolium salts **16** and **17** were obtained by first reacting a N-substituted imidazole with a large excess of 1,2-dibromoethane or 1,3-dibromopropane to yield monocondensates **10c** and **13a** (see below), which were then reacted further with another N-substituted imidazole. Asymmetric

diimidazolium salts with a methylene bridge could not be obtained following this synthetic route, as even in a large excess of dibromomethane the dicondensate is synthesized.[10]

An overview of various monoimidazolium salts synthesized by conventional heating is presented in Table A.3. Monocondensates [**10c**]Br and [**13a**]Br were obtained by using an excess of alkyl dihalide and stirring at 35 – 40 °C, in order to avoid the formation of an inseparable mixture of mono- and dicondensate. Compound [**11h**]I could be obtained in good yields by stirring at room temperature, as iodomethane is highly reactive towards substitution reactions. Imidazolium salt [**14a**]Br has been synthesized before by stirring the reagents in dimethylacetamide (DMA), although column chromatography was necessary to obtain the pure compound.[12]

Table A.3. Overview of imidazolium salts obtained in this study.

Cation	R-Im	R′	X	Yield (%) [a]	Solvent and conditions [b]
10c	**1c**	CH_2CH_2Br	Br	86	THF, R-Im : R′-X = 1 : 5, 40 °C
11h	**1h**	Me	I	84	THF, RT
12c	**1c**	Bn	Br	82	1,4-dioxane
12e	**1e**	Bn	Br	63	THF
13a	**2a**	$(CH_2)_3Br$	Br	33	THF, R-Im : R′-X = 1 : 6, 35 °C
14a	**2a**	Bn	Br	97	THF, 16 h
				96 [12]	DMA, 50 °C, 16 h
15b	**3b**	Bn	Br	95	1,4-dioxane

[a] Isolated yield (%); [b] Standard conditions: R-Im : R′-X = 1 : 1.1–3.0; with THF: 80 °C, 2-3 d; with 1,4-dioxane: 100 °C, 16 h.

All (di)imidazolium salts are insoluble in 1,4-dioxane, THF, diethyl ether and hydrocarbons, sparingly soluble in dichloromethane and soluble in methanol, DMSO and water, except for the highly substituted imidazolium bromide [**15b**]Br, which was found also soluble in 1,4-dioxane, and was isolated only after precipitation by the addition of diethyl ether. The (di)imidazolium salts were analyzed by ^{1}H and ^{13}C NMR spectrometry, infrared spectroscopy, mass spectrometry and elemental analysis. The characteristic NCHN resonances in the ^{1}H and ^{13}C NMR spectra were present around 9 – 10 and 135 ppm, respectively, with the resonances of the benzimidazolium and 4,5-diphenylimidazolium salts shifted more downfield. Interestingly, the mass spectra of benzyl and *tert*-butyl substituted imidazolium salts showed a defragmentation pattern consistent with partial loss of these substituents.

A.3 Conclusion

In conclusion, three methods for the synthesis of (di)imidazolium salts are discussed and evaluated. Microwave-assisted synthesis of a number of salts was shown to be a fast method; however, the products obtained are often not pure. The

most efficient synthetic route is heating the reagents in 1,4-dioxane at elevated temperatures, leading to high yields and pure products. In total, nineteen novel imidazolium salts were synthesized and characterized.

A.4 Experimental Section

General Procedures. All quaternization reactions were performed under an atmosphere of dry argon, using standard Schlenk techniques, except for the microwave-assisted syntheses, which were performed in a closed pressure tube, which was loaded in air. THF and 1,4-dioxane were distilled from CaH_2 and stored on molecular sieves under argon. The compounds 1-(bromomethyl)-2,4,6-trimethylbenzene,[13] **1b**,[14] **1c**,[15] **1f**,[15] **1g**,[16] **1h**,[17] **3b**,[18] 1,3-di-O-tosylpropane,[19] 1,2-di-O-tosylethane,[20] and 1,2-di-O-mesylethane[21] were prepared according to literature procedures. Compounds **1e**[22] and **1j**[23] are known compounds, but were prepared following different synthetic routes. NMR data of these compounds, however, match those reported in literature. Other chemicals were obtained commercially and used as received. Microwave-assisted syntheses were performed on an Emrys Optimizer laboratory microwave. ^{1}H NMR and ^{13}C NMR spectra were recorded on a Bruker DPX300 spectrometer. Chemical shifts are reported as referenced against the residual solvent signals and quoted in ppm relative to tetramethylsilane (TMS). IR spectra were recorded with a Perkin-Elmer FT-IR Paragon 1000 spectrophotometer equipped with a golden-gate ATR device, using the reflectance technique (4000-300 cm^{-1}; resolution 4 cm^{-1}). Electrospray mass spectra were recorded on a Finnigan TSQ-quantum instrument using an electrospray ionization technique (ESI-MS), using a water/acetonitrile or water/methanol mixture as solvent. C,H,N,S elemental analyses were carried out with a Perkin-Elmer series II CHNS/O analyzer 2400.

1-(2,4,6-trimethylbenzyl)imidazole (1e). To a solution of imidazole (1.36 g, 20 mmol) in 40 mL DMSO was added powdered potassium hydroxide (1.68 g, 30 mmol) and the mixture was stirred at room temperature for 45 min. Then 1-(bromomethyl)-2,4,6-trimethylbenzene (4.24 g, 20 mmol) was added and the solution was stirred vigorously for 3 h, while cooling with a water bath at room temperature. The resulting solution was diluted with 350 mL water and extracted six times with 50 mL chloroform. The combined extracts were washed with water, dried with magnesium sulfate and the solvent was evaporated. The remaining oil was vacuum distilled at 170 °C to yield the product as a pale yellow oil. Yield: 3.40 g (84%). ^{1}H NMR (300 MHz, DMSO-d_6, 300 K): δ 7.48 (s, 1H, NCHN), 6.89 (s, 2H, Ar-H), 6.86 (s, 1H, NCH), 6.83 (s, 1H, NCH), 5.14 (s, 2H, NCH_2), 2.22 (s, 3H, CH_3), 2.21 (s, 6H, CH_3). ^{13}C NMR (75 MHz, DMSO-d_6, 300 K): δ 137.3 (2 × C_q), 136.9 (NCHN), 129.5 (C_q), 129.1 (C_{Ar}), 128.3 (NCH), 118.8 (NCH), 43.9 (NCH_2), 20.5 (CH_3), 19.2 (CH_3). IR (neat): 2918 (w), 1613 (w), 1507 (m), 1464 (m), 1225 (m), 1108 (m), 1073 (s), 1024 (s), 906 (m), 853 (m), 733 (m), 686 (s), 662 (s), 617 (m) cm^{-1}.

1,3-bis(1-imidazolyl)propane (1j). To a solution of imidazole (5.72 g, 84 mmol) and 1,3-dibromopropane (4.25 mL, 42 mmol) in 60 mL acetonitrile was added 30 mL 25% aqueous sodium hydroxide solution and the mixture was vigorously stirred for 3 days. After evaporation of all solvents, the remaining solids were extracted into chloroform, dried with magnesium sulfate, and filtered. Evaporation of the solvent yielded the product as a pale yellow oil. Yield: 4.23 g (57%). ^{1}H NMR (300 MHz, $CDCl_3$, 300 K): δ 7.45 (s, 2H, NCHN), 7.10

(s, 2H, NCH), 6.89 (s, 2H, NCH), 3.91 (t, 4H, *J* = 7 Hz, NCH_2), 2.29 (pent, 2H, *J* = 7 Hz, CH_2). ^{13}C NMR (75 MHz, $CDCl_3$, 300 K): δ 137.0 (NCHN), 130.2 (NCH), 118.5 (NCH), 43.3 (NCH_2), 31.9 (CH_2).

General synthesis of diimidazolium salts by conventional heating in THF (method A). A solution of alkyl dihalide, alkyl ditosylate, or alkyl dimesylate and 2.0 – 2.5 equivalents of N-substituted imidazole or N-substituted imidazole derivative in dry THF was stirred and refluxed using an oil bath under an argon atmosphere for 2-3 days. The resulting white to off-white precipitate was isolated by filtration, washed with THF and diethyl ether and dried *in vacuo*. In the case that the reaction resulted in a two-phase mixture, the two layers were separated. The product layer was washed with THF and diethyl ether and the product crystallized upon drying *in vacuo*.

General microwave-assisted synthesis of diimidazolium salts (method B). To a 5 mL pressure tube were added N-substituted imidazole, 1,2-dibromoethane, 1.5 mL toluene and a stir bar. The tube was capped and heated with stirring in the microwave cavity, while keeping the solution at a preset temperature. After cooling, the cap was removed and the off-white to yellow solid product was isolated by filtration and washed with toluene. The product was recrystallized from methanol/diethyl ether and obtained as off-white to white solids.

General synthesis of diimidazolium salts by conventional heating in 1,4-dioxane (method C). As method A, using dry 1,4-dioxane as solvent for the reaction and stirring at 100 °C for 16 h. The product was washed with THF and diethyl ether.

1,1′-tert-butyl-3,3′-(1,1-methylene)diimidazolium dibromide ([4c]Br_2). Following method C, the compound was obtained as a white solid from **1c** (3.97 g, 32.0 mmol) and dibromomethane (2.61 g, 15.0 mmol) in 30 mL 1,4-dioxane. Yield: 2.65 g (42%). NMR spectra are identical to those reported.[5]

1,1′-dibenzyl-3,3′-(1,1-methylene)diimidazolium dibromide ([4d]Br_2). Following method C, the compound was obtained as a white solid from **1d** (5.06 g, 32.0 mmol) and dibromomethane (2.61 g, 15.0 mmol) in 30 mL 1,4-dioxane. Yield: 2.50 g (30%). NMR spectra are identical to those reported.[10]

1,1′-dimethyl-3,3′-(1,2-ethanediyl)diimidazolium ditosylate ([5a][OTos]$_2$). Method B: **1a** (0.36 g, 4.4 mmol) and 1,2-di-O-tosylethane (0.74 g, 2.0 mmol) in 1.5 mL toluene at 125 °C for 250 sec. The compound was further purified by recrystallization from methanol/diethyl ether. Yield: 0.95 g (86%). Method C: **1a** (0.41 g, 5.0 mmol) and 1,2-di-O-tosylethane (0.74 g, 2.0 mmol) in 15 mL 1,4-dioxane. Yield: 1.02 g (95%). ^1H NMR (300 MHz, DMSO-d_6, 300 K): δ 9.01 (s, 2H, NCHN), 7.69 (s, 2H, NCH), 7.58 (s, 2H, NCH), 7.48 (d, 4H, *J* = 8 Hz, Ar-H), 7.09 (d, 4H, *J* = 8 Hz, Ar-H), 4.66 (s, 4H, NCH_2), 3.81 (s, 6H, NCH_3), 2.27 (s, 6H, $ArCH_3$). ^{13}C NMR (75 MHz, DMSO-d_6, 300 K): δ 137.7 (C_q), 137.2 (NCHN), 128.1 (C_{Ar}), 125.5 (C_{Ar}), 123.9 (NCH), 122.4 (NCH), 48.4 (NCH_2), 35.9 (NCH_3), 20.8 (CH_3). IR (neat): 3088 (m), 1559 (m), 1188 (s), 1163 (s), 1121 (s), 1030 (s), 1008 (s), 819 (s), 747 (m), 680 (s), 619 (s), 554 (s) cm^{-1}. ESI-MS: *m*/*z* 191 ($[M - 2\ OTos - H]^+$), 363 ($[M - OTos]^+$, 100%). Anal. Calcd for $C_{24}H_{30}N_4O_6S_2$: C, 53.92; H, 5.66; N, 10.48; S, 11.99. Found: C, 54.02; H, 5.65; N, 10.39; S, 11.86.

1,1′-diisopropyl-3,3′-(1,2-ethanediyl)diimidazolium dibromide ([5b]Br_2). Following method A, the compound was isolated as an off-white solid from **1b** (2.42 g, 22.0 mmol) and

1,2-dibromoethane (1.97 g, 10.5 mmol) in 30 mL THF. Yield: 3.30 g (75%). NMR spectra are identical to those reported.[5]

1,1′-di-tert-butyl-3,3′-(1,2-ethanediyl)diimidazolium dibromide ([5c]Br$_2$). Method A: **1c** (2.60 g, 20.9 mmol) and 1,2-dibromoethane (1.95 g, 10.4 mmol) in 25 mL THF yielded a mixture of the mono- and dicondensate, according to the NMR spectra. Method B: **1c** (0.55 g, 4.4 mmol) and 1,2-dibromoethane (0.38 g, 2.0 mmol) in 1.5 mL toluene, 250 s at 130 °C. Yield: 0.35 g (35%). Method C: **1c** (5.50 g, 44.3 mmol) and 1,2-dibromoethane (4.13 g, 22.0 mmol) in 45 mL 1,4-dioxane. Yield: 7.49 g (78%). NMR spectra are identical to those reported.[5]

1,1′-dibenzyl-3,3′-(1,3-ethanediyl)diimidazolium dibromide ([5d]Br$_2$). Method A: **1d** (8.22 g, 52.0 mmol) and 1,2-dibromoethane (4.70 g, 25.0 mmol) in 40 mL THF. Yield: 8.20 g (65%). Method B: **1d** (0.70 g, 4.4 mmol), and 1,2-dibromoethane (0.38g, 2.0 mmol) in 1.5 mL toluene, 250 s at 125 °C. Yield: 0.44 g (43%). NMR spectra are identical to those reported.[10]

1,1′-dibenzyl-3,3′-(1,2-ethanediyl)diimidazolium ditosylate ([5d][OTos]$_2$). Following method A, the product was obtained as a white solid from **1d** (1.27 g, 8.0 mmol) and 1,2-di-O-tosylethane (1.48 g, 4.0 mmol) in 12 mL dry THF. Yield: 2.60 g (95%). ^{1}H NMR (300 MHz, DMSO-d_6, 300 K): δ 9.20 (s, 2H, NCHN), 7.79 (s, 2H, NCH), 7.65 (s, 2H, NCH), 7.48 (d, 4H, J = 8 Hz, Ar-H), 7.38 (m, 10H, Ar-H), 7.10 (d, 4H, J = 8 Hz, Ar-H), 5.37 (s, 4H, NCH$_2$), 4.70 (s, 4H, NCH$_2$), 2.27 (s, 6H, ArCH$_3$). ^{13}C NMR (75 MHz, DMSO-d_6, 300 K): δ 145.5 (C$_q$), 137.8 (C$_q$), 136.9 (NCHN), 134.6 (C$_q$), 129.0 (C$_{Ar}$), 128.8 (C$_{Ar}$), 128.3 (C$_{Ar}$), 128.1 (C$_{Ar}$), 125.5 (C$_{Ar}$), 122.9 (2 × NCH), 52.1 (NCH$_2$), 48.5 (NCH$_2$), 20.8 (CH$_3$). IR (neat): 3090 (m), 1567 (w), 1453 (w), 1219 (s), 1183 (s), 1121 (s), 1035 (m), 1011 (m), 813 (s), 684 (s), 562 (s) cm^{-1}. ESI-MS: m/z 253 ([M – 2 OTos – Bn]$^+$), 342 ([M – 2 OTos – H]$^+$), 515 ([M – OTos]$^+$), 100%). Anal. Calcd for C$_{36}$H$_{38}$N$_4$O$_6$S$_2$: C, 62.95; H, 5.58; N, 8.16; S, 9.34. Found: C, 62.82; H, 5.56; N, 8.19; S, 9.17.

1,1′-dibenzyl-3,3′-(1,2-ethanediyl)diimidazolium dimesylate ([5d][OMs]$_2$). Method A: **1d** (1.27 g, 8.0 mmol) and 1,2-di-O-mesylethane (0.87 g, 4.0 mmol) in 12 mL dry THF. Yield: 1.60 g (75%). Method B: **1d** (0.70 g, 4.4 mmol) and 1,2-di-O-mesylethane (0.44g, 2.0 mmol) in 1.5 mL toluene, 250 s at 150 °C. Yield: mixture of mono- and dicondensates. Analytical sample obtained from method A: ^{1}H NMR (300 MHz, DMSO-d_6, 300 K): δ 9.21 (s, 2H, NCHN), 7.80 (s, 2H, NCH), 7.65 (s, 2H, NCH), 7.40 (m, 10H, Ar-H), 5.39 (NCH$_2$), 4.69 (NCH$_2$), 2.20 (s, 6H, CH$_3$). ^{13}C NMR (75 MHz, DMSO-d_6, 300 K): δ 137.0 (NCHN), 134.6 (C$_q$), 129.0 (C$_{Ar}$), 128.8 (C$_{Ar}$), 128.3 (C$_{Ar}$), 123.2 (NCH), 122.9 (NCH), 52.0 (NCH$_2$), 48.4 (NCH$_2$), 39.3 (SCH$_3$). IR (neat): 3090 (m), 3034 (m), 1558 (m), 1456 (w), 1337 (w), 1557 (s), 1040 (s), 774 (s), 715 (s), 639 (m), 551 (s), 521 (s) cm^{-1}. ESI-MS: m/z 253 ([M – 2 OMs – Bn]$^+$), 343 ([M – 2 OMs – H]$^+$), 439 ([M – OMs]$^+$, 100%). Anal. Calcd for C$_{24}$H$_{30}$N$_4$O$_6$S$_2$·H$_2$O: C, 52.16; H, 5.84; N, 10.14. Found: C, 52.23; H, 5.71; N, 9.98.

1,1′-(1,2-ethanediyl)-3,3′-(2,4,6-trimethylbenzyl)diimidazolium dibromide ([5e]Br$_2$). Method B: **1e** (0.88 g, 4.4 mmol) and 1,2-dibromoethane (0.38 g, 2.0 mmol) in 1.5 mL toluene at 130 °C for 400 s. Yield: 0.32 g (27%). Method C: **1e** (2.0 g, 10.0 mmol) and 1,2-dibromoethane (0.84 g, 4.5 mmol) in 15 mL dry 1,4-dioxane. Yield: 1.75 g (66%). ^{1}H NMR (300 MHz, DMSO-d_6, 300 K): δ 8.81 (s, 2H, NCHN), 7.63 (2 × s, 4H, NCH), 6.96 (s, 4H, Ar-H), 5.33 (s, 4H, NCH$_2$), 4.64 (s, 4H, NCH$_2$), 2.24 (s, 6H, CH$_3$), 2.19 (s, 12H, CH$_3$). ^{13}C NMR (75 MHz, DMSO-d_6, 300 K): δ 142.0 (NCHN), 138.6 (C$_q$), 138.1 (C$_q$), 129.4 (C$_{Ar}$), 126.5 (C$_q$), 122.7 (NCH), 48.3 (NCH$_2$), 47.1 (NCH$_2$), 20.6 (CH$_3$), 19.3 (CH$_3$). IR (neat): 3059 (m), 1612 (w), 1559 (m), 1447 (w), 1337 (w), 1156 (s), 850 (m), 758 (m), 634 (s) cm^{-1}. ESI-MS: m/z 295 ([M + 2H]$^{2+}$,

100%), 427 ([M – 2Br – H]$^+$), 509 ([M – Br]$^+$). Anal. Calcd for $C_{28}H_{36}Br_2N_4 \cdot 0.9H_2O$: C, 55.62; H, 6.30; N, 9.27. Found: C, 55.63; H, 6.29; N, 9.36.

1,1′-dimesityl-3,3′-(1,2-ethanediyl)diimidazolium dibromide ([5f]Br$_2$). Method A: **1f** (4.10 g, 22.0 mmol) and 1,2-dibromoethane (1.88 g, 10.0 mmol) in 30 mL THF. Yield: 2.20 g (39%). Method B: **1f** (0.82 g, 4.4 mmol) and 1,2-dibromoethane (0.38 g, 2.0 mmol) in 1.5 mL toluene, 600 s at 130 °C, followed by 300 s at 145 °C. Yield 0.24 g (21%). Method C: **1f** (3.17 g, 17.0 mmol) and 1,2-dibromoethane (1.41 g, 7.5 mmol) in 20 mL 1,4-dioxane. Yield: 2.95 g (70%). NMR spectra are identical to those reported.[10]

1,1′-(1,2-ethanediyl)-3,3′-ditrityldiimidazolium dibromide ([5g]Br2). Following method C, from **1g** (3.41 g, 11.0 mmol) and 1,2-dibromoethane (0.94 g, 5.0 mmol) in 20 mL 1,4-dioxane a mixture of mono- and dicondensate was obtained, which could not be separated.

1,1′-(1,2-ethanediyl)-3,3′-(2-methoxyphenyl)diimidazolium dibromide ([5h]Br$_2$). Following method A, **1h** (1.74 g, 10.0 mmol) and 1,2-dibromoethane (0.94 g, 5.0 mmol) in 20 mL dry THF yielded the product as an off-white solid, which was recrystallized from methanol/diethyl ether and dried *in vacuo*. Yield: 1.14 g (42%). ^{1}H NMR (300 MHz, DMSO-d_6, 300 K): δ 9.67 (s, 2H, NCHN), 8.14 (s, 2H, NCH). 7.96 (s, 2H, NCH), 7.61 (m, 4H, Ar-H), 7.36 (d, 2H, J = 8 Hz, Ar-H), 7.16 (t, 2H, 8 Hz, Ar-H), 4.94 (s, 4H, NCH_2), 3.81 (s, 6H, OCH_3). ^{13}C NMR (75 MHz, DMSO-d_6, 300 K): δ 152.0 (C_q), 137.8 (NHCN), 131.8 (C_{Ar}), 126.0 (C_{Ar}), 123.9 (NCH), 123.2 (C_q), 122.4 (NCH), 121.0 (C_{Ar}), 113.3 (C_{Ar}), 56.4 (OCH_3), 48.6 (NCH_2). IR (neat): 3055 (m), 1604 (w), 1557 (s), 1502 (s), 1446 (m), 1254 (s), 1206 (m), 1129 (m), 1067 (m), 1022 (m), 868 (w), 757 (s), 634 (s) cm^{-1}. ESI-MS: m/z 188 ([M – 2Br]$^{2+}$, 100%), 375 ([M – 2Br – H]$^+$). Anal. Calcd for $C_{22}H_{24}Br_2N_4O_2$: C, 49.27, H, 4.51; N, 10.45. Found: C, 49.42; H, 4.42; N, 10.35.

1,1-dimethyl-3,3′-(1,3-propanediyl)diimidazolium ditosylate ([6a][OTos]$_2$). Following method A, the product was obtained as a hygroscopic white solid from **1a** (0.66 g, 8.0 mmol) and 1,3-di-O-tosylpropane (1.54 g, 4.0 mmol) in 12 mL dry THF. Yield: 2.05 g (93%). ^{1}H NMR (300 MHz, DMSO-d_6, 300 K): δ 9.11 (s, 2H, NCHN), 7.74 (s, 2H, NCH), 7.71 (s, 2H, NCH), 7.47 (d, 4H, J = 8 Hz, Ar-H), 7.10 (d, 4H, J = 8 Hz, Ar-H), 4.20 (t, 4H, J = 7 Hz, NCH_2), 3.82 (s, NCH_3), 2.36 (pent, 2H, J = 7 Hz, CH_2), 2.27 (s, 6H, $ArCH_3$). ^{13}C NMR (75 MHz, DMSO-d_6, 300 K): δ 145.5 (C_q), 137.8 (C_q), 136.9 (NCHN), 128.0 (C_{Ar}), 125.4 (C_{Ar}), 123.7 (NCH), 122.1 (NCH), 45.7 (NCH_2), 35.7 (NCH_3), 29.4 (CH_2), 20.7 ($ArCH_3$). IR (neat): 3094 (w), 1575 (w), 1191 (s), 1118 (s), 1029 (s), 1008 (s), 812 (m), 678 (s), 617 (m), 559 (s) cm^{-1}. ESI-MS: m/z 205 ([M – 2 OTos – H]$^+$), 377 ([M – OTos]$^+$, 100%). Anal. Calcd for $C_{25}H_{32}N_4O_6S_2 \cdot 0.5H_2O$: C, 53.84; H, 5.96; N, 10.05; S, 11.50. Found: C, 53.39; H, 6.28; N, 10.03; S, 11.30.

1,1′-dibenzyl-3,3′-(1,3-propanediyl)diimidazolium dibromide ([6d]Br$_2$). Following method C, a reaction between **5d** (0.95 g, 6.0 mmol) and 1,3-dibromopropane (0.50 g, 2.5 mmol) in 10 mL 1,4-dioxane yielded the compound as a white solid. Yield: 0.78 g (60%). ^{1}H NMR (300 MHz, DMSO-d_6, 300 K): δ 9.49 (s, 2H, NCHN), 7.87 (t, 2H, J = 2 Hz, NCH), 7.82 (t, 2H, J = 2 Hz, NCH), 7.43 (m, 10H, Ar-H), 5.45 (s, 4H, NCH_2Ph), 4.28 (t, 4H, J = 7 Hz, NCH_2), 2.43 (pent, 2H, J = 7 Hz, CH_2). ^{13}C NMR (75 MHz, DMSO-d_6, 300 K): δ 136.4 (NCHN), 134.7 (C_q), 129.0 (C_{Ar}), 128.8 (C_{Ar}), 128.4 (C_{Ar}), 122.8 (NCH), 122.6 (NCH), 51.9 (NCH_2), 46.0 (NCH_2), 29.3 (CH_2). IR (neat): 3068 (w), 2969 (m), 1549 (m), 1447 (m), 1213 (w), 1180 (m), 1149 (s), 846 (m), 748 (m), 718 (s), 702 (s), 636 (s) cm^{-1}. ESI-MS: m/z 267 ([M – 2 Br – Bn]$^+$, 100%), 357 ([M – 2 Br – H]$^+$), 437 ([M – Br]$^+$). Anal. Calcd for $C_{23}H_{26}Br_2N_4$: C, 53.30; H, 5.06; N, 10.81. Found: C, 53.09; H, 5.07; N, 10.80.

1,1-dibenzyl-3,3′-(1,3-propanediyl)diimidazolium ditosylate ([6d][OTos]$_2$). Following method A the product was obtained as a white solid from **5d** (1.27 g, 8.0 mmol) and 1,3-di-O-tosylpropane (1.54 g, 4.0 mmol) in 15 mL dry THF. Yield: 2.61 g (93%). ^{1}H NMR (300 MHz, DMSO-d_6, 300 K): δ 9.31 (s, 2H, NCHN), 7.78 (2 × s, 4H, NCH), 7.48 (d, 4H, J = 8 Hz, Ar-H), 7.42 (m, 10H, Ar-H), 7.10 (d, 4H, J = 8 Hz, Ar-H), 5.40 (NCH_2Ar), 4.23 (t, 4H, J = 7 Hz, NCH_2), 2.39 (t, 2H, J = 7 Hz, CH_2), 2.27 (s, 6H, $ArCH_3$). ^{13}C NMR (75 MHz, DMSO-d_6, 300 K): δ 145.5 (C_q), 137.8 (C_q), 136.5 (NCHN), 134.7 (C_q), 129.0 (C_{Ar}), 128.8 (C_{Ar}), 128.4 (C_{Ar}), 128.2 (C_{Ar}), 125.5 (C_{Ar}), 122.8 (NCH), 122.6 (NCH), 51.9 (NCH_2), 46.1 (NCH_2), 29.4 (CH_2), 20.8 (CH_3). IR (neat): 3096 (m), 1567 (m), 1455 (m), 1192 (s), 1120 (s), 1033 (s), 1011 (s), 875 (w), 810 (m), 679 (s), 561 (s) cm^{-1}. ESI-MS: m/z 267 ([M – 2 OTos – Bn]$^+$), 357 ([M – 2 OTos – H]$^+$), 529 ([M – OTos]$^+$, 100%). Anal. Calcd for $C_{37}H_{40}N_4O_6S_2$: C, 63.41; H, 5.75; N, 7.99. Found: C, 63.01; H, 5.61; N, 8.01.

1,1′-(3-nitro-6-hydroxyphenylmethyl)-3,3′-(1,3-propanediyl)diimidazolium dibromide ([6k]Br$_2$). To a solution of α-bromo-4-nitro-o-cresol (2.78 g, 12.0 mmol) in 15 mL dry 1,4-dioxane and 5 mL acetonitrile was added **1j** (0.88 g, 5.0 mmol) and the mixture was stirred 3 days at 100 °C. The resulting two layers were separated and the product layer was washed with THF and dissolved in methanol. Addition of diethyl ether yielded again a two-phase system. After separation, the product layer slowly crystallized *in vacuo* and the product was isolated as a pale yellow solid. Yield: 2.75 g (86%). ^{1}H NMR (300 MHz, DMSO-d_6, 300 K): δ 11.7 (s, 2H, OH), 9.31 (s, 2H, NCHN), 8.40 (d, 2H, J = 3 Hz, Ar-H), 8.18 (dd, 2H, J = 9 Hz, J = 3 Hz, Ar-H), 7.81 (s, 4H, NCH), 7.11 (d, 2H, J = 9 Hz, Ar-H), 5.42 (s, 4H, NCH_2), 4.24 (t, 4H, J = 7 Hz, NCH_2), 2.37 (m, 2H, CH_2). ^{13}C NMR (75 MHz, DMSO-d_6, 300 K): δ 163.5 (C_q), 143.0 (NCHN), 140.7 (C_q), 128.5 (C_{Ar}), 128.2 (C_{Ar}), 124.1 (NCH), 123.7 (NCH), 122.8 (C_q), 117.2 (C_{Ar}), 48.7 (NCH_2), 47.2 (NCH_2), 30.8 (CH_2). IR (neat): 3030 (m), 1594 (m), 1557 (m), 1520 (m), 1495 (m), 1435 (m), 1336 (s), 1281 (s), 1151 (m), 1088 (s), 932 (m), 747 (m), 639 (m) cm^{-1}. ESI-MS: m/z 328 ([M – 2Br – $O_2NC_7H_5OH$]$^+$, 100%), 479 ([M – 2Br – H]$^+$), 561 ([M – Br]$^+$). Anal. Calcd for $C_{23}H_{24}Br_2N_6O_6 \cdot 1.7CH_3OH$: C, 42.70; H, 4.47; N, 12.10. Found: C, 42.44; H, 4.35; N, 12.31.

1,1′-dimethyl-3,3′-(1,2-ethanediyl)dibenzimidazolium dibromide ([7a]Br$_2$). Method A: **2a** (4.22 g, 32.0 mmol) and 1,2-dibromoethane (2.81 g, 15.0 mmol) in 35 mL THF yielded 2.0 g of a mixture of mono- and dicondensates. Method B: **2a** (0.58 g, 4.4 mmol) and 1,2-dibromoethane (0.38 g, 2.0 mmol) in 1.5 mL toluene, 250 s at 150 °C. Yield: 0.33 g (37%). Method C: **2a** (4.22 g, 32.0 mmol) and 1,2-dibromoethane (2.81 g, 15.0 mmol) in 35 mL 1,4-dioxane. Yield: 3.70 g (55%). NMR spectra are identical to those reported.[5]

1,1′-dimethyl-3,3′-(1,3-propanediyl)dibenzimidazolium ditosylate ([8a][OTos]$_2$). Following method C, the product was isolated as a white, hygroscopic solid from **2a** (1.59 g, 12.0 mmol) and 1,3-di-O-tosylpropane (1.92g, 5.0 mmol) in 10 mL 1,4-dioxane. Yield: 2.94 g (94%). ^{1}H NMR (300 MHz, DMSO-d_6, 300 K): δ 9.71 (s, 2H, NCHN), 8.03 (m, 4H, Ar-H), 7.69 (m, 4H, Ar-H), 7.45 (d, 4H, J = 8 Hz, Ar-H), 7.09 (d, 4H, J = 8 Hz, Ar-H), 4.65 (t, 4H, J = 7Hz, NCH_2), 4.05 (s, 6H, NCH_3), 2.57 (pent, 2H, J = 7 Hz, CH_2), 2.26 (s, 6H, CH_3). ^{13}C NMR (75 MHz, DMSO-d_6, 300 K): δ 146.8 (C_q), 144.3 (NCHN), 139.0 (C_q), 133.0 (C_q), 132.1 (C_q), 129.3 (C_{Ar}), 127.7 (2 × C_{Ar}), 126.7 (C_{Ar}), 114.8 (C_{Ar}), 144.7 (C_{Ar}), 45.0 (NCH_2), 34.5 (NCH_3), 29.4 (CH_2), 22.0 (CH_3). IR (neat): 3054 (w), 1570 (m), 1463 (w), 1429 (w), 1183 (s), 1121 (s), 1031 (s), 1009 (s), 811 (m), 762 (s), 681 (s), 559 (s) cm^{-1}. ESI-MS: m/z 153 ([M – 2 OTos]$^{2+}$, 100%), 305 ([M – 2 OTos – H]$^+$), 477 ([M – OTos]$^+$). Anal. Calcd for $C_{31}H_{36}N_4O_6S_2 \cdot 0.25C_6H_5CH_3$: C, 60.72; H, 5.91; N, 8.65; S, 9.90. Found: C, 60.86; H, 5.61; N, 8.59; S, 9.45.

1,1′-diisopropyl-3,3′-(1,2-ethanediyl)bis-4,5-diphenylimidazolium dibromide ([9b]Br$_2$). The product was obtained as a white solid from a mixture of **3b** (2.10 g, 8.0 mmol) and 1,2-dibromoethane (0.75 g, 4.0 mmol) in 20 mL 1,4-dioxane following method C. Yield: 1.50 g (53%). ^{1}H NMR (300 MHz, DMSO-*d*$_6$, 300 K): δ 10.18 (s, 2H, NCHN), 7.48 (m, 8H, Ar-H), 7.41 (m, 8H, Ar-H), 7.07 (m, 4H, Ar-H), 4.54 (s, 4H, NCH$_2$), 4.41 (sept, 2H, *J* = 7 Hz, NCH), 1.46 (d, 12H, *J* = 7 Hz, CH$_3$). ^{13}C NMR (75 MHz, DMSO-*d*$_6$, 300 K): δ 135.0 (NCHN), 131.1 (C$_q$), 131.0 (C$_q$), 130.7 (2 × C$_{Ar}$), 130.4 (C$_{Ar}$), 130.2 (C$_{Ar}$), 129.1 (C$_{Ar}$), 129.0 (C$_{Ar}$), 124.9 (C$_q$), 124.1 (C$_q$), 50.9 (NCH), 46.4 (NCH$_2$), 22.4 (CH$_3$). IR (neat): 2930 (w), 2882 (w), 1557 (m), 1443 (w), 1357 (w), 1210 (m), 1110 (w), 1022 (w), 771 (m), 701 (s), 667 (m) cm^{-1}. ESI-MS: *m*/*z* 276 ([M – 2Br]$^{2+}$, 100%), 551 ([M – 2Br – H]$^+$), 633 ([M – Br]$^+$). Anal. Calcd for C$_{38}$H$_{40}$Br$_2$N$_4$: C, 64.05; H, 5.66; N, 7.86. Found: C, 64.34; H, 5.79; N, 7.92.

1-(2-bromoethyl)-3-tert-butylimidazolium bromide ([10c]Br). A mixture of **1c** (2.48 g, 20.0 mmol) and 1,2-dibromoethane (8.66 mL, 100 mmol) in 40 mL dry THF was stirred 3 days at 40 °C. The resulting colorless oil was isolated after decantation, washing with THF and diethyl ether and drying *in vacuo*. Yield: 5.40 g (86%). ^{1}H NMR (300 MHz, DMSO-*d*$_6$, 300 K): δ 9.45 (s, 1H, NCHN), 8.08 (s, 1H, NCH), 7.91 (s, 1H, NCH), 4.59 (t, 2H, *J* = 6 Hz, CH$_2$), 3.98 (t, 2H, *J* = 6 Hz, CH$_2$), 1.58 (s, 9H, CH$_3$). ^{13}C NMR (75 MHz, DMSO-*d*$_6$, 300 K): δ 135.0 (NCHN), 122.7 (NCH), 120.2 (NCH), 59.6 (C$_q$), 50.0 (CH$_2$), 31.2 (CH$_2$), 29.0 (CH$_3$). IR (neat): 3028 (m), 1560 (s), 1382 (s), 1293 (m), 1203 (s), 1134 (s), 870 (w), 700 (s), 658 (s), 628 (s), 583 (m) cm^{-1}. ESI-MS: *m*/*z* 175 ([M – Br – ^{t}Bu]$^+$), 231 ([M – Br]$^+$, 100%).

1-(2-methoxyphenyl)-3-methylimidazolium iodide ([11h]I). A solution of **1h** (1.74 g, 10.0 mmol) and methyl iodide (1.56 g, 11.0 mmol) in 15 mL dry THF was stirred for 16 h at room temperature. The resulting pale yellow suspension was filtered, washed with THF and dried *in vacuo* to yield a white solid. Yield: 2.65 g (84%). ^{1}H NMR (300 MHz, DMSO-*d*$_6$, 300 K): δ 9.49 (s, 1H, NCHN), 8.03 (s, 1H, NCH), 7.90 (s, 1H, NCH), 7.59 (m, 2H, Ar-H), 7.35 (d, 1H, *J* = 8 Hz, Ar-H), 7.17 (t, 1H, *J* = 8 Hz, Ar-H), 3.95 (s, 3H, CH$_3$), 3.87 (s, 3H, CH$_3$). ^{13}C NMR (75 MHz, DMSO-*d*$_6$, 300 K): δ 152.1 (C$_q$), 137.6 (NCHN), 131.6 (C$_{Ar}$), 126.2 (C$_{Ar}$), 123.6 (NCH), 123.4 (NCH), 123.3 (C$_q$), 121.1 (C$_{Ar}$), 113.2 (C$_{Ar}$), 56.4 (CH$_3$), 36.1 (CH$_3$). IR (neat): 2973 (m), 1576 (m), 1557 (m), 1500 (s), 1438 (m), 1339 (w), 1268 (s), 1159 (m), 1121 (m), 1016 (s), 880 (m), 768 (s), 748 (s), 694 (m), 651 (m), 620 (s) cm^{-1}. ESI-MS: *m*/*z* 189 ([M – I]$^+$, 100%). Anal. Calcd for C$_{11}$H$_{13}$IN$_2$O: C, 41.79; H, 4.14; N, 8.86. Found: C, 41.85; H, 4.16; N, 8.85.

1-tert-butyl-3-benzylimidazolium bromide ([12c]Br). Following method C, the product was obtained from **1c** (1.88 g, 15.1 mmol) and benzyl bromide (3.42 g, 20 mmol) in 20 mL dry 1,4-dioxane. Yield: 3.65 g (82%). ^{1}H NMR (300 MHz, DMSO-*d*$_6$, 300 K): δ 9.54 (s, 1H NCHN), 8.04 (s, 1H, NCH), 7.84 (s, 1H, NCH), 7.42 (m, 5H, Ar-H), 5.40 (s, 2H, NCH$_2$), 1.59 (s, 9H, CH$_3$). ^{13}C NMR (75 MHz, DMSO-*d*$_6$, 300 K): δ 134.9 (C$_q$), 134.6 (NCHN), 128.9 (C$_{Ar}$), 128.6 (C$_{Ar}$), 128.2 (C$_{Ar}$), 122.5 (NCH), 120.7 (NCH), 59.6 (C$_q$), 51.9 (NCH$_2$), 28.9 (CH$_3$). IR (neat): 3048 (m), 3012 (m), 1557 (m), 1451 (w), 1380 (m), 1201 (m), 1136 (m), 772 (m), 760 (s), 723 (s), 662 (s), 632 (m) cm^{-1}. ESI-MS: *m*/*z* 159 ([M – Br – ^{t}Bu + H]$^+$), 215 ([M – Br]$^+$, 100%). Anal. Calcd for C$_{14}$H$_{19}$BrN$_2$: C, 56.96; H, 6.49; N, 9.49. Found: C, 56.76; H, 6.44; N, 9.55.

1-benzyl-3-(2,4,6-trimethylbenzyl)imidazolium bromide ([12e]Br). The white product was prepared according to method A from **1e** (0.80 g, 4.0 mmol) and benzyl bromide (0.75 g, 4.4 mmol) in 10 mL dry THF. However, the reaction mixture was refluxed for only 16 h. Yield: 0.93 g (63%). ^{1}H NMR (300 MHz, DMSO-*d*$_6$, 300 K): δ 9.23 (s, 1H, NCHN), 7.84 (s, 1H, NCH), 7.58 (s, 1H, NCH), 7.40 (m, 5H, Ar-H), 6.95 (s, 2H, Ar-H), 5.39 (s, 2H, NCH$_2$), 5.36 (s, 2H,

NCH_2), 2.23 (s, 3H, CH_3), 2.22 (s, 6H, CH_3). ^{13}C NMR (75 MHz, DMSO-d_6, 300 K): δ 138.5 (C_q), 138.0 (C_q), 135.7 (NCHN), 135.0 (C_q), 129.4 (C_{Ar}), 128.9 (C_{Ar}), 128.6 (C_{Ar}), 128.1 (C_{Ar}), 126.8 (C_q), 122.7 (NCH), 122.6 (NCH), 51.8 (NCH_2), 47.0 (NCH_2), 20.6 (CH_3), 19.3 (CH_3). IR (neat): 3033 (w), 1558 (m), 1452 (m), 1158 (s), 1031 (w), 849 (w), 799 (w), 749 (s), 732 (s), 696 (m), 641 (s) cm^{-1}. ESI-MS: *m*/*z* 133 ($[M - Br - BnIm + H]^+$), 159 ($[BnIm + H]^+$), 291 ($[M - Br]^+$, 100%). Anal. Calcd for $C_{20}H_{23}BrN_2 \cdot 0.1H_2O$: C, 64.38; H, 6.27; N, 7.51. Found: C, 64.36; H, 6.52; N, 7.51.

1-(3-bromopropyl)-3-methylbenzimidazolium bromide ([13a]Br). A mixture of **2a** (1.32 g, 10.0 mmol) and 1,3-dibromopropane (12.1 g, 60.0 mmol) in 10 mL dry THF was stirred 2 days at 35 °C. The resulting white precipitate was isolated by filtration and washed with THF and diethyl ether. Yield: 1.0 g (33%). ^1H NMR (300 MHz, DMSO-d_6, 300 K): δ 9.78 (s, 1H, NCHN), 8.09 (m, 1H, Ar-H), 8.02 (m, 1H, Ar-H), 7.69 (m, 2H, Ar-H), 4.61 (t, 2H, *J* = 7 Hz, NCH_2), 4.06 (s, 3H, CH_3), 3.61 (t, 2H, *J* = 7 Hz, $BrCH_2$), 2.42 (m, 2H, CH_2). ^{13}C NMR (75 MHz, DMSO-d_6, 300 K): δ 143.0 (NCHN), 131.8 (C_q), 130.9 (C_q), 126.6 (C_{Ar}), 126.5 (C_{Ar}), 113.6 (C_{Ar}), 113.4 (C_{Ar}), 45.1 (CH_2), 33.3 (CH_3), 31.5 (CH_2), 30.7 (CH_2). IR (neat): 3001 (w), 1570 (m), 1464 (w), 1426 (w), 1258 (m), 1225 (m), 1124 (w), 823 (w), 760 (s), 591 (s), 554 (s) cm^{-1}. ESI-MS: *m*/*z* 253 ($[M - Br]^+$, 100%). Anal. Calcd for $C_{11}H_{14}Br_2N_2$: C, 39.55; H, 4.22; N, 8.39. Found: C, 39.89; H, 4.27; N, 8.54.

1-benzyl-3-methylbenzimidazolium bromide ([14a]Br). The compound was obtained as a white solid following method A, starting from **2a** (1.32 g, 10.0 mmol) and benzylbromide (1.88 g, 11.0 mmol) in 20 mL THF. Yield: 2.95 g (97%). NMR spectra are identical to those reported.[12]

1-benzyl-3-isopropyl-4,5-diphenylimidazolium bromide ([15b]Br). The product was obtained following method C from **3b** (0.26 g, 1.0 mmol) and benzyl bromide (0.51 g, 3.0 mmol) in 10 mL dry 1,4-dioxane. In this case, however, the product was precipitated from the reaction mixture by the addition of diethyl ether and filtered to yield an off-white solid. Yield: 0.41 g (95%). ^1H NMR (300 MHz, DMSO-d_6, 300 K): δ 9.98 (s, 1H, NCHN), 7.46 (m, 5H, Ar-H), 7.40 – 7.20 (m, 8H, Ar-H), 7.02 (m, 2H, Ar-H), 5.40 (s, 2H, CH_2), 4.41 (sept, 1H, *J* = 7 Hz, NCH), 1.48 (d, 6H, *J* = 7 Hz, CH_3). ^{13}C NMR (75 MHz, DMSO-d_6, 300 K): δ 134.6 (NCHN), 134.2 (C_q), 131.5 (C_q), 131.3 (C_q), 131.0 (C_{Ar}), 130.7 (C_{Ar}), 130.2 (C_{Ar}), 130.0 (C_{Ar}), 129.0 (C_{Ar}), 128.7 (2 × C_{Ar}), 128.3 (C_{Ar}), 127.6 (C_{Ar}), 125.3 (C_q), 125.0 (C_q), 50.7 (NCH), 50.4 (NCH_2), 22.4 (CH_3). IR (neat): 2927 (m), 2850 (m), 1554 (m), 1446 (m), 1248 (m), 1210 (m), 1116 (s), 889 (w), 871 (s), 774 (s), 700 (s), 612 (m) cm^{-1}. ESI-MS: *m*/*z* 353 ($[M - Br]^+$, 100%). Anal. Calcd for $C_{25}H_{25}BrN_2$: C, 69.29; H, 5.81; N, 6.46. Found: C, 69.05; H, 6.01; N, 6.46.

1-(1-(3-methylbenzimidazolium))-3-(1-(3-methylimidazolium))propanediyl dibromide ([16]Br_2). A suspension of **[13a]Br** (1.0 g, 3.0 mmol) and **1a** (0.41 g, 5.0 mmol) in 15 mL 1,4-dioxane was stirred for 3 days at 100 °C. The resulting white precipitate was isolated by filtration, washed with 1,4-dioxane and diethyl ether, recrystallized from methanol/diethylether and dried *in vacuo*. Yield: 0.72 g (58%). ^1H NMR (300 MHz, DMSO-d_6, 300 K): δ 9.92 (s, 1H, NCHN), 9.26 (s, 1H, NCHN), 8.12 (m, 1H, Ar-H), 8.05 (m, 1H, Ar-H), 7.83 (s, 1H, NCH), 7.71 (m, 2H, Ar-H), 7.69 (s, 1H, NCH), 4.59 (t, 2H, *J* = 7 Hz, NCH_2), 4.36 (t, 2H, *J* = 7 Hz, NCH_2), 4.10 (s, 3H, NCH_3), 3.84 (s, 3H, NCH_3), 2.55 (m, 2H, CH_2). ^{13}C NMR (75 MHz, DMSO-d_6, 300 K): δ 142.9 (NCHN), 136.8 (NCHN), 131.8 (C_q), 130.8 (C_q), 126.5 (2 × C_{Ar}), 123.7 (NCH), 122.2 (NCH), 113.6 (2 × C_{Ar}), 45.8 (NCH_2), 43.6 (NCH_2), 35.8 (CH_3), 33.3 (CH_3), 28.8 (CH_2). IR (neat): 2954 (m), 1573 (m), 1463 (w), 1423 (w), 1162 (m), 1027 (w), 808 (m), 760

(s), 618 (s) cm^{-1}. ESI-MS: *m*/*z* 128 ($[M - 2Br]^{2+}$, 100%), 255 ($[M - 2Br - H]^{+}$). Anal. Calcd for $C_{15}H_{20}Br_2N_4 \cdot 0.5CH_3OH$: C, 43.08; H, 5.13; N, 12.96. Found: C, 43.08; H, 5.44; N, 13.25.

1-benzyl-1′-tert-butyl-3,3′-(1,2-ethanediyl)diimidazolium dibromide ([17]Br_2). To a suspension of **[10c]Br** (1.56 g, 5.0 mmol) in 25 mL 1,4-dioxane was added **1d** (0.79 g, 5.0 mmol) and the mixture was stirred for 16 h at 100 °C. The resulting hygroscopic white solid was isolated by filtration and washed with 1,4-dioxane and diethyl ether and dried *in vacuo*. Yield: 2.06 g (87%). ^{1}H NMR (300 MHz, DMSO-d_6, 300 K): δ 9.33 (s, 1H, NCHN), 9.29 (s, 1H, NCHN), 8.01 (s, 1H, NCH), 7.81 (s, 1H, NCH), 7.68 (s, 1H, NCH), 7.66 (s, 1H, NCH), 7.40 (m, 5H, Ar-H), 5.42 (s, 2H, NCH_2Ar), 4.74 (m, 2H, NCH_2), 4.68 (m, 2H, NCH_2), 1.55 (s, 9H, CH_3). ^{13}C NMR (75 MHz, DMSO-d_6, 300 K): δ 136.8 (NCHN), 135.2 (NCHN), 134.5 (C_q), 129.0 (C_{Ar}), 128.7 (C_{Ar}), 128.3 (C_{Ar}), 122.9 (NCH), 122.8 (2 × NCH), 120.4 (NCH), 59.7 (C_q), 51.9 (NCH_2), 48.4 (NCH_2), 48.3 (NCH_2), 28.9 (CH_3). IR (neat): 3051 (s), 1557 (s), 1447 (m), 1379 (m), 1322 (w), 1210 (s), 1157 (s), 1134 (s), 778 (m), 716 (s), 634 (s) cm^{-1}. ESI-MS: *m*/*z* 253 ($[M - 2Br - {}^tBu]^+$, 100%), 309 ($[M - 2Br - H]^+$), 389 ($[M - Br]$). Anal. Calcd for $C_{19}H_{26}Br_2N_4 \cdot 0.7H_2O$: C, 47.46, H, 5.72; N, 11.60. Found: C, 47.26; H, 5.45; N, 11.71.

A.5 References

(1) Welton, T. *Chem. Rev.* **1999**, *99*, 2071.
(2) In, S.; Cho, S. J.; Kang, J. M. *Supramol. Chem.* **2005**, *17*, 443.
(3) Alcalde, E.; Alvarez-Rua, C.; Garcia-Granda, S.; Garcia-Rodriguez, E.; Mesquida, N.; Perez-Garcia, L. *Chem. Commun.* **1999**, 295.
(4) Voges, M. H.; Romming, C.; Tilset, M. *Organometallics* **1999**, *18*, 529.
(5) Scherg, T.; Schneider, S. K.; Frey, G. D.; Schwarz, J.; Herdtweck, E.; Herrmann, W. A. *Synlett* **2006**, 2894.
(6) Lidstrom, P.; Tierney, J.; Wathey, B.; Westman, J. *Tetrahedron* **2001**, *57*, 9225.
(7) de la Hoz, A.; Diaz-Ortiz, A.; Moreno, A. *Chem. Soc. Rev.* **2005**, *34*, 164.
(8) Varma, R. S.; Namboodiri, V. V. *Chem. Commun.* **2001**, 643.
(9) Deetlefs, M.; Seddon, K. R. *Green Chem.* **2003**, *5*, 181.
(10) Lee, H. M.; Lu, C. Y.; Chen, C. Y.; Chen, W. L.; Lin, H. C.; Chiu, P. L.; Cheng, P. Y. *Tetrahedron* **2004**, *60*, 5807.
(11) Torres, J.; Lavandera, J. L.; Cabildo, P.; Claramunt, R. M.; Elguero, J. *Bull. Soc. Chim. Belg.* **1992**, *101*, 29.
(12) Vik, A.; Hedner, E.; Charnock, C.; Tangen, L. W.; Samuelsen, O.; Larsson, R.; Bohlin, L.; Gundersen, L. L. *Bioorg. Med. Chem.* **2007**, *15*, 4016.
(13) Niehues, M.; Kehr, G.; Erker, G.; Wibbeling, B.; Frohlich, R.; Blacque, O.; Berke, H. *J. Organomet. Chem.* **2002**, *663*, 192.
(14) Starikova, O. V.; Dolgushin, G. V.; Larina, L. I.; Ushakov, P. E.; Komarova, T. N.; Lopyrev, V. A. *Russ. J. Organ. Chem.* **2003**, *39*, 1467.
(15) Liu, J. P.; Chen, J. B.; Zhao, J. F.; Zhao, Y. H.; Li, L.; Zhang, H. B. *Synthesis* **2003**, 2661.
(16) Davis, D. P.; Kirk, K. L.; Cohen, L. A. *J. Heterocycl. Chem.* **1982**, *19*, 253.
(17) Pratt, D. A.; Pesavento, R. P.; van der Donk, W. A. *Org. Lett.* **2005**, *7*, 2735.
(18) Chianese, A. R.; Kovacevic, A.; Zeglis, B. M.; Faller, J. W.; Crabtree, R. H. *Organometallics* **2004**, *23*, 2461.
(19) Bell, T. W.; Choi, H. J.; Harte, W.; Drew, M. G. B. *J. Am. Chem. Soc.* **2003**, *125*, 12196.
(20) Bode, R. H.; Bol, J. E.; Driessen, W. L.; Hulsbergen, F. B.; Reedijk, J.; Spek, A. L. *Inorg. Chem.* **1999**, *38*, 1239.
(21) Tahtaoui, C.; Parrot, I.; Klotz, P.; Guillier, F.; Galzi, J. L.; Hibert, M.; Ilien, B. *J. Med. Chem.* **2004**, *47*, 4300.
(22) Kamijo, T.; Yamamoto, R.; Harada, H.; Iizuka, K. *Chem. Pharm. Bull.* **1983**, *31*, 1213.
(23) Sato, K.; Onitake, T.; Arai, S.; Yamagishi, T. *Heterocycles* **2003**, *60*, 779.

Samenvatting

Nikkel N-heterocyclische carbeencomplexen in homogene katalyse

Inleiding

Hoewel de bijzondere chemie van N-heterocyclische carbenen (NHCs) al ruim veertig jaar wordt onderzocht, is het gebied pas in de afgelopen tien jaar tot volle ontwikkeling gekomen. Ofschoon NHCs voornamelijk werden gezien als een laboratoriumeigenaardigheid, staan ze nu bekend als stabiele, economisch aantrekkelijke en zeer veelzijdige liganden voor een groot aantal toepassingen in homogene katalyse. In eerste instantie werden NHCs voornamelijk onderzocht als fosfaananaloga in door ruthenium en palladium gekatalyseerde reacties, maar tegenwoordig worden NHC-complexen van deze en andere overgangsmetalen gebruikt in vele nieuwe transformaties. Daarom is het opmerkelijk dat nikkel-NHC-complexen nog relatief weinig worden gebruikt in katalytische reacties. Het doel van het in dit proefschrift beschreven onderzoek was de synthese van nikkel-NHC-complexen, met een nadruk op chelerende liganden, en om deze complexen te gebruiken in een verscheidenheid aan homogene katalytische reacties.

Hoofdstuk 1 begint met een overzicht van elektronische en sterische eigenschappen van N-heterocyclische carbenen en hun overgangsmetaal-complexen. Daarna volgt een samenvatting van de verschillende methodes om NHCs en hun complexen te maken. Het hoofdstuk wordt afgerond met een overzicht van katalytische reacties waarin overgangsmetaal-NHC-complexen een rol spelen, met speciale aandacht voor nikkel-NHC-complexen.

Zilver(I) complexen van N-heterocyclische carbenen

Men heeft aangetoond dat de transmetallering van NHCs van zilver(I) naar andere overgangsmetalen een efficiënte route is voor de synthese van overgangsmetaal-NHC-complexen. Pogingen om zilver(I)-NHC-complexen te maken, leidden uiteindelijk tot de bepaling van de kristalstructuur van een dimeer van een zilver(I)-bromidecomplex met een monodentaat NHC, zoals beschreven in Hoofdstuk 2. Verrassend genoeg werd door een andere onderzoeksgroep een beduidend andere structuur gevonden, terwijl een vrijwel identieke syntheseroute werd gevolgd. In dit geval bestond de structuur uit een mononucleair zilver(I)-bromidecomplex met twee monodentate NHC liganden. Een aantal studies, waaronder NMR- en kristallisatie-experimenten is ondernomen om te achterhalen wat de structuur van de verbinding in oplossing is en om te ontdekken waardoor

twee verschillende kristalstructuren konden worden gevonden onder vrijwel dezelfde reactiecondities. De uiteindelijke conclusie is dat het ontstaan van de [$(NHC)_2AgBr$]-structuur een toevalstreffer moet zijn. Daarnaast is een nieuwe classificatie van alle bekende kristalstructuren van zilver-NHC-complexen geïntroduceerd.

Het zilver(I)-NHC-complex is gebruikt voor de synthese van het overeenkomstige nikkel(II)-dihalidecomplex, wat de haalbaarheid demonstreert van de transmetallering van monodentate NHCs van zilver(I) naar nikkel(II).

Nikkel N-heterocyclische carbenen in homogene katalyse

In Hoofdstuk 1 is een aantal door nikkel-NHC-complexen gekatalyseerde reacties geïntroduceerd. Het doel van het onderzoek is het gebruik van nikkel-NHC-complexen in homogene katalyse uit te breiden en te verbeteren. Uiteindelijk is het gebruik van nikkel-NHC-complexen succesvol onderzocht in drie verschillende katalysetypes: de hydrosilylering van interne alkynen, de Kumada-koppeling van arylhalides met een aryl-Grignardreagens, en de vinylpolymerizatie van norborneen.

Monodentate NHC liganden - Hydrosilylering

De synthese van een aantal nikkel(II)-dihalidecomplexen met monodentate N-heterocyclische carbeenliganden met kleine substituenten is beschreven in Hoofdstuk 3. Deze complexen zijn gebruikt als katalysator in de hydrosilylering van interne alkynen, wat een belangrijke syntheseroute is voor vinylsilanen. Het grootste deel van de tot nu toe gepubliceerde onderzoeken naar katalytische hydrosilylering is gefocust op eindstandige alkynen en gebruikt kostbare metalen als katalysator. In de in dit proefschrift beschreven studie is de actieve katalysator een nikkel(0)-deeltje, welke *in situ* wordt verkregen door een reactie van het nikkel(II)-precursorcomplex met diethylzink. Met een protocol waarin de katalysator wordt geactiveerd voordat de substraten worden toegevoegd, lieten twee van de $Ni(NHC)_2I_2$-complexen de hoogste activiteit zien; volledige conversie van 3-hexyn met triethylsilaan werd bereikt binnen 60 minuten met 5 mol% katalysator bij 50 °C. In alle gevallen werd selectief het (E)-product verkregen, waarin het waterstofatoom en de silylgroep aan dezelfde zijde van de dubbele band zitten.

Aangezien de NHC-liganden in dit katalytische systeem slechts als monodentaat ligand gebonden zijn, bestaat de mogelijkheid dat het ligand dissocieert, wat kan leiden tot vrij nikkelmetaal, of tot nanodeeltjes. Om er zeker van te zijn dat de waargenomen katalytische activiteit niet resulteert uit de aanwezigheid van heterogene nikkeldeeltjes, zijn twee testen uitgevoerd die homogene en heterogene katalyse kunnen onderscheiden. Ten eerste werden alle katalytische experimenten herhaald in aanwezigheid van 100 equivalenten kwik, een bekende deactivator voor heterogene katalysatoren. Ten tweede werd de katalysator-

concentratie gevarieerd, daar in een homogeen systeem de katalytische activiteit linear afhangt van de katalysatorconcentratie, terwijl dit voor een heterogeen systeem niet het geval hoeft te zijn. De resultaten van deze testen laten duidelijk zien dat de activiteit veroorzaakt wordt door een homogene katalysator.

Chelerende NHC liganden – Kumada koppeling

Vroege pogingen om *cis*-chelerende bisNHC-nikkeldihalidecomplexen te verkrijgen waren niet succesvol en leverden slechts dikationische homoleptische tetracarbeencomplexen of onscheidbare mengsels op. Het enige in de literatuur bekende *cis*-[(bisNHC)NiX$_2$]-complex werd gesynthetiseerd uit een cyclisch bisimidazoliumzout, waarin de twee imidazoliumringen verbonden zijn door twee C$_4$-bruggen. De succesvolle synthese en karakterisering van een aantal nikkel(II)-dihalidecomplexen met bidentate, op benzimidazool gebaseerde bisNHC-liganden is beschreven in Hoofdstuk 4. De kristalstructuren van vier van deze complexen werden bepaald door middel van röntgendiffractie en daarmee werd bewijs geleverd voor de veronderstelde vlakvierkante *cis*-geometrie. Daarnaast werden twee nikkelcomplexen met macrocyclische bisNHC-liganden succesvol gesynthetiseerd.

De nieuwe nikkel-bisNHC-complexen werden onderzocht op hun katalytische activiteit in de Kumada-koppeling van arylchlorides en -bromides met fenylmagnesiumchloride bij kamertemperatuur. Deze reactie is een effectieve en economisch aantrekkelijke route voor de synthese van C–C gekoppelde diarylen, hoewel het een vrij lage functionele-groeptolerantie heeft. Met uitzondering van de complexen met macrocyclische liganden waren alle complexen redelijk tot zeer actief in deze reactie. De meest effectieve katalysator voor beide arylhalides gevonden in deze studie is een benzylgesubstitueerd nikkel-bisNHC-complex, welke volledige conversie gaf van 4-chloroanisool in minder dan 14 uur, met een selectiviteit van 99% voor het gewenste product 4-methoxybifenyl met 3 mol% katalysator; met 4-bromoanisool werd volledige conversie bereikt in 75 minuten met een selectiviteit van 82% onder vergelijkbare reactieomstandigheden. Daarnaast werd waargenomen dat de katalytische activiteit van de nikkelcomplexen afhangt van de bulk van de substituenten op het bisNHC-ligand: in het geval van 4-bromoanisool ging de reactiesnelheid omlaag met grotere substituenten, terwijl in het geval van 4-chloroanisool de reactiesnelheid omhoog ging. Hieruit is geconcludeerd dat de snelheidsbepalende stap van de katalytische cyclus afhangt van de vertrekkende groep van het substraat.

De voortgezette zoektocht naar een efficiënte katalysator voor de Kumada-koppeling is beschreven in Hoofdstuk 5. Er werd besloten te proberen nikkelcomplexen te synthetiseren met chelerende NHC-liganden, waarin het NHC-ligand is gefunctionaliseerd met anionische donorgroepen. Op basis van de synthese van bekende complexen werd een aantal complexen met amido- en benzimidazolatogesubstitueerde NHCs bereid en gekarakteriseerd met één-kristal

röntgendiffractie. Verrassend genoeg zijn deze complexen hoogst actief in de Kumada-koppeling van 4-chloroanisool met fenylmagnesiumchloride, onder de condities zoals beschreven in Hoofdstuk 4. Het benzimidazolatogefunctionaliseerde complex laat de hoogst bekende reactiviteit en effectiviteit in deze reactie zien, met een kwantitatieve opbrengst van het gewenste product binnen 30 minuten met slechts 1 mol% katalysator. Zelfs het minder reactieve 4-fluoroanisool kon in 150 minuten kwantitatief worden gekoppeld, onder dezelfde omstandigheden. Verondersteld wordt dat de hoge snelheid van deze katalysatoren kan worden toegeschreven aan een coöperatieve interactie tussen de anionische N-donorgroep, magnesiumhalide en het substraat, waardoor de oxidatieve additie van het substraat aan het nikkelatoom sneller verloopt.

DFT studies

Om het onderzoek naar de nikkelgekatalyseerde Kumada-koppeling te vervolmaken is een poging gedaan om de katalytische resultaten beschreven in Hoofdstuk 4 te rationaliseren. Met behulp van density functional theory (DFT) werd de complete katalytische cyclus van deze reactie met nikkel-bisNHC-complexen berekend. De resultaten van deze kwantumchemische berekeningen worden besproken in Hoofdstuk 6 en laten de waarschijnlijkheid zien van de algemeen geaccepteerde cyclus, welke bestaat uit de oxidatieve additie van het arylhalide, transmetallering van het halide-ion met de arylgroep van het Gignard-reagens, en de reductieve eliminatie van het product. Het is aangetoond dat de oxidatieve additie begint met de coördinatie van het arylhalide aan het initiële Ni(0)-complex, gevolgd door insertie van het nikkelatoom in de C–halide band, wat een *cis*-gecoördineerd nikkel(II)-complex geeft. In de tweede stap is het arylmagnesiumchloride gecoördineerd tussen de nikkelgebonden aryl en de halide waarna via een overgangstoestand bestaande uit een Ni–C–Mg–halide ring de nieuwe arylgroep en het halide van positie wisselen. Dit resulteert in een MgXCl-groep, gecoördineerd tussen twee nikkelgebonden arylringen, welke vervolgens dissocieert. In de derde stap vormen, via een drieledige overgangstoestand, de twee overgebleven arylringen een C–C-band en het gekoppelde product dissocieert waarna het nikkel(0)-complex achterblijft.

Naast de cyclus die leidt tot het gewenste product is een route voorgesteld die, uitgaande van een intermediair uit de transmetalleringsstap, effectief leidt tot een uitwisseling van de arylringen van de twee uitgangsstoffen. Deze route verklaart uitstekend alle bijproducten die experimenteel zijn geobserveerd.

De berekende energieën van de complete katalytische cyclus laten zien dat de drie stappen in de cyclus barrières hebben van vrijwel gelijke grootte. Dit is in overeenstemming met de verandering van snelheidsbepalende stap bij verandering van vertrekkende groep. Helaas verhindert dit ook de bepaling van wat nu echt de snelheidsbepalende stap is onder experimentele omstandigheden.

Vinylpolymerisatie van norborneen

Het laatste type homogene katalyse dat in het kader van dit proefschrift experimenteel is onderzocht is de vinylpolymerisatie van norborneen, welke beschreven staat in Hoofdstuk 7. Vanwege hun goede thermische weerstand en transparantie zijn norborneenpolymeren van belang voor optische en elektronische toepassingen en hun katalytische synthese is gerapporteerd met verscheidene nikkelcomplexen met N-, O- en P-donor liganden. Slechts twee voorbeelden van nikkel-NHC-katalysatoren zijn bekend in deze reactie en er werd besloten om een aantal van de complexen die beschreven zijn in Hoofdstukken 3-5 te testen, namelijk een complex met monodentate NHC-liganden, twee complexen met een chelerend bisNHC-ligand en twee complexen met anionische, bidentate N-donorgefunctionaliseerde NHC liganden.

Na activering met een relatief lage 500-voudige overmaat methylaluminoxaan lieten de drie typen complexen goede tot hoge activiteit zien, bij verschillende temperaturen in dichloormethaan en 1,2-dichloorethaan. Met behulp van IR-spectroscopie en NMR-spectrometrie werd aangetoond dat de polymeerproducten van het vinylgepolymeriseerde type zijn met een hoog moleculair gewicht en een lage polydispersiteit (zoals bepaald met size exclusion chromatografie). Van de drie onderzochte katalysatortypes waren de complexen met N-donorgefunctionaliseerde liganden het minst actief, terwijl de hoogste activiteit van 2.6×10^7 g/(mol kat)·h werd behaald met het kleine complex diiodidobis(1,3-dimethylimidazol-2-ylideen)nikkel(II).

List of publications

'The autoxidation activity of new mixed-ligand manganese and iron complexes with tripodal ligands'

R. van Gorkum, J. Berding, D. M. Tooke, A. L. Spek, J. Reedijk, E. Bouwman, *J. Catal.* **2007**, *252*, 110

'The synthesis, structures and characterisation of new mixed-ligand manganese and iron complexes with tripodal, tetradentate ligands'

R. van Gorkum, J. Berding, A. M. Mills, H. Kooijman, D. M. Tooke, A. L. Spek, I. Mutikainen, U. Turpeinen, J. Reedijk, E. Bouwman, *Eur. J. Inorg. Chem.* **2008**, 1487

'Synthesis of novel chelating benzimidazole-based carbenes and their nickel(II) complexes; activity in the Kumada coupling reaction'

J. Berding, M. Lutz, A. L. Spek, E. Bouwman, *Organometallics* **2009**, *28*, 1845

'Another silver complex of 1,3-dibenzylimidazol-2-ylidene: solution and solid state structures'

J. Berding, H. Kooijman, A. L. Spek, E. Bouwman, *J. Organomet. Chem.* **2009**, *694*, 2217

'N-donor functionalized N-heterocyclic carbene nickel(II) complexes in the Kumada coupling'

J. Berding, T. F. van Dijkman, M. Lutz, A. L. Spek, E. Bouwman, *Dalton Trans.* **2009**, 6948

'$NiX_2(NHC)_2$ complexes in the hydrosilylation of internal alkynes'

J. Berding. J. A. van Paridon, V. H. S. van Rixel, E. Bouwman, *Eur. J. Inorg. Chem.* **2009**, submitted

'Theoretical study on the nickel (bisNHC) complex catalyzed Kumada coupling'

J. Berding, F. Buda, A. W. Ehlers, E. Bouwman, in preparation

'Nickel N-heterocyclic carbene complexes in the vinyl polymerization of norbornene'

J. Berding, E. Bouwman, in preparation

Curriculum Vitae

De auteur van dit proefschrift werd op 20 december 1980 geboren te Den Haag. Na het behalen van het VWO-diploma aan het Christelijk Gymnasium Sorghvliet te Den Haag in 1999, begon hij in september van dat jaar aan de studie Scheikunde aan de Universiteit Leiden. Het propedeutisch jaar werd *cum laude* afgerond. De hoofdvakstage werd uitgevoerd onder leiding van prof.dr. J. Reedijk op het gebied van de coördinatiechemie en homogene katalyse. Voor het stageverslag ontving de auteur de Unilever Research Prijs 2004. De bijvakstage werd uitgevoerd onder leiding van prof.dr. H.S. Overkleeft op het gebied van de organische synthese. Daarnaast is een zomerstage uitgevoerd aan Grinnell College te Grinnell, Iowa onder leiding van prof.dr. M. Minelli op het gebied van de anorganische synthese. Het doctoraal examen werd afgelegd op 18 januari 2005.

De auteur was van 1 februari 2005 tot 1 juli 2009 als promovendus in dienst van de Universiteit Leiden. In die periode werd het in dit proefschrift beschreven onderzoek verricht onder leiding van dr. E. Bouwman en prof.dr. J. Reedijk. Naast het onderzoek werden die hiermee samenhangende onderwijstaken vervuld op de eerste- en tweedejaars practica voor scheikunde- en molecular science-studenten. Daarnaast heeft de auteur een aantal studenten begeleid bij een research-practicum, onderzoeks project, bachelor- of masterstage. Een deel van het onderzoek werd uitgevoerd aan de Westfälische Wilhelms-Universität Münster, Duitsland in de groep van prof.dr. F.E. Hahn.

Tijdens zijn promotieperiode heeft de auteur onder meer de volgende cursussen bijgewoond en met goed gevolg afgerond: de NIOK-cursus 'Catalysis – an integrated approach' op Schiermonnikoog in 2005; de NIBHV-cursus 'Bedrijfshulpverlening met adembescherming' te Leiden in 2006; de cursus 'Scientific writing in English' van het talencentrum van de Universiteit Leiden in 2008.

Delen van het in dit proefschrift beschreven werk werden door de auteur gepresenteerd tijdens nationale (NCCC VI – NCCC X te Noordwijkerhout in 2005-2009; de HRSMC autumn school 'Advanced Metal Organic Chemistry' te Oegstgeest in 2006; de NWO bijeenkomst 'Ontwerp & Synthese, Structuur & Reactviteit, Biomoleculaire Chemie' te Lunteren in 2006; het HRSMC-symposium te Amsterdam in 2008) en internationale (de 35e Gordon Conference on Organometallic Chemistry te Newport, RI, VS in 2007; de 23e International Conference on Organometallic Chemistry te Rennes, Frankrijk in 2008, IRTG-bijeenkomst te Münster, Duitsland in 2008) bijeenkomsten.

Nawoord

The doubter is a true man of science; he doubts only himself and his interpretations, but he believes in science.
Claude Bernard (An Introduction to the Study of Experimental Medicine, 1865. Vertaald uit het Frans door H.C. Greene in 1927)

Zoals hierboven aangegeven, is een wetenschapper een twijfelaar. Gelukkig was er tijdens mijn promotietijd een aantal personen die mij direct of indirect hebben gesteund en geholpen door het wegnemen van een aantal van mijn twijfels. Nu het onderzoek en het beschrijven ervan tot een goed eind zijn gebracht, wil ik graag die mensen noemen die op verschillende manieren hier aan hebben bijgedragen.

In de ruim vier jaar promotieonderzoek heeft een flink aantal studenten voor kortere of langere tijd mij in mijn onderzoek geholpen. Een aantal van hen noem ik hier. Martijn van der Ster, de syntheses van gefunctionaliseerde complexen die ik voor je Master-stage had bedacht bleken toch lastiger dan ik had gehoopt. Het was hoe dan ook een leerzame ervaring. Tom van Dijkman, jouw Bachelor-stage op het gebied van de N-donor-gefunctionaliseerde NHC-complexen (hoofdstuk 5) heeft zelfs geleid tot een mooie publicatie. Joris Dokter, John van Paridon en Vincent van Rixel, jullie hebben voor jullie Bachelor-stage gewerkt aan de hydrosilylering. Hopelijk herken je een deel van je werk terug in hoofdstuk 3. Het bleek helaas een moeilijker onderwerp dan vooraf gedacht, maar jullie hebben er hard aan gewerkt en nuttig was het zeker.

Ik noem natuurlijk graag 'de harde kern' van HB514: Jimmy, Marta, Raja en Tiddo. Marta and Raja, you're both defending your theses within two weeks after me. I'm glad we could support each other in writing during the last few months and I wish you both good luck. Jimmy en Tiddo, jullie moeten (mogen!) nog even en ik wens jullie veel succes daarbij. Ik denk met plezier terug aan de fijne (wetenschappelijke) discussies en de gezelligheid. Andere collega's die in de afgelopen vier jaar een kortere of langere tijd in ons kantoortje en op ons lab hebben gewerkt, wil ik ook graag noemen: Stefania, Tom, Meenal, Prasad en Susmit. I enjoyed very much the good atmosphere in the office and in the lab.

De CBAC-groep is groter dan alleen HB514. De volgende namen mogen dan ook niet ontbreken in het lijstje van mensen die het werk de afgelopen jaren tot een mooie ervaring hebben gemaakt: Paul, Eva, Patricia, Ariadna, Sudeshna, Nuria, Geoff, Sylvestre, Ira, Patrick, José, Laurent, Remy, Karlijn, Steven, Gé, Wen Tian en vele binnen- en buitenlandse studenten. En tegen de vele Spanjaarden, die met mij in de CBAC-groep zaten, wil ik graag nog zeggen: Estoy avergonzado que después de tener tantos compañeros de trabajo españoles, todavía no puedo hablar Español, but I'm sure you'll forgive me.

Van een aantal mensen waren de technische kennis en vaardigheden van groot belang voor het proefschrift: Jos van Brussel, het was altijd weer een feestje als een elementanalyse goed uitpakte en ook het vervangen van GC-injectiespuiten zal ik missen. John van Dijk, vooral de polymeren uit hoofdstuk 7 hebben je flink bezig gehouden en bleken helaas niet erg oplosbaar. Ik hoop dat de database waar we samen aan hebben gewerkt nog een lange tijd mee zal gaan. Jopie Erkelens leverde mijn zeer geroutineerd de nodige massaspectra. Fons Lefeber en Kees Erkelens waren zeer hulpvaardig en geduldig bij mijn NMR-metingen. Huub Kooijman en Martin Lutz van Universiteit Utrecht waren verantwoordelijk voor het bepalen van de kristalstructuren van de nikkel- en zilvercomplexen in dit proefschrift. Hun expertise was van onschatbare waarde.

Andreas Ehlers (UvA) en Francesco Buda hebben advies geleverd bij de DFT-berekeningen beschreven in hoofdstuk 6. Franco, fijn dat ik gebruik kon maken van je rekentijd op het Mistress-cluster. Andreas, je kritische vragen en opmerkingen hebben geleid tot de uiteindelijke versie van het hoofdstuk. Een deel van het werk beschreven in hoofdstuk 4 is uitgevoerd in de groep van prof.dr. F.E. Hahn in Münster. Für ihre Gastfreundlichkeit sollten Mareike Jahnke und Florian Hupka erwähnt werden.

Dan zijn er eigenlijk nog teveel mensen die ik moet noemen vanwege hun steun in het leven buiten het lab en het zorgen voor voldoende ontspanning. Twee mensen wil ik in het bijzonder noemen. Vincent, als alfa *pur sang* zul je mijn werk nooit helemaal begrijpen, maar je interesse en vriendschap waardeer ik zeer. David, ik ben vereerd dat je mijn paranimf wilt zijn. Ik wens je veel succes met je eigen promotieonderzoek.

Dan als laatsten de mensen die niet genoeg genoemd kunnen worden: mijn lieve ouders en zusjes. Zonder de vele jaren van jullie onvoorwaardelijke steun had ik nooit zo ver kunnen komen.

Lieve Paulyn, over jou heb ik nooit hoeven twijfelen.

Joris